Fourth edition

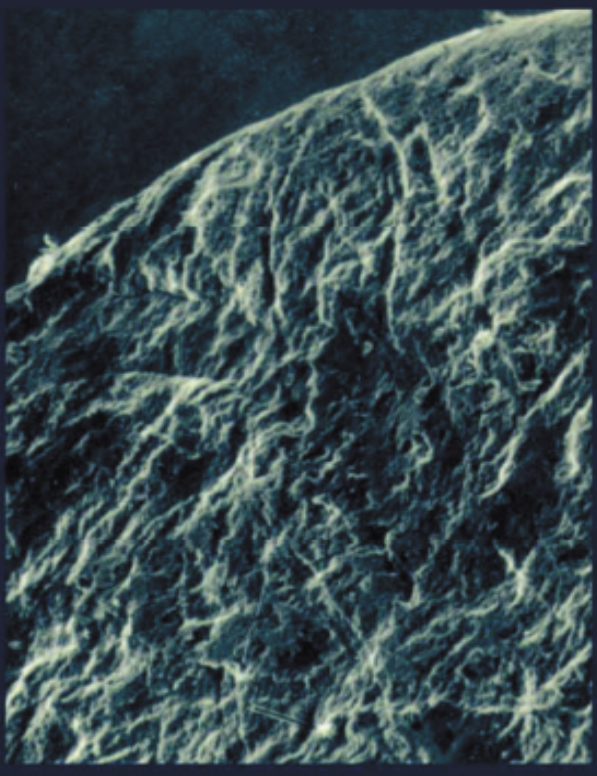

PRINCIPLES AND APPLICATIONS OF ELECTROCHEMISTRY

D. R. Crow

Principles and Applications of Electrochemistry

Principles and Applications of Electrochemistry

Fourth edition

D. R. CROW
Professor of Electrochemistry and Dean of Research
University of Wolverhampton


Chapman & Hall/CRC
Taylor & Francis Group
Boca Raton London New York

Published in 1994 by
Chapman & Hall/CRC
Taylor & Francis Group
6000 Broken Sound Parkway NW, Suite 300
Boca Raton, FL 33487-2742

Chapman & Hall/CRC is an imprint of Taylor & Francis Group
First edition 1974, Second edition 1979, Third edition, 1988, This edition 1994
Originally published by Chapman & Hall

International Standard Book Number-10: 0-7514-0168-4 (Softcover)
International Standard Book Number-13: 978-0-7514-0168-4 (Softcover)
Library of Congress catalog number: 94-70122

Library of Congress Cataloging-in-Publication Data

Catalog record is available from the Library of Congress

informa
Taylor & Francis Group
is the Academic Division of Informa plc.

Visit the Taylor & Francis Web site at
http://www.taylorandfrancis.com

and the CRC Press Web site at
http://www.crcpress.com

Preface

It has been my good fortune to have had the various editions of this book in print for rather more than twenty years. Those who have used it have been kind enough to comment on its appropriateness for them as either teacher or student, and their identification of errors and obscurities has always been communicated to me with diplomacy. There are now many more books, both general and specific, which deal with the subject of Electrochemistry: in some of them I flatter myself that there is evidence of the influence of earlier editions of this text in regard to structure and treatment. There is always something to learn from different approaches and I acknowledge their help to me in formulating my own ideas for presenting this update.

This fourth edition represents a considerable revision. Structurally it is different from its predecessors in that principles and applications are separated. Several derivations which at first (and maybe even subsequent) readings of their context, may be omitted without in any way detracting from the main theme have been placed in Appendices. Other areas have been re-ordered, expanded or given greater prominence. An example is the section on Electrochemical Sensors which now forms a chapter on its own; another area is that of Electro-analytical Techniques which again has a chapter devoted to it and which includes a number of modern methods not included in earlier editions.

Maintenance of a proper balance between selectivity and detail is always a problem in writing a text such as this one: however, in producing this new edition, which is both re-structured and modestly expanded, the aim has been to bring the essentials into focus and context, but to point the way to further study, expanded treatment and greater intellectual depth. Above all, it has been my concern that the *shape* of the subject of Electrochemistry should be stated at the outset and not lost or obscured during the reading of particular parts, that its coherence should be evident and that its wider application should be appreciated.

There are a number of people whose help I would wish to acknowledge. In terms of this edition I am indebted to my typist Ms Tracey Simcox whose speed and accuracy of word-processing, combined with an ability to decipher my drafts, contributed to my keeping to the schedule agreed with the publishers. Which leads me to express my gratitude to the various editors and staff of Chapman and Hall with whom I have worked over the years: their courtesy, understanding and help have always been so suppor-

tive. My immediate colleagues and my own students are among those already mentioned whose use of earlier editions and association with various undergraduate courses have provided me with feedback on the effectiveness of the book.

Finally, I am thankful for the inestimable benefit of a happy and settled home where my wife Margaret, despite a busy academic life of her own, is a constant source of support and encouragement.

D. R. C.

Contents

1 The development and structure of electrochemistry

1.1 The ubiquitous nature of electrochemistry

The subject of electrochemistry is concerned with the study and exploitation of the transference of electrical charges across interfaces and through solution. Transfer of material across biological membranes, storage of electricity in batteries, the production of nylon, electroplating, nerve action, corrosion—these are some areas in which few people would argue that the phenomena are electrochemical.

Yet within the more academic tradition, electrochemistry has been seen as a large and important area of physical chemistry—in many respects rightly so. The subject finds its place in courses of physical chemistry and it appears in chapters of books of that subdivision of the subject of chemistry. Still, it is difficult to define the limits of electrochemistry, for its influence permeates so much of wider chemistry.

The Periodic Table of the Elements, the foundation of systematic inorganic chemistry, is complemented by the Electrochemical Series. Any discussion of periodicity quickly introduces such terms as *electronegativity* and *ionic* character—and the language has turned inexorably to that of electrochemistry. Metal extraction and chemical analysis require electrochemical principles for their understanding and effective exploitation, both on an industrial and on a laboratory scale. Organic synthesis increasingly sees electrochemistry put to use; modern development owes much to the control of electrochemical parameters made possible by modern instrumentation although the Kolbe synthesis was established in the mid-nineteenth century.

1.2 The historical dimension

Publication of the laws of electrochemical conversion some 160 years ago by Michael Faraday established quantitative electrochemistry: direct application of those laws is seen in coulometry.

The nineteenth century saw the building and emergence of the discipline of *Thermodynamics*—a tool of enormous power and an intellectual insight of awesome proportions. Electrochemistry played its part in this development: formulation of the Third Law in particular owed much to investigations of the temperature dependence of cell emf's. Largely under the

influence of Nernst, electrochemistry was itself given, and seen as having, a thermodynamic foundation. Indeed, the dominance of Nernst and electrochemical thermodynamics was to have something of a retarding influence on earlier twentieth century progress in Western electrochemistry. Development of electrochemical kinetics owed more to the researches of Central and Eastern Europe. In retrospect, the work of Heyrovsky, starting in Prague in the late twenties, bridges and ultimately leads to a proper regard for the thermodynamic and kinetic principles in electrochemistry.

1.3 The domains of electrochemistry

Electrochemistry is concerned with charges and with their movement and transfer from one medium to another. The ultimate unit of charge is that carried by the electron; electrons are important in electrochemistry and their functions here are similar to some of those which they exhibit in related disciplines more usually regarded as the province of physics. The science of *Thermionics* is built on the exchange of electrons between a solid and a vacuum; that of *transistor electronics* is based on their transfer between one solid phase and another.

When electrons exchange between metals (or other *electronic* conductors), in this context usually termed *electrodes*, and species in solution within which that metal is placed, *Electrodics* is a suitable name to give to the discipline which emerges.

The behaviour of species in solution with an excess or deficiency of electrons, so that they form the negatively or positively charged entities termed *ions*, is the interest of the science which may be called *Ionics*. Electrodics, concerned with electrode processes, and ionics, concerned with the behaviour of ions in solution, constitute much of the fabric ofelectrochemistry.

Separating the solid (or sometimes liquid) material of an electrode and a solution there exists an interfacial region of great importance. The interplay of these three regions is implied by Figure 1.1.

The extremely large field gradients at electrode/solution interfaces caused by imposed potential differences, induce gross distortions in the positions (orbitals) which electrons may occupy in solute ions and in electrodes. Such constraints affect the transfer of electrons between the solid and solution species.

Systems of the sort shown in Figure 1.1 only take on practical significance when combined in pairs to form *electrochemical cells* (Figure 1.2). Differing chemical characteristics of systems labelled 1 and 2 give rise to voltages across terminals connected to the electrodes. This is the arrangement in the wide range of batteries commercially available, except that pastes often replace solutions, render the arrangement stationary and lead to the description *dry*. In cases where the processes which generate the cell voltage

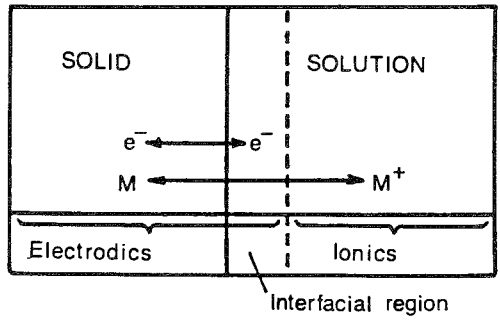

Figure 1.1 Electrodics is concerned with the exchange of electrons between electrodes and species in solution (these are frequently ions). Ionics is the discipline concerned with the behaviour of ions in solution.

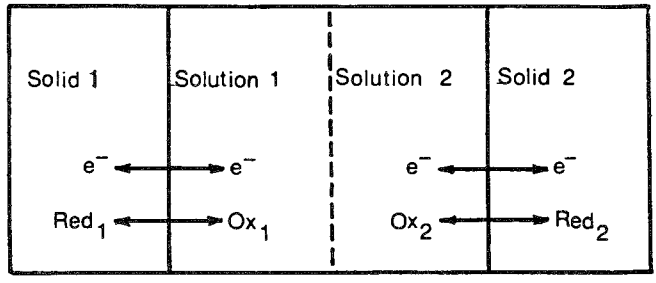

Figure 1.2 General arrangement of an electrochemical cell. Spontaneous generation of a voltage occurs by interfacing of certain electrode/solution pairs of differing chemical characteristics. Imposition of external voltage can reverse the discharge process in rechargeable cells. Supply of 'fuels' to solution sectors under conditions that electron exchange may occur between them and the electrodes can generate an exploitable voltage.

can be reversed, after discharge, by imposition of an external voltage, the battery is rechargeable. The efficiency of such processes is largely governed by the absence of side reactions, the lead–acid cell installed in our motor cars being particularly effective. In other variations, a voltage is generated by the transfer of electrons between the electrodes and *fuels* continuously supplied to the adjacent solution sectors. This is easier said than done and it is necessary to have appropriate catalysts incorporated to ensure rapid electron transfer. Manned spacecraft use hydrogen and oxygen in such *fuel cells* to provide a major part of the electricity requirements, and to supplement the water supply by this product of the process.

The arrangement shown in Figure 1.2 is quite general and of particular practical importance is the variant where one *half-cell* has its properties maintained constant so that relative changes in the other half may be investigated. This approach is the basis of much of electroanalytical chemistry.

The nature, behaviour and structure of species in solution are closely linked with the way in which they undergo electron exchange reactions. Changing the *form* of these species, such as by complexation, often produces a change in electrode behaviour. The nature of metallic deposits produced in electroplating is, for example, significantly affected by the presence of additives to the solution. Even today the reasons for this are far from completely understood and the production of many plated surfaces remains as much an art as a science.

In many arrangements, the magnitudes of currents and voltages are related to the *concentrations* of dissolved solutes. Measurement of such quantities, under carefully controlled experimental conditions, constitutes the very large area of electroanalytical chemistry. Much recent effort has been devoted to the development of electrochemical *sensors*. These are systems which miniaturize and confine complex solution chemistry and electrochemistry to small probes whose sensitive and reversible responses to specific solution components allows their concentration to be determined. A particularly attractive type of sensor is that based on the specific reactions of enzymes.

Implicit in the demonstration and implementation of Faraday's laws are the concepts of atomicity and the nature of ions and electrons. Evidently charges transferred through solutions and across electrode/solution interfaces are 'atomic' in nature.

The two laws are tersely expressed as follows:

1. In electrolytic processes the amount of chemical decomposition is proportional to the *quantity of electricity* passed.
2. The masses of different species dissolved from or deposited at electrodes *by the same quantity of electricity* are in direct proportion to M_R/z for each species. M_R is the relative molar mass, z the change in charge number which occurs in the electrode reaction which may be represented in general terms by

$$A^{n+} \pm ze \rightleftharpoons A^{(n\mp z)+}$$

Thus, when a given current is caused to pass for a given time through a series of electrolyte solutions, the extent of decomposition is always the same in terms of $1/z$ moles. In this statement lies the definition of the Faraday constant as the amount of electricity required to deposit a mole of any species from solution. It has the value $96\,487\,\mathrm{C\,mol^{-1}}$ and its units emphasize the fact that 96 487 coulombs is the amount of electricity associated with '1 mole of unit charges, or electrons'. For practical purposes throughout the following chapters the value of the constant is rounded to $96\,500\,\mathrm{C\,mol^{-1}}$.

Faraday's laws, while allowing a measure of *how much* electrochemical

change occurs, can say nothing about *how* (or why) such changes take place. Further, the electron exchange reactions involve species which originate in the solution and which must travel to the electrode to become involved in the process there. In the bulk of the solution electroactive solutes will behave in a way dependent on their structure, their interaction with the solvent and the prevailing conditions. Such factors will influence the transfer of an ion through the solution to the edge of the interfacial region and its subsequent negotiation of that region. Each of these circumstances constitutes an area (or areas) of study in their own right. Their influence is augmented in the *overall* electrochemical processes quantitatively expressed in terms of Faraday's laws. In short, the behaviour of ions may be considered in the bulk of a solution, at interfaces and at electrodes—three domains of electrochemistry. In Table 1.1 important features of the subject, upon which subsequent chapters focus, are listed within these domains.

The sequence of Chapters 2–7, concerned with *principles*, reflects directly the journey of an ion in solution to an electrode and its reaction there. Chapters 8–11 are concerned with the exploitation of those principles in a range of *applications*.

Table 1.1 Features of electrochemistry

Ionics	Interfacial phenomena	Electrodics
Nature and behaviour of ions in solution and fused state	Double layer theory	Kinetics and mechanism of electrode reactions
Ionic equilibria	Adsorption	
Acid–base theory	Zeta potential	Electron-transfer processes
Transport processes	Electrokinetic phenomena	
Potential-determining ion reactions and reversible half-cell potentials	Colloidal systems	Electrocatalytic processes
Sensor systems	Ion-exchange processes	

PART I PRINCIPLES

2 Ionic interaction: the ways in which ions affect each other in solution

2.1 The nature of electrolytes

Electrolytes are species giving rise to ions to a greater or lesser extent, strong electrolytes being completely ionized even in the solid and fused states. In the latter case, and also when dissolved in a solvent, the ions become free to move and the highly ordered lattice structure characteristic of crystals is destroyed. Weak electrolytes, on the other hand, are ionized to only a small extent in solution, ionization increasing with dilution according to the well-known Ostwald Law considered in Chapter 3.

2.1.1 Ion–ion and ion–solvent interactions

Although strong electrolytes are completely ionized, their ions are not entirely free to move independently of one another through the body of a solution, except when this is infinitely dilute. A fairly realistic picture of the situation in a solution containing the oppositely charged ions of an electrolyte is as follows. Ions will move randomly with respect to one another due to fairly violent thermal motion. Even in this condition, however, coulombic forces will exert their influence to some extent with the result that each cation and anion is surrounded on a time average by an 'ion atmosphere' containing a relatively higher proportion of ions carrying charge of an opposite sign to that on the central ion.

Movement of ions under the influence of an applied field will be very slow and subject to disruption by the thermal motion. Under the influence of such a field, movement of the atmosphere occurs in a direction opposite to that of the central ion, resulting in the continuous breakdown and reformation of the atmosphere as the ion moves in one direction through the solution. The time lag between the restructuring of the atmosphere and the movement of the central ion causes the atmosphere to be asymmetrically distributed around the central ion causing some attraction of the latter in a direction opposite to that of its motion. This is known as the *asymmetry*, or *relaxation* effect. In addition, central ions experience increased viscous hindrance to their motion on account of solvated atmosphere ions which, on account of the latter's movement in the opposite direction to the central ion, produce movement of solvent in this opposing direction as well. This is known as the *electrophoretic* effect.

Such interactions must obviously increase in significance with increasing concentration of the electrolyte. In the extreme condition of infinite dilution, all interionic effects are eliminated, ions move without the above restrictions, current may pass freely and conductivity reaches a maximum value. In another extreme situation, interionic attraction may become so great that the formation of discrete ion pairs may occur. The most favourable conditions for such behaviour are high electrolyte concentration and high charges on the ions. Ion pairs consist of associated ions, the formation of which must be regarded as a time-averaged situation since in any such system there will be a continual interchange of ions amongst the pairs. For a species to be regarded as an ion pair, it must be a 'kinetically distinct' species. That is, although it is an unstable and transient entity, it nevertheless has a lifetime of such duration that it can experience a number of kinetic collisions before exchanging an ion partner.

2.1.2 Dissolution, solvation and heats of solution

Very many salts are known to dissolve readily in solvents with heats of solution that are usually fairly small in magnitude and which may be exothermic or endothermic. At first sight this is a phenomenon rather difficult to account for, since crystal structures have high lattice energies. A lattice energy is the large-scale analogue of the dissociation energy of an individual ionic 'molecule'. In a crystal, the energies of a large number of component ion formula units contribute to the total lattice energy which is effectively the energy evolved when the lattice is built up from free ions. Since such energies are large, we are led to suppose that a large amount of energy is required to break down the ordered structure and liberate free ions. A way in which the observed easy dissolution can be explained is by the simultaneous occurrence of another process which produces sufficient energy to compensate for that lost in the rupture of the lattice bonds. Exothermic reactions of individual ions with the solvent—giving rise to the heat of solvation—provide the necessary energy. From the First Law of Thermodynamics, the algebraic sum of the lattice and solvation energies is the heat of solution. This explains both why the heats of solution are usually fairly small and why they may be endothermic or exothermic—depending upon whether the lattice energy or the solvation energy is the greater quantity.

A great difficulty when dealing with electrolytes is to ascribe individual properties to individual ions. Individual thermodynamic properties cannot be determined, only mean ion quantities being measurable. Interionic and ion–solvent interactions are so numerous and important in solution that, except in the most dilute cases, no ion may be regarded as behaving independently of others. On the other hand, there is no doubt that certain dynamic properties such as ion conductances, mobilities and transport

numbers may be determined, although values for such properties are not absolute but vary with ion environment.

2.2 Ion activity

Since the properties of one ion species are affected by the presence of other ions with which it interacts electrostatically, except at infinite dilution, the concentration of a species is an unsatisfactory parameter to use in attempting to predict its contribution to the bulk properties of a solution. What is rather required is a parameter similar to, and indeed related to, concentration, i.e. the actual number of ions present, but which expresses the availability of the species to determine properties, to take part in a chemical reaction or to influence the position of an equilibrium. This parameter is know as activity (a) and is related to concentration (c) by the simple relationship

$$a_i = \gamma_i c_i \tag{2.1}$$

γ_i is known as an activity coefficient which may take different forms depending on the way in which concentrations for a given system are expressed, i.e. as molarity, molality or mole fraction. For instance, the chemical potential (μ_i) of a species i may be expressed in the form

$$\mu_i = \mu_i^{\ominus} + RT \ln x_i \gamma_i \tag{2.2}$$

where x_i is the mole fraction and γ_i is known as the rational activity coefficient. Similar expressions in terms of molar or molal concentrations may be used.

2.2.1 Chemical and electrochemical potential

Before going any further it is necessary to be quite clear what chemical potential (μ_i) really means; somewhat formal definitions, while necessary, tend to obscure the mental picture and experiment required to understand the practical relevance of such parameters.

In essence, μ_i is the *change in free energy* of a system when 1 mole of *uncharged* species i is added to it (in fact to such a large amount of the system under fixed conditions that no other changes of significant size occur).

In a solution where individual particles do *not* interact with one another (an *ideal* solution), μ_i is given by

$$\mu_i = \mu_i^{\ominus} + RT \ln x_i \tag{2.3}$$

In a (non-ideal) solution where particles interact with one another equation (2.3) must be modified to

$$\mu_i = \mu_i^{\ominus} + RT \ln a_i$$

$$= \mu_i^{\ominus} + RT \ln x_i \gamma_i \qquad \text{(See equation (2.2))}$$

or

$$\mu_i = \mu_i^{\ominus} + RT \ln x_i + RT \ln \gamma_i \tag{2.4}$$

In equation (2.4) the term $RT \ln \gamma_i$ may be seen as a modifying function to correct the ideal equation for the effects of interaction.

If solute species are ions, particularly strong interactions occur because of the electrostatic forces between charges. Equation (2.4) will no longer take account of their energy contribution to the system.

Charges on ions already present in the system will generate an electrical potential, ϕ. Addition of 1 mole of further changes, of magnitude z_i, will induce an *extra* change in free energy of magnitude $z_i F\phi$. Thus, the free energy of the system is increased by both the transfer of matter and by the transfer of charge. The sum of these contributions is known as the *electrochemical* potential $\tilde{\mu}_i$. Thus

$$\tilde{\mu}_i = \mu_i + z_i F\phi \tag{2.5}$$

or, in terms of equation (2.4)

$$\tilde{\mu}_i = \mu_i^{\ominus} + RT \ln a_i + z_i F\phi$$

and

$$\tilde{\mu}_i = \mu_i^{\ominus} + RT \ln x_i + RT \ln \gamma_i + z_i F\phi \tag{2.6}$$

2.2.2 Mean ion activity

Until about 1923, activity coefficients were purely empirical quantities in that when concentrations were modified by their use, correct results could be predicted for the properties of a system. On the basis of the Debye–Hückel theory, to be discussed shortly, activity coefficients become rationalized and theoretically predictable quantities.

For the purposes of deriving relationships in which activity coefficients occur it is very convenient to make use of the idea of individual ion activities and activity coefficients. However, as already stressed, such quantities are incapable of measurement and so are meaningless in a practical sense. One ion species, deriving from dissolved electrolyte, cannot on its own determine properties of a system; it will always do so in concert with an equivalent number of oppositely charged ions. It is therefore only possible to use a form of activity or activity coefficient which takes account of both types of ions characteristic of an electrolyte. Such forms are known as mean ion activities ($a_\pm$) and mean ion activity coefficients ($\gamma_\pm$) and are defined by

$$(a_\pm)^\nu = a_+^{\nu_+} \cdot a_-^{\nu_-} \tag{2.7a}$$

and

$$(\gamma_{\pm})^{\nu} = (\gamma_{+})^{\nu_{+}} \cdot (\gamma_{-})^{\nu_{-}} \tag{2.7b}$$

where $\nu = \nu_{+} + \nu_{-}$, the latter being the number of cations and anions respectively deriving from each formula unit of the electrolyte.

2.3 The Debye–Hückel equation

Equation (2.6) in many ways sets the scene for this present treatment of electrochemistry. Three things should be emphasized about it:

1. Its origin is in thermodynamics, with its starting point the Gibbs definition of chemical potential.
2. The third term, $RT \ln \gamma_i$, is the one of immediate interest and provides the starting point for attempting to predict values of γ_i from know physical parameters.
3. The fourth term, $z_i F\phi$, will feature prominently in later chapters and is the foundation for interpreting interfacial behaviour and electrode potentials.

2.3.1 A theoretical model for calculating activity coefficients

In this section the outline thinking of Debye and Hückel is given: detailed derivations of important relationships required are given in Appendix I.

A potential ϕ exists in the vicinity of an ion by virtue of the charge which it carries: this may be resolved into *two* parts. One contribution is due to the ion itself, the other due to its atmosphere of appropriately signed net charge.

Thus

$$\phi = \phi_0 + \phi_i \tag{2.8}$$

where ϕ_0 has been used to represent the contribution of the ion itself and ϕ_i that due to its atmosphere.

It is clear that the term $RT \ln \gamma_i$ has the units of energy per mole: the crucial step in the derivation of Debye and Hückel is the identification of $RT \ln \gamma_i$ with the contribution that the *ion atmosphere* makes to the total (molar) energy of ion species i. In the case of an individual ion, the contribution is $kT \ln \gamma_i$ and this may be equated to the work which must be performed to give an ion its charge, $z_i\epsilon$, ϵ being the electronic charge.

The work done, dw, in charging an ion by an increment of charge, dϵ, is given by

$$dw = \phi \, d\epsilon \tag{2.9}$$

Therefore

$$dw = \phi_0 d\epsilon + \phi_i d\epsilon$$

Thus $kT \ln \gamma_i$ may be equated to that part of the work, w_i, providing the ion with its charge, which is associated with ϕ_i, i.e. to

$$w_i = \int_0^{z_i\epsilon} \phi_i \, d\epsilon \tag{2.10}$$

The laws of electrostatics (Appendix I) may be used to rationalize the terms in equation (2.8) as follows

$$\phi = \pm \left(\frac{z_i \epsilon}{4\pi\varepsilon_0 \varepsilon} \right) \frac{1}{a} \mp \left(\frac{z_i \epsilon}{4\pi\varepsilon_0 \varepsilon} \right) \left(\frac{\kappa}{1 + \kappa a} \right) \tag{2.11}$$

where ε_0 is the permittivity of a vacuum and ε is the relative permittivity (dielectric constant) of the solvent. The two terms of equation (2.11) have the general form of the potential at the *surface of a charged sphere*: the signs for the two contributions are seen to be consistent with the opposite charges associated with ion and atmosphere. The term a represents the distance of closest approach of an ion and another from the atmosphere, both regarded as spheres (Figure 2.1).

The expression

$$\frac{\kappa}{1 + \kappa a}$$

in the second term on the right-hand side of equation (2.11) corresponds to $1/a$ in the first term. Thus the expression $(1 + \kappa a)/\kappa$ is an effective radius—that of the ion atmosphere. Thus, the effect of the atmosphere on the potential of a given ion is equivalent to the effect of the same charge distributed over a sphere of radius $(1 + \kappa a)/\kappa$ or $(1/\kappa + a)$. In fact, it is the quantity $1/\kappa$ which is usually defined as the thickness of the ion atmosphere or Debye length. This is reasonable in dilute solution where $1/\kappa \gg a$ but becomes unrealistic in more concentrated solutions to the extent that a calculated value of $1/\kappa$ may become less than a, implying that the edge of the atmosphere resides at a distance less than the distance of closest approach. It is seen that κa is the ratio of the ion diameter to the atmosphere radius.

Combining equations (2.10) and (2.11) gives w_i as

$$w_i = -\int_0^{z_i\epsilon} \left(\frac{z_i \epsilon}{4\pi\varepsilon_0 \varepsilon} \right) \left(\frac{\kappa}{1 + \kappa a} \right) d\epsilon$$

(assuming i to be a positive ion), therefore

$$w_i = -\frac{z_i^2 \epsilon^2 \kappa}{8\pi\varepsilon_0 \varepsilon (1 + \kappa a)}$$

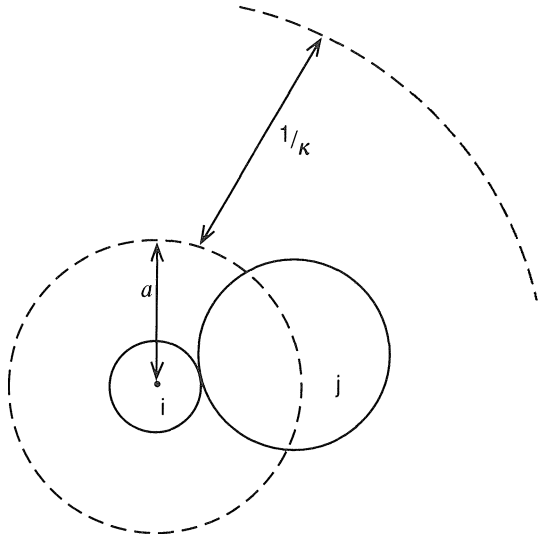

Figure 2.1 The distance of closest approach, a, for ion i and atmosphere ion j, and the Debye length, $1/\kappa$. Radius of ion atmosphere $= 1/\kappa + a \sim 1/\kappa$ when $1/\kappa \ll a$ as is the case for dilute solutions.

so that

$$kT \ln \gamma_i = -\left(\frac{z_i^2 \epsilon^2}{8\pi\varepsilon_0\varepsilon}\right)\left(\frac{\kappa a}{1+\kappa a}\right)$$

or, in terms of the mean ion activity coefficient of the electrolyte

$$\ln \gamma_{\pm} = -\frac{\epsilon^2}{8\pi\varepsilon_0\varepsilon kT} |z_+ z_-| \left(\frac{\kappa}{1+\kappa a}\right) \tag{2.12}$$

It is shown in Appendix II that κ may be expressed in the form

$$\kappa = \left(\frac{2 \times 10^3 \epsilon^2 N}{\varepsilon_0 \varepsilon kT}\right)^{\frac{1}{2}} \sqrt{I} \tag{2.13}$$

where N is the Avogadro constant and I is the ionic strength of the solution given by

$$I = \tfrac{1}{2}\sum m_i z_i^2 \tag{2.14}$$

m_i being the concentration of the electrolyte in the units mol kg^{-1}.

Substitution of equation (2.13) into equation (2.12), after conversion to logarithms to base 10 gives

$$\log \gamma_{\pm} = -\frac{\epsilon^2 N}{2 \cdot 3(8\pi\varepsilon_0\varepsilon RT)} |z_+ z_-| \frac{\left(\frac{2 \times 10^3 \epsilon^2 N^2}{\varepsilon_0 \varepsilon RT}\right)^{\frac{1}{2}} \sqrt{I}}{1 + \left(\frac{2 \times 10^3 \epsilon^2 N^2}{\varepsilon_0 \varepsilon RT}\right)^{\frac{1}{2}} a\sqrt{I}}$$

(Note that $k = R/N$.) Or, more simply, in a form which collects constants,

$$-\log \gamma_{\pm} = \frac{|z_+ z_-| A\sqrt{I}}{1 + Ba\sqrt{I}} \tag{2.15}$$

This is the Debye–Hückel equation in which A and B are constant for a particular solvent at a given temperature and pressure and which are given explicity by

$$A = \frac{\epsilon^2 N}{2 \cdot 3RT(8\pi\varepsilon_0\varepsilon)} \left(\frac{2 \times 10^3 N^2 \epsilon^2}{\varepsilon_0 \varepsilon RT}\right)^{\frac{1}{2}}$$

$$B = \left(\frac{2 \times 10^3 N^2 \epsilon^2}{\varepsilon_0 \varepsilon RT}\right)^{\frac{1}{2}}$$

The above constants may be calculated for water at 298 K by substitution of the data.

$$\epsilon = 1.6021 \times 10^{-19}\,\text{As};\ \text{N} = 6.023 \times 10^{23}\,\text{mol}^{-1}$$

$$\varepsilon_0 = 8.8542 \times 10^{-12}\,\text{kg}^{-1}\,\text{m}^{-3}\,\text{s}^4\,\text{A}^2;\ \varepsilon = 78.54$$

$$R = 8.314\,\text{J K}^{-1}\,\text{mol}^{-1};\ T = 298\,\text{K}$$

Thus

$$A = 0.509\,\text{mol}^{-\frac{1}{2}}\,\text{kg}^{\frac{1}{2}}$$

$$B = 3.290 \times 10^9\,\text{m}^{-1}\,\text{mol}^{-\frac{1}{2}}\,\text{kg}^{\frac{1}{2}}$$

In view of the fact that the product Ba in equation (2.15) is frequently of the order of unity, it is common practice for activity coefficients to be calculated via the simplified form

$$-\log \gamma_{\pm} \sim \frac{|z_+ z_-| A\sqrt{I}}{1 + \sqrt{I}} \tag{2.16}$$

2.3.2 Limiting and extended forms of the Debye–Hückel equation

For very dilute solutions the denominator of equation (2.15) is very little different from unity. Under such conditions the 'Limiting Law' expression holds, viz.

$$-\log \gamma_{\pm} = |z_+ z_-| A\sqrt{I} \tag{2.17}$$

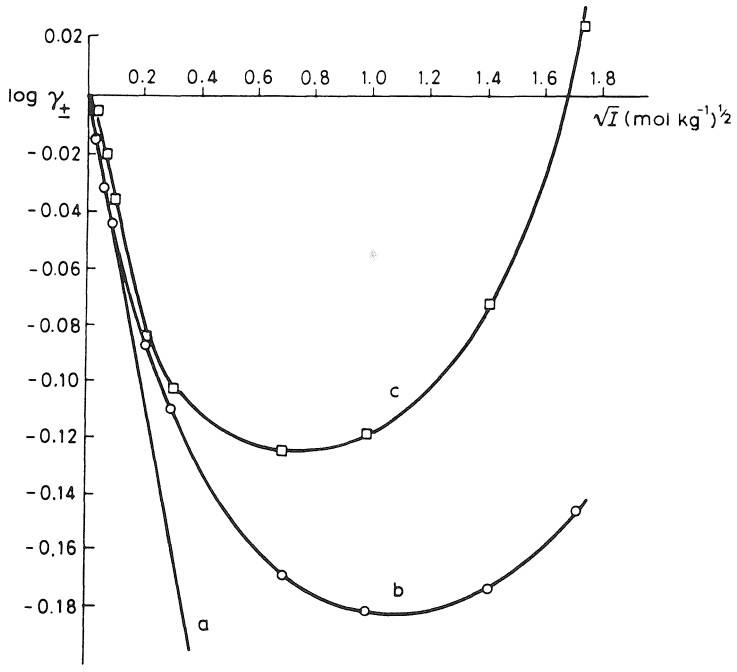

Figure 2.2 Variation of mean ion activity coefficients with ionic strength ($\log \gamma_{\pm}$ versus $\sqrt{I}$). (a) Limiting law line for a 1:1 electrolyte, (b) experimental graph for NaCl, (c) experimental graph for KOH.

An experimental test of the Debye–Hückel model as represented by equation (2.15) may be undertaken by rearranging this expression to the form

$$-\frac{A\,|\,z_+z_-\,|\,\sqrt{I}}{\log \gamma_{\pm}} = 1 + Ba\sqrt{I} \tag{2.18}$$

The left-hand side of equation (2.18) may be determined experimentally under conditions where the limiting law holds. Then, if B for the solvent is known, the left-hand side of the equation may be plotted as a function of $\sqrt{I}$ to give a value of the distance of closest approach, a, from the slope of the graph. Here a drawback is encountered since very often the values obtained for a are physically meaningless in that they are far too small or even negative. Nevertheless, with the assumption of a reasonable magnitude for a (~ 0.4 nm) equation (2.15) does hold for many electrolytes up to $I \sim 0.1\,\text{mol kg}^{-1}$.

In practice activity coefficients initially decrease with increasing concentration of electrolyte (Figure 2.2). Such behaviour is entirely consistent with both the Debye–Hückel equation and its limiting form. However, in

(*a*) [+ −]
(*b*) [+ − +]$^+$, [− + −]$^-$
(*c*) [+ − + −], [− + − +]

Figure 2.3 Possible associations in a 1:1 electrolyte. (a) ion pairs, zero net charge; (b) triple ions, unit charge; (c) quadruple ions, zero net charge.

practice, activity coefficients show a turning point at some value of I, after which they progressively increase. It is thus seen to be necessary to modify equation (2.15) by the addition of a further term which is an increasing function of I, i.e.

$$\log \gamma_{\pm} = -\frac{A\,|z_+z_-|\sqrt{I}}{1 + Ba\sqrt{I}} + bI \tag{2.19}$$

This last relationship has become known as the Hückel equation.

2.4 Ion association

Mean ion activity coefficients cannot always be realistically predicted from the Debye–Hückel equation: this suggests that the model used to describe the distribution of ions about other ions does not apply. This idea is supported by the observation that for many cases experimental values of conductances are lower than those predicted by the Onsager equation (see Chapter 4).

2.4.1 Ionization, dissociation and association

Strong electrolytes are fully *ionized*: this applies to the solid, solution and fused states. Dilution of a solution of a strong electrolyte does not change the state of ionization unlike the case for a weak electrolyte where undissociated molecular species are in equilibrium with ions

$$BA \rightleftharpoons B^+ + A^-$$

Here the proportion of ions to undissociated species increases with dilution.

In the solid state, strong electrolytes are fully *associated* within a rigidly geometrical distribution of discrete ions.

It was suggested by Bjerrum that, under certain conditions, a *degree of association* of oppositely charged ions in solution is feasible. High electrolyte concentration, strong interionic forces (favoured by solvents of *low* dielectric constant since coulombic forces are inversely proportional to ε), small ions and high charges are the factors which should encourage such behaviour.

There is experimental evidence for the formation of ion pairs, triple ions and even quadruple ions (Figure 2.3).

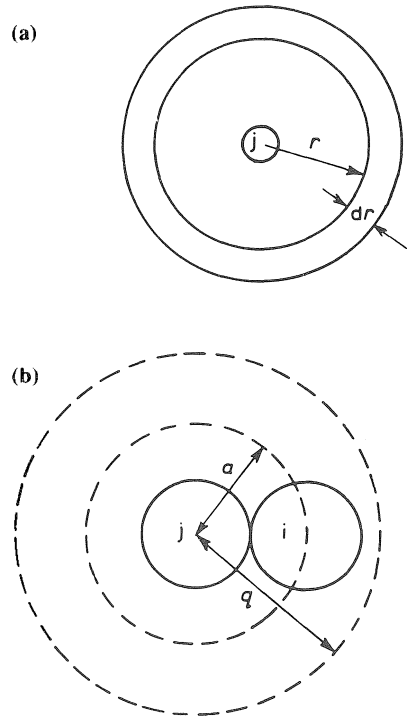

Figure 2.4 (a) Model for determination of distribution of i ions within shells of specified dimensions about j ions (b) Relation of a to q for ion pairing.

Such evidence is provided by rationalization of the discrepancies relating to such parameters as conductivity referred to above and by experimental measurement of association constants for processes such as

$$B^+ + A^- \rightleftharpoons [B^+A^-]$$

2.4.2 The Bjerrum equation

Association leads to a smaller number of particles in a system and associated species have a lower charge than non-associated ones. This will obviously serve to diminish the magnitudes of properties of a solution which are dependent on the number of solute particles and the charges carried by them.

Bjerrum's basic assumption was that the Debye–Hückel theory holds so long as the oppositely charged ions of an electrolyte are separated by a distance q greater than a certain minimum value given by

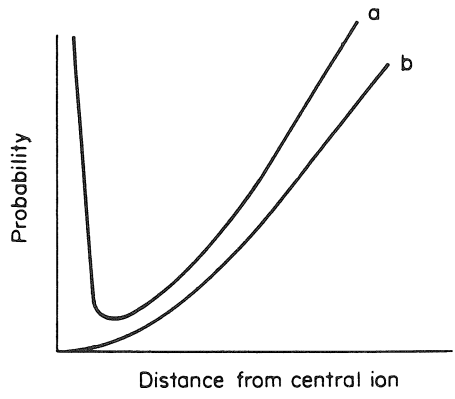

Figure 2.5 Shapes of probability curves for distribution of (a) i ions about j ions; (b) j ions about j ions.

$$q = \frac{z_i z_j \epsilon^2}{8\pi\varepsilon_0 \varepsilon kT} \tag{2.20}$$

When the ion separation is less than q, ion pairing is regarded as taking place. Equation (2.20) may be derived from consideration of the Boltzmann distribution of i-type ions in a thin shell of thickness dr at a distance r from a central j-type ion (Figure 2.4)

The number of i-type ions in such a shell is given by

$$dN_i = N_i \exp\left[\pm\frac{z_i \epsilon \phi_j}{kT}\right] 4\pi r^2 \, dr \tag{2.21}$$

The potential at a small distance from the central j-ion may be assumed to arise almost entirely from that ion and is given by equation (2.11) as

$$\phi_j = \pm\frac{z_j \epsilon}{4\pi\varepsilon_0 \varepsilon r} \tag{2.22}$$

Thus,

$$dN_i = 4\pi N_i \exp\left(-\frac{z_i z_j \epsilon^2}{4\pi\varepsilon_0 \varepsilon kTr}\right) r^2 \, dr \tag{2.23}$$

We expect to find decreasing probability of finding i-type ions per unit volume at increasing values of r. However, the volumes of the concentric shells increase outwards from a j-ion so that, in fact, the probability passes through a minimum at some critical distance. A plot of calculated probability versus r shows such a minimum (Figure 2.5).

It may be seen from the minimum condition, $dN_i/dr = 0$, that this distance is given by equation (2.20).

For a 1:1 electrolyte in aqueous solution at 298 K, q has the value 0.357 nm. Should the sum of the respective ionic radii be less than this figure then ion-pair formation will be favoured.

It is evident that for a given electrolyte at constant temperature, lowering of dielectric constant will encourage association. For tetraisoamylammonium nitrate the sum of ion radii is of the order of 0.7 nm. This gives a value of about 42 for ε by substitution into equation (2.20) and implies that, for solvents of greater dielectric constant than 42, there should be no association but rather complete dissociation, i.e. the Debye–Hückel theory should hold good. Conductance measurements have verified that, in fact, virtually all ion pairing has ceased for $\varepsilon > 42$.

Problems

2.1 Estimate the radius of the ion atmosphere surrounding a given ion at 298 K in an aqueous solution of (i) a 1:1 electrolyte, (ii) a 1:2 electrolyte for the concentrations 0.1, 0.01, 0.001 and 0.0001 mol kg^{-1}. Note the dependence of the value of the atmosphere radius upon ionic strength and also upon the relative permittivity (dielectric constant) of a medium by comparing values of $1/\kappa$ for water (ε = 78.54) and for *N*,*N*-dimethylformamide (ε = 36.70).

2.2 Calculate the ionic strength of an aqueous solution of magnesium chloride of concentration 0.0015 mol kg^{-1} at 298 K. In terms of the Debye–Hückel limiting law, calculate (i) the activity coefficients of the Mg^{2+} and Cl^- ions in the solution, (ii) the mean ion activity coefficient of the ions, $\gamma_\pm$.

2.3 Calculate the ionic strength of (i) a solution of lanthanum nitrate, $La(NO_3)_3$ at 298 K at a concentration of 0.001 mol kg^{-1}, (ii) a solution containing lanthanum nitrate and sodium chloride at concentrations of 0.001 and 0.002 mol kg^{-1}, respectively.

2.4 Determine the mean activity coefficient of $La(NO_3)_3$ in the environments of the previous question (i) from the Debye–Hückel Limiting Law, (ii) from the extended form of the law.

2.5 Estimate the values of the Debye–Hückel constants A and B for water as solvent at 298 K.

2.6 The following values of mean ion activity coefficients are reported (R. H. Stokes and R. A. Robinson (1955) *Electrolyte Solutions*, Butterworths, London, p. 234) for sodium chloride in water at 298 K for the range of molalities shown.

m mol kg^{-1}	0.001	0.002	0.005	0.01	0.02	0.05	0.10
$\gamma_\pm$	0.9649	0.9519	0.9273	0.0922	0.8706	0.8192	0.7784

By a suitable graphical procedure, calculate the distance of closest approach of the ions.

2.7 Calculate the Bjerrum critical distance for ion pairing in water at 298 K for 1:1, 2:2 and 3:3 electrolytes.

3 Ionic equilibria: the behaviour of acids and bases

3.1 Classical theory. The Arrhenius dissociation model

Arrhenius put forward the idea of incomplete dissociation of weak electrolytes on the basis of observed anomalies in the values of colligative properties for electrolytes. Thus, the depression of freezing point of water containing a non-electrolyte is less than that with the same molar proportion of a weak electrolyte. Except at very high dilutions, however, the depression does not approach that to be expected for the total number of ions to which the complete dissociation of the electrolyte gives rise. The classical dissociation theory, concerned essentially with aqueous solutions, rests on the concept of incomplete dissociation of weak electrolytes which increases with dilution. The Arrhenius theory considers the parent electrolyte and ions produced from it as behaving in their own right, any chemical interaction with solvent molecules being ignored, the solvent being simply regarded as a medium within which dissociation and dispersal of ions may occur.

The Arrhenius theory similarly attempts to define acids and bases as isolated species in solution giving rise, respectively, to hydrogen ions and hydroxyl ions. While this view accounts for some properties of acids and bases and their reactions, it cannot begin to explain acidic and basic characteristics in non-aqueous media. Acidic and basic properties are, in fact, *consequent upon* interaction with the solvent and until such interaction has taken place the properties are not shown.

Despite the shortcomings of the classical theory, the relations derived from its use do allow the calculation of reliable equilibrium data for weak electrolytes, including acids and bases, in aqueous solution.

Consider a solution of a binary electrolyte, MX, at a concentration C mol dm^{-3}. If only a fraction α, of MX ionizes, there will result an equilibrium mixture of $C(1 - \alpha)$ mol dm^{-3} of MX in company with $C\alpha$ of both M^+ and X^- ions. The equilibrium for the dissociation process

$$MX \rightleftharpoons M^+ + X^-$$

is then given by

$$K' \sim \frac{[M^+][X^-]}{[MX]} = \frac{\alpha^2 C}{(1 - \alpha)} \tag{3.1}$$

The approximation sign accounts for the use of concentrations in place of activities. Equation (3.1) has become known as the Ostwald Dilution Law and, for a very weak electrolyte where $\alpha \ll 1$, takes the form $K' \sim \alpha^2 C$.

3.2 The Brønsted–Lowry concept of acids and bases

In studies of catalysis of solution reactions by acids and bases, Brønsted observed that catalytic activity was shown by species which at the time were not regarded as acids or bases. An extension of the classical view of acids and bases became desirable and a general definition of such substances to include both aqueous and non-aqueous media was necessary.

Earlier definitions of acids and bases as species producing, respectively, hydrogen ions and hydroxyl ions are only valid in aqueous solution. The concept of Brønsted and Lowry, while extending the classical definition, does not exclude the treatment of Arrhenius for aqueous media. The extended view regards acids as proton donors and bases as proton acceptors regardless of whether substances concerned are ionic or neutral. A terse summary of this definition may be given as follows

$$\text{acid} \rightleftharpoons \text{base} + \text{proton} \tag{3.2}$$

As examples, the following equilibria may be cited

$$\begin{aligned} H_2SO_4 &\rightleftharpoons HSO_4^- + H^+ \\ HSO_4^- &\rightleftharpoons SO_4^{2-} + H^+ \\ H_3O^+ &\rightleftharpoons H_2O + H^+ \\ H_2O &\rightleftharpoons OH^- + H^+ \\ OH^- &\rightleftharpoons O^{2-} + H^+ \end{aligned} \tag{3.3}$$

The species on the right-hand side of equation (3.3), along with the protons, are in each case what are known as the conjugate bases of the various acids. In a similar way we may define conjugate acids of appropriate bases. It is apparent that some species, known as ampholytes, are capable of behaving as both acids and bases. In this respect the nature of water when acting as a solvent is of particular significance, as it means that all acidic and basic properties in aqueous solution will set up equilibria involving the solvent.

3.2.1 The importance of solvent in generating acid–base properties

Owing to the fact that unsolvated protons cannot exist in solution, equations (3.3) are meaningless as written. They may, however, prove useful when considering coupled acid–base systems provided that it is borne in mind that H^+ refers to the solvated proton. Thus, the reaction of sulphuric acid and ammonia may be considered as

$$H_2SO_4 \rightleftharpoons HSO_4^- + H^+$$

$$\frac{NH_3 + H^+ \rightleftharpoons NH_4^+}{H_2SO_4 + NH_3 \rightleftharpoons HSO_4^- + NH_4^+} \tag{3.4}$$

Or, in general,

$$\text{acid}_1 + \text{base}_2 \rightleftharpoons \text{base}_1 + \text{acid}_2 \tag{3.5}$$

where base_1 is the conjugate base of the original acid_1 and acid_2 is the conjugate acid of the original base_2.

3.2.2 Relative strengths of conjugate pairs

The position of equilibrium in systems represented by equation (3.5) is determined by the relative strengths of the two acids and bases. If acid_1 is stronger than acid_2 or, which comes to the same thing, if base_2 is stronger than base_1, the equilibrium is displaced to the right. To such reversible systems the Law of Mass Action may be applied to give for the equilibrium constant

$$K \sim \frac{[\text{base}_1][\text{acid}_2]}{[\text{acid}_1][\text{base}_2]} \tag{3.6}$$

where K is dependent only upon temperature and the nature of the solvent. Equation (3.6) may be used for dilute solutions where the effects of ion interaction are minimized.

Relationships so far used show no involvement of solvent and obscure the fact that acidic and basic properties are *consequent upon* interaction of species with solvent.

3.2.3 Types of solvent and general acid–base theory

Equation (3.5) may be applied quite generally to all dissociation processes, e.g. to acid dissociations such as

$$HNO_3 + H_2O \rightleftharpoons NO_3^- + H_3O^+ \tag{3.7}$$

and to self-ionization (or autoprotolytic) reactions such as

$$\begin{gathered} H_2O + H_2O \rightleftharpoons H_3O^+ + OH^- \\ NH_3 + NH_3 \rightleftharpoons NH_4^+ + NH_2^- \\ C_2H_5OH + C_2H_5OH \rightleftharpoons C_2H_5O^- + C_2H_5OH_2^+ \\ H_2SO_4 + H_2SO_4 \rightleftharpoons HSO_4^- + H_3SO_4^+ \end{gathered} \tag{3.8}$$

The last processes are important for almost all solvents.

There are four types of solvent which may be distinguished in terms of acid–base theory:

1. Acidic or protogenic solvents. These provide protons, common examples being sulphuric and ethanoic acids.
2. Basic or protophilic solvents. These have the ability to bind protons, liquid ammonia being typical.
3. Amphoteric or amphiprotic solvents such as water and ethanol which behave as either acids or bases.
4. Aprotic solvents. Such solvents show no self-ionization. Most, like benzene, do not take part in protolytic reactions although some, such as dimethylformamide and dimethylsulphoxide show basic properties.

The term lyonium ion is often given to the ion species resulting from proton solvation (e.g. H_3O^+, NH_4^+) while the solvent residue (less the proton) is called the lyate ion (e.g. $C_2H_5O^-, NH_2^-$).

The proton affinities of the solvent and its lyate ion decide the acid–base characteristics of a particular solute in that solvent. Thus, if a solute has a greater proton affinity than that of the lyate ion deriving from the solvent, it will behave as a base in that solvent. On the other hand, if the conjugate base to a solute has a smaller proton affinity than the solvent itself, the solute behaves as an acid.

For example, the conjugate base of benzoic acid, $C_6H_5COO^-$, has less affinity for protons than water so that the reaction

$$C_6H_5COOH + H_2O \rightleftharpoons C_6H_5COO^- + H_3O^+ \tag{3.9}$$

occurs in aqueous solution which is in accord with experience, benzoic acid behaving as a weak acid in aqueous solution. This, however, is not the case in concentrated sulphuric acid. Here benzoic acid has a greater proton affinity than the lyate ion from sulphuric acid, HSO_4^-, so that the reaction

$$C_6H_5COOH + H_2SO_4 \rightleftharpoons C_6H_5COOH_2^+ + HSO_4^- \tag{3.10}$$

occurs in this medium, i.e. benzoic acid is now behaving as a base. Aniline in liquid ammonia behaves as a weak acid because the solvent has a rather greater affinity for protons that does the species $C_6H_5NH^-$

$$C_6H_5NH_2 + NH_3 \rightleftharpoons C_6H_5NH^- + NH_4^+ \tag{3.11}$$

On the other hand, in glacial ethanoic acid, aniline has a much greater proton affinity than does the lyate ion CH_3OO^- and so behaves as a strong base

$$C_6H_5NH_2 + CH_3COOH \rightleftharpoons C_6H_5NH_3^+ + CH_3COO^- \tag{3.12}$$

3.3 Strengths of acids and bases in aqueous solution

Somewhat vague reference was made above to the relative strengths of acids and bases. It is necessary to give quantitative significance to such terms.

The strengths of acids for a particular solvent are measured and expressed with respect to a chosen standard for that solvent: for water, the standard is the acid–base pair H_3O^+/H_2O. The strength of some other acid, HA, may then be defined with respect to the reaction

$$HA + H_2O \rightleftharpoons A^- + H_3O^+ \tag{3.13}$$

For example

$$CH_3COOH + H_2O \rightleftharpoons CH_3COO^- + H_3O^+ \tag{3.14}$$

A^- is the conjugate base of HA, while the ethanoate ion, CH_3COO^-, is the conjugate base of ethanoic acid, CH_3COOH.

3.3.1 Dissociation constants of acids and the self-ionization constant of water

The equilibrium constant for reaction (3.13) gives a measure of the strength of HA in that it defines the extent to which the reaction proceeds to the left or right, i.e.

$$K = \frac{[A^-][H_3O^+]}{[HA][H_2O]}$$

or

$$K_a = \frac{[A^-][H_3O^+]}{[HA]} \tag{3.15}$$

where K_a is the dissociation constant of HA; $K_a = K[H_2O]$, the term $[H_2O]$ being omitted from the denominator and absorbed into the constant, K_a, since it is very large and approximately constant for dilute solution. If HA is the water molecule itself then the equilibrium constant refers to the self-ionization of water, viz.

$$H_2O + H_2O \rightleftharpoons H_3O^+ + OH^- \tag{3.16}$$

for which

$$K = \frac{[H_3O^+][OH^-]}{[H_2O]^2}$$

It is usual in this case to absorb $[H_2O]^2$ into the constant K to give

$$K_w = [H_3O^+][OH^-] \tag{3.17}$$

where K_w is known as the ionic product of water which has the value 10^{-14} at 298 K.

3.3.2 Dissociation constants of bases

The strength of a base, B, is defined in terms of the hydroxyl ions produced in water, i.e. by the reaction

$$B + H_2O \rightleftharpoons BH^+ + OH^- \tag{3.18}$$

For example

$$NH_3 + H_2O \rightleftharpoons NH_4^+ + OH^- \tag{3.19}$$

BH^+ is the conjugate acid of B, while the ammonuim ion is the conjugate base of NH_3. The dissociation constant, K_b of the base B may now be expressed as

$$K_b = \frac{[BH^+][OH^-]}{[B]} \tag{3.20}$$

Equation (3.15) and equation (3.20) will now be developed a little further in the examples provided by ethanoic acid and ammonia. For ethanoic acid equation (3.15) becomes

$$K_a = \frac{[CH_3COO^-][H_3O^+]}{[CH_3COOH]} \tag{3.21}$$

If both sides of equation (3.21) are multiplied by K_w, it may be rewritten as

$$K_a = \frac{[CH_3COO^-][H_3O^+]}{[CH_3COOH]} \cdot \frac{K_w}{[H_3O^+][OH^-]}$$

Therefore

$$K_a = \frac{[CH_3COO^-]}{[CH_3COOH][OH^-]} \cdot K_w \tag{3.22}$$

Now

$$\frac{[CH_3COO^-]}{[CH_3COOH][OH^-]} = \frac{1}{K_b'} = \frac{1}{K_h} \tag{3.23}$$

where K_b' is the dissociation constant of the *conjugate base* of CH_3COOH, that is the ethanoate ion. K_b' takes its form from the reaction.

$$CH_3COO^- + H_2O \rightleftharpoons CH_3COOH + OH^- \tag{3.24}$$

K_b' is alternatively expressed as K_h, the *hydrolysis constant.* In a similar way equation (3.20) may be considered as applied to ammonia for which it becomes

$$K_b = \frac{[NH_4^+][OH^-]}{[NH_3]} \tag{3.25}$$

and

$$K_b = \frac{[NH_4^+][OH^-]}{[NH_3]} \cdot \frac{K_w}{[H_3O^+][OH^-]}$$

Therefore

$$K_b = \frac{[NH_4^+]}{[NH_3][H_3O^+]} \cdot K_w \tag{3.26}$$

Now

$$\frac{[NH_4^+]}{[NH_3][H_3O^+]} = \frac{1}{K_a'} = \frac{1}{K_h} \tag{3.27}$$

where K_a' is the dissociation constant of the *conjugate acid* of NH_3, that is the ammonium cation, K_a' taking its form from the reaction

$$NH_4^+ + H_2O \rightleftharpoons NH_3 + H_3O^+ \tag{3.28}$$

Again, an alternative designation of K_a' is K_h.

Thus for both of the above cases

$$K_a = \frac{K_w}{K_b'} \text{ or } K_b = \frac{K_w}{K_a'} \tag{3.29}$$

i.e. the dissociation constant of an acid or base is given by K_w divided by the dissociation constant of the corresponding conjugate base or acid.

It should be clear that the foregoing only relates to weak acids and bases. Dissociation constants have no meaning for the cases of completely ionized strong acids and bases.

3.3.3 Zwitterions

Amino acids carry both amino and carboxyl groups and belong to a class of species known as 'zwitterions' carrying both positively and negatively charged centres. Glycine, the simplest with the basic formula NH_2CH_2CO OH, exists in aqueous solution as the zwitterion $^+H_3NCH_2COO^-$. Such species clearly combine the acidic and basic properties described above.

In the presence of base, glycine ($G^\pm$) will form a salt of the anion $H_2NCH_2COO^-$, (G^-), while with an acid it produces a salt of the cation $^+H_3NCH_2COOH$, (G^+). It is apparent that the acid–base properties of glycine will be characterized by two acid dissociation constants which may be defined in terms of the equilibria.

$$\underset{(G^+,\text{ acid solution})}{^+H_3NCH_2COOH} \rightleftharpoons \underset{(G^\pm,\text{ neutral solution})}{^+H_3NCH_2COO^-} + H^+ \rightleftharpoons \underset{(G^-,\text{ basic solution})}{H_2NCH_2COO^-} + 2H^+$$

$$K_{a1} \cong \frac{[H^+][G^\pm]}{[G^+]}\,;\; K_{a2} \cong \frac{[H^+][G^-]}{[G^\pm]} \tag{3.30}$$

3.3.4 The values of dissociation constants

Experimental values of K_a, K_b vary over many orders of magnitude. Rather than deal with such an unwieldy range of values, it is more convenient to express strengths of acids or bases on a logarithmic scale. The logarithmic exponent (pK) of a dissociation constant is defined as

$$pK = -\log_{10} K \tag{3.31}$$

the negative sign indicating that a high pK value is to imply a weaker acid and stronger base while a low value implies a stronger acid and weaker base.

3.4 Extent of acidity and the pH scale

A consideration of the self-ionization of water,

$$2H_2O \rightleftharpoons H_3O^+ + OH^-$$

makes it clear that this solvent is neutral owing to equal concentrations of H_3O^+ and OH^- ions. At 298 K each of these is equal to 10^{-7} mol dm^{-3}. It must be remembered that, since K_w is temperature dependent, so also is the concentration of H_3O^+ and OH^- corresponding to the condition of neutrality. Owing to the vast range of acidity possible, concentrations of H_3O^+ and OH^- are better expressed in logarithmic form in the same way as dissociation constants. Again, negative exponents are considered, thus,

$$pH = -\log a_{H_3O^+} \sim -\log [H_3O^+] \tag{3.32}$$

and

$$pOH = -\log [OH^-]$$

Also

$$\log [H_3O^+] + \log [OH^-] = \log K_w \tag{3.33}$$

or,

$$pH + pOH = pK_w \text{ (at 298 K)} \tag{3.34}$$

so that for most practical purposes the scale may be regarded as extending from 0 to 14.

These simple relationships may be used to calculate the pH values of solutions of acids, bases and various types of salt.

3.4.1 Calculation of pH for solutions of strong acids and bases

It should be clear from equation (3.32) that solutions of hydrochloric acid at concentration 0.1, 0.01 and 0.001 mol dm^{-3} have pH values which are respectively 1, 2 and 3. In a complementary way, application of equation

(3.34) shows that solutions of sodium hydroxide at concentrations 0.1, 0.01 and 0.001 mol dm^{-3} have pH values of 13, 12 and 11, respectively.

Similarly, it is readily calculated that a solution of 0.05 mol dm^{-3} HCl has a pH of 1.30 while that of a 0.003 mol dm^{-3} solution of this strong monobasic acid is 2.52: a solution of 0.005 mol dm^{-3} NaOH may be calculated to have a pOH value of 2.30 and a pH of 11.70. At these concentrations, the contributions of H_3O^+ and OH^- from the solvent are negligible by comparison with their concentrations deriving from dissolved acid or base. However, at concentrations much lower than those considered above, this simple process cannot be continued. It only holds so long as the contributions to $[H_3O^+]$ and $[OH^-]$ by water itself are very small relative to those of added acids or bases. In view of the magnitude of the ionic product of water, as soon as the concentrations of H_3O^+ or OH^- deriving from added acid or base become of the same order as the water equilibrium values of 10^{-7} mol dm^3, the contributions to pH from *both* solvent and solute must be taken account of.

Values of pH calculated for some hydrochloric acid solutions of low concentration are given in Table 3.1.

Table 3.1 Calculation of pH values of solutions of low concentration of strong acid

Concn. of added acid (mol dm^{-3})	Total concn. of H_3O^+ (mol dm^{-3})	pH
10^{-5}	1.01×10^{-5}	4.996
10^{-6}	1.10×10^{-6}	5.95
10^{-7}	2.00×10^{-7}	6.70
10^{-8}	1.10×10^{-7}	6.96

Values for a similar range of solutions of sodium hydroxide are collected in Table 3.2.

Table 3.2 Calculation of pH values of solutions of low concentrations of strong base

Concn. of added base (mol dm^{-3})	Total concn. of OH^- (mol dm^{-3})	pOH	pH
10^{-5}	1.01×10^{-5}	4.996	9.004
10^{-6}	1.10×10^{-6}	5.95	8.05
10^{-7}	2.00×10^{-7}	6.70	7.30
10^{-8}	1.10×10^{-7}	6.96	7.04

3.4.2 Calculation of pH for solutions of weak acids and bases

For the case of a weak acid equation (3.15) contains the quantity $[H_3O^+]$ which is required to calculate pH. This expression may be manipulated as follows

$$K_a = \frac{[A^-][H_3O^+]}{[HA]} \sim \frac{[H_3O^+]^2}{C} \tag{3.35}$$

since $[A^-] = [H_3O^+]$ and $[HA] \sim C$, the analytical concentration of acid if the extent of dissociation is small. Thus

$$[H_3O^+] = K_a^{\frac{1}{2}} C^{\frac{1}{2}}$$

So that in terms of $pH = -\log_{10}[H_3O^+]$

$$pH = -\tfrac{1}{2}\log K_a - \tfrac{1}{2}\log C$$

which, in terms of equation (3.31) becomes

$$pH = \tfrac{1}{2}(pK_a - \log C) \tag{3.36}$$

Similarly, for the case of a weak base equation (3.20) contains the quantity $[OH^-]$ which provides a value of pOH. This expression may be approximated as follows

$$K_b = \frac{[BH^+][OH^-]}{[B]} \sim \frac{[OH^-]^2}{C} \tag{3.37}$$

C now being the concentration of base.
Thus

$$[OH^-] = K_b^{\frac{1}{2}} C^{\frac{1}{2}}$$

So that in terms of $pOH = -\log_{10}[OH^-]$

$$\begin{aligned} pOH &= -\tfrac{1}{2}\log K_b - \tfrac{1}{2}\log C \\ &= \tfrac{1}{2}(pK_b - \log C) \end{aligned}$$

Therefore the pH of the solution is given in terms of equation (3.34) by

$$pH = pK_w - \tfrac{1}{2}(pK_b - \log C) \tag{3.38}$$

Equation (3.36) and equation (3.38) provide a rapid route to calculation of pH when the values of dissociation constants are known.

3.5 Hydrolysis. Salt solutions showing acid–base properties

Reactions such as

$$CH_3COO^- + H_2O \rightleftharpoons CH_3COOH + OH^- \qquad \text{(see(3.24))}$$

and

$$NH_4^+ + H_2O \rightleftharpoons NH_3 + H_3O^+ \qquad \text{(see (3.28))}$$

are *hydrolysis* reactions for salts of a weak acid and base, respectively.

In the first case it is also necessary to have cations and in the second anions present in solution since individual ion species cannot exist on their own. If these other ions do not show acidic or basic character they play no part in the hydrolysis equilibria. Thus a solution of sodium ethanoate shows a *basic* reaction in aqueous solution, sodium ions showing no hydrolysis while the ethanoate ions undergo reaction (3.24). Similarly a solution of ammonium chloride is *acidic* in aqueous solution: chloride ions are not hydrolysed and the acidity is produced by reaction (3.28).

A salt derived from both a weak acid and a weak base will show hydrolysis reactions for both cation and anion.

3.6 Calculation of the pH of salt solutions

The procedure here is very much like that adopted in the case of solutions of weak acids and bases: the equation representing the reaction of the hydrolysable components with water is manipulated via approximations to give an explicit relationship between hydrogen ion concentration and a dissociation constant.

3.6.1 Salts derived from weak acids and strong bases

For the case of sodium ethanoate, the hydrolysis reaction is (3.24) for which K_h(or K_b') is

$$K_h = \frac{[CH_3COOH][OH^-]}{[CH_3COO^-]} \qquad \text{(see equation (3.23))}$$

Since $[CH_3COOH] = [OH^-]$, it follows that

$$K_h = \frac{[OH^-]^2}{[CH_3COO^-]} \tag{3.39}$$

If the degree of hydrolysis is small, which in practical terms means a K_h value less that 0.01, $[CH_3COO^-]$ is approximately the concentration of sodium ethanoate, C, originally dissolved. Thus,

$$K_h \sim \frac{[OH^-]^2}{C} \tag{3.40}$$

and

$$[OH^-] \sim \sqrt{K_h C}$$

therefore,

$$[H_3O^+] = \frac{K_w}{[OH^-]} \sim \frac{K_w}{\sqrt{K_h C}}$$

and

$$[H_3O^+] = \left(\frac{K_w K_a}{C}\right)^{\frac{1}{2}}$$

Or, taking logarithms

$$pH = \tfrac{1}{2}(pK_w + pK_a + \log C) \tag{3.41}$$

In equation (3.41), pK_a refers to the *parent weak acid*, CH_3COOH.

3.6.2 Salts derived from weak bases and strong acids

For the case of ammonium chloride, whose hydrolysis reaction is (3.28), K_h (or K_a') is given by

$$K_h = \frac{[NH_3][H_3O^+]}{[NH_4^+]} \qquad \text{(see equation (3.27))}$$

Since $[NH_3] = [H_3O^+]$ it follows that

$$K_h = \frac{[H_3O^+]^2}{[NH_4^+]} \tag{3.42}$$

Also, if K_h is small, $[NH_4^+] \sim C$, the concentration of ammonium chloride taken, so that

$$[H_3O^+] \sim \sqrt{K_h C} = \left(\frac{K_w C}{K_b}\right)^{\frac{1}{2}}$$

or, taking logarithms

$$pH = \tfrac{1}{2}(pK_w - pK_b - \log C) \tag{3.43}$$

where pK_b refers to the *parent weak base*, NH_3.

3.6.3 Salts derived from weak acids and weak bases

In the case of the salt ammonuim ethanoate both hydrolysis reactions (3.24) and (3.28) occur and it is readily shown that

$$K_h = \frac{K_w}{K_a K_b} \tag{3.44}$$

Let it be supposed that the concentration of dissolved salt is C and that $[NH_3] \sim [CH_3COOH]$, i.e. the two hydrolysis reactions have proceeded to

the same extent. If K_h is small, $[NH_4^+]$ and $[CH_3COO^-]$ are both approximately C. In terms of these approximations, K_h is given by

$$K_h = \frac{[NH_3][CH_3COOH]}{[NH_4^+][CH_3COO^-]} \sim \frac{[CH_3COOH]^2}{C^2}$$

or,

$$[CH_3COOH] = CK_h^{\frac{1}{2}} = C\left(\frac{K_w}{K_a K_b}\right)^{\frac{1}{2}} \tag{3.45}$$

Now K_a for the parent acid is given by

$$K_a = \frac{[CH_3COO^-][H_3O^+]}{[CH_3COOH]}$$

so that

$$[CH_3COOH] = \frac{C[H_3O^+]}{K_a} \tag{3.46}$$

Combining equations (3.45) and (3.46) provides an explicit relationship between K_a, K_b, K_w and $[H_3O^+]$, viz.

$$[H_3O^+] = \left(\frac{K_a K_w}{K_b}\right)^{\frac{1}{2}} \tag{3.47}$$

or, in terms of pH,

$$pH = \tfrac{1}{2}(pK_w + pK_a - pK_b) \tag{3.48}$$

3.7 Buffer systems

Bufffer systems consist of weak acids or bases dissolved in company with one of their completely ionized salts. The purpose of such systems is to maintain an almost constant pH which is only slightly affected by the addition of acids or bases.

3.7.1 The Henderson–Hasselbalch equation

Consider the system ethanoic acid/sodium ethanoate in which the state of ionization of the various species may be represented as follows:

$$CH_3COOH + H_2O \rightleftharpoons CH_3COO^- + H_3O^+$$
$$CH_3COO^- + Na^+$$

The presence of the fully dissociated ethanoate salt will suppress the protolysis of the acid so that this remains virtually undissociated. This means

that the concentration of free ethanoic acid, $[CH_3COOH]$, in the system is to all intents and purposes the original concentration, $[acid]_0$. Similarly, the concentration of ethanoate ion $[CH_3COO^-]$ is very close to that of the salt, $[salt]_0$.

Thus, the acid dissociation constant may be given in the form

$$K_a \sim \frac{[salt]_0}{[acid]_0} \cdot [H_3O^+]$$

or

$$[H_3O^+] \sim K_a \frac{[acid]_0}{[salt]_0} \tag{3.49}$$

or, taking logarithms,

$$pH = pK_a + \log \frac{[salt]_0}{[acid]_0} \tag{3.50}$$

Equation (3.50) is one form of the Henderson–Hasselbalch equation which states that the pH of a buffer solution is a function of the dissociation constant of the weak acid and the acid: salt ratio.

For a weak base in company with one of its completely ionized salts, the argument is similar. Consider the case of ammonia in the presence of ammonium chloride:

$$NH_3 + H_2O \rightleftharpoons NH_4^+ + OH^-$$
$$NH_4^+ + Cl^-$$

Since the ammonium chloride is almost completely dissociated, $[NH_4^+] \sim [salt]_0$ and $[NH_3] \sim [base]_0$ so that

$$K_b = \frac{[salt]_0}{[base]_0} \cdot [OH^-]$$

therefore,

$$[OH^-] = \frac{[base]_0}{[salt]_0} \cdot K_b \tag{3.51}$$

or

$$pH = pK_w - pK_b - \log \frac{[salt]_0}{[base]_0} \tag{3.52}$$

This is a further form of the Henderson–Hasselbalch equation (3.52) being complementary to equation (3.50).

Addition of small amounts of strong acid or base serve only to interconvert small amounts of the weak acid or base and the salt comprising the buffer so that the concentration ratio remains almost constant. The most effective buffers have this ratio of the order of unity.

Amino acids such as glycine may form acidic and basic buffers. In terms of equation (3.30) it may be readily seen that

$$[H^+]^2 \sim K_{a1}K_{a2}\frac{[G^+]}{[G^-]}$$

or,

$$pH \cong \tfrac{1}{2}pK_{a1} + \tfrac{1}{2}pK_{a2} - \tfrac{1}{2}\log\frac{[G^+]}{[G^-]}$$

A solution of pure glycine thus shows a pH (the isoelectric point) of $\frac{1}{2}(2.34 + 9.78) = 6.06$, the pK_a values used being the accepted ones for 298 K. In the presence of strong acid, only the $G^+/G^{\pm}$ equilibrium is of significance so that

$$pH \cong pK_{a1} + \log\frac{[G^{\pm}]}{[G^+]} \tag{3.53}$$

Correspondingly, in the presence of base, only the $G^{\pm}/G^-$ equilibrium is of significance and

$$pH \cong pK_{a2} + \log\frac{[G^-]}{[G^{\pm}]} \tag{3.54}$$

3.7.2 *Efficiency of buffer systems: buffer capacity*

The efficiency of a buffer system is measured in terms of its 'buffer capacity', β, which, for an acidic buffer may be defined by

$$\beta = \frac{d[B]}{dpH} \tag{3.55}$$

Equation (3.55) gives β as the change of concentration of strong base, d[B], which is required for a given pH change. For a basic buffer, the buffer capacity is given by

$$\beta = -\frac{d[A]}{dpH} \tag{3.56}$$

where d[A] is now the change of concentration of strong acid required to produce the change dpH. Acidic buffer solutions may be prepared by mixing a weak acid, HA and a strong base, BOH, so that the following interaction occurs

$$HA + BOH \rightleftharpoons B^+ + A^- + H_3O^+$$

the pH of the resulting solution being given by

$$pH = pK_a + \log\frac{[A^-]}{[HA]}$$

or

$$\mathrm{pH} = \mathrm{p}K_\mathrm{a} + \log \frac{x}{a - x} \tag{3.57}$$

where $a = [\mathrm{HA}] + [\mathrm{A}^-]$ and $x = [\mathrm{B}^+]$.

β is obtained from this expression by differentiation as

$$\beta = \frac{\mathrm{d}[\mathrm{B}]}{\mathrm{dpH}} = \frac{\mathrm{d}x}{\mathrm{dpH}} = 2.3x\left(1 - \frac{x}{a}\right) \tag{3.58}$$

Basic buffer solutions may be prepared by mixing a weak base and strong acid so that the following interaction occurs

$$\mathrm{BOH} + \mathrm{HA} \rightleftharpoons \mathrm{BH}^+ + \mathrm{A}^- + \mathrm{OH}^-$$

the pH of the resulting solution now being given by

$$\mathrm{pH} = \mathrm{p}K_\mathrm{w} - \mathrm{p}K_\mathrm{b} + \log \frac{[\mathrm{BOH}]}{[\mathrm{BH}^+]}$$

or,

$$\mathrm{pH} = \mathrm{p}K_\mathrm{w} - \mathrm{p}K_\mathrm{b} + \log \frac{(a - x)}{x} \tag{3.59}$$

where $a = [\mathrm{BOH}] + [\mathrm{BH}^+]$ and $x = [\mathrm{BH}^+]$. Here

$$\beta = -\frac{\mathrm{d}x}{\mathrm{dpH}} = 2.3x\left(\frac{x}{a} - 1\right) \tag{3.60}$$

Buffering is only satisfactory when the salt:acid or salt:base ratios lie between 0.1 and 10 so that the effective buffer range of any system, in terms of the dissociation constants of the acid or base involved, is given by

$$\mathrm{pH} = \mathrm{p}K_\mathrm{a} \pm 1$$

and

$$\mathrm{pOH} = \mathrm{p}K_\mathrm{b} \pm 1 \tag{3.61}$$

The variation of buffer capacity with variation of the salt:acid ratio is shown in Figure 3.1.

It is seen from equations (3.58) and (3.60) that for β to be a maximum, $\mathrm{d}\beta/\mathrm{d}x = 0$, i.e. $x_\mathrm{max} = \frac{1}{2}a$, which corresponds to a 1:1 ratio of acid or base to salt. It is clear from equation (3.57) that, under the above conditions, $\mathrm{pH} = \mathrm{p}K_\mathrm{a}$. The variation of β with pH is shown in Figure 3.2.

Calculations of pH from the given forms of the Henderson–Hasselbalch equation are only valid when the buffer ratios may be calculated from the quantities of components used to make the solution. Such procedure is

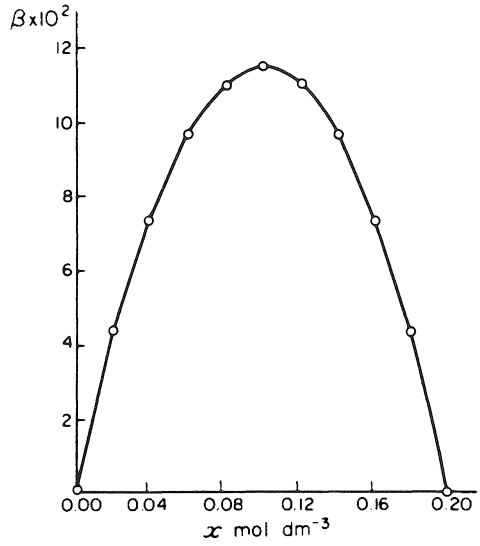

Figure 3.1 Variation of buffer capacity for an acid buffer with the proportion of salt to acid. Points calculated from equation (3.58) using $a = 0.2\,\text{mol dm}^{-3}$; $x = 0\text{–}0.2\,\text{mol dm}^{-3}$.

only justified for the range $4 < \text{pH} < 10$; outside this range, the values of concentrations involved in the buffer ratio will differ considerably from those initially dissolved. Consider firstly the case of a solution with $\text{pH} < 4$ containing a buffer system represented by HA/A^-. It is now no longer true to say that very little acid will ionize; it is of sufficient strength that the amount of free unionized acid is significantly less than that originally dissolved. There is correspondingly more of the anion, A^-, than can be accounted for by the total ionization of the salt, alone. In order to establish the amounts of free acid and anion that will be present in the buffer system, It is necessary to consider the equilibrium

$$\text{HA} + \text{H}_2\text{O} \rightleftharpoons \text{H}_3\text{O}^+ + \text{A}^-$$

from which it is readily seen that

$$[\text{HA}] = [\text{HA}]_0 - [\text{H}_3\text{O}^+]$$

and

$$[\text{A}^-] = [\text{A}^-]_0 + [\text{H}_3\text{O}^+]$$

The Henderson–Hasselbalch equation now takes the form

$$\text{pH} = \text{p}K_\text{a} + \log \frac{[\text{A}^-]_0 + [\text{H}_3\text{O}^+]}{[\text{HA}]_0 - [\text{H}_3\text{O}^+]} \tag{3.62}$$

Similar arguments hold for a buffer system of pH greater than 10, which we

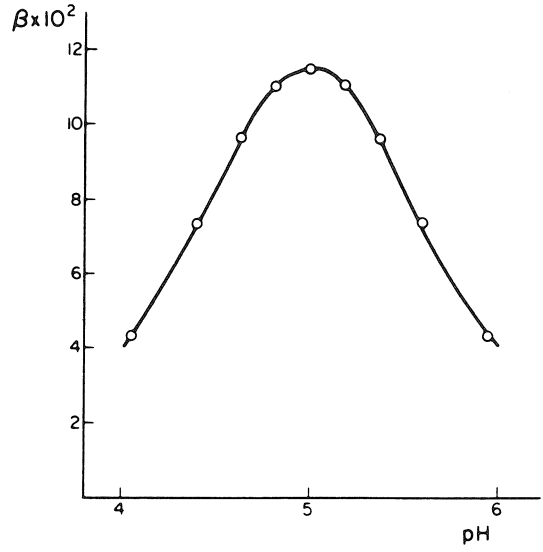

Figure 3.2 Variation of buffer capacity with pH for an acid buffer. Points calculated from equations (3.58) and (3.57) using $pK_a = 5$; $a = 0.2\,\text{mol dm}^{-3}$.

may represent by B/BH^+. It is now necessary to make suitable allowance for the equilibrium

$$B + H_2O \rightleftharpoons BH^+ + OH^-$$

The base now ionizes to a far from negligible extent so the $[B] < [B]_0$ and $[B] = [B]_0 - [OH^-]$. Further, $[BH^+] = [BH^+]_0 + [OH^-]$. Thus,

$$pH = pK_w - pK_b - \log \frac{[BH^+]_0 + [OH^-]}{[B]_0 - [OH^-]} \tag{3.63}$$

3.8 Operation and choice of visual indicators

In an acid–base titration there will only be observed a pH of 7 at the equivalence point if both titrant and titrand are strong electrolytes. If one is weak, the salt formed will undergo hydrolysis and the solution at the equivalence point will be either slightly acid or alkaline.

Acid-base indicators show differing colours with varying hydrogen ion concentration in a solution. The change in colour occurs in general over a 'colour change interval' of some two pH units. It is necessary to select indicators for particular titrations which show clear colours at pH values close to those known to hold at the equivalence point.

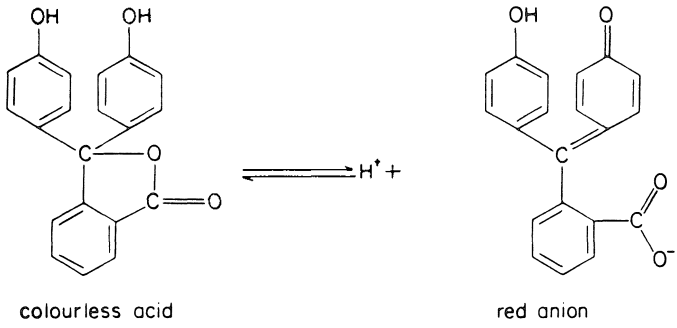

Figure 3.3 The acidic and anionic forms of phenolphthalein.

3.8.1 Functioning of indicators

Indicators are themselves weak organic acids or bases whose undissociated forms differ in colour from the ionic forms due to their considerably different electronic structure and hence absorption spectra.

The dissociation of an acid indicator molecule in water occurs according to

$$\underset{\text{colour 1}}{HIn} + H_2O \rightleftharpoons H_3O^+ + \underset{\text{colour 2}}{In^-} \tag{3.64}$$

In dilute solution the equilibrium constant, K_i, for this reaction is

$$K_i = \frac{[H_3O^+][In^-]}{[HIn]} \tag{3.65}$$

from which

$$[H_3O^+] = K_i \frac{[HIn]}{[In^-]} \tag{3.66}$$

or,

$$pH = pK_i + \log \frac{[In^-]}{[HIn]} \tag{3.67}$$

The titration exponent, pK_i, may be defined as the pH at which the concentrations of basic (In^-) and acidic (HIn) forms of the indicator are equal.

Phenolphthalein is an acid indicator of this type with acidic and basic species given in Figure 3.3.

Equation (3.66) may alternatively be expressed in terms of the fraction, x, of indicator in the alkaline form

$$[H_3O^+] = K_i \frac{1-x}{x} \tag{3.68}$$

The latter is sometimes known as the indicator equation: it is quite general in its application to both indicator acids and bases.

3.8.2 Titrimetric practice

It is found in practice that an observer can normally detect no change from a full acid or full alkaline colour until at least 9% of the indicator is in the alkaline- or acid-coloured form, respectively. Thus in passing from an acid to an alkaline solution, no change in colour is apparent until 9% of the indicator assumes the alkaline form, i.e. $x = 0.09$ and $1 - x = 0.91$. Insertion of these values into equation (3.68) gives

$$[H_3O^+] = \frac{0.91}{0.09} K_i \sim 10K_i$$

or

$$pH = pK_i - 1 \tag{3.69}$$

Similarly, in passing from alkaline to acid solution,

$$[H_3O^+] = \frac{0.09}{0.91} K_i \sim 0.1K_i$$

or

$$pH = pK_i + 1 \tag{3.70}$$

The effective range of pH over which colour changes can be detected is therefore given by

$$pH = pK_i \pm 1 \tag{3.71}$$

Problems

(Use concentrations rather than activities except where indicated otherwise)

3.1 Calculate the pH of the following solutions: (i) 0.001 mol dm^{-3} hydrochloric acid, (ii) 0.001 mol dm^{-3} sulphuric acid, (iii) 0.002 mol dm^{-3} sodium hydroxide, (iv) 0.0015 mol dm^{-3} calcium hydroxide, (v) 0.01 mol dm^{-3} ethanoic acid, (vi) 0.02 mol dm^{-3} ammonium hydroxide.

3.2 The pH of a 0.01 mol dm^{-3} aqueous solution of adipic acid is observed to be 3.22. Calculate the pH of a 0.15 mol dm^{-3} solution of adipic acid at the same temperature.

3.3 Calculate the volume of 0.2 mol dm^{-3} sodium hydroxide which must be added to 200 cm^3 of 0.2 mol dm^{-3} ethanoic acid at 298 K($K_a = 1.75 \times 10^{-5}$) to produce a solution with a pH of 5.50.

3.4 Calculate the pH of the following salt solutions at 298 K: (i) 0.2 mol dm^{-3} ammonium chloride, (ii) 0.1 mol dm^{-3} sodium ethanoate, (iii) 0.1 mol dm^{-3} ammonium ethanoate. For ammonia, $pK_b = 4.75$; for ethanoic acid $pK_a = 4.76$.

3.5 (i) Estimate the pH of the solution containing 0.02 mol dm^{-3} ethanoic acid and 0.03 mol dm^{-3} sodium ethanoate (pK_a of ethanoic acid = 4.76). (ii) Estimate the pH of the solution containing 0.02 mol dm^{-3} ammonium hydroxide and 0.01 mol dm^{-3} ammonium chloride (pK_b of ammonia = 4.75).

3.6 To 25 cm^3 of a solution of isopropylamine of concentration 0.15 mol dm^{-3} are added 10 cm^3 of 0.12 mol dm^{-3} hydrochloric acid. The total volume is made up to 250 cm^3 with distilled water. What is the pH of the resulting solution? (pK_b for isopropylamine = 4.03.)

3.7 Calculate the pH of the following glycine-based buffer solutions: (i) 25 cm^3 0.02 mol dm^{-3} glycine +10 cm^3 0.02 mol dm^{-3} NaOH, (ii) 25 cm^3 0.02 mol dm^{-3} glycine +18 cm^3 0.02 mol dm^{-3} NaOH, (iii) 25 cm^3 0.02 mol dm^{-3} glycine +8 cm^3 0.02 mol dm^{-3} HCl, (iv) 25cm^3 0.02 mol dm^{-3} glycine +16 cm^3 0.02 mol dm^{-3} HCl. (The pK_{a1}, pK_{a2} values of glycine are 2.34 and 9.78 respectively.)

3.8 Calculate the pH of an aqueous phosphate buffer solution at 298 K which has been prepared by mixing equal volumes of 0.1 mol dm^{-3} solutions of Na_2HPO_4 and NaH_2PO_4. The second dissociation constant of phosphoric acid may be taken as $K_{a2} = 6.34 \times 10^{-8}$. (Use the Debye–Hückel equation for calculation of ion activity coefficients.)

3.9 Consider the titration of 10 cm^3 of 0.1 mol dm^{-3} lactic acid ($K_a = 1.38 \times 10^{-4}$) with 0.1 mol dm^{-3} sodium hydroxide. Calculate the pH of the solution at the following stages during the titration: (i) at the start (no NaOH added), (ii) at quarter neutralization (2.5 cm^3 NaOH added), (iii) at half neutralization (5.0 cm^3 NaOH added), (iv) at three-quarters neutralization (7.5 cm^3 NaOH added), (v) at neutralization (10 cm^3 NaOH added), (vi) when a total of 20 cm^3 of NaOH has been added.

3.10 The pH of an aqueous solution of sodium benzoate at 298 K is 8.32 for a concentration of 0.04 mol dm^{-3}. Given that the ionization constant of benzoic acid at 298 K is 6.31×10^{-5}, calculate a value for the ionic product of water at this temperature. Use the Debye-Hückel equation for the estimation of the mean ion activity coefficient.

3.11 A 0.05 mol dm^{-3} solution of ammonium chloride in water at 273 K has a pH of 6.08. The thermodynamic dissociation constant of ammonium hydroxide at 273 K is 1.227×10^{-4}. Calculate the value of the thermodynamic ionic product of water at 273 K.

4 The conducting properties of electrolytes

4.1 The significance of conductivity data

Experimental determinations of the conducting properties of electrolyte solutions are important essentially in two respects. Firstly, it is possible to study quantitatively the effects of interionic forces, degrees of dissociation and the extent of ion pairing. Secondly, conductance values may be used to determine quantities such as solubilities of sparingly soluble salts, ionic products of self-ionizing solvents, dissociation constants of weak acids and to form the basis for conductimetric titration methods.

The resistance of a portion of an electrolyte solution may be defined in the same way as for a metallic conductor by

$$R = \rho\left(\frac{l}{A}\right) \tag{4.1}$$

ρ being the specific resistance or resistivity and l and A the length (m) and area (m^2) respectively of the portion of solution studied. $1/R$ is known as the conductance of the material. Of greater importance here is the reciprocal of ρ, known as the conductivity, κ, i.e.

$$\kappa = \frac{1}{\rho} = \frac{l}{RA} \tag{4.2}$$

κ has the units $\Omega^{-1}\,m^{-1}$ or Sm^{-1}, S (Siemens) being the unit of reciprocal resistance.

4.1.1 Measurement of conductivity

A Wheatstone bridge arrangement may be used to measure the resistance of a portion of a solution bounded by electrodes of fixed area held at a fixed separation from each other. These electrodes are usually of platinum with a coating of finely divided platinum (platinum black) electrodeposited on their surfaces. Two complications are immediately apparent: firstly, application of a direct voltage across the electrodes is likely to cause electrolysis and the electrodes are said to become polarized: secondly, it is difficult to measure the area of the electrodes and the distance between them (maintaining these parameters at fixed values can also present some problems). To overcome the first difficulty, it is essential to use an alternating voltage

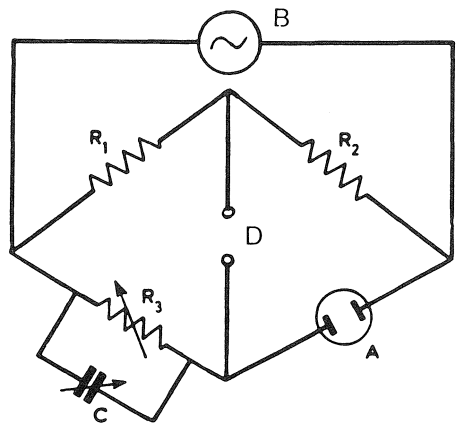

Figure 4.1 A.c. bridge circuit for conductivity determination. (A) Conductivity cell. (B) Oscillator. (C) Capacitance (variable) to balance capacitance of cell. (D) Detector.

source so that no significant accumulation of electrolysis products can occur at the electrodes, the changes occurring in one half-cycle being reversed in the next half-cycle. The catalytic properties of the platinum black ensure that the electrode reactions occur rapidly and stay in phase with the applied alternating voltage. The second problem is solved by determining a cell constant with a solution of accurately known κ. What is actually measured, of course, is the resistance R, with κ determined from

$$R = \left(\frac{1}{\kappa}\right)\left(\frac{l}{A}\right) \tag{4.3}$$

If κ for a standard solution of a reference electrolyte is known, l/A (the cell constant) may be calculated from an observed resistance using the cell in question and the standard electrolyte. Potassium chloride is the accepted standard for which accurately determined values of κ at different concentrations and temperature in aqueous solution are available. Once the cell constant is known the conductivity of any electrolyte may be determined from its measured resistance using equation (4.3). The essential circuit is shown in Figure 4.1.

The variable condenser connected in parallel with the variable resistance, R_3, serves to balance the capacity effects of the conductance cell. Adjustment of C and R_3 is made until the detector indicates zero voltage difference between the opposite junctions of the network. In this condition of bridge balance, the resistance R_C may be found from the expression $R_1/R_2 = R_3/R_C$. The position of balance may be indicated by a minimum signal on an oscilloscope.

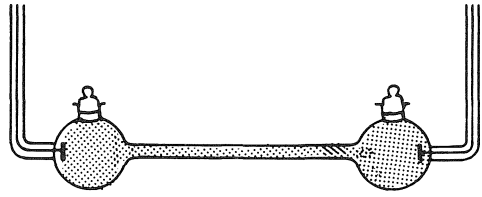

Figure 4.2 Conductivity cell with high cell constant; suitable for precision measurement of high conductivities.

For maximum sensitivity in measuring high conductivities, a high cell constant is required. Here the cell should be of the type shown in Figure 4.2 with small electrodes separated by a large distance. Conversely, for the measurement of small conductivities, l/A should be as small as possible as in Figure 4.3. This latter design is very adaptable as a 'dip-type' cell.

4.1.2 Molar conductivity

Conductivity as a practical quantity has restricted use since it is not possible to compare values for different electrolyte concentrations owing to the section of solution investigated containing different numbers of ions. Molar conductivity, given the symbol Λ, on the other hand, is defined in such a way that at any concentration the conductivity of one mole of any electrolyte may be determined.

Imagine two electrodes held at a separation of 1 m. If a solution has a concentration $C\,\mathrm{mol\,m^{-3}}$ then the volume of solution containing one mole $= 1/C\,\mathrm{m^3}$ and both electrodes would have to have an area $1/C\,\mathrm{m^2}$, for a separation of 1 m, if one mole of electrolyte were to be held between them at concentration C. The molar conductivity is thus given by the conductivity, κ, multiplied by the volume which contains one mole of electrolyte, i.e. by

$$\Lambda(\Omega^{-1}\,\mathrm{m^2\,mol^{-1}}) = \frac{\kappa(\Omega^{-1}\,\mathrm{m^{-1}})}{C(\mathrm{mol\,m^{-3}})} \tag{4.4a}$$

In terms of the centimetre as the unit of length, it is acceptable to express κ in the units $\Omega^{-1}\,\mathrm{cm^{-1}}$ and C in $\mathrm{mol\,cm^{-3}}$ and to obtain Λ as

$$\Lambda(\Omega^{-1}\,\mathrm{cm^2\,mol^{-1}}) = \frac{\kappa(\Omega^{-1}\,\mathrm{cm^{-1}})}{C(\mathrm{mol\,cm^{-3}})} \tag{4.4b}$$

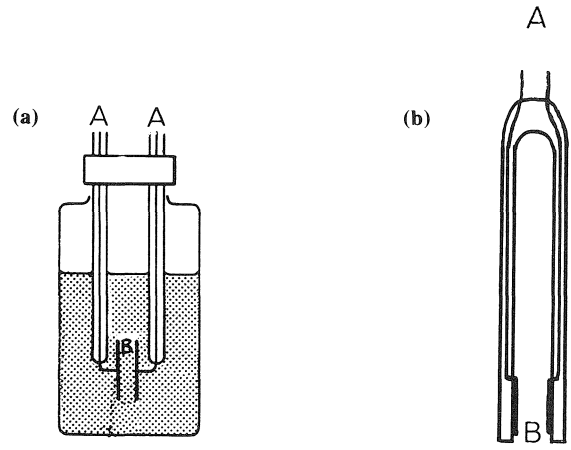

Figure 4.3 Conductivity cells with low cell constant. (a) Bottle-type (b) Dip-type: A. Contact wires sealed into insulating glass envelope. B. Exposed surfaces of platinised platinum electrodes.

Indeed, to many people the latter units produce values for Λ which are more convenient (Table 4.1) than those obtained with SI units (Table 4.2).

However, the more usual units of concentration are mol dm^{-3} which, when combined with κ in the units Ω^{-1} cm^{-1}, require modification of equation (4.4b) to

$$\Lambda(\Omega^{-1}\,\text{cm}^2\,\text{mol}^{-1}) = \frac{1000\kappa(\Omega^{-1}\,\text{cm}^{-1})}{C(\text{mol}\,\text{dm}^{-3})} \tag{4.4c}$$

To correct molar conductivities in the units Ω^{-1} cm^2 mol^{-1} to Ω^{-1} m^2 mol^{-1} it is necessary to divide the former by 10^4.

The usually accepted numerical values of equilibrium constants are obtained by the use of concentrations in the units mol dm^{-3} or mol kg^{-1} and the values for the dissociation constant of ethanoic acid given in Table 4.3, and estimated via equation (4.8) are those corresponding to the latter units.

Clearly, it is necessary to be familiar with the units which may be used for the various quantities and, in particular, to exercise the greatest care and consistency in combining them.

4.1.3 Empirical variation of molar conductivity of electrolyte solutions with concentration

In respect of the variation of their molar conductivities with concentration, strong and weak electrolytes show distinct characteristics. For *strong*

electrolytes Kohlrausch established an empirical relationship between Λ and $\sqrt{C}$, viz.

$$\Lambda_C = \Lambda_0 - k\sqrt{C} \tag{4.5}$$

which holds up to concentrations in the region of $5\,\text{mol}\,\text{m}^{-3}$, extrapolation of a plot of Λ_C versus $\sqrt{C}$ giving Λ_0 the molar conductivity at infinite dilution.

Weak electrolytes show no such linear relationship. Their dissociation is considered to increase with increasing dilution of the solution so that the dissociation constant of ethanoic acid may be expressed in the manner already considered in Chapter 3.

$$\begin{array}{lccccc} & \mathrm{CH_3COOH} & \rightleftharpoons & \mathrm{CH_3COO^-} & + & \mathrm{H^+} \\ \text{Equilibrium concentrations} & (1-\alpha)C & & \alpha C & & \alpha C \end{array}$$

$$K = \frac{[\mathrm{CH_3COO^-}][\mathrm{H^+}]}{[\mathrm{CH_3COOH}]} = \frac{\alpha^2 C}{(1-\alpha)} \tag{4.6}$$

For such electrolytes, Arrhenius showed that α, the degree of dissociation, may be given quite well by the following

$$\alpha = \frac{\Lambda_C}{\Lambda_0} \tag{4.7}$$

Λ_C being the measured molar conductivity at a finite electrolyte concentration. Such an expression is obviously meaningless for strong electrolytes where ionization is complete at all concentrations. A combination of equations (4.6) and (4.7) gives

$$K = \frac{C\Lambda_C^2}{\Lambda_0^2\left(1 - \dfrac{\Lambda_C}{\Lambda_0}\right)} = \frac{C\Lambda_C^2}{\Lambda_0(\Lambda_0 - \Lambda_C)} \tag{4.8}$$

In order to apply equation (4.8) to the determination of dissociation constants it is necessary to have independent means of determining Λ_0. This is made possible by the Independent Migration Principle considered in the next section.

4.1.4 The independent migration of ions

Kohlrausch demonstrated that each ion of an electrolyte makes its own unique contribution to the total molar conductivity of the electrolyte which is independent of the other ion(s). The phenomenon has expression as the Law of Independent Migration of Ions in the form, for a 1:1 electrolyte

$$\Lambda_0 = \lambda_+^0 + \lambda_-^0 \tag{4.9}$$

λ_0^+, λ_0^- being the ionic conductivities at infinite dilution. Equation (4.9) has been written for infinite dilution since it is only under such conditions, when ion–ion interactions are at a minimum, that the law strictly holds. It is then applicable to both strong and weak electrolytes. Its validity is demonstrated in the data of Table 4.1.

Table 4.1 Infinite dilution values of molar conductivities of some strong electrolytes at 298 K (Ω^{-1} cm^2 mol^{-1})

Salt	Λ_0	Salt	Λ_0	$\Delta\Lambda_0$
KCl	130	NaCl	108.9	21.1
KNO_3	126.3	$NaNO_3$	105.2	21.1
$\Delta\Lambda_0$	3.7		3.7	

In quoting the Λ or Λ_0 value for a given electrolyte, it is necessary to be very careful to specify the formula unit to which the value applies. The molar conductivity of an electrolyte solution reflects the amount of current that it can carry, i.e. the rate of transfer of charge through it. When comparing values for different electrolytes, it is essential to define 1 mole in all cases as the amount associated with 1 mole of unit charges (i.e. 6.023×10^{23} elementary units).

There is no problem in the case of uni-univalent electrolytes such as potassium chloride where the mole is specified as KCl but for magnesium sulphate or sodium sulphate a mole would be specified as $\frac{1}{2}MgSO_4$ and $\frac{1}{2}Na_2SO_4$, respectively (rather than $MgSO_4$ or Na_2SO_4).

Thus,

$$\Lambda_0(MgSO_4) = 2.662 \times 10^{-2}\,\Omega^{-1}\,m^2\,mol^{-1}$$

but

$$\Lambda_0(\tfrac{1}{2}MgSO_4) = 1.331 \times 10^{-2}\,\Omega^{-1}\,m^2\,mol^{-1}$$

and

$$\Lambda_0(Na_2SO_4) = 2.604 \times 10^{-2}\,\Omega^{-1}\,m^2\,mol^{-1}$$

but

$$\Lambda_0(\tfrac{1}{2}Na_2SO_4) = 1.302 \times 10^{-2}\,\Omega^{-1}\,m^2\,mol^{-1}$$

We clearly have to be equally careful in the case of ion conductivities. There is, for example, no significance in comparing the values of $\lambda^0(Na^+)$, $\lambda^0(Mg^{2+})$ and $\lambda^0(Fe^{3+})$ but there is real significance in a comparison of $\lambda^0(Na^+)$, $\lambda^0(1/2Mg^{2+})$ and $\lambda^0(1/3Fe^{3+})$ in that molar values thus defined are referred in each case to the amount of species associated with 1 mole of electrons. Some values of limiting ion conductivities are listed in Table 4.2.

Table 4.2 Limiting molar conductivities of some ion species at 298 K

Cation	$\lambda_0^+ (\Omega^{-1} m^2 mol^{-1})$	Anion	$\lambda_0^- (\Omega^{-1} m^2 mol^{-1})$
H_3O^+	3.499×10^{-2}	OH^-	1.976×10^{-2}
Na^+	0.502×10^{-2}	MnO_4^-	0.613×10^{-2}
Ag^+	0.619×10^{-2}	Cl^-	0.764×10^{-2}
$1/2\,Ca^{2+}$	0.595×10^{-2}	$1/2\,SO_4^{2-}$	0.800×10^{-2}
$1/3\,Fe^{3+}$	0.680×10^{-2}	$1/3\,Fe(CN)_6^{3-}$	0.991×10^{-2}

In the application of the Kohlrausch law, the values of molar ion conductivities used must refer to the quantity of ions contained in the specified amount of electrolyte. Thus

$$\begin{aligned}\Lambda_0(\tfrac{1}{2}Na_2SO_4) &= \lambda^0(Na^+) + \lambda^0(\tfrac{1}{2}SO_4^{2-}) \\ &= (0.502 + 0.800) \times 10^{-2}\,\Omega^{-1}\,m^2\,mol^{-1} \\ &= 1.302 \times 10^{-2}\,\Omega^{-1}\,m^2\,mol^{-1}\end{aligned}$$

It is, of course, equally true to write

$$\begin{aligned}\Lambda_0(Na_2SO_4) &= \lambda^0(2Na^+) + \lambda^0(SO_4^{2-}) \\ &= (1.004 + 1.600) \times 10^{-2}\,\Omega^{-1}\,m^2\,mol^{-1} \\ &= 2.604 \times 10^{-2}\,\Omega^{-1}\,m^2\,mol^{-1}\end{aligned}$$

A more general form of the Kohlrausch law is thus seen to be

$$\Lambda_0 = \nu_+\lambda_+^0 + \nu_-\lambda_-^0 \tag{4.10}$$

where ν_+, ν_- are the numbers of moles of cation and anion, respectively, to which 1 mole of the electrolyte gives rise in solution.

The Kohlrausch law is required to establish the value of Λ_0 for weak electrolytes. For example Λ_0 for ethanoic acid may be calculated from experimentally determined values of Λ_0 for hydrochloric acid, sodium ethanoate and sodium chloride (all strong electrolytes). From the Kohlrausch relation we may write

$$\begin{aligned}{}_{HCl}\Lambda_0 &= (\lambda_{H^+})^0 + (\lambda_{Cl^-})^0 && \text{(i)} \\ {}_{NaEtO}\Lambda_0 &= (\lambda_{Na^+})^0 + (\lambda_{EtO^-})^0 && \text{(ii)} \\ {}_{NaCl}\Lambda_0 &= (\lambda_{Na^+})^0 + (\lambda_{Cl^-})^0 && \text{(iii)}\end{aligned} \tag{4.11}$$

Addition of (i) and (ii) followed by subtraction of (iii) gives

$$({}_{HCl}\Lambda_0 + {}_{NaEtO}\Lambda_0) - {}_{NaCl}\Lambda_0 = (\lambda_{H^+})^0 + (\lambda_{EtO^-})^0 \tag{4.12}$$

Experimental values at 298 K for hydrochloric acid, sodium ethanoate and sodium chloride are 4.262×10^{-2}, 0.910×10^{-2} and $1.265 \times 10^{-2}\ \Omega^{-1}\ m^2\ mol^{-1}$, respectively. Insertion of these data into equation (4.12) gives a value of $3.907 \times 10^{-2}\ \Omega^{-1}\ m^2\ mol^{-1}$ for the limiting molar conductivity of ethanoic acid at 298 K. This value, combined with measured values at infinite concentrations, was used to calculate the dissociation constant of ethanoic acid according to equation (4.8) and the results are shown in Table 4.3.

Table 4.3 Values of dissociation constant of ethonaic acid calculated from experimental values of Λ at 298 K

C(mol dm^{-3})	$K \times 10^5$
0.001	1.851
0.005	1.851
0.010	1.846
0.050	1.771
0.100	1.551

The results may be taken to verify the validity of equation (4.8). Values of K show fairly satisfactory constancy but a pronounced trend towards a limiting value at the lowest concentrations. This confirms the approach of activity coefficients to unity in this region, extrapolation to $C = 0$ providing the limiting (thermodynamic) value of K.

4.2 Conductivity and the transport properties of ions

Transport is the general term used for the movement of matter of various sorts; here it is the movement of ions through solution which is of concern. There are *four* factors which encourage ions to move through solution namely

(i) concentration gradients;
(ii) potential gradients;
(iii) temperature gradients;
(iv) mechanical stirring.

All of these have significance in various electrochemical contexts; the convective effects represented by (iii) and (iv) above will be of greater concern in later chapters dealing with electrode processes and their exploitation. For the present it is the effects of concentration and potential gradients which are important and in the treatment which follows the convective processes are assumed to be excluded. In practical terms they are easily controlled via thermostatic control and protection of apparatus from vibration and shock.

In Chapter 2, the electrochemical potential, $\tilde{\mu}_i$ of ion species i was defined by

$$\tilde{\mu}_i = \mu_i + z_i F\phi \tag{4.13}$$

where μ_i is the chemical potential while ϕ is an electrical potential experienced by the ion. It has been shown that in an electrolyte solution, ϕ arises from both the charge on the ions and from that on the atmospheres by which they are surrounded.

In terms of the conventional thermodynamic definition of μ_i, equation (4.13) may be expressed in a form involving the concentration of the ion, thus

$$\tilde{\mu}_i \sim \mu_i^{\ominus} + RT \ln c_i + z_i F\phi \tag{4.14}$$

This is seen to be of similar form to equation (2.4) except that molar concentration $c_i(\text{mol dm}^{-3})$ is more conveniently used than mole fraction x_i. The expression is applicable in dilute solution where concentration may be approximated for activity.

Spontaneous movement of i will take place from regions in solution of higher to those of lower electrochemical potential. The rate of such movement, v_i, is proportional to the gradient $(\partial\tilde{\mu}_i/\partial x)$ in which x is the distance of i from a reference plane so that

$$v_i = k_i \left(\frac{\partial \tilde{\mu}_i}{\partial x}\right) \tag{4.15}$$

where k_i is a proportionality constant.

Then, in terms of equation (4.14), the rate of movement becomes

$$v_i = k_i \left[RT\left(\frac{\partial \ln c_i}{\partial x}\right) + z_i F \frac{\partial \phi}{\partial x}\right] \tag{4.16}$$

It is now necessary to introduce the idea of the flux, j_i, of ion i. This is defined as the quantity which passes normally across a plane of unit area in unit time, its units being either $\text{mol s}^{-1}\text{m}^{-2}$ or $\text{mol s}^{-1}\text{cm}^{-2}$. Thus, in terms of $\text{d}n_i$, moles crossing the plane in time $\text{d}t$ we can write

$$j_i = \frac{\text{d}n_i}{\text{d}t} = c_i v_i \tag{4.17}$$

so that, in terms of equation (4.16) the flux becomes

$$j_i = k_i c_i \left[RT\left(\frac{\partial \ln c_i}{\partial x}\right) + z_i F\left(\frac{\partial \phi}{\partial x}\right)\right] \tag{4.18}$$

emphasizing that it is a function of both the concentration and the potential gradients.

4.2.1 *Diffusion and conductivity: the Nernst–Einstein equation*

It is useful to consider the significance of the two gradient terms separately. Thus, when $(\partial\phi/\partial x) = 0$, equation (4.18) becomes

$$j_i = k_i c_i RT \left(\frac{\partial \ln c_i}{\partial x}\right)$$

$$= k_i RT \left(\frac{\partial c_i}{\partial x}\right)$$

or

$$j_i = D_i \left(\frac{\partial c_i}{\partial x}\right) \tag{4.19}$$

Equation (4.19) gives expression to Fick's first law of diffusion and introduces the diffusion coefficient of i, defined as $D_i = k_i RT$, and having the units $m^2\,s^{-1}$ or $cm^2\,s^{-1}$.

Under conditions of zero concentration gradient, the flux may be expressed by

$$j_i = k_i c_i z_i F \left(\frac{\partial\phi}{\partial x}\right)$$

i.e.

$$j_i = c_i \left(\frac{D_i}{RT}\right) z_i F \left(\frac{\partial\phi}{\partial x}\right) \tag{4.20}$$

or, in terms of the passage of charge

$$z_i F_{j_i} = i = c_i \left(\frac{D_i}{RT}\right) z_i^2 F^2 \left(\frac{\partial\phi}{\partial x}\right) \tag{4.21}$$

i ($C\,s^{-1}\,m^2$ or $A\,m^{-2}$) being the current density.

In the simplest formulation conductivity, κ, is given by equation (4.2) as

$$\kappa = \frac{l}{RA}$$

$$= \frac{lI}{EA} \quad \begin{array}{l}\text{(Substituting } \frac{1}{R} = \frac{I}{E} \text{ by Ohm's Law}\\ \text{where } I = \text{current, } E = \text{potential)}\end{array}$$

or

$$\kappa = \frac{I/A}{E/l} = \frac{\text{current density}}{\text{potential gradient}}$$

Therefore

$$\kappa = \frac{i}{\left(\frac{\partial\phi}{\partial x}\right)} = \frac{i}{\vec{F}} \tag{4.22}$$

using the symbol $\vec{F}$ for field strength or potential gradient. By inserting the expression for i (equation (4.21)) into equation (4.22) the conductivity, κ_i, of ion i becomes

$$\kappa_i = \frac{c_i D_i z_i^2 F^2}{RT} \tag{4.23}$$

or,

$$\lambda_i = \frac{\kappa_i}{c_i} = \frac{D_i z_i^2 F^2}{RT} \tag{4.24}$$

Introducing the general Kohlrausch law as expressed in equation (4.10) it is possible to write for a general electrolyte

$$\Lambda_0 = \frac{F^2}{RT}\left[\nu_+ D_+^0 z_+^2 + \nu_- D_-^0 z_-^2\right]$$

and since $\nu_+ z_+ = \nu_- z_-$

$$\Lambda_0 = \frac{\nu_+ z_+ F^2}{RT}\left[z_+ D_+^0 + z_- D_-^0\right] \tag{4.25}$$

or, in the case that $\nu_+ = \nu_- = 1$; $z_+ = z_- = z$ and equation (4.25) becomes

$$\Lambda_0 = \frac{z^2 F^2}{RT}\left[D_+^0 + D_-^0\right] \tag{4.26}$$

Equations (4.24), (4.25) and (4.26) are all forms of the Nernst–Einstein equation.

4.2.2 Ion speeds and conductivity: the Einstein and Stokes–Einstein equations

Since the conductivity of an electrolyte is a measure of the current it can carry, and therefore of the rate of charge transfer, it is also a function of the rate with which the constituent ions carry their charge through a solution. This rate depends upon the concentration and valency of the ions as well as upon their speeds.

Movement of ions through a solution may be induced by the imposition of an electric field—a consequence of an applied potential between the electrodes. The electric field force experienced by an ion causes it to accelerate. This acceleration, however, is opposed by the retarding forces of the asymmetry and electrophoretic effects as well as by the solvent viscosity (Chapter 2), so that an ion ultimately moves with a uniform velocity determined by a balance of these opposing forces. For a strong electrolyte at concentration c, giving rise to cations with charge z_+ at concentration c_+ and anions with charge z_- at concentration c_-, the amount of charge crossing unit area of solution in unit time is given by

$$c_+\nu_+z_+F + c_-\nu_-z_-F = i_+ + i_- = i \tag{4.27}$$

where i is the current density, i_+, i_- are the current density contributions from cation and anion while ν_+, ν_- are the speeds of the two ionic species.

In the case of a weak electrolyte, where each molecule produces ν_+ cations and ν_- anions, with a degree of ionization α, then

$$c_+ = \alpha\nu_+c \quad \text{and} \quad c_- = \alpha\nu_-c$$

Substitution for c_+, c_- into equation (4.27) gives

$$i = \alpha cF(\nu_+v_+z_+ + \nu_-v_-z_-) \tag{4.28}$$

Now, the speeds with which ions move are linear functions of the field strength, $\vec{F}$, so we may write,

$$v_+ = u_+\vec{F} \quad \text{and} \quad v_- = u_-\vec{F} \tag{4.29}$$

Here the proportionality constants u_+, u_- are the *mobilities* of the respective ionic species, i.e. their speeds under a unit field strength at a specified concentration.

Introducing the expressions v_+, v_- from equations (4.29) into equation (4.28) gives

$$i = \alpha cF\vec{F}(\nu_+u_+z_+ + \nu_-u_-z_-) \tag{4.30}$$

Therefore, in terms of equation (4.22) the conductivity becomes

$$\kappa_c = \frac{1}{\vec{F}} = \alpha cF(\nu_+u_+z_+ + \nu_-u_-z_-)$$

or

$$\Lambda_c = \frac{\kappa_c}{c} = \alpha F(\nu_+u_+z_+ + \nu_-u_-z_-) \tag{4.31}$$

Now, at infinite dilution $\alpha = 1$ and u_+, u_- will reach limiting values u_+^0, u_-^0; Equation (4.31) then becomes

$$\Lambda_0 = F(\nu_+u_+^0z_+ + \nu_-u_-^0z_-) \tag{4.32}$$

and since

$$\Lambda_0 = \nu_+\lambda_+^0 + \nu_-\lambda_-^0 \qquad \text{(equation (4.10))}$$

then

$$\Lambda_0 = \nu_+u_+^0z_+F + \nu_-u_-^0z_-F \tag{4.33}$$

where

$$\lambda_+^0 = u_+^0z_+F \quad \text{and} \quad \lambda_-^0 = u_-^0z_-F \tag{4.34}$$

Equations (4.32), (4.33) and (4.34) are clearly valid for both strong and weak electrolytes at infinite dilution.

It should be noted with caution that some workers have used the term 'mobility' in place of molar ion conductivity. Such practice is misleading and should be avoided; the distinction between molar ion conductivity, as a measure of the amount of current that an ion can carry, and mobility, which is a speed in a field of unit potential gradient, should be clearly understood.

Evidently equations (4.34) make possible the calculation of the speeds with which ions move under the influence of an applied field when their limiting molar conductivities are known.

Consider the case of a singly charged cation for which $\lambda_+^0 = 0.5 \times 10^{-2}$ $\Omega^{-1}\,m^2\,mol^{-1}$

$$u_+^0 = \frac{\lambda_+^0}{F} = \frac{0.5 \times 10^{-2}\,\Omega^{-1}m^2\,mol^{-1}}{96\,500\,C\,mol^{-1}}$$

$$= 5.2 \times 10^{-8}\frac{\Omega^{-1}\,m^2}{A\,s}$$

$$= 5.2 \times 10^{-8}\frac{m^2}{V\,s}$$

$$= 5.2 \times 10^{-8}\frac{m\,s^{-1}}{V\,m^{-1}}$$

i.e. at infinite dilution the cation moves with a speed of $5.2 \times 10^{-8}\,m\,s^{-1}$ in a potential gradient of $1\ V\,m^{-1}$. Or, as the mobility would more usually be expressed,

$$u_+^0 = 5.2 \times 10^{-8}\,m^2\,s^{-1}V^{-1}$$

Table 4.4 Ion mobilities at 298 K in aqueous solution

Ion	$u^0\ (m^2s^{-1}V^{-1})$
H_3O^+	36.3×10^{-8}
OH^-	20.5×10^{-8}
Li^+	4.0×10^{-8}
Na^+	5.2×10^{-8}
K^+	7.6×10^{-8}
Ag^+	6.4×10^{-8}
Mg^{2+}	5.5×10^{-8}
Zn^{2+}	5.5×10^{-8}
Cl^-	7.9×10^{-8}
Br^-	8.1×10^{-8}
NO_3^-	7.4×10^{-8}
SO_4^{2-}	8.3×10^{-8}

A list of ion mobilities is given in Table 4.4. It is seen that H_3O^+ and

OH^- ions in aqueous solution are exceptional in having extremely high mobilities. In view of what has become known about the extent of association of water molecules ('iceberg' structures) such large values cannot be accounted for on the basis of the independent migration of H_3O^+ and OH^- species. In fact, a somewhat unique transport mechanism operates whereby protons are exchanged between neighbouring solvent molecules producing movement of charge and causing continuous destruction and reformation of the species. A very similar mechanism operates in the case of $H_3SO_4^+$ and HSO_4^- in systems where concentrated sulphuric acid is used as solvent. For the other ions listed it is to be noted that the speeds are very small indeed, even in the extreme condition of infinite dilution when they can move unencumbered by other ions. It follows that electrical migration should be interpreted as a very slow drift of ions towards electrodes superimposed on their much more rapid thermal motions.

A combination of the general form of equation (4.34) with equations (4.17) and (4.19) allows a relationship between diffusion coefficient and mobility to be derived. If the migration of ions induced by an applied field exactly balanced their diffusion then

$$D_i \left(\frac{\partial c_i}{\partial x} \right) - c_i u_i \vec{F} = 0 \tag{4.35}$$

The Boltzmann distribution law may be used to express the concentration of ion species i, $c_i(x)$ at a point where the applied potential is $\phi(x)$ in terms of the concentration c_i^0 at $\phi(x) = 0$, i.e.

$$c_i(x) = c_i^0 \exp\left[-\frac{z_i F \phi(x)}{RT} \right]$$

Therefore

$$\left(\frac{\partial c_i}{\partial x} \right) = c_i^0 \left[\frac{\partial}{\partial \phi} \exp\left(-\frac{z_i F \phi(x)}{RT} \right) \right] \frac{\partial \phi}{\partial x}$$

$$= c_i^0 \left(-\frac{z_i F}{RT} \right) \exp\left(-\frac{z_i F \phi(x)}{RT} \right) \frac{\partial \phi}{\partial x}$$

$$= c_i(x) \left[-\frac{z_i F}{RT} \right] \frac{\partial \phi}{\partial x}$$

$$= \left[\frac{c_i(x) z_i F}{RT} \right] \vec{F}$$

Therefore

$$D_i \left(\frac{c_i z_i F}{RT} \right) \vec{F} = c_i u_i \vec{F}$$

or

$$D_i = \frac{u_i RT}{z_i F} \tag{4.36}$$

Equation (4.36) is the Einstein equation.

The mobility of an ion species may be related to the viscosity of the solvent medium by combining a form of equation (4.15) with the Stokes equation. The latter may be written in terms of the viscous force on a single solvated ion of radius r_i under terminal velocity v_i and may be equated to the diffusion force experienced by that ion, viz.

$$6\pi r_i v_i \eta = \frac{1}{N} \left(\frac{\partial \mu_i}{\partial x} \right) \tag{4.37}$$

The right-hand side of equation (4.37) requires the factor $1/N$ for consideration of a single ion and has been expressed in terms of μ_i rather than $\tilde{\mu}_i$ if no external field is applied. Under these circumstances equation (4.15) becomes

$$v_i = k_i \left(\frac{\partial \mu_i}{\partial x} \right) = \frac{D_i}{RT} \left(\frac{\partial \mu_i}{\partial x} \right)$$

Therefore,

$$\left(\frac{\partial \mu_i}{\partial x} \right) = \frac{v_i RT}{D_i} = 6\pi r_i v_i \eta N$$

and

$$D_i = \frac{RT}{6\pi r_i \eta N} \tag{4.38}$$

Equation (4.38) is the Stokes–Einstein equation. The right-hand side may be equated to the corresponding expression in the Einstein equation so that

$$\frac{RT}{6\pi r_i \eta N} = \frac{u_i RT}{z_i F}$$

or

$$u_i = \frac{z_i F}{6\pi r_i \eta N}$$

Substitution of $\lambda_i^0 = F z_i u_i^0$ yields, after rearrangement

$$\lambda_i^0 \eta = \frac{z_i^2 F^2}{6\pi r_i N} \tag{4.39}$$

Equation (4.39) is the theoretical expression of Walden's rule which in its earlier empirical form suggested that the product of λ_i^0 and η should be approximately constant for the same solute species in different solvents. Differing degrees of solvation in different solvents cause effective ionic radii as well as viscosity to vary with solvent; in consequence, gross departures from the 'rule' may be observed.

4.3 Rationalization of relationships between molar conductivity and electrolyte concentration

Three classes of behaviour may be distinguished. In the case of strong, completely dissociated electrolytes any variation of conductivity with concentration can be traced to the varying interaction between ions as their proximity is varied by concentration changes. For weak, incompletely dissociated electrolytes changes in conductivity may be expected to occur as their degree of dissociation is forced to increase by increasing dilution. The conditions under which the ions deriving from strong electrolytes may associate into ion pairs have already been considered. Since such associations reduce the effective number of conducting species, occurrence of such phenomena may be expected to reduce the conductivity below values which would be obtained were all the ions to be unassociated.

4.3.1 Strong, completely dissociated electrolytes

Onsager attempted formulation and quantitative assessment of the relaxation and electrophoretic effects (Chapter 2). Since these are functions of the nature of ion atmospheres, it is to be expected that expressions resulting from the Debye–Hückel theory will have some significance in such formulation. There has developed some variation in the form of the original expression derived by Onsager: in part this has arisen because of changes in, and rationalization of, units. The ion conductivity λ_+, of a cation species in a very dilute solution of a strong electrolyte may be expressed as

$$\lambda_+ = \lambda_+^0 - \left[|z_+ z_-| \left(\frac{\epsilon^2 N}{12\pi\varepsilon\varepsilon_0 RT} \right) \left(\frac{q}{1+\sqrt{q}} \right) \lambda_+^0 + \left(\frac{F^2 z_+}{6\pi\eta N} \right) \right] \frac{\kappa}{1+\kappa a} \quad (4.40)$$

where

$$q = \frac{|z_+ z_-|(\lambda_+^0 + \lambda_-^0)}{(|z_+| + |z_-|)(|z_+|\lambda_-^0 + |z_-|\lambda_+^0)} \quad (4.41)$$

so that, if $\kappa a < 1$ and κ is replaced by its expression in equation (2.13)

$$\lambda_+ = \lambda_+^0 - \left(\frac{2 \times 10^3 N^2 \epsilon^2}{\varepsilon\varepsilon_0 RT}\right)^{\frac{1}{2}} \times \left[|z_+ z_-| \left(\frac{\epsilon^2 N}{12\pi\varepsilon\varepsilon_0 RT}\right)\left(\frac{q}{1+\sqrt{q}}\right)\lambda_+^0 + \left(\frac{F^2 z_+}{6\pi\eta N}\right)\right]\sqrt{I} \qquad (4.42)$$

Since a complementary expression to equation (4.40) may be written for λ_- in terms of λ_-^0 and z_-, addition of λ_+ and λ_- gives the molar conductivity according to the Kohlrausch principle, viz.

$$\Lambda_+ = \Lambda_0 - B\left[|z_+ z_-| \left(\frac{\epsilon^2 N}{12\pi\varepsilon\varepsilon_0 RT}\right)\left(\frac{q}{1+\sqrt{q}}\right)\Lambda_0 + \frac{F^2(|z_+| + |z_-|)}{6\pi\eta N}\right]\sqrt{I} \qquad (4.43)$$

where B is the factor in the Debye–Hückel equation. For a 1:1 electrolyte $q = 0.5$ $|z_+| = |z_-| = 1$, so that for water as solvent at 298 K, using $\varepsilon = 78.5$ and $\eta = 8.937 \times 10^{-4}\,\mathrm{kg\,m^{-1}s^{-1}}$ (0.008937 poise) equation (4.43) may be expressed in terms of the values for the various constants as

$$\Lambda = \Lambda_0 - (3.290 \times 10^9)[2.381 \times 10^{-10}(0.294)\Lambda_0 + 1.842 \times 10^{-12}]C^{\frac{1}{2}}$$

therefore

$$\Lambda = \Lambda_0 - (0.230\Lambda_0 + 6.060 \times 10^{-3})C^{\frac{1}{2}} \qquad (4.44)$$

for Λ in the units $\Omega^{-1}\,\mathrm{m^2\,mol^{-1}}$.

Or, in general,

$$\Lambda_C = \Lambda_0 - (B_1\Lambda_0 + B_2)C^{\frac{1}{2}} \qquad (4.45)$$

which is of the same form as the empirical square-root law (equation (4.5)) established by Kohlrausch.

In equation (4.45) the constants have had the subscripts 1 and 2 attached to distinguish them from the Debye–Hückel constant B, but to emphasize their relationship with that constant.

In Figure 4.4 is shown an example of the variation of experimentally determined Λ_C values as a function of $C^{\frac{1}{2}}$ for a 1:1 electrolyte. The Onsager relation is a limiting one in that it only holds good for 1:1 electrolytes at concentrations less than 0.001 M, deviations occurring as shown at higher concentrations due to the neglect of higher terms in the limiting equation. The theoretical Onsager slope may be calculated from equation (4.44) as

$$0.23\Lambda_0 + 60.60 = 89.68\left(\frac{\Omega^{-1}\,\mathrm{cm^2\,mol^{-1}}}{\mathrm{mol^{1/2}\,dm^{-3/2}}}\right) \qquad (4.46)$$

which is in good agreement with the value indicated for the limiting slope in Figure 4.4. Deviations for electrolytes with higher valency products occur at

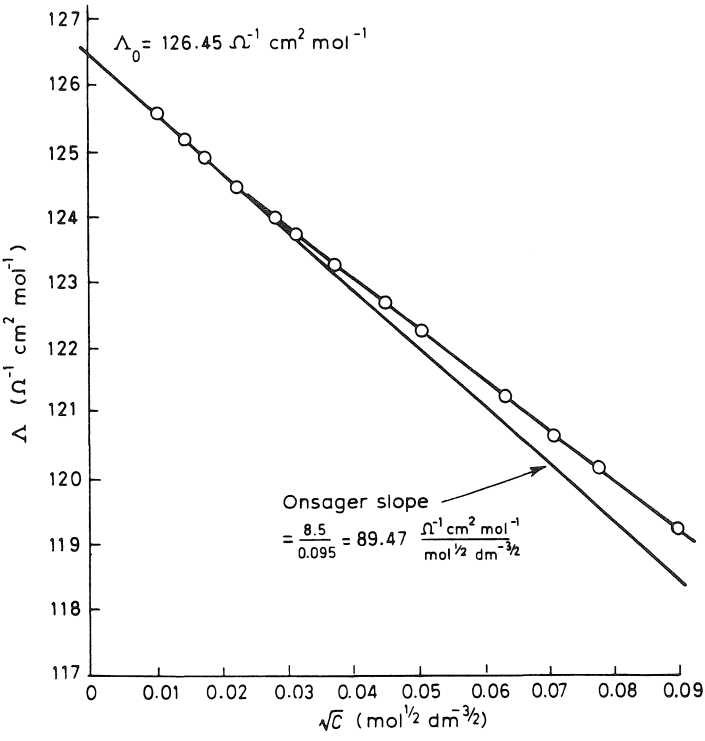

Figure 4.4 Experimental plot of molar conductivity versus square root of concentration for sodium chloride in water at 298 K.

even lower concentrations. Electrolytes with a valency product equal to or greater than 4 show marked negative deviations. These are attributed to ion association and are to be distinguished from positive deviations associated with shortcomings of the Onsager equation.

Rearrangement of equation (4.45) gives

$$\Lambda_0 = \frac{\Lambda_C + B_2 C^{1/2}}{1 - B_1 C^{1/2}} \tag{4.47}$$

Shedlovsky observed that the value of Λ_0 as calculated from equation (4.47) was not constant, but showed almost linear variation with concentration. The linear extrapolation function

$$\Lambda_0' = \frac{\left(\Lambda_C + B_2\sqrt{C}\right)}{\left(1 - B_1\sqrt{C}\right)}$$

when plotted against concentration yields a further value of Λ_0 when

extrapolated to zero concentration. This value can be defined in terms of an empirical relationship

$$\Lambda_0 = \frac{\left(\Lambda_C + B_2\sqrt{C}\right)}{\left(1 - B_1\sqrt{C}\right)} - bC \tag{4.48}$$

where b is an empirical constant.

Rearrangement of equation (4.48) yields

$$\Lambda_C = \Lambda_0 - (B_1\Lambda_0 + B_2)\sqrt{C} + bC\left(1 - B_1\sqrt{C}\right) \tag{4.49}$$

This equation holds good for a number of electrolytes up to a concentration of 0.1 M.

In conclusion, we can see that in an ideal solution of a strong electrolyte Λ is independent of concentration. An approach to this condition is made in very dilute solution as seen in the portion BC of the graph of Λ versus dilution given in Figure 4.5 for sodium chloride solutions in water at 298 K. Over the region AB extreme departures from ideality occur and, with increasing concentration, ion–ion and ion–solvent interactions become more and more significant. Over this region a conductivity coefficient of may be defined by

$$\frac{\Lambda}{\Lambda_0} = g_\Lambda \tag{4.50}$$

4.3.2 Weak, incompletely dissociated electrolytes

Experimental use of equations (4.5) and (4.7) from the Arrhenius theory does make possible the determination of dissociation constants even though both equations are based upon erroneous assumptions. Ions, even in dilute solution, do not behave as ideal solutes and their conductivities are functions of concentration. The reasons that equilibrium constants determined by the Arrhenius equations are fairly good are that, firstly, interactions between ions are less numerous than for a strong electrolyte and secondly, and more important, corrections to α by the use of the Onsager equation and introduction of activity coefficients from the Debye–Hückel theory almost compensate one another. The Onsager equation in the case of a weak electrolyte becomes

$$\Lambda_C = \alpha\left[\Lambda_0 - (B_1\Lambda_0 + B_2)\sqrt{(\alpha C)}\right] \tag{4.51}$$

and equation (4.50) now takes the form

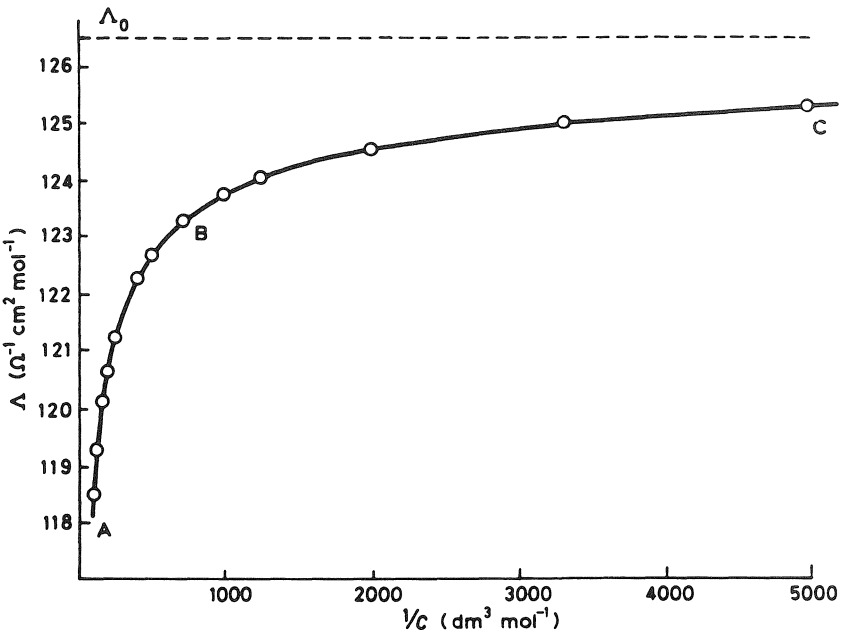

Figure 4.5 Plot of experimental molar conductivity versus dilution for a strong, completely ionized electrolyte (NaCl) in water at 298 K.

$$\frac{\Lambda}{\Lambda_0} = \alpha g_\Lambda \tag{4.52}$$

which may be regarded as the precise form of equation (4.7).

4.3.3 Electrolyte systems showing ion pairing

It has been seen that deviations from the Onsager equation in its limiting form occur for uni-univalent electrolytes at higher concentrations where observed molar conductivities are somewhat higher than predicted so that the slope of the Λ versus $C^{1/2}$ graph is somewhat lower than the theoretical Onsager slope.

Electrolytes with a valency product < 4 show fair to good agreement with the Onsager equation at low concentrations, although the upper concentration limit at which deviation begins to occur becomes progressively lower as the valency product increases. When this product is > 4 it is no longer possible to perform experiments at the extremely high dilutions where the Onsager equation might be expected to hold. Even for the lowest concentrations accessible the deviations are now extreme (Figure 4.6).

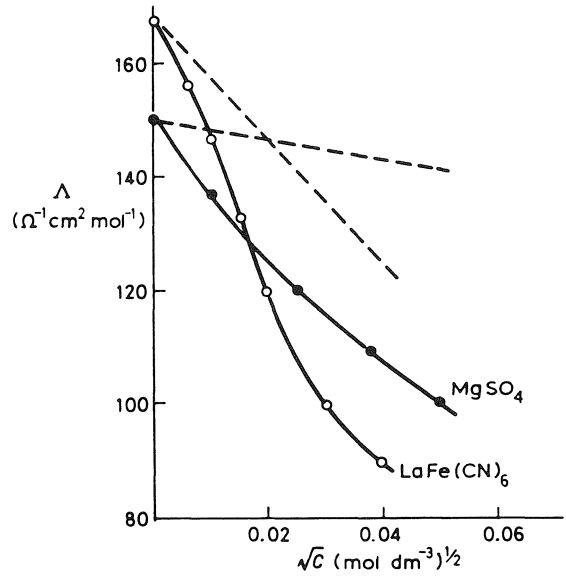

Figure 4.6 Deviations from the Onsager equation, shown by electrolytes with valency products 4 and 6, indicating ion pairing. The dashed lines are the Onsager slopes.

However, such deviations occur in the opposite sense to those obtained with low-valency product electrolytes, i.e. observed conductivities are now substantially lower than those predicted. Such deviations indicate a drastic reduction in the number of conducting species in solution, i.e. association to form ion pairs has taken place. Such deviations become more marked in solvents of low dielectric constant. In such cases the molar conductivity versus $C^{1/2}$ graph may show a minimum (Figure 4.7) and this is attributed to the formation of triple ions which, unlike ion pairs, carry a net charge.

4.4 Conductivity at high field strengths and high frequency of alternation of the field

In normal fields of the order of a few volts per centimetre, conductivities show no measurable variation with field. Wien, however, using fields of the other of 100 kV cm^{-1} observed an increase in conductivity whose magnitude is a function of both the concentration and the charge on the ions of the electrolyte. For a given concentration of a particular electrolyte, a limiting value of conductivity is reached at higher field strengths.

Under the influence of such high field strengths, the ions move very rapidly indeed (up to m s^{-1}). Since the rearrangement time of the atmosphere

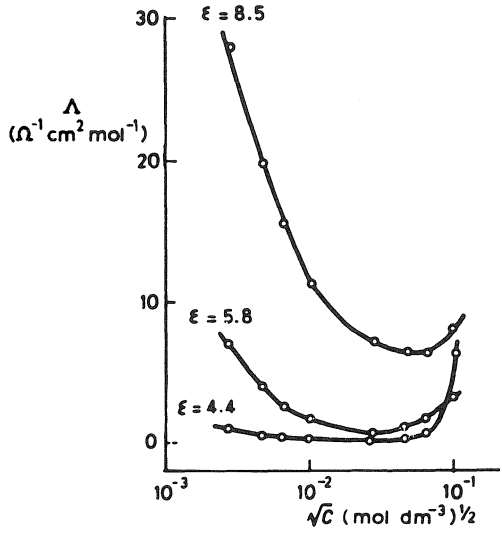

Figure 4.7 Plots of molar conductivity versus $\sqrt{C}$ for tetraisoamylammonium nitrate at various values of dielectric constant.

about an ion is slow by comparison, the retardation of the ion's motion by the electrophoretic and relaxation effects becomes progressively smaller as the field strength becomes larger. This effect is only observed for strong electrolytes.

The conductivity of weak electrolytes, e.g. weak acids, is also increased under the influence of high fields. This dissociation field effect, or second Wien effect, is caused quite differently from that described for strong electrolytes. The high field in this case changes the values of the dissociation constants of weak electrolytes. For an acid dissociation

$$HA \underset{k_{-1}}{\overset{k_1}{\rightleftharpoons}} H^+ + A^-$$

where k_1,k_{-1} are the forward and backward rate constants, the dissociation constant, K_a, is given by

$$K_a = \frac{k_1}{k_{-1}}$$

Since the H–A bond has some electrostatic character, the acid molecule has, to a limited extent, the properties of an ion pair. While the rate of formation of an ion pair is independent of an external field, the dissociation rate is increased, i.e. k_1 increases relative to k_{-1} with consequent increase

in K_a. The equilibrium shifts to a new position corresponding to a higher concentration of H^+ and A^-.

An increase in conductivity of strong electrolytes is also observed with high-frequency fields operating at frequencies greater than 5 megacycles per second. At such frequencies, a central ion oscillates at a frequency comparable to the relaxation time of the atmosphere. The relaxation effect thus becomes smaller the greater the frequency and the conductivity rises. The electrophoretic effect remains unchanged.

4.5 Electrical migration and transport numbers

Section 4.2 showed that electrolyte conductivities are dependent upon the transport properties of the constituent ions in the solvent considered. The phenomenon of electrical migration, i.e. the movement of cations and anions under the influence of an applied electrical field, may be used to identify properties of individual ions.

In order to determine λ_+, λ_- from measurements of the conductance of the electrolyte, it is necessary to know the fraction of the total current passed which is carried by each ion type. Such fractions are known as transport numbers, t. By definition, the sum of the transport numbers of all ion species in an electrolyte solution is unity.

Equation (4.27) gave the anion and cation current density contributions,

$$i_+ = c_+ v_+ z_+ F; \quad i_- = c_- v_- z_- F$$

and

$$i = i_+ + i_- = c_+ v_+ z_+ F + c_- v_- z_- F$$

So that the fraction, t_+, of the current density carried by the cation is

$$t_+ = \frac{i_+}{i_+ + i_-} = \frac{c_+ v_+ z_+ F}{F(c_+ v_+ z_+ + c_- v_- z_-)} \tag{4.53}$$

For a uni-univalent electrolyte, $c_+ = c_- = c$ and $|z_+| = |z_-| = 1$, so that equation (4.53) becomes

$$t_+ = \frac{v_+}{v_+ + v_-} \tag{4.54}$$

Similarly, for the anion,

$$t_- = \frac{v_-}{v_+ + v_-} \tag{4.55}$$

The concentration dependence of transport numbers is implicit in equations (4.54) and (4.55) owing to the concentration dependence of ion speeds.

For a solution containing several electrolytes, the transport number of an individual species is defined similarly, viz.

$$t_+ = \frac{v_+}{\Sigma v}; \quad t_- = \frac{v_-}{\Sigma v} \tag{4.56}$$

From such expressions it is evident that transport number values are very much dependent on the nature and concentration of other ion species present. The greater the number of other ion species, the smaller will be the fraction of the total current carried by the ion under consideration and hence the smaller its transport number. This phenomenon is made use of in a number of electroanalytical techniques to be described later; if the transport number of a particular species can be made so small that it approaches zero, a condition has been reached where that species ceases to migrate and no current is carried by it.

Now, from equation (4.29)

$$v_+ = u_+\vec{F} \quad \text{and} \quad v_- = u_-\vec{F}$$

so that equation (4.53) may equally well be written

$$t_+ = \frac{c_+u_+z_+}{c_+u_+z_+ + c_-u_-z_-}$$

and since $c_+ = \alpha\nu_+ c$ and $c_- = \alpha\nu_- c$

$$t_+ = \frac{\alpha\nu_+cu_+z_+}{\alpha\nu_+cu_+z_+ + \alpha\nu_-cu_-z_-}$$

Therefore

$$t_+ = \frac{\nu_+u_+z_+}{\nu_+u_+z_+ + \nu_-u_-z_-}$$

Also for electroneutrality, $|\nu_+z_+| = |\nu_-z_-|$.

Therefore

$$t_+ = \frac{u_+}{u_+ + u_-} \quad \text{and} \quad t_- = \frac{u_-}{u_+ + u_-} \tag{4.57}$$

Now $\lambda_+^0 = u_+^0 z_+ F$; $\lambda_-^0 = u_-^0 z_- F$ (see equation (4.34))

So that for the special case of infinite dilution,

$$t_+^0 = \frac{u_+^0}{u_+^0 + u_-^0} \quad \text{and} \quad t_-^0 = \frac{u_-^0}{u_+^0 + u_-^0}$$

Therefore

$$t_+^0 = \frac{\lambda_+^0/z_+F}{\lambda_+^0/z_+F + \lambda_-^0/z_-F}; \quad t_-^0 = \frac{\lambda_-^0/z_-F}{\lambda_+^0/z_+F + \lambda_-^0/z_-F} \tag{4.58}$$

and remembering again that $|\nu_+z_+| = |\nu_-z_-|$ the last relationships become

$$t_+^0 = \frac{\nu_+\lambda_+^0}{\nu_+\lambda_+^0 + \nu_-\lambda_-^0}; \quad t_-^0 = \frac{\nu_-\lambda_-^0}{\nu_+\lambda_+^0 + \nu_-\lambda_-^0}$$

or, in terms of the modified Kohlrausch law given in equation (4.10)

$$t_+^0 = \frac{\nu_+\lambda_+^0}{\Lambda_0}\,;\; t_-^0 = \frac{\nu_-\lambda_-^0}{\Lambda_0} \tag{4.59}$$

Equations (4.59) enable λ_+^0, λ_-^0 to be determined from a knowledge of t_+^0, t_-^0 and Λ_0, the transport numbers at infinite dilution being calculated by extrapolating to zero concentration a series of values obtained by measurements made over a range of electrolyte concentration.

Equations (4.59) hold for both strong and weak electrolytes at infinite dilution. At finite concentrations the same *form* of equations (4.59) holds approximately for strong electrolytes, the quantities having values corresponding to the concentration used. In the case of a weak electrolyte the approximate relationships must include the degree of ionization corresponding to its concentration.

It is apparent from the above relationships that t_+, t_- are related by the expression

$$t_+ + t_- = 1 \tag{4.60}$$

The experimental determination of transport numbers is considered in Chapter 8.

Problems

4.1 The resistance of a 0.005 mol dm^{-3} solution of sodium chloride at 298 K was found to be $2.619 \times 10^3\ \Omega$. In a separate experiment (using the same conductivity cell) the resistance of 0.1 mol dm^{-3} potassium chloride was determined as 122.6 Ω. Given that the conductivity of 0.1 mol dm^{-3} potassium chloride at 298 K is 0.01289 Ω^{-1} cm^{-1}, calculate the molar conductivity of the sodium chloride solution.

4.2 Given that the molar conductivities at infinite dilution at 298 K for sodium propionate, sodium nitrate and nitric acid are 0.859×10^{-2}, 1.2156×10^{-2} and $4.2126 \times 10^{-2}\ \Omega^{-1}\ m^2\ mol^{-1}$ respectively, calculate the molar conductivity of propionic acid at infinite dilution at 298 K.

4.3 If the mobility of the silver ion in aqueous solution at 298 K is $6.40 \times 10^{-8}\ m^2\ s^{-1}\ V^{-1}$, calculate (i) the diffusion coefficient of the silver ion, (ii) its molar ion conductivity and (iii) its effective radius. The viscosity of water at 298 K is $8.94 \times 10^{-4}\ kg\ m^{-1}\ s^{-1}$.

5 Interfacial phenomena: double layers

5.1 The interface between conducting phases

At the interface between any pair of conducting phases a potential difference exists whose magnitude is a function of both the composition and nature of the phases. There are many types of interface for which this phenomenon is of practical importance, for example,

(i) metal/electrolyte solution;
(ii) metal/metal;
(iii) electrolyte solution/electrolyte solution;
(iv) solution of lower concentration/semipermeable membrane/solution of higher concentration.

The observed potentials are produced by the electrical double layer whose structure is responsible for many of the properties of a given system; the double layer itself arises from an excess of charges at the interface which may be ions, electrons or oriented dipoles.

To understand why this is so, it is necessary to consider the nature of a metallic conductor and how its introduction to an electrolyte solution disturbs the ion distribution considered in Chapter 2. Metals consist of an ordered arrangement of positive nuclei surrounded by mobile electrons which occupy closely spaced levels, culminating in that of the highest energy at what is known as the Fermi level. Transfer of electrons to and from this level is involved in electrode processes but these are not the concern for the moment. It is the electrostatic effect of the surface accumulation of negative charges on other charged species and dipoles in solution which is of immediate importance here.

5.2 The electrode double layer

The expression 'double layer' is something of a misnomer and arose from the original simple view of an organized arrangement of positive ions from solution, to compensate for the negative charges in the surface, to form an interfacial region similar to a parallel plate condenser (Figure 5.1). The terminology, with qualifications, has persisted. Although double layers are a general interfacial phenomena, some attention will be paid here to electrode–electrolyte interfaces because of their importance in electrode kinetics. Fur-

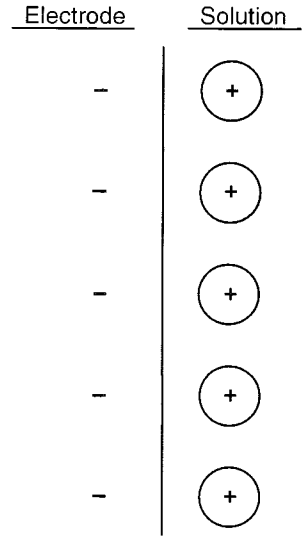

Figure 5.1 Simple condenser (Helmholtz) model of the double layer.

ther, the theory leads to a proper interpretation of electrokinetic phenomena, to an understanding of the factors affecting colloid stability and to the elucidation of cell membrane and ion-exchange processes.

For the case of an electrode dipping into a solution of an electrolyte, it is clear that, for electroneutrality, the excess charge residing on the electrode surface must be exactly balanced by an equal charge of opposite sign on the solution side. It is the *distribution* of this latter charge that is of interest. When only electrostatic interaction operates, ions from the solution phase may approach the electrode only so far. The surface array of ions is 'cushioned' from the electrode surface by a layer of solvent (in this case water) molecules (Figure 5.2). The line drawn through the centre of such ions at this distance of closest approach marks a boundary known as the 'outer Helmholtz plane' (OHP). The region within this plane constitutes the compact part of the double layer or the Helmholtz layer.

The size of the ions forming up at the outer Helmholtz plane are such that sufficient of them to neutralize the charge on the electrode cannot all fit here. The remaining charges are held with increasing disorder as the distance from the electrode surface increases, where electrostatic forces become weaker and where dispersion by thermal motion is more effective. This less-ordered arrangement of charges of sign opposite to that on the electrode constitutes the *diffuse part of the double layer*. Thus, all the charge which neutralizes that on the electrode is held in a region between the outer Helmholtz plane and the bulk of the electrolyte solution. The variation of potential, ϕ, with distance from the electrode surface is shown in Figure 5.3.

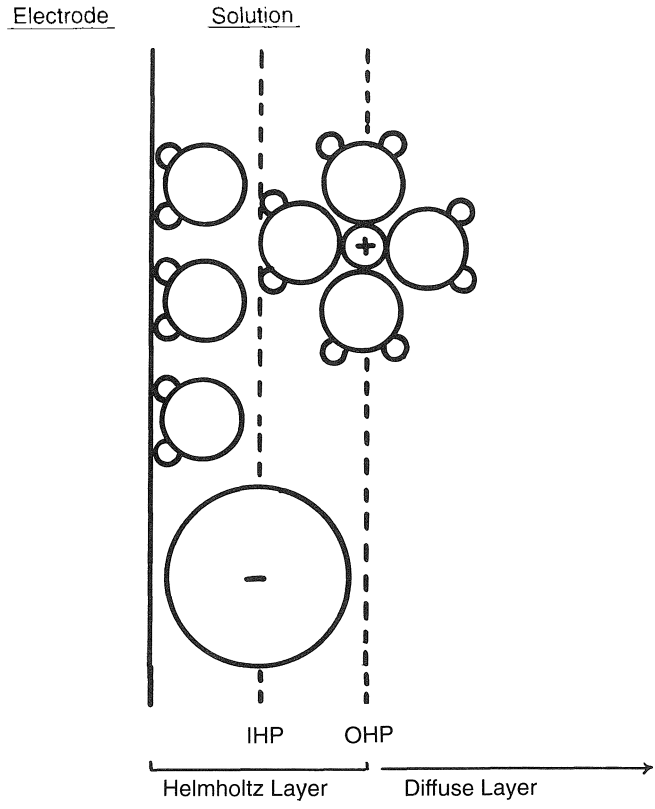

Figure 5.2 Relative positions of inner and outer Helmholtz planes of electrode double layer.

This is only the case for purely electrostatic interaction between the electrode and ions in solution. In other cases, specific adsorption of ions may occur in which van der Waals and chemical forces participate. Most anions are specifically adsorbed, thereby losing most, if not all, of their inner hydration shell. This behaviour contrasts with that of most cations, which retain their hydration molecules. Specifically adsorbed species can evidently approach much closer to the electrode surface as has been shown in Figure 5.2.

A line drawn through the centres of such species aligned at the electrode surface defines a further boundary within the Helmholtz layer—the so-called inner Helmholtz plane. The extent to which specific adsorption occurs is controlled by the nature of ions in solution as well as by the nature of the electrode material and any potential applied to it.

Uncharged species, if they are less polar than the solvent or are attracted to the electrode material by van der Waals or chemical forces, will accumulate at the interface. Such species are known as *surfactants*. Where specific

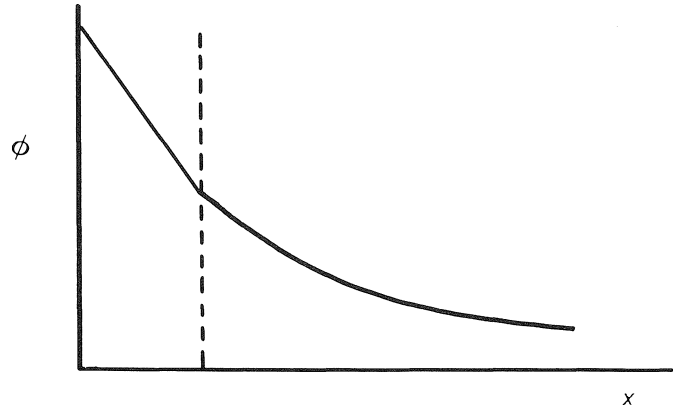

Figure 5.3 Varition of potential with distance from electrode surface.

adsorption occurs the charge distribution in the diffuse layer will change to maintain electroneutrality.

5.3 Polarized and non-polarized electrodes

These terms sometimes cause difficulty, but this is not really necessary: to polarize something is quite simply to cause a charge separation as in the classical Helmholtz model. If the metallic conductor considered above behaves as an *ideal polarized electrode* it allows no movement of charge between itself and the solution phase. In such cases it is possible to control the charge distribution by the imposition of an externally applied potential and to effectively change the character of the surface 'condenser'. In contrast, an ideal non-polarized electrode allows free and unimpeded exchange of electrons across the interface.

There is something which should be clearly understood in advance of later chapters concerned with non-polarized electrodes. Although a double layer is identifiable with the structure and behaviour of a polarized electrode, it is also present in non-polarized electrodes: this is why it is an important influence on electrode processes. However, the origin in the latter case is different and involves *charge transfer* across the interface.

5.4 Electrocapillarity: the Lippman equation

It has been noted that the potential of an ideal polarized electrode may be varied at will by altering its charge distribution through variation of applied potential, but without altering the equilibrium position at the interface.

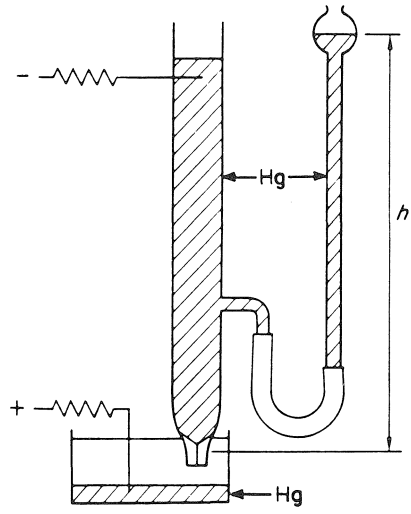

Figure 5.4 Principle of the Lippmann electrometer.

Such a system is equivalent to a perfect condenser without leakage and, like a perfect condenser, it may be charged by connection to a reference electrode and source of emf. It will then retain the imposed potential when the source is removed.

In practice, this behaviour is difficult to attain. However, the mercury electrode in potassium chloride and similar electrolyte solutions approaches very closely to the behaviour required of an ideal polarized electrode. *Within a certain range of potentials*, ions do not react at its surface nor does the metal dissolve, i.e. neither electrochemical reactions nor the establishment of electrochemical equilibria occur.

5.4.1 Variation of charge with applied potential at a mercury/solution interface

Interfacial tension measurements on liquid metal electrodes, such as mercury, have provided a great deal of information about double layer structure and have indicated the factors governing adsorption at a charged interface. The interfacial tension, γ, of a mercury/solution interface may be observed with the Lippmann electrometer, which is shown schematically in Figure 5.4. The mercury meets the solution in a fine-bore capillary, the meniscus being observed by means of a microscope. If a potential is applied to the mercury, the position of the meniscus is seen to change but may be restored to its original position by changing the reservoir height, h. The

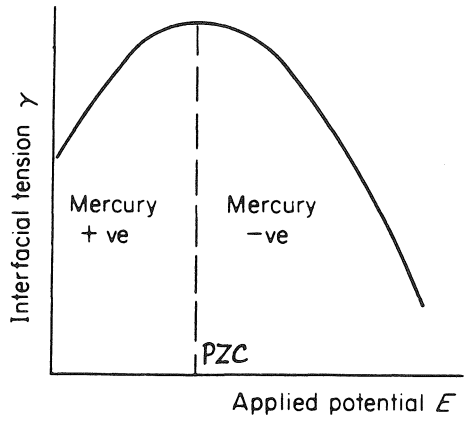

Figure 5.5 Schematic variation of interfacial tension with applied potential (electrocapillary curve) for a mercury/aqueous electrolyte solution interface.

amount by which h is required to be changed is a function of the change in interfacial tension caused by the applied potential. Mercury takes up a positive charge with respect to an aqueous solution; when a small negative potential is applied, some of this charge is neutralized and the interfacial tension rises. A point is reached where all the positive charge is neutralized and γ will then reach its maximum value. As an excess of negative charge is added with further increase in negative potential, γ will again decrease (Figure 5.5).

The dependence of interfacial tension on applied potential may be derived by application of the Gibbs adsorption isotherm to the system of phases in equilibrium in an electrochemical cell incorporating an almost ideal polarized electrode.

The Gibbs adsorption isotherm is expressed in the form

$$d\gamma + \Sigma\Gamma_i \, d\mu_i = 0 \tag{5.1}$$

where γ is the interfacial tension between two phases and Γ_i is the interfacial concentration of adsorbed species, i, this latter being neutral so that its chemical potential, μ_i, is a function of the pressure, temperature and composition of the phase.

The concern here, however, is with *charged* species. When i carries charge its chemical potential is also a function of the electrical potential, ϕ, of the phase in which it exists. Thus, for ions of charge z_i, the electrochemical potential, $\tilde{\mu}_i$ (see equation (2.5)) has been defined by

$$\tilde{\mu}_i = \mu_i + z_i F\phi \tag{5.2}$$

So that, for ions, the Gibbs adsorption isotherm is express in terms of electrochemical potential by

$$d\gamma + \Sigma\Gamma_i d\tilde{\mu}_i = 0 \tag{5.3}$$

Equation (5.3) clearly relates the interfacial tension to the electrical potential difference between the phases.

Application of equation (5.3) to the series of interfaces involved in the cell incorporating the mercury/electrolyte solution interface of the Lippmann electrometer allows derivation of the following expression

$$\left(\frac{\partial\gamma}{\partial E}\right)_{P,T,\mu} = -\sigma \tag{5.4}$$

This is known as the Lippmann equation and relates the variation of interfacial tension with applied potential to σ, the number of charges per unit area at the interface.

Derivation of equation (5.4) is given in Appendix III and, since this involves a consideration of the series of interfaces in an electrochemical cell, its detailed scrutiny is probably better left until Chapter 6 has been read.

Expressing σ as the product CE, where C is the capacitance of the double layer regarded as a condenser and E the applied potential, then at constant T, P and μ,

$$d\gamma = -CE\,dE \tag{5.5}$$

which, on integration, gives

$$\gamma = -\frac{C}{2}E^2 + \text{constant} \tag{5.6}$$

This last expression is a form of the equation to a parabola. At the maximum of the curve

$$\left(\frac{\partial\gamma}{\partial E}\right) = 0$$

a situation corresponding to the potential of zero charge (PZC) where the Helmholtz distribution of charges is destroyed.

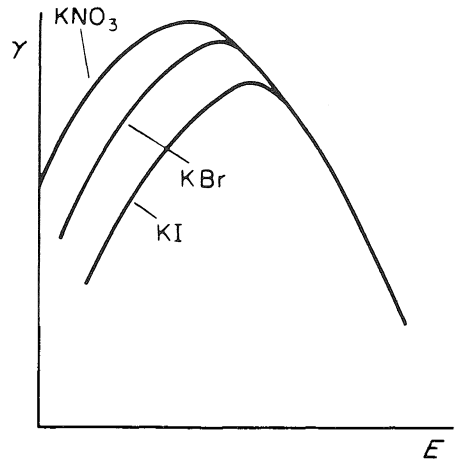

Figure 5.6 Effect on electrocapillary curves of specific adsorption of anions.

5.4.2 *Specific adsorption*

Electrocapillary curves obtained with the Lippmann electrometer are not usually parabolic. For a few electrolytes, such as potassium nitrate (and even then within a limited concentration range) parabolic curves are found but more usually the curves show varying degrees of distortion. Such behaviour is always found with cations and anions which are specifically adsorbed.

The capacity of the double layer formed at the interface may be found by differentiating the Lippmann equation.

$$\left(\frac{\partial^2 \gamma}{\partial E^2}\right)_{P,T,\mu} = -\frac{\partial \sigma}{\partial E} = C \tag{5.7}$$

Were C to be a constant for a given electrode, identical electrocapillary curves would be obtained whatever the electrolyte dissolved in solution. Alkali metal nitrates do show almost identical parabolas, but other salts of given alkali metals each give their own characteristic curves (Figure 5.6.)

It is seen that the variations in electrocapillary curves for such salts occur only on the part of the curves which correspond to a positive charge being carried by the mercury electrode: they are regarded as arising from specific adsorption of the various anions into the double layer. Surface active cations similarly affect the side of the curve which corresponds to mercury adopting a negative charge. Non-electrolytes which are surface active, such as gelatin, also modify the shape of electrocapillary curves (often quite drastically) and this will be seen to be of significance in the technique of polarography to be considered in Chapter 9.

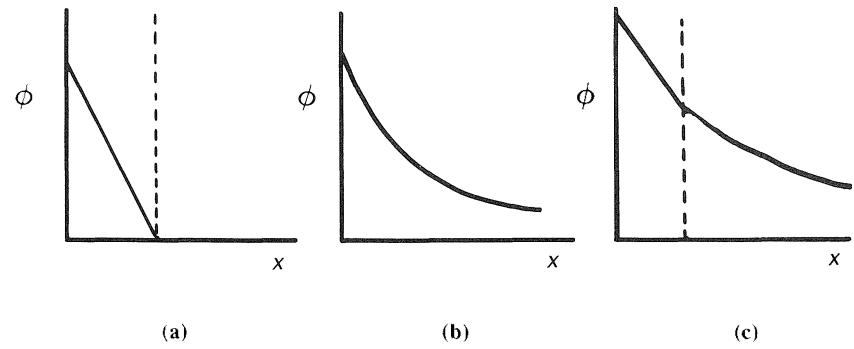

Figure 5.7 Potential variations at electrode/solution interfaces according to (a) Helmholtz, (b) Gouy and Chapman, (c) Stern.

5.5 Models for the double layer

The nature of the interfacial region considered in section 5.2 and represented schematically in Figure 5.2 has evolved via a number of theoretical models. All of these explain some experimental phenomena and do so in terms of electrostatic forces.

5.5.1 Distribution of charge according to Helmholtz, Gouy and Chapman, and Stern

Helmholtz considered the interfacial region to be limited to the condenser model described by Figure 5.1, the potential variation across the region being linear as in Figure 5.7(a). Gouy and Chapman, by contrast, appreciated that a large charged plane surface presented to the ions of an electrolyte in solution would, rather like a 'giant ion', induce a one-dimensional charge distribution similar to that proposed in three dimensions for the Debye–Hückel model of electrolyte behaviour. In this approach the potential variation is non-linear (Figure 5.7(b)) and the interfacial region extends further into the electrolyte solution; in fact, so far as to a position where the ions may be considered to behave in the way they would before the introduction of the metal.

In experimental terms these two models represent extremes of behaviour in terms of electrolyte concentration and modern interpretations are based on the compromise model proposed by Stern. This distinguishes the Helmholtz and the diffuse regions as parts of the whole interfacial region and identifies corresponding linear and non-linear variations of ϕ with distance according to Figure 5.7(c).

Modern interpretation of the interfacial region as represented by Figure 5.2 is based on the Stern model but includes the effects of specific

adsorption (particularly associated with the work of Graham) and takes account of solvation of electrolyte ions and of the electrode surface.

5.5.2 *The diffuse double layer*

The similarity of the three-dimensional Debye–Hückel treatment for the distribution of ions in solution and that possible for a one-dimensional distribution normal to the electrode surface has been mentioned. But what, it may be asked, does this achieve? It provides an expression for the potential at any point within the diffuse, non-linear region and, particularly important, the potential at the OHP as a limiting condition. Derivation of this expression is given in Appendix IV and it may be written as

$$\phi = \frac{\sigma}{\varepsilon_0 \varepsilon \kappa} e^{\kappa(a-x)} \tag{5.8}$$

where σ is the charge density at the electrode surface i.e. the charge per unit area at the position where $x = 0$. Distance from the electrode surface is represented by x while a now stands for the distance of closest approach of ions to the surface (defined in terms of the position of the OHP identified in Figure 5.2).

The constant κ has similar significance to its use in Debye–Hückel theory: in the latter $1/\kappa$ was the radius of the ion atmosphere, here it may be identified with δ, the thickness of the diffuse layer.

5.5.3 *The zeta potential*

In the condition that x approaches a, i.e. the outer limit of the Helmholtz layer, $(a - x) \rightarrow 0$. Under these conditions ϕ will be designated ϕ_0; i.e.

$$\phi_0 = \frac{\sigma}{\varepsilon_0 \varepsilon \kappa} = \zeta \tag{5.9}$$

ϕ_0 may, for present purposes, be identified approximately with ζ (the 'zeta' potential), i.e. the potential at the point where the potential difference across the interface ceases to be uniform, viz. the edge of the outer Helmholtz layer where the diffuse layer begins.

The capacity, C_D, of the (electrolyte concentration dependent) diffuse layer is given by

$$C_D = \frac{\sigma}{\zeta} = \varepsilon_0 \varepsilon \kappa$$

therefore,

$$\zeta = \frac{\sigma \delta}{\varepsilon_0 \varepsilon} \tag{5.10}$$

This equation forms the basis for the explanation and description of all electrokinetic phenomena.

There are effectively two components which make up the total potential drop across the interface; viz. ϕ_0 across the diffuse part, and $(\phi - \phi_0)$ across the fixed part. The total capacitance of the double layer, C, is made up of that due to the inner (adsorption) layer, which we may designate C_H, and that due to the diffuse layer, C_D. Since these capacitances are connected in series

$$\frac{1}{C} = \frac{1}{C_H} + \frac{1}{C_D}$$

or

$$C = \frac{C_H C_D}{C_H + C_D} \tag{5.11}$$

Now, if the electrolyte solution is very dilute, $C_D \ll C_H$ and $C \sim C_D$. The double layer is now essentially all diffuse, and this was the model adopted by Gouy and Chapman in their work on the double layer. On the other hand, when the solution is very concentrated $C_D \gg C_H$ and $C \sim C_H$ which defines the earliest model of the double layer due to Helmholtz.

The relationship between ϕ, ϕ_0 and ζ is summarized in Figure 5.8.

5.6 Electrokinetic phenomena

Electrokinetic properties are associated with phases in contact with each other and are of particular significance for colloidal systems, although by no means restricted to these. Imposition of an emf across such interfaces causes movements of the phases with respect to one another while forced movement of the phases produces a characteristic emf. Thus cause and effect are readily interchangeable. Electrokinetic effects may be summarized as in Table 5.1.

Table 5.1 Electrokinetic phenomena

Motion caused by imposed emf	Emf produced by movement of phases
Electro-osmosis—liquid caused to move through a static diaphragm	*Streaming potential*—potential produced by liquid being forced through a diaphragm
Electrophoresis—solid particles caused to move through a stationary liquid	*Sedimentation potential*—potential produced by the free fall of particles through a liquid (the Dorn effect)

When motion, by whichever means, occurs it does so along a shear plane separating those ions or molecules intimately attached to the solid surface and others moving relative to them. This plane must be close to *yet outside* the OHP and it follows that while the potential at his plane of movement, the ζ potential, will often be close to ϕ_0 it will *not* identify exactly with it.

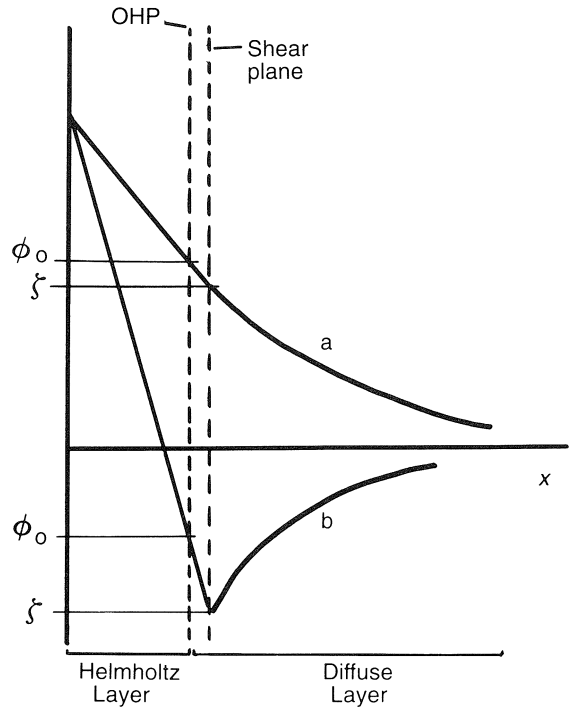

Figure 5.8 Potential variations across electrode/solution interface showing relationship between ϕ_0 and the ζ potential (a) without specific adsorption and (b) with specific adsorption.

5.6.1 Electro-osmosis

A diaphragm through which liquid is forced by imposition of an emf may be regarded as comprising a series of capillaries around the internal surface of which there exists a double layer of separated charges (Figure 5.9).

Let it be assumed that, during the movement of liquid through such a capillary, the fall of velocity is confined to the double layer by frictional forces. The velocity gradient in the layer is then v/δ, while the potential gradient down the length of the tube is $E/l = V(\mathrm{V\,m^{-1}})$.

If the surface charge per unit area is σ, then the electrical force per unit area $= V\sigma$.

The viscous force per unit area $= \eta(v/\delta)$, η being the coefficient of viscosity of the liquid. If liquid flows through the capillaries at a constant rate the electrical force balances the viscous force, i.e.

$$\eta = \left(\frac{v}{\delta}\right) = V\sigma \tag{5.12}$$

therefore,

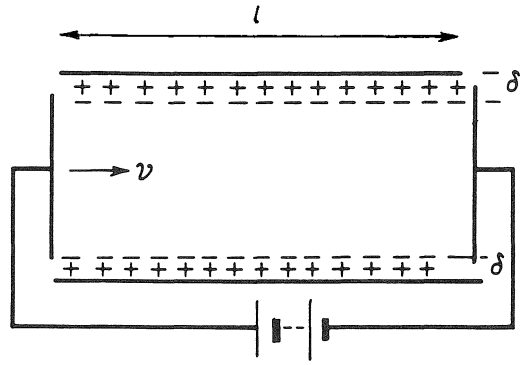

Figure 5.9 Cylindrically symmetrical double layer around the surface of a capillary.

$$\sigma = \left(\frac{\eta}{V}\right)\left(\frac{v}{\delta}\right) \tag{5.13}$$

Now

$$\zeta = \left(\frac{\delta}{\varepsilon_0 \varepsilon}\right)\sigma \qquad \text{(see equation (5.10))}$$

therefore,

$$\zeta = \frac{\eta v}{\varepsilon_0 \varepsilon V} \quad \text{or} \quad v = \frac{\zeta \varepsilon_0 \varepsilon V}{\eta} \tag{5.14a}$$

For a potential gradient of $1\,\mathrm{V\,m^{-1}}$, v is identified with u_0 the electro-osmotic mobility. Therefore,

$$\zeta = \frac{\eta u_0}{\varepsilon_0 \varepsilon} \tag{5.14b}$$

or,

$$u_0 = \frac{\zeta \varepsilon_0 \varepsilon}{\eta} \tag{5.14c}$$

Equations (5.14a)–(5.14c) are all forms of the Smoluchowski equation. If the volume flow per unit time and the cross-sectional area of all capillaries are Φ and q respectively, then

$$v = \frac{\Phi}{q} \tag{5.15}$$

and

$$\zeta = \frac{\eta \Phi}{\varepsilon_0 \varepsilon V q} \tag{5.16}$$

and, since for a single capillary, $q = \pi r^2$

$$\Phi = \frac{\zeta \varepsilon_0 \varepsilon V \pi r^2}{\eta} \tag{5.17}$$

or

$$\zeta = \frac{\eta \Phi}{\varepsilon_0 \varepsilon V \pi r^2} \tag{5.18}$$

Equation (5.18) may be used to determine the zeta potential from measurements of Φ, r and V. Since it is often by no means easy to measure V precisely, it is better to measure the current flowing, I, and the conductivity of the liquid, κ, and to replace V in equation (5.18) by $I/q\kappa$. Thus,

$$\zeta = \frac{\eta \Phi}{\varepsilon_0 \varepsilon V q} = \frac{\eta \Phi \kappa}{\varepsilon_0 \varepsilon I} \tag{5.19}$$

It is also possible to determine ζ from measurements on a single capillary, for under these conditions the Poiseuille equation may be used, viz.

$$\Phi = \frac{\pi P r^4}{8 \eta l}$$

where P is the driving pressure. This equation may be substituted into equation (5.18), the significance of P now being the difference in pressure at the ends of the capillary resulting from electro-osmotic flow, i.e.

$$P = \frac{8 \varepsilon_0 \varepsilon V l \zeta}{r^2} \tag{5.20}$$

5.6.2 *Streaming potential*

The velocity of a liquid flowing in a capillary varies with the distance from the centre of the tube as shown in Figure 5.10. The liquid at the surface of the tube is stationary so that the double layer at the interface consists of a stationary and a moving part. It is the relative movement of these two planes of the double layer which gives rise to the streaming potential. The velocity of the liquid at any point on the parabolic front distance x from the wall is given by

$$u = \frac{P(r^2 - x^2)}{4 \eta l} \tag{5.21}$$

Thus, the moving part of the double layer, at a distance $(r - \delta)$ from the centre of the tube, moves with a velocity u_δ given by

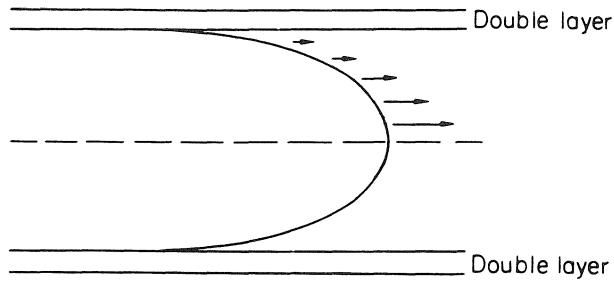

Figure 5.10 Variation of liquid velocity through a capillary with distance from the centre.

$$u_\delta = \frac{P}{4\eta l}\left[r^2 - (r-\delta)^2\right]$$
$$= \frac{P}{4\eta l}(2r\delta - \delta^2)$$

therefore

$$u_\delta \sim \frac{Pr\delta}{2\eta l} \quad \text{since } \delta^2 \ll 2r\delta \tag{5.22}$$

As the movement of the front of liquid forces one layer of charges past the other, a current is produced which must be given by the product of the total charge around a unit length of tube and the velocity of the moving part of the layer, i.e.

$$I = 2\pi r\sigma u_\delta \tag{5.23}$$

which, on substitution for u_δ from equation (5.22) becomes

$$I = \frac{\pi r^2 \sigma \delta P}{\eta l} \tag{5.24}$$

If the liquid has conductivity κ, the conductance of the liquid in the capillary is $\pi r^2\kappa/l$ and its resistance $l/\pi r^2\kappa$. Thus, by Ohm's Law,

$$E_s = \frac{Il}{\pi r^2 \kappa}$$

where E_s is the streaming potential.

So

$$E_s = \frac{\sigma \delta P}{\eta \kappa} \qquad \text{(by substitution for } I \text{ from equation (5.24))}$$

but

$$\zeta = \frac{\sigma\delta}{\varepsilon_0\varepsilon} \qquad \text{(see equation (5.10))}$$

from which

$$\sigma\delta = \zeta\varepsilon_0\varepsilon$$

so that

$$E_s = \frac{\zeta\varepsilon_0\varepsilon P}{\eta\kappa} \tag{5.25}$$

It is seen from a comparison of equations (5.19) and (5.25) that

$$\frac{E_s}{P} = \frac{\Phi}{I} \tag{5.26}$$

Equation (5.26) has indeed been experimentally verified.

5.6.3 Electrophoresis

Here solid particles, which may be of colloidal dimensions or even larger, are caused to move through a static solvent under the influence of an electric field. The electrophoretic velocity, v, in a field V is given by

$$v = \frac{\zeta\varepsilon_0\varepsilon V}{\eta} \qquad \text{(see equation (5.14a))}$$

where it is assumed that the thickness of the double layer is small in comparison with the size of the particles.

The velocity attained by an ion moving in the field is

$$v = \frac{z_i\epsilon V}{R} \tag{5.27}$$

where R is the viscous resistance to the motion of the ion given by Stokes' Law for a spherical particle of radius r by

$$R = 6\pi\eta r$$

Therefore

$$v = \frac{z_i\epsilon V}{6\pi\eta r} \tag{5.28}$$

Now, such particles experience the electrophoretic and relaxation effects. To discuss the electrophoretic effect, it is assumed that each particle is surrounded by a diffuse double layer of a thickness dependent upon the concentrations of ions in the solution. During migration through a solution a particle drags with it a layer of liquid of thickness d (say): d is usually

less than δ. Within this layer there are a number of ions and their presence modifies the effective charge on the moving particle. If the effective charge is $\Delta z\epsilon$, equation (5.28) may be written as

$$v = \frac{\Delta z\epsilon V}{6\pi\eta(r + d)} \tag{5.29}$$

For a spherical condenser we have, from equation (5.10)

$$C = \frac{\Delta z\epsilon}{\zeta}$$

also,

$$C = (r + d)4\pi\varepsilon_0\varepsilon$$

for the spherical condenser of radius $(r + d)$; therefore,

$$\Delta z\epsilon = 4\pi\varepsilon_0\varepsilon\zeta(r + d) \tag{5.30}$$

From equations (5.29) and (5.30)

$$v = \frac{\varepsilon_0\varepsilon\zeta V}{\left(\frac{3}{2}\right)\eta} \tag{5.31}$$

It is seen that equation (5.31) is of the same form as equation (5.14a) but contains a different numerical factor.

In solutions of high ionic concentration, i.e. the condition where a very thin double layer is formed equation (5.14a) is expected to apply. On the other hand, in very dilute solutions equation (5.31) will be the more likely form. Corrections for the relaxation effect are rather difficult to assess for large particles on account of the Onsager correction only being applicable to cases where a central ion is *small* in comparison with its atmosphere.

The determination of electrophoretic velocities may be carried out experimentally by the use of methods suitable for transport number measurements. Moving boundary techniques have proved useful despite the problem of a difficulty in selecting suitable indicator ions. Reliable estimates of electrophoretic velocities make possible the determination of zeta potentials. Since colloids migrate at characteristic rates under the influence of an electric field, electrophoresis provides an important means of separation. Coatings, such as rubber or graphite, may be deposited on metal electrodes by this means and additives to these may be co-deposited.

Of particular importance is the separation and purification of proteins. Ampholytic protein particles migrate in an electric field at a rate which is characteristic, not only of their surface properties and charge and composition of the solution, but also of the pH. This is because the charge which the particles acquire by their own loss or gain of protons is a function

of pH. At a given pH, different proteins are thus dissociated to different extents and have characteristic mobilities. An originally sharp boundary between a buffer solution containing various proteins and another buffer solution without proteins, splits into several boundaries corresponding to each species. A purified protein shows a characteristic variation of migration velocity with pH (the so-called 'mobility curve'). The velocity has a different sign on either side of the isoelectric point and is zero at this point. The slope of the velocity versus pH plot at the isoelectric point is a characteristic of a given protein.

5.7 Behaviour of colloidal systems

5.7.1 Stability of colloidal dispersions

The stability of colloid particles is attributed to the nature of the double layer which exists at the interface between their surfaces and the solution in which they are dispersed. Breakdown of colloidal systems, i.e. aggregation for flocculation, is similarly caused by changes in the double layer structure.

The concern here is with lyophobic colloids. Lyophilic colloid systems, on account of their affinity for the solvent, form thermodynamically stable solvated systems. Lyophobic colloids, on the other hand, are in a state of unstable equilibrium with the medium and are susceptible to irreversible breakdown when the equilibrium is subjected to even small disturbances. Lyophobic colloid particles carry similar charges, as may be confirmed by the direction of their migration in an electric field, and these usually originate from the preferential adsorption of ions from the solution. For example, negatively charged hydrosulphide ions are adsorbed at the surface of colloidal particles of arsenic(III) sulphide. Consequently, the diffuse double layer, surrounding each particle, must contain an equivalent number of positively charged (hydrogen) ions—the 'counterions' or 'gegenions'.

The repulsive forces between such particles are usually large due to the fairly large number of unit charges which each carries. Not only are the forces of repulsion large, they are of long range in comparison with the short-range attractive (dispersion) forces. The overriding repulsive forces prevent the particles aggregating, and their magnitude controls the stability of the colloid system. The magnitude of these forces may be changed by changing the number of charges carried by the particles. Adsorption of oppositely charged ions, leading to partial or complete neutralization of those on the particles, reduces the repulsive forces, allows more free play of the attractive van der Waals forces and, if occurring to a sufficiently large extent, results in aggregation. The observed effects of adding electrolytes to lyophobic colloid systems are qualitatively in agreement with

this interpretation, so that, for instance, the higher the charges carried by the ions of an added electrolyte, the more efficient it is found to be and the lower the concentration required to induce aggregation.

5.7.2 *Colloidal electrolytes*

Some electrolytes containing large ions, particularly soaps, dyes and many synthetic detergents, behave as normal electrolytes only in very dilute solution. At higher concentrations they show unusually low osmotic pressures and their conductivities show large deviations from the Onsager relationship. Such behaviour may be attributed to the formation of micelles by aggregation of similarly charged ions. This process of micelle formation occurs at a critical concentration for each system and is encouraged by large ion size. For example, cetylpyridinium salts show the Onsager dependence of molar conductivity on the square root of electrolyte concentration at very low concentrations (10^{-3} M). Beyond a critical concentration, however, the conductivity declines very rapidly and ultimately assumes a minimum almost constant value. Micelle formation, caused by the aggregation of about 68 cetylpyridinium ions, causes the observed drop in conductivity. In these micelles the cations are arranged with the cationic groups facing the solvent and with the hydrocarbon chains pointing inwards. The gegenions contained in the double layer surrounding the particles then reduce the latter's effective charge and mobility and give rise to the sharp drop in conductivity. With a knowledge of the transport numbers of cation and anion over the concentration range, the ion conductivities may be calculated. The conductivity of the cetylpyridinium ion increases sharply beyond the critical concentration due to the increased mobility of the hydrocarbon chain constituent. There is lower frictional resistance offered to the movement of the micelle than to that of the total number of original individual particles, and this more than outweighs the effects of the more dense ion atmosphere due to the increased concentration of charges in the micelle.

After the critical concentration the conductivity of the anion is observed to drop very sharply to zero and to pass into negative values. This is the same type of transport number behaviour as that shown by cadmium iodide (Chapter 8) and indicates that the anions are preferentially transported to the cathode rather than to the anode. It is evident that ion association between anions and positively charged micelles is the cause. Hartley calculated that in cetylpyridinium bromide about 53 bromide ions are associated with each micelle of 68 cationic species to give a net charge of +15.

5.7.3 *Polyelectrolytes*

Micelle particles are usually spherical in shape due to the fact that the constituent ions tend to orientate themselves with lyophobic fragments pointing

inwards away from the solvent. Consequently the distribution of charge will tend to be spherically symmetrical. Polyelectrolytes, by contrast, are long-chain polymeric species which carry ionizable groups along the chain. Depending on their proximity to one another, charged groups along such a chain interact and the extent of interaction may be affected by changing the conditions of the system. Thus, in a dilute solution of sodium polymethacrylate, the repulsion between neighbouring carboxylate groups causes almost complete extension of the chain. In the parent acid, however, which is weak with ionization of the acid groups occurring to only a small extent, the chain is coiled. The coils open when alkali is added to neutralize the acid groups and increase the number of carboxylate repulsions. The addition of other salts to solutions of the full extended poly salt causes the latter to recoil due to the increased ionic strength which reduces the intergroup repulsions.

Measurements of conductance and transport numbers similar to those used for micelles confirm the importance of association of counterions for polyelectrolytes. An interesting feature is that in an electric field such polyions exhibit abnormally high induced dipoles. It is apparent that the associated counterions have considerable mobility along the length of the chain so that the field causes polarization and orientation of the chain along the field direction.

Problems

5.1 Calculate the approximate thickness (δ) of the diffuse double layer which is established at a negatively charged plane solid surface in contact with a 0.001 mol dm^{-3} aqueous solution of sodium sulphate at 298 K. Relative permittivity of water = 78.54.

5.2 Particles of the colloidal dispersion of a noble metal have have an effective mean radius of 0.25 μm in a 0.04 mol dm^{-3} aqueous solution of a 1:1 electrolyte and have an electrophoretic mobility of 3.50×10^{-8} m^2 V^{-1} at 298 K. Calculate an approximate value for the zeta (ζ) potential. Viscosity of water at 298 K = 8.94×10^{-4} kg m^{-1} s^{-1}, relative permittivity of water at 298 K = 78.5. Comment upon the magnitude of the quantity κa in relation to the range of values calculated for the examples to Chapter 2.

5.3 A glass tube 15 cm long and mean internal diameter 1.2 mm is filled with water from a static source while a potential difference of 250 V is applied between its ends. A temperature of 298 K is maintained throughout the time of imposition of the potential difference. Calculate the rate of electro-osmotic flow of the water at 298 K given that the zeta (ζ) potential for a glass/water interface is -40 mV, the viscosity of water is 8.9×10^{-4} kg m^{-1} s^{-1}, and its relative permittivity is 78.5 at this temperature.

6 Electrode potentials and electrochemical cells

6.1 Comparison of chemical and electrochemical reactions

In this chapter the transfer of electrons through the electrode/solution interface is considered. Since such transfer requires electrons to exchange between species in solution and the Fermi level in the electrode, those species become chemically changed in the process. In this sense the phenomena considered here are fundamentally different to those shown under conditions of polarization considered in Chapter 5. A rather different model is now required for the electrode/solution interface.

Electrode reactions are oxidation–reduction processes of a somewhat unique type which obey the scheme:

$$\text{oxidant} + ne \rightleftharpoons \text{reductant} \tag{6.1}$$

ne representing a transfer of n unit charges, i.e. electrons.

The difference between chemical and electrochemical reactions lies in the different sources of electrons. A chemical oxidation–reduction system is made up of two individual systems,

$$Ox_1 + ne \rightleftharpoons Red; \text{ e.g. } Fe^{3+} + e \rightleftharpoons Fe^{2+}$$
$$Red_2 - ne \rightleftharpoons Ox_2; \text{ e.g. } Ce^{3+} - e \rightleftharpoons Ce^{4+}$$

Overall

$$Ox_1 + Red_2 \rightleftharpoons Red_1 + Ox_2$$
$$\text{e.g.} \qquad Fe^{3+} + Ce^{3+} \rightleftharpoons Fe^{2+} + Ce^{4+} \tag{6.2}$$

It is not normally possible to isolate the two contributing processes, since it is only possible to observe changes in one system by coupling it with the second.

Electrochemically, the individual processes may be separated, however. It is, for example, often possible for a metallic conductor, dipping into a solution of an oxidizing or reducing agent, to exchange electrons with such species and effectively bring about their reduction or oxidation. Such reactions are in some ways simpler in that if the electrode is only providing or taking up electrons, it may otherwise be regarded as inert.

It is possible to control precisely the rate with which electrons are provided (or taken up) by an electrode by variation of a potential applied to it

via an externally connected emf source (the circuit being completed by the inclusion of a suitable reference electrode).

There are two ways in which such electron exchange reactions may occur. They may be forced to occur, which is the situation encountered in electrolysis or they may occur spontaneously as happens in batteries and galvanic cells.

When two electrochemical redox systems are coupled together, one electrode providing and the other taking up electrons, the net effect is similar to that of the chemical scheme. Such is the situation observed with electrochemical cells for which there are associated overall chemical reactions. Owing to the precision with which electrochemical measurements may be made for such systems, it is often possible to use them to obtain precise thermodynamic data characteristic of the reactions occurring within cells.

In considering electron exchange reactions *at* electrodes it must not be forgotten that an oxidant or reductant in solution has to have some means of *reaching* the electrode so that the electrochemistry can take place. There are a number of ways in which mass transfer can occur and the interplay between the relative rates of mass transfer and of electron exchange processes will be important in later chapters. For the present it is possible to arrive at preliminary conclusions by assuming virtually infinite rates for *all* processes.

6.2 Electrode potentials: their origin and significance

A metal dipping into a solution of its ions has an equilibrium such as

$$M^{n+} + ne \rightleftharpoons M \tag{6.3}$$

eventually established at its surface. For many such systems equilibrium is established rapidly; in other cases the approach to equilibrium is slow, at least at room temperature.

Such an electrode will adopt a potential difference with respect to the solution whose value is a function of the position of equilibrium (6.3). If this is established rapidly, the potential difference (the electrode potential) may be easily measured by means of a potentiometer device which compares it with another (reference) electrode. If the process is a slow one, a continuously variable potential will be observed and no steady value may be determined experimentally.

Other electrodes involve gases in equilibrium with ions in solution, e.g. hydrogen and chlorine electrodes function through operation of the following equilibria

$$\tfrac{1}{2}H_2 \rightleftharpoons H^+ + e \tag{6.4}$$

and

$$\tfrac{1}{2}\,Cl_2 + e \rightleftharpoons Cl^- \tag{6.5}$$

These require the gas to be bubbled over the surface of some inert electrode material dipping into a solution of the ions of the gas. Surface adsorbed gas molecules enter into equilibrium with ions in solution and cause the electrode to adopt a potential characteristic of the position of equilibrium.

For the hydrogen electrode it is seen that the oxidized form is in solution; for the chlorine electrode the oxidized form is adsorbed at the surface. In redox electrodes both oxidized and reduced forms are present in solution, electrons being exchanged at an inert conductor immersed in the solution. A platinum wire placed in the Fe(III)–Fe(II) system constitutes such an electrode operating on the equilibrium

$$Fe^{3+} + e \rightleftharpoons Fe^{2+} \tag{6.6}$$

Each electrode system described constitutes what is known as a 'half-cell'; it is necessary to couple two such half-cells to form a complete electrochemical cell. When all the equilibrium components of a half-cell are in their standard states of unit activity, the electrode is said to be a standard electrode and to adopt its standard potential.

6.2.1 Types of potential operating at the electrode/solution interface

It is necessary to clarify what is measured by the potentiometric means referred to above and to understand which of a number of potentials applicable to interfaces are capable of experimental measurement.

On the face of it the problem is a simple one in which it is required to determine the difference in potential of an electrode material and that of the solution with which it is in contact. In terms of the model represented in Figure 6.1, it is required to measure $\Delta\phi$ given by

$$\Delta\phi = \phi_M - \phi_S \tag{6.7}$$

where ϕ_M, ϕ_S are the *inner*, or Galvani, potentials of the two phases.

Up until now the symbol ϕ has been used somewhat indiscriminately to represent a potential: it is now necessary to be more circumspect and to introduce new symbols to represent a number of types of potential which need to be distinguished.

This model is rather different to that considered in Chapter 5. Implicit in equilibrium (6.3) is the *polarizability* of the electrode, i.e. transfer of charge can occur. It must be remembered, however, that charges transferred between the two phases have to pass through the non-homogeneous sections of the interfacial region. A consideration of the journey of a charge from

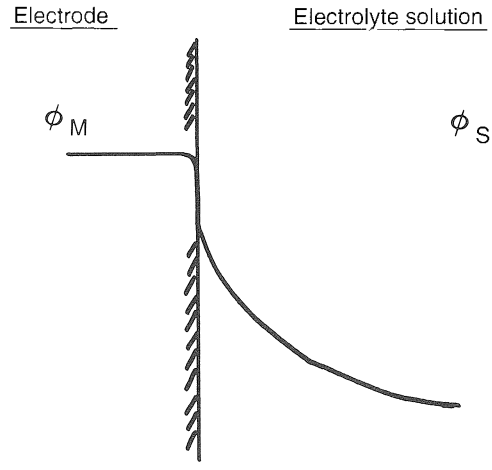

Figure 6.1 Relationship between Galvani potentials of electrode and solution phases.

solution to electrode and vice versa brings into better focus the differing regions of potential which the charge must negotiate.

It is necessary to perform a mental experiment whereby the electrode and solution are separated from one another but with the charge distributions considered to be the same as when combined. It is then possible to imagine the influence of the electrode on a charge approaching it from the solution side and passing through its surface and similarly to imagine the influence of the solution on a charge approaching it from the electrode side and emerging through the solution surface.

Consider first the transfer of charge from solution to electrode: at a position some 100 nm from its surface a potential now to be designated ψ, due to the electrode, will be experienced. This is analogous to the potential arising in the vicinity of an ion considered in Chapter 2.

ψ is the *outer*, or Volta, potential. The charge, moving from this position through the diffuse region of rising ψ, will eventually experience a sharp variation of potential *at the surface* designated χ.

After penetration of the surface the charge experiences the inner region of the electrode where the constant (Galvani) potential is ϕ. This process is shown in Figure 6.2(a).

Figure 6.2(b) represents the complementary mental experiment for the electrode-to-solution journey which requires the introduction of inner (ϕ_S), outer (ψ_S), and surface (χ_S) potentials for the solution. It is clear that for both media and in general the Galvani potential may be expressed by

$$\phi = \chi + \psi \tag{6.8}$$

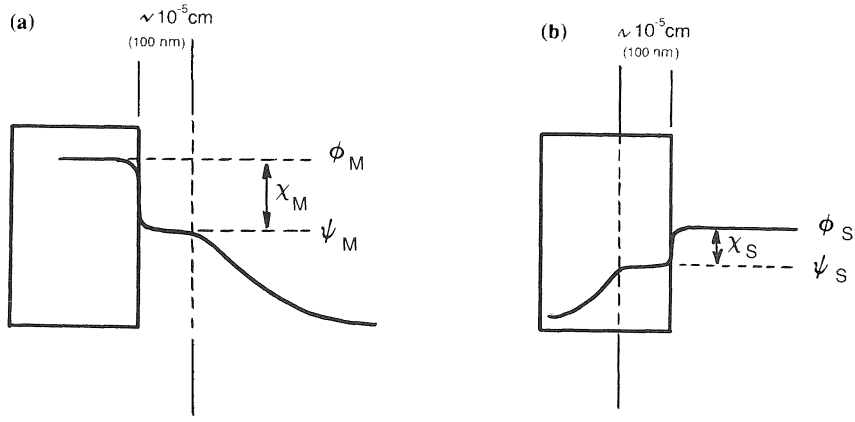

Figure 6.2 Relationship between inner, outer and surface potentials. (a) solution-to-electrode charge transfer; (b) electrode-to-solution charge transfer.

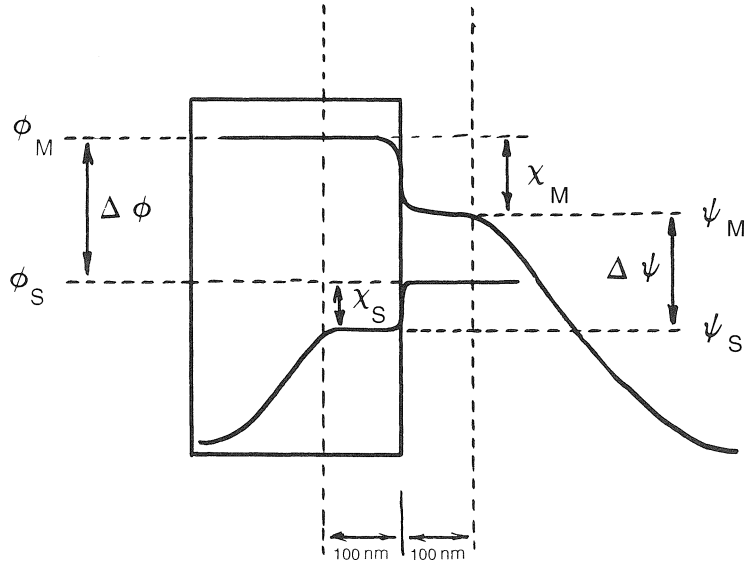

Figure 6.3 Combination of the components of Figure 6.2 to show the relationship between ϕ, ψ and χ for electrode and solution phases.

The relationship between ϕ_M and ϕ_S and that between ψ_M and ψ_S is better understood when the two curves of Figure 6.2 are brought together as shown in Figure 6.3.

6.2.2 *Measurable and non-measurable quantities*

Outer (Volta) potentials can be measured; surface potentials cannot. This is apparently a considerable problem for it means that ϕ cannot be measured. This implies that $\Delta\phi$ cannot be measured which at first sight may seem to be somewhat at odds with the comments made about *experimental* potentiometric measurement in section 6.2. What *can* be measured is a value of $\Delta\phi$ *relative to a reference* $\Delta\phi$: such relative values are known as *electrode potentials* (E). It is perhaps appropriate now to summarize these important concepts.

(i) electrode potential, $E = \Delta\phi = \phi_M - \phi_s$, is expressed in terms of non-measurable quantities;
(ii) a reference electrode potential, $E_{ref} = \Delta\phi_{ref}$ may be defined, quite arbitrarily, for convenience;
(iii) the difference, $E - E_{ref} = \Delta\phi - \Delta\phi_{ref}$, can be measured by potentiometric means.

If E_{ref} is designated zero and is the common reference for *all* measurements of $E - E_{ref}$, then it is possible to draw up an internationally agreed series of values of E. This series, within the IUPAC system, is considered in more detail in a later section.

6.3 Electrode potentials and activity: the Nernst equation

Consider a redox half-reaction of the type given by equation (6.3), e.g.

$$Cu^{2+} + 2e \rightleftharpoons Cu \tag{6.9}$$

This equilibrium is established at room temperature when a piece of metallic copper is immersed in a solution of copper(II) sulphate.

When equilibrium is established, the electrochemical potentials to the left must equal those to the right, thus

$$\tilde{\mu}_{Cu^{2+}} + 2\tilde{\mu}_e = \tilde{\mu}_{Cu} \tag{6.10}$$

Now, for *each phase*, $\tilde{\mu}$ is given by

$$\tilde{\mu}_i = \mu_i^{\ominus} + RT \ln a_i + z_i F\phi \qquad \text{(see equation (2.5))} \tag{6.11}$$

Equation (6.11) may be substituted for each phase into equation (6.9) to obtain the equality:

$$[\mu^{\ominus}_{Cu^{2+}} + RT \ln a_{Cu^{2+}} + 2F\phi_{Cu^{2+}}] + [2\mu_e^{\ominus} + 2RT \ln a_e - 2F\phi_e] = [\mu^{\ominus}_{Cu} + RT \ln a_{Cu} + 0F\phi_{Cu}] \tag{6.12}$$

It should be noted that a negative sign is associated with the term $2F\phi_e$ since electrons carry negative charge, and that the term involving ϕ_{Cu} becomes zero due to the neutrality of copper atoms.

Thus, since $\Delta\phi = \phi_{electrode} - \phi_{solution} = \phi_{Cu} - \phi_S$ is required.

$$[0F\phi_{Cu} - 2F\phi_{Cu^{2+}} + 2F\phi_e] = [\phi_e - \phi_{Cu^{2+}}]2F$$
$$= \mu^{\ominus}_{Cu^{2+}} + 2\mu^{\ominus}_e - \mu^{\ominus}_{Cu} + RT \ln a_{Cu^{2+}} - RT \ln a_{Cu}$$

or,

$$\Delta\phi = \frac{\mu^{\ominus}_{Cu^{2+}} + 2\mu^{\ominus}_e - \mu^{\ominus}_{Cu}}{2F} + \frac{RT}{2F} \ln \frac{a_{Cu^{2+}}}{a_{Cu}}$$

or

$$\Delta\phi = \Delta\phi^{\ominus} + \frac{RT}{2F} \ln \frac{a_{Cu^{2+}}}{a_{Cu}} \tag{6.13}$$

Equation (6.13) is known as the Nernst equation which may be expressed in the general form applicable to the general half-reaction process

$$oOx + ne \rightleftharpoons r\ Red \tag{6.14}$$

$$E = E^{\ominus} + \frac{RT}{nF} \ln \frac{(a_{ox})^o}{(a_{red})^r} \tag{6.15}$$

In equations (6.13) and (6.14), $\Delta\phi^{\ominus}$ and $E^{\ominus}$ are symbols for the standard electrode potential. Although equation (6.13) has been expressed in terms of $\Delta\phi$ and $\Delta\phi^{\ominus}$ to emphasize that electrode potentials are Galvani potential differences, the following sections will adopt the more familiar notation of E and $E^{\ominus}$.

A shortened, and for many purposes an adequate alternative, derivation of the Nernst expression may be effected as follows.

The van't Hoff reaction equation expresses the free energy change for a chemical reaction in the form

$$\Delta G = \Delta G^{\ominus} + RT \ln \frac{\prod(\text{activities of products})}{\prod(\text{activities of reactants})} \tag{6.16}$$

So that for the electrode reaction (6.3) as written, equation (6.16) takes the form

$$\Delta G = \Delta G^{\ominus} + RT \ln \frac{a_M}{a_{M^{n+}}} \tag{6.17}$$

Now, the free energy change of a reversible electrode reaction is related to the electrode potential by

$$\Delta G = -nEF \tag{6.18}$$

and, for the standard state

$$\Delta G^{\ominus} = -nE^{\ominus}F \tag{6.19}$$

Relationships (6.18) and (6.19) follow from simple reasoning: reduction of one mole of M^{n+} to M requires the passage of n Faradays, or a quantity of electricity nF coulombs. Passage of charge nF through a potential difference of E volts constitutes electrical work of nFE joules. This work, done by the system, at constant temperature and pressure, is equal to the decrease in free energy of the system, $-\Delta G$. Hence the equality (6.18) and, under standard conditions (6.19).

Substitution of equations (6.18) and (6.19) into equation (6.17) gives

$$nEF = nE^{\ominus}F + RT \ln \frac{a_{M^{n+}}}{a_M}$$

or,

$$E = E^{\ominus} + \frac{RT}{nF} \ln a_{M^{n+}} \tag{6.20}$$

where a_M has been omitted as the activity of the metal may be regarded as constant and unity. The logarithmic term always involves a ratio of terms characteristic of the oxidized form to those characteristic of the reduced form. Thus, for a redox electrode, e.g. the Fe(III)–Fe(II) system

$$E = E^{\ominus} + \frac{RT}{F} \ln \frac{a_{Fe^{3+}}}{a_{Fe^{2+}}} \tag{6.21}$$

and for a chlorine electrode,

$$\begin{aligned} E &= E^{\ominus} + \frac{RT}{F} \ln \frac{(a_{Cl_2})^{\frac{1}{2}}}{a_{Cl^-}} \\ &= E^{\ominus} + \frac{RT}{F} \ln \frac{1}{a_{Cl^-}} \end{aligned} \tag{6.22}$$

since $a_{Cl_2}^{\frac{1}{2}} = 1$ at 1 atmosphere pressure.

Thus, in general,

$$E_{eq} = E^{\ominus} + \frac{RT}{nF} \ln \frac{a_{Ox}}{a_{red}} \sim E^{\ominus} + \frac{RT}{nF} \ln \frac{[Ox]}{[Red]} \tag{6.23a}$$

At 298 K, with the value of R as $8.314\,J\,K^{-1}mol^{-1}$ and F as $96\,500\,C\,mol^{-1}$, equation (6.23a) may be expressed as

$$E_{eq} \sim E^{\ominus} + \frac{0.02567}{n} \ln \frac{[Ox]}{[Red]} \tag{6.23b}$$

or as

$$E_{eq} \sim E^{\ominus} + \frac{0.05913}{n} \log \frac{[Ox]}{[Red]} \tag{6.23c}$$

These are forms of the Nernst equation, in which E_{eq} has been used to emphasize that it is an equilibrium potential referring to the position of dynamic equilibrium between oxidized and reduced forms which is established rapidly at the electrode surface. Only to such a system can this—a thermodynamic equation—be applied.

6.4 Disturbance of the electrode equilibrium

The equilibrium at the electrode may be disturbed by making it more oxidizing or reducing by superimposing an external emf. Thus, if a potential, E, is applied such that $E < E_{eq}$, some of the oxidized form is reduced until a new equilibrium position is reached where $E'_{eq} = E$. Conversely, if $E > E_{eq}$, some of the reduced form is oxidized. Such changes may only be made within limits which are consistent with equilibrium being maintained at the electrode. While such an approach may be useful, it is much oversimplified; electron exchanges proceed with finite rates which vary widely and mass transfer processes occur at finite speeds. It is, however, convenient to consider cases where (i) the electron exchange rate > mass transfer rate and (ii) mass transfer rate > electron transfer rate.

6.4.1 Why electrons transfer

Clearly if electrons are to exchange between the material of an electrode and a species in solution it is required that the two participants approach to within a minimum distance of each other. To achieve this there will be rearrangements of hydration molecules in the surface, interface and solute species. Such processes will be considered later: for the present it is the energetic requirements for electron transfer when the two media may be assumed to be appropriately oriented which are of interest.

Electron exchanges will occur between the highest available energy level in the electrode (the Fermi level) and the lowest energy orbitals of the solute species. These energy levels are related to the various potentials considered in section 6.2, in terms of the schematic plan given in Figure 6.4.

If $U_F \sim U_{solute}$ it is easy for electrons to transfer in either direction. Shift of U_F by imposition of an external potential will disturb the equilibrium.

6.4.2 The distinction between fast and slow systems

If equilibrium between metal M and its ion M^+ is established rapidly a characteristic potential will be adopted by M relative to that of the constant

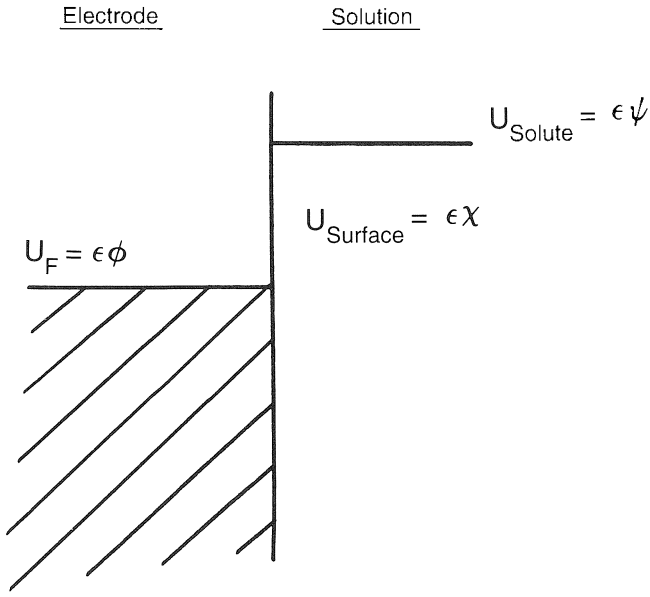

Figure 6.4 Energy levels relating to the various potentials at the electrode–solution interface.

potential of a reference electrode. A plausible model for this state of affairs is given in Figure 6.5 where an approximate coincidence is shown of the energy of the Fermi level U_F and the energy U_{M^+} of the maximum of the electronic energy distribution curve of the ion.

No net current will be observed since identical current components flow in either direction due to identical movements of charge. As soon as a potential is applied more negative (more reducing, or more cathodic) than the equilibrium value, E_{eq}, a net flow of electrons occurs from electrode to solution, i.e. from U'_F to U_{M^+} and the process $M^+ + e \rightarrow M$ is accelerated relative to the reverse reaction. A net cathodic current flows (Figure 6.6).

If a potential is applied more positive (more oxidizing, or more anodic) than E_{eq} a net current flows in the opposite direction since the process $M \rightarrow M^+ + e$ now occurs with electrons flowing from U_{M^+} to U''_F. The current–voltage graph takes the form shown in Figure 6.7.

Similar considerations apply to oxidation and reduction processes at inert electrodes. Let us consider the same metal ion M^+ and its reduction at such an inert electrode, i.e. one with which it does not react or enter into equilibrium. In this case no current will be observed until E_{eq} is reached, since only the oxidized form, M^+, is present with none of the reduced form, M. If the reduced form, M, can be dissolved in the electrode, e.g. in the form of an amalgam in the case of a mercury electrode, the corresponding anodic current–voltage curve may be obtained. To do this the amalgam

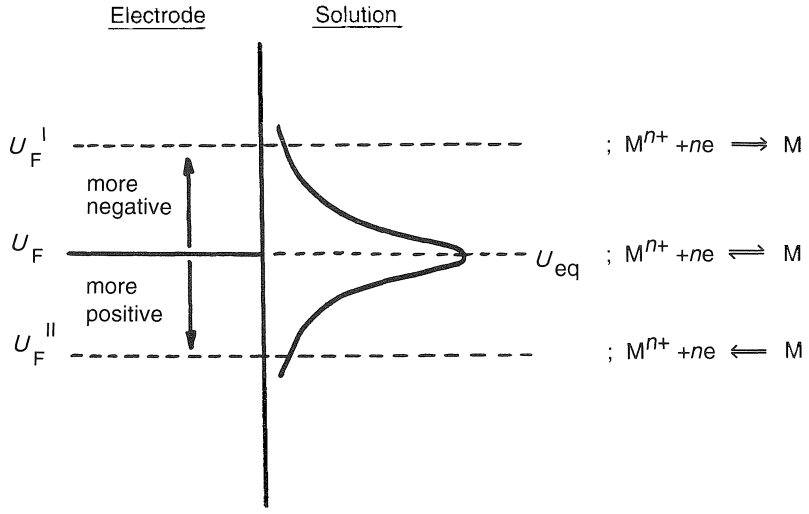

Figure 6.5 Dependence of the nature of an electrode reaction on the Fermi level of the electrode.

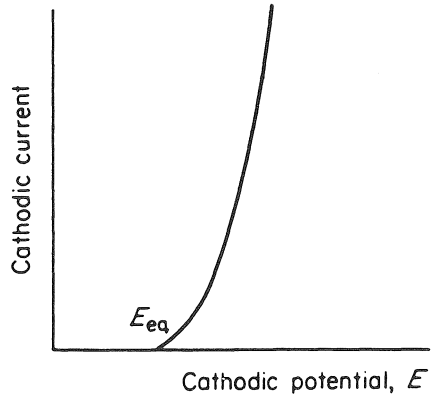

Figure 6.6 Current–potential curve for a cathodic process.

electrode and reference electrode would have to be placed in a solution containing no M^+ but some indifferent electrolyte to act as current carrier. At potentials with respect to the reference electrode more negative than E_{eq} no net current would be observed, but at more positive values a net anodic current would appear (Figure 6.8).

Consider now a redox system, e.g. M^{3+}/M^{2+}, and let both forms be present in a solution into which are placed an inert electrode and a suitable

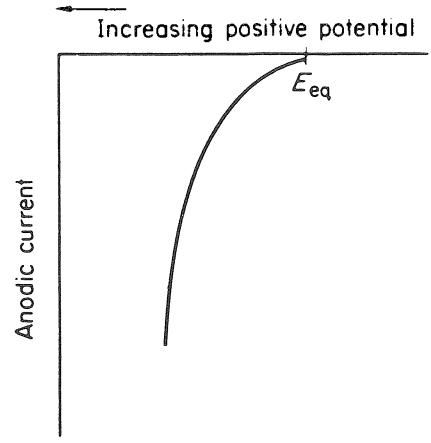

Figure 6.7 Current–potential curve for an anodic process.

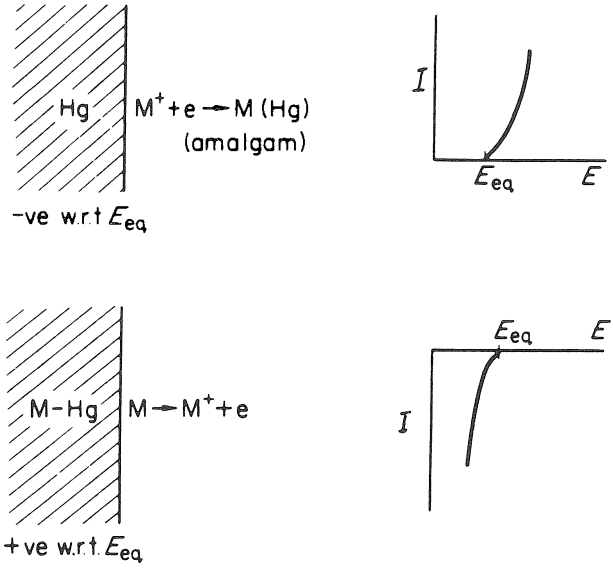

Figure 6.8 Cathodic and anodic reactions, with corresponding current–potential curves, at an inert electrode in which the reduced form is soluble.

reference electrode. If the equilibrium

$$M^{3+} + e \rightleftharpoons M^{2+}$$

is established instantaneously at the electrode surface then, with no exter-

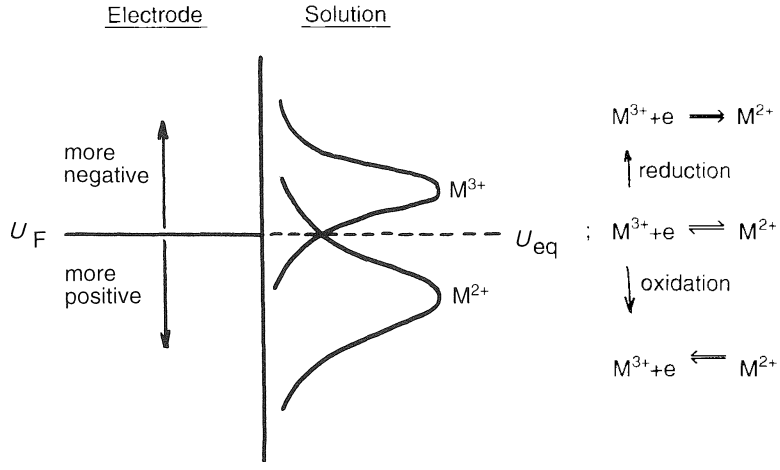

Figure 6.9 The nature of the net redox process shown as a function of the interaction of the Fermi level of the (inert) electrode and the energy distribution curves of the oxidized and reduced forms of the couple.

nally applied potential, the inert electrode adopts a characteristic potential, E_{eq} corresponding to $U_F = U_{redox}$ (Figure 6.9).

The distribution of electronic energy levels in M^{3+} and M^{2+} will differ to a small extent due to differing degrees of solvation consequent upon differing ion charges.

At potentials more negative than E_{eq} the current–voltage curve for the process $M^{3+} + e \rightarrow M^{2+}$ may be developed while at more positive potentials the curve for the process $M^{2+} - e \rightarrow M^{3+}$ occurs in a complementary way, the one passing smoothly into the other through E_{eq} (Figure 6.10).

All systems considered so far in this section may be classed as fast or reversible, the term 'fast' referring to the rapid attainment of equilibrium between an electrode and species in solution.

Figure 6.10 shows the variation of *net* current with applied potential (dashed curve) in relation to the currents of the individual forward and backward processes. This shows more clearly the flow of equal and opposite currents at E_{eq}; these being denoted by I_0, the exchange current. For such a system at potentials only slightly removed from E_{eq}, a net oxidation or reduction may be made to occur under almost reversible conditions with the Nernst equation applying.

In the case of slow or 'irreversible' systems, equilibrium is established so slowly that the condition is never seen to be reached. No significant current is seen near to E_{eq} and applied potentials well removed to both cathodic and anodic sides of this value are often required to produce currents of the same order of magnitude as those obtained for a fast system. Evidently

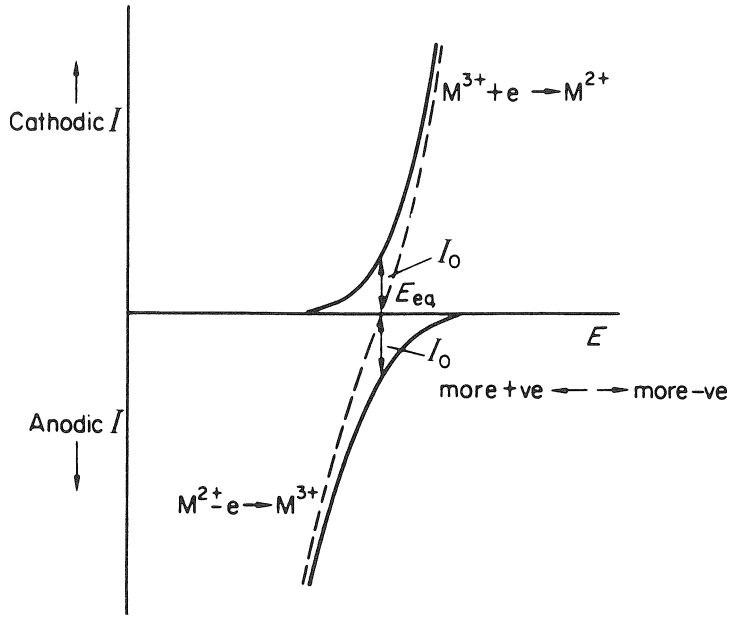

Figure 6.10 Anodic–cathodic current–potential curve for a 'fast' system.

the average energies of the electronic levels are both significantly removed from U_F (Figure 6.11).

In Figure 6.12 are shown schematically the shapes of current–voltage curves to be expected for a slow anodic–cathodic reaction. It is seen that, not only is a considerably more negative potential required for the slow system in order to obtain the same current as for the fast one, but the rate of increase of current is much less for the slow process. For the fast system the current rises almost vertically. In practice this would show some small deviation from the vertical and this reflects the influence of the comparative slowness of mass transfer processes. Slow electrochemical systems are said to require large overvoltage, $(E - E_{eq})$ or $(E_{eq} - E)$, in order to produce a significant net current and take place under irreversible conditions.

When an electrochemical reaction occurs the concentration of oxidizable or reducible species at the electrode surface is depleted and if fresh material is not provided electrolysis stops. In fact, mass transfer occurs, which tends to maintain surface concentrations constant. If the electrode reaction occurs much more rapidly than mass transfer processes, the latter are rate determining and control the magnitude of current which flows. This gives rise finally to a stationary state in which material reaching the electrode is oxidized or reduced as fast as it arrives at the surface. Later chapters

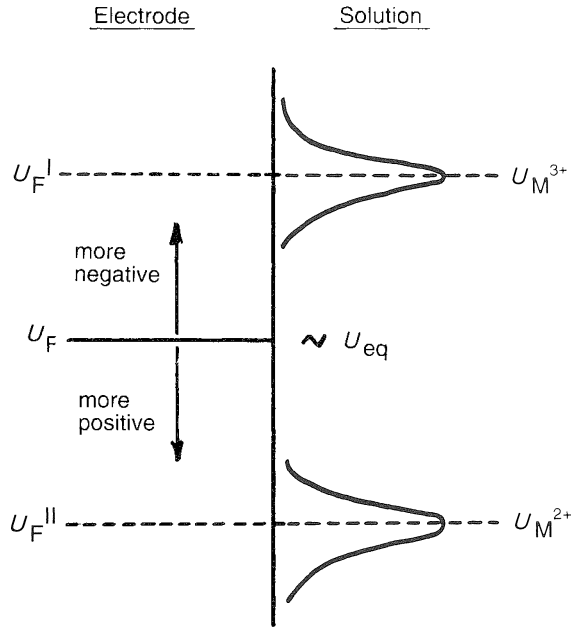

Figure 6.11 The energies of electronic levels of oxidized and reduced forms are both well removed from U_F and substantial additional energy, in the form of extra applied potential, is required to induce net reaction.

will consider the important implications of such situations for analytical electrochemistry.

6.5 The hydrogen scale and the IUPAC convention

In the last section variation of the relative value of the potential of an electrode with respect to some reference value was considered. It has been established that it is impossible to determine absolute values of potentials adopted by electrodes. What *can* be done is to measure the value of $\Delta\phi$ for one redox system relative to that for another reference value. In more colloquial terms, the emf of a cell obtained by coupling the electrode (half-cell) in question with another electrode can be measured. If the latter is so constructed that it maintains an almost constant potential *whatever the potential difference* between the two electrodes, electrode potentials can be measured with respect to an arbitrarily chosen standard and given physical significance. The internationally agreed standard is the hydrogen electrode; this device operating with hydrogen gas at 1 atmosphere pressure, in contact with platinized platinum, in a solution of hy-

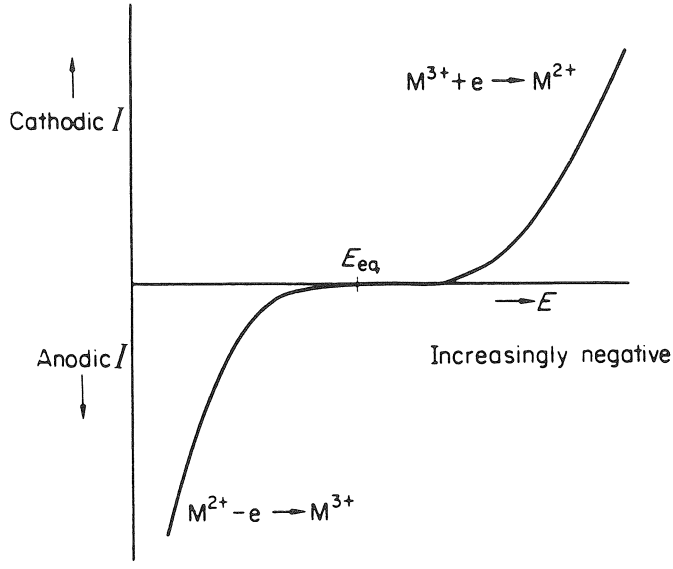

Figure 6.12 Anodic–cathodic current–potential curve for a 'slow' system.

drogen ions of unit activity, is assigned a potential of zero *at all temperatures.*

6.5.1 The standard hydrogen electrode

The hydrogen electrode, depending for its operation on establishment of the equilibrium

$$\tfrac{1}{2}H_2 \rightleftharpoons H^+ + e$$

requires that gaseous hydrogen and hydrogen ions in solution be brought together at the surface of a suitable catalyst. Equilibrium is attained rapidly at platinum black. The finely divided platinum is supported on platinum foil acting as an electronic conductor. This part of the electrode is made by first cleaning the foil in chromic acid and then plating it in a solution of 1% platinum(IV) chloride with an anode of platinum. The necessary thin layer of the catalytic material is in this way cathodically deposited on the foil. Unfortunately, this process causes the occlusion of some chlorine in the deposit and this must be removed by making the electrode the cathode for a short-term electrolysis in dilute sulphuric acid. Chlorine is swept away in the stream of electrolytically generated hydrogen.

In operation this electrode dips into a solution of hydrogen ions of constant activity while hydrogen gas passes over its surface. In Figure 6.13

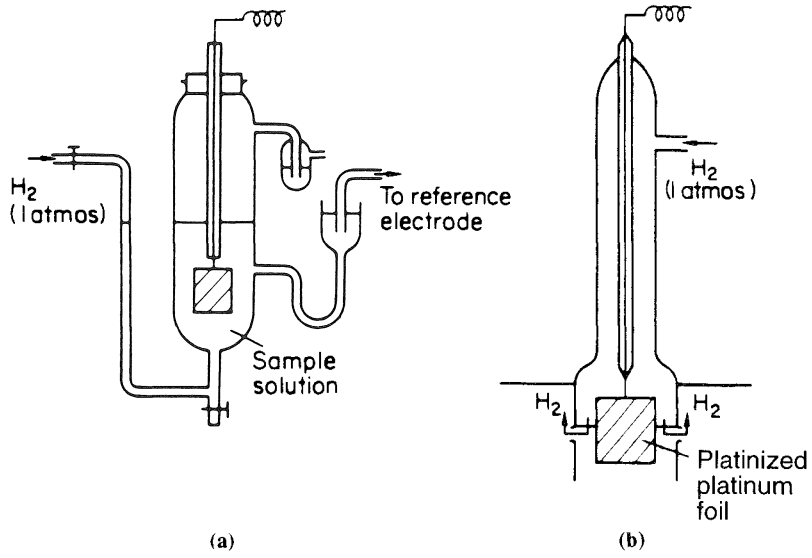

Figure 6.13 Two forms of hydrogen electrode. (a) Lindsey type: hydrogen bubbles upwards over the platinum foil surface. (b) Hildebrand type: a series of holes are blown in the glass envelope surrounding the platinum foil. The gas flow rate is adjusted so that hydrogen only escapes through these. The level of solution inside the envelope fluctuates so that part of the foil is exposed alternately to solution and gas.

are shown two types of hydrogen electrode: the one has the electrolyte solution enclosed and protected from possible air contamination, the other may be dipped into a solution whose hydrogen ion concentration is to be determined. The former is more desirable for the determination of electrode potentials; the latter is suited for following changes in hydrogen ion concentrations as in titrations.

It is vital that the hydrogen gas is pure and for the most accurate work even commercially pure hydrogen should be bubbled through alkaline pyrogallol or passed over heated palladized asbestos to remove the last traces of oxygen. Since the passage of gas through the electrode solution can cause a change of its concentration, prior passage of the purified gas through a sample of this solution is desirable.

Satisfactory functioning of the hydrogen electrode is, above all, dependent on the complete absence of catalyst poisons such as mercury and arsenic and particularly sulphur compounds. Consequently, rubber tubing should not be used for connections; PVC or polythene are much more reliable materials. Before using a hydrogen electrode to determine the emf of a cell formed by coupling it with another half-cell, it should be checked against a duplicate electrode. The steady emf of a cell made up of two identical hydrogen half-cells should, of course, be zero. In operation hydrogen

electrode should be found to assume a steady potential within 20 min and this should be independent of the rate of bubbling. Dependence of the potential on bubbling rate is characteristic of poisoning as are also slowness in reaching equilibrium and general variability of potential. Under these conditions it is necessary to clean and replatinize the electrode surface.

By applying the Nernst equation to the hydrogen electrode equilibrium it is seen that the potential of a hydrogen electrode is given by

$$E = E^{\ominus} + \frac{RT}{F} \ln \frac{a_{H^+}}{(a_{H_2})^{\frac{1}{2}}} = E^{\ominus} + \frac{RT}{F} \ln a_{H^+} - \frac{RT}{2F} \ln P_{H_2} \tag{6.24}$$

where P_{H_2} is the pressure of hydrogen gas.

When both the activities of hydrogen and hydrogen ion are unity, $E = E^{\ominus}$, which is arbitrarily given the value zero at all temperatures. Potentials of all other electrodes may then be given values relative to this standard.

6.5.2 *Electrode potential and cell emf sign conventions*

The signs which are to be given to electrode potentials and cell emf follow the convention adopted by the International Union of Pure and Applied Chemistry (IUPAC).

By the electrode potential of the half-cell M^{n+}/M is implied the emf of the cell formed by coupling the latter with a hydrogen half-cell. Since the potential of the latter is zero under standard conditions, the emf determined is the electrode potential of the M^{n+}/M couple. The cell may be represented by

$$Pt, H_2(a = 1)|H^+(a = 1)||M^{n+}|M \tag{6.25}$$

the electrode potential of the couple M^{n+}/M then being defined by

$$E_{cell} = E_{right} - E_{left} \tag{6.26}$$

with $E_{left} = 0$ for a standard hydrogen electrode.

In equation (6.25) a number of symbols commonly used in such cell representations are given. A vertical line usually implies a phase boundary between the species or components brought into equilibrium, e.g. an electrode and an electrolyte. A double vertical line usually represents the introduction of a salt bridge (see section 6.7) while a dotted vertical line may be used to represent the interface between two solutions in which electrical contact is maintained without short-term mixing. Commas usually link the components of an electrode or electrolyte system.

The sign of the electrode potential is decided very easily by whether hydrogen gas is evolved or hydrogen ionizes at the left-hand electrode. If on closing the circuit of cell (6.25) the hydrogen electrode becomes the positive pole by giving up electrons to hydrogen ions to give gaseous hydrogen, the

unknown electrode potential is negative and equal to the emf developed by the cell. On the other hand, if the hydrogen electrode becomes the negative pole, taking up electrons as hydrogen ionizes, the unknown electrode potential is positive and again equal to the emf developed by the cell. A table of International Standard Electrode Potentials on the hydrogen scale is given in Table 6.1.

Table 6.1 Standard electrode potentials, $E^{\ominus}$ (volts with respect to the Standard hydrogen electrode), at 298 K

Electrode	$E^{\ominus}$	Electrode	$E^{\ominus}$
Li^+/Li	−3.05	Cu^{2+}/Cu^+	+0.16
Ca^{2+}/Ca	−2.87	Bi^{3+}/Bi	+0.23
Na^+/Na	−2.71	Cu^{2+}/Cu	+0.34
Mg^{2+}/Mg	−2.37	O_2/OH^-	+0.40
Al^{3+}/Al	−1.66	Fe^{3+}/Fe^{2+}	+0.76
Zn^{2+}/Zn	−0.76	Ag^+/Ag	+0.80
Cd^{2+}/Cd	−0.40	Hg^{2+}/Hg	+0.80
Ni^{2+}/Ni	−0.25	Hg^{2+}/Hg_2^{2+}	+0.92
Pb^{2+}/Pb	−0.13	Cl_2/Cl^-	+1.36
H^+/H	0.00	Ce^{4+}/Ce^{3+}	+1.61

When an electrochemical cell is formed from two half-cells, one of which is not the hydrogen half-cell, the emf may be calculated from rule (6.26) using the individual half-cell potentials determined with respect to hydrogen. The electrode which has the more negative potential is always written on the left as the negative pole of the cell, while that with the more positive electrode potential is always written on the right as the positive pole of the cell. When this rule is followed, no ambiguity as to signs arises. It is seen that only in the *determination* of the sign of a half-cell potential is there a possibility of having a negative pole on the right; but here we are seeking to establish in which direction a particular cell reaction (involving the standard hydrogen electrode) is spontaneous. For a half-cell with established sign and magnitude of E, the direction of the spontaneous cell reaction is specified. Consider the Daniell cell in which one electrode is zinc dipping into a zinc sulphate solution, the other being copper dipping into copper sulphate solution. The two solutions are prevented from mixing by a porous membrane separating them. In accordance with the convention this cell may be represented by

$$Zn|ZnSo_4 \vdots CuSO_4|Cu$$

i.e.

$$Zn|Zn^{2+} \vdots Cu^{2+}|Cu$$

It is instructive to investigate such a cell more analytically in terms of

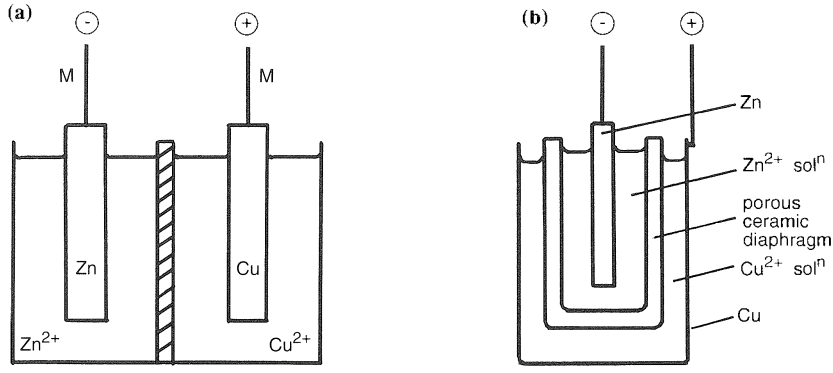

Figure 6.14 The Daniell cell. (a) Schematic form; (b) practical arrangement.

the potential differences at the various interfaces which it involves. For these purposes it is useful to visualize the cell in the schematic form of Figure 6.14(a), although the practical arrangement is as shown in Figure 6.14(b).

Combining equation (6.26) with the general expression for the potential of the two half-cells, viz.

$$E_{\text{half-cell}} = \Sigma\Delta\phi_{\text{interfaces}} \tag{6.27}$$

the expression for the emf of the cell becomes:

$$E_{\text{cell}} = ({}_{\text{R}}\phi_{\text{M}} - \phi_{\text{Cu}}) + (\phi_{\text{Cu}} - \phi_{\text{Cu}^{2+}}) + (\phi_{\text{Cu}^{2+}} - \phi_{\text{Zn}^{2+}}) + (\phi_{\text{Zn}^{2+}} - \phi_{\text{Zn}}) + (\phi_{\text{Zn}} - {}_{\text{L}}\phi_{\text{M}}) \tag{6.28}$$

There are *two* ways of using equation (6.28). Firstly, it may be expressed in terms of various $\Delta\phi$ terms as follows:

$$E_{\text{cell}} = \Delta\phi^{\text{M}}_{\text{Cu}} + \Delta\phi^{\text{Cu}}_{\text{Cu}^{2+}} \pm (\Delta\phi^{\text{Cu}^{2+}}_{\text{Zn}^{2+}}) - \Delta\phi^{\text{Zn}}_{\text{Zn}^{2+}} - \Delta\phi^{\text{M}}_{\text{Zn}} \tag{6.29}$$

Equation (6.29) emphasizes the existence of the small but significant liquid junction potential, $\Delta\phi^{\text{Cu}^{2+}}_{\text{Zn}^{2+}}$ a quantity difficult to measure accurately but easily minimized. Secondly, cancellation of like terms in equation (6.28) yields the simple expression

$$E_{\text{cell}} = {}_{\text{R}}\phi_{\text{M}} - {}_{\text{L}}\phi_{\text{M}} \tag{6.30}$$

Equation (6.30) emphasizes that the cell emf is the difference in inner potentials of the two connecting wires.

6.5.3 *Calculation of cell emf values from tabulated data*

It is a useful exercise to write down all the information, including electrode reactions, which is implied by the use of data from Table 6.1 applicable to the half-cell components to left and right. Thus, for the Daniell cell, knowing only the values of $E^{\ominus}_{Cu^{2+}|Cu}$ and $E^{\ominus}_{Zn^{2+}|Zn}$ it is possible to summarize its behaviour and orientation in the following way

Left-hand electrode	*Right-hand electrode*
ANODE	CATHODE
Negative pole	Positive pole
Oxidation occurs	*Reduction* occurs
$Zn \rightarrow Zn^{2+} + 2e$	$Cu^{2+} + 2e \rightarrow Cu$
$E^{\ominus} = -0.76\,V$	$E^{\ominus} = +0.34\,V$

Overall

$$Zn + Cu^{2+} \rightarrow Zn^{2+} + Cu$$

$$E^{\ominus}_{cell} = +0.34 - (-0.76)$$
$$= +1.10\,V$$

It can be seen that when the cell is represented correctly there is no ambiguity in regard to the direction in which the reaction proceeds spontaneously.

The meaning and significance of the terms *anode* and *cathode* which have been introduced above should be clearly understood. It is particularly important to distinguish them from *polarities*. The term *cathode* describes the electrode at which *reduction* occurs: in a spontaneous cell, as discussed here, this will be the *more positive* pole of the cell, but in an electrolysis cell where such processes are *induced*, such an electrode will be the more negative pole. In a complementary way, the term *anode* describes the electrode at which *oxidation* occurs: for a spontaneous cell this will be the more negative pole but the more positive one in an electrolysis cell.

6.6 Other reference electrodes

It is often more convenient to use subsidiary or secondary reference electrodes whose potentials have been accurately determined with respect to that of the hydrogen electrode. A number of useful systems give reproducible potentials over a long period. Quite apart from the experimental inconveniences of the hydrogen electrode, secondary reference electrodes may be chosen which do not show the major disadvantages of the primary standard. The latter cannot be used in solutions containing chemically reducible species and is susceptible to poisoning.

The most useful reference systems are those described as electrodes of the second kind. These are quite different to systems such as Cu/Cu^{2+} and Zn/Zn^{2+} which are electrodes of the first kind.

Electrodes of the second kind have the following form: metal, in contact with one of its sparingly soluble salts, placed in a solution containing a strongly ionized salt with a common anion. The calomel electrode is a case in point and is represented by

$$Hg|Hg_2Cl_2(s),\ KCl\,aq.$$

The term *calomel* deriving from the earlier trivial name for mercury(I) chloride.

Other examples are the silver/silver chloride and mercury/mercury(I) sulphate electrodes

$$Ag|AgCl(s), KCl\,aq.$$

and

$$Hg|Hg_2SO_4(s), K_2SO_4\,aq.$$

It is important to be very clear in regard to the reactions upon which the operation of such electrodes depends. For the calomel half-cell the reaction is

$$Hg_2Cl_2 + 2e \rightleftharpoons 2Hg + 2Cl^-$$

and similarly for the silver–silver chloride electrode

$$AgCl + e \rightleftharpoons Ag + Cl^-$$

In particular it should be noted that the structure and reaction of the silver/silver chloride electrode is quite distinct from those of the silver/silver ion electrode.

The potential adopted by each of these reference electrodes is controlled by the activity of the *anion* in solution. This may be shown quite simply by considering a calomel electrode in which the chloride ion activity is a_{Cl^-}. The potential adopted by the *mercury* depends upon the activity of the Hg_2^{2+} ion, so that

$$E = E^{\ominus}_{Hg} + \frac{RT}{2F} \ln a_{Hg_2^{2+}} \tag{6.31}$$

Now, $a_{Hg_2^{2+}} \times a^2_{Cl^-} = K_{Hg_2Cl_2}$, the solubility product of calomel, i.e.

$$a_{Hg_2^{2+}} = \frac{K_{Hg_2Cl_2}}{a^2_{Cl^-}} \tag{6.32}$$

Substitution of equation (6.32) into equation (6.31) gives

$$E = E^{\ominus}_{Hg} + \frac{RT}{2F} \ln \frac{K_{Hg_2Cl_2}}{a^2_{Cl^-}} \tag{6.33}$$

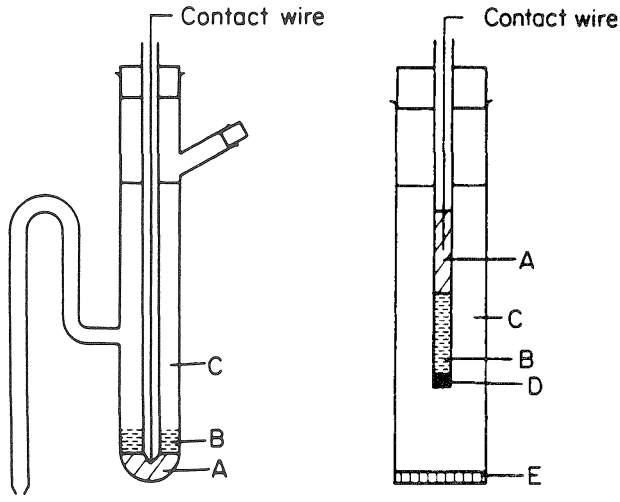

Figure 6.15 Two forms of calomel electrode. A. Mercury. B. Mercury–calomel paste. C. Potassium chloride solution. D. Asbestos or glass wool plug. E. Sintered glass.

or

$$E = \left[E^{\ominus}_{Hg} + \frac{RT}{2F} \ln K_{Hg_2Cl_2}\right] - \frac{RT}{2F} \ln a^2_{Cl^-} \qquad (6.34)$$

Since the terms in brackets form a constant, which we may denote by $E^{\ominus}_{Hg_2Cl_2}$, equation (6.34) may take the form

$$E = E^{\ominus}_{Hg_2Cl_2} - \frac{RT}{F} \ln a_{Cl^-} \qquad (6.35)$$

Three types of calomel have been commonly used, distinguishable by different concentration of potassium chloride. Their characteristics are summarized in Table 6.2.

Table 6.2 Potentials adopted by calomel electrodes with different concentrations of KCl

Electrode	Potential (V, versus Standard hydrogen electrode)
0.1 mol dm^{-3} KCl	+0.336
1 mol dm^{-3} KCl	+0.283
Saturated KCl	+0.242

plus1.5bp

Two forms of calomel electrode are shown in Figure 6.15.

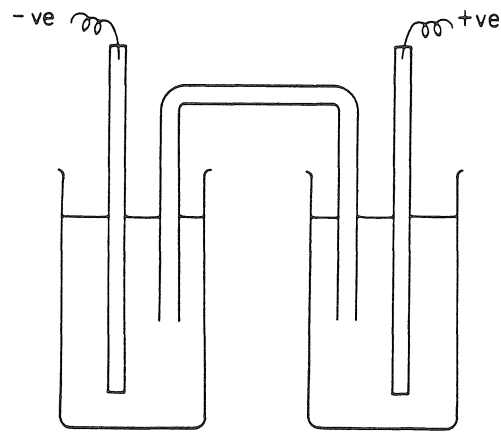

Figure 6.16 Connection of half-cells by means of a salt bridge containing a suitable electrolyte to eliminate the junction potential. For KCl and NH_4NO_3, $t_+ \sim t_- \sim 0.5$.

6.7 Concentration cells and emf measurements

It has been seen that the coupling of two half-cells produces an electrochemical cell which may be used to produce an emf. In the Daniell cell the two half-cell components are brought into electrical contact by a porous membrane separating the copper sulphate and zinc sulphate solutions. There will inevitably be interdiffusion of zinc and copper ions. Usually the ions from such solutions in contact will diffuse at different rates, leading to a charge separation across the interface which will give rise to a potential difference in this region which ultimately becomes steady. Any measurement of the cell emf will under these conditions include a contribution from this diffusion or liquid junction potential. Liquid junction potentials are extremely difficult to reproduce in practice and, even though their magnitudes do not normally exceed 100 mV, it is wisest for them to be eliminated if at all possible. This may be achieved by connecting solutions in two half-cells by means of a salt bridge (Figure 6.16). This is either a glass or flexible tube containing a saturated solution of either potassium chloride or ammonium nitrate. To prevent excessive diffusion, the ends of the tubes are often plugged with porous material, such as filter paper or glass wool, and the electrolytes are frequently set in agar gel. Transport numbers of cation and anion in solutions of potassium chloride and ammonium nitrate are approximately equal and if such species serve to carry current in a salt bridge between two half-cells the rates of movement of charge in either direction will be approximately equal. Such minimization of charge separation may serve to reduce liquid junction potentials to a few millivolts.

Cell emf's may be measured potentiometrically by comparison with a standard cell of known reproducible emf. A Weston Standard Cadmium

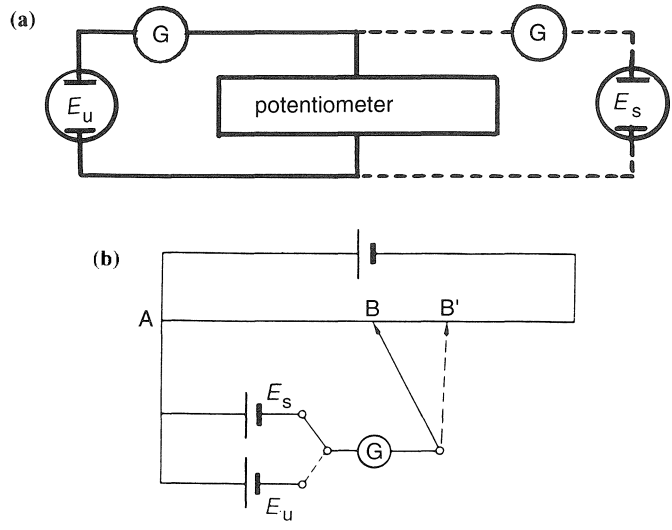

Figure 6.17 (a) Schematic circuit for determination of cell emf. **(b)** Poggendorf potentiometric circuit for determination of cell emf. E_s = emf of standard, E_u = emf of unknown. $E_u/E_s = AB'/AB$.

cell is frequently used for such purposes to calibrate coils or, more historically, the slide-wire of a potentiometer (Figure 6.17). By means of such a device the natural emf of a cell is balanced by an equal and opposite applied emf. Balance in this 'null-point' method is identified by approach to the equilibrium potential E_{eq} along the path identified in Figure 6.9 and recognized by zero deflection in the galvanometer.

It is clearly necessary for the two emfs to act *in opposition* : if the polarity of a cell is unknown this will be soon remedied for only if connection is made in accordance with this property will balance be obtainable.

6.8 Concentration cells without liquid junctions

Concentration cells are made up of two half-cells which are similar chemically but which differ in the activity of some common component: the difference gives rise to an emf because of the difference in potential of the two half-cells. The activity difference may be either between the solutions or between the electrode materials.

6.8.1 Cells with amalgam electrodes

Such a cell is formed by two metal amalgam electrodes of different metal activity dipping into a common solution of a soluble salt of the metal, e.g.

$$\begin{array}{lccl} \textit{Anode}\ (-\text{ve pole}) & \text{Hg, Tl} & |\text{TlNO}_3| & \text{Tl, Hg (+ve pole) } \textit{cathode} \\ & a_2 & & a_1 \quad (a_2 > a_1) \\ & E_2 & & E_1 \end{array}$$

activity of Tl^+ ions in solution $= a_+$.

$$\begin{array}{cc} \textit{Oxidation} & \textit{Reduction} \\ \text{Tl}(a_2) \rightarrow \text{Tl}^+ + \text{e} & \text{Tl}^+ + \text{e} \rightarrow \text{Tl}(a_1) \\ E_2 = E^{\ominus}_{\text{Tl}} + \dfrac{RT}{F} \ln \dfrac{a_+}{a_2} & E_1 = E^{\ominus}_{\text{Tl}} + \dfrac{RT}{F} \ln \dfrac{a_+}{a_1} \end{array}$$

Overall $\text{Tl}(a_2) \rightarrow \text{Tl}(a_1)$. Since $a_2 > a_1, E_1 > E_2$. Therefore,

$$E_{\text{cell}} = E_1 - E_2 = \frac{RT}{F} \ln \frac{a_2}{a_1} \tag{6.36}$$

It should be noted that equation (6.36) gives the instantaneous cell emf which will fall as the ratio a_2/a_1 decreases due to transfer of material. Overall, the cell reaction involves the passage of thallium from the higher to the lower activity. When these activities become equal, the potentials of both electrodes are the same and the cell ceases to operate. For the passage of 1 Faraday, the free energy change accompanying the movement of 1 mole of thallium from a_2 to a_1 is

$$\Delta G = -RT \ln \frac{a_2}{a_1}$$

and since $\Delta G = -nEF$ (and $n = 1$)

$$E_{\text{cell}} = \frac{RT}{F} \ln \frac{a_2}{a_1} \qquad \text{(see equation (6.36))}$$

6.8.2 *Cells with gas electrodes operating at different pressures*

Here we may consider a cell consisting of two hydrogen electrodes operating at different pressures dipping into a common solution of hydrochloric acid, e.g.

$$\begin{array}{lccl} \textit{Anode} & (-\text{ve pole}) & & (+\text{ve pole}) \quad \textit{Cathode} \\ & \text{Pt, } H_2 & | \text{ HCl } | & H_2, \text{ Pt} \\ & P_2 & & P_1 (P_2 > P_1) \\ & E_2 & & E_1 \end{array}$$

Oxidation	*Reduction*
$\frac{1}{2}H_2(P_2) \rightarrow H^+ + e$	$H^+ + e \rightarrow \frac{1}{2}H_2(P_1)$
$E_2 = E^{\ominus}_{H_2} + \frac{RT}{F}\ln\frac{a_{H^+}}{(a_{H_2})^{1/2}}$	$E_1 = E^{\ominus}_{H_2} + \frac{RT}{F}\ln\frac{a_{H^+}}{(a_{H_2})^{1/2}}$
$= \frac{RT}{F}\ln a_{H^+} - \frac{RT}{F}\ln(P_2)^{1/2}$	$= \frac{RT}{F}\ln a_{H^+} - \frac{RT}{F}\ln(P_1)^{1/2}$

Overall $\frac{1}{2}H_2(P_2) \rightarrow \frac{1}{2}H_2(P_1)$.

Again, $E_1 > E_2$. Therefore,

$$E_{cell} = E_1 - E_2 = \frac{RT}{2F}\ln\frac{P_2}{P_1} \tag{6.37}$$

6.8.3 *Concentration cells without transference*

One can form such a cell by connecting two cells of the Harned type in opposition to one another; in this way a composite cell is formed.

The simplest type of Harned cell is

Anode	*Cathode*
(−ve pole)	(+ve pole)
H_2(1 atm), Pt | HCl |	AgCl(s), Ag

Oxidation	*Reduction*
$\frac{1}{2}H_2 \rightarrow H^+ + e$	$AgCl(s) + e \quad Ag(s) + Cl^-$

Overall cell reaction:

$$H_2(1\text{ atm}) + AgCl(s) \rightarrow Ag(s) + Cl^- + H^+$$

Thus, the free energy change for the passage of 1 Faraday is

$$\Delta G = -nFE = \Delta G^{\ominus} + RT\ln\frac{a_{Ag}a_{H^+}a_{Cl^-}}{(a_{H_2})^{\frac{1}{2}}a_{AgCl}}$$

which, since the activities of silver, hydrogen and silver chloride are constant and unity, becomes

$$\Delta G = \Delta G^{\ominus} + RT\ln a_{H^+}a_{Cl^-}$$

or

$$E = E^{\ominus} - \frac{RT}{F}\ln a_{H^+}a_{Cl^-} = E^{\ominus} - \frac{2RT}{F}\ln(a_{\pm})_{HCl} \tag{6.38}$$

Such cells are useful for determining mean ion activity coefficients of acid in the central solution (see Chapter 8).

A composite of two such cells may be represented as

$$\underset{\substack{(a_\pm)_2\\E_2}}{\text{Ag, AgCl(s)|HCl|Pt, H}_2\text{(1 atm)}} \quad \underset{\substack{(a_\pm)_1\\E_1}}{\text{Pt, H}_2\text{(1 atm)|HCl|AgCl(s), Ag}}$$

The left-hand cell has electrodes reversed with respect to the Harned cell considered above, i.e.

$$E_{\text{left cell}} = \frac{2RT}{F} \ln (a_\pm)_2 - E^\ominus = -E_2 \qquad \text{(according to equation (6.38))}$$

The right-hand cell has electrodes in the conventional arrangement, i.e.

$$E_{\text{right cell}} = E^\ominus - \frac{2RT}{F} \ln (a_\pm)_1 = E_1$$

The resultant emf of the composite cell is thus given by

$$E_{\text{cell}} = E_{\text{left}} + E_{\text{right}} = -E_2 + E_1 = \frac{2RT}{F} \ln \frac{(a_\pm)_2}{(a_\pm)_1} \tag{6.39}$$

In order for this to be positive, it is necessary that $(a_\pm)_2 \geq (a_\pm)_1$ so that $E_1 > E_2$. No physical transfer of material occurs from one side to the other but, if $(a_\pm)_2 > (a_\pm)_1$, the net effect during the working of the cell is the deposition of H^+ and Cl^- at their respective reversible electrodes in the left-hand cell and dissolution of H^+ and Cl^- at appropriate electrodes on the right. If the cell is allowed to discharge, the resultant effect is a spontaneous decline in $(a_\pm)_2$ and increase in $(a_\pm)_1$.

If the cell is rewritten with the hydrogen electrodes at extreme left and right, the section of the composite cell containing the higher mean activity of HCl, $(a_\pm)_2$, must now appear on the right as follows:

$$\underset{\substack{(a_\pm)_1\\E_1}}{\text{Pt, H}_2\text{(1 atm)|HCl|AgCl(s), Ag}} \quad \underset{\substack{(a_\pm)_2\\E_2}}{\text{Ag, AgCl(s)|HCl|Pt, H}_2\text{(1 atm)}}$$

The left-hand cell now has the conventional Harned orientation so that

$$E_{\text{left cell}} = E^\ominus - \frac{2RT}{F} \ln (a_\pm)_1 = E_1$$

Conversely, the right-hand cell is now reversed and its emf is given by

$$E_{\text{right cell}} = \frac{2RT}{F} \ln (a_\pm)_2 - E^\ominus = -E_2$$

so that the resultant emf of the composite cell is given by

$$E_{\text{cell}} = E_{\text{left}} + E_{\text{right}} = E_1 - E_2 = \frac{2RT}{F} \ln \frac{(a_\pm)_2}{(a_\pm)_1}$$

which is seen to be identical to equation (6.39).

The electrode at extreme right adopts a relatively positive potential (due to deposition of H^+ from $(a_\pm)_2$) with respect to the electrode at extreme left which adopts a relatively negative potential (due to dissolution of H^+ into $(a_\pm)_1$). The overall effect in a discharging cell remains a spontaneous decline in $(a_\pm)_2$.

In the general case with an electrolyte comprising ν_+ cations and ν_- anions ($\nu_+ + \nu_- = \nu$) equation (6.39) becomes

$$E = \frac{\nu}{\nu_\pm} \cdot \frac{RT}{F} \ln \frac{(a_\pm)_2}{(a_\pm)_1} \tag{6.40}$$

ν_+ or ν_- being used in the latter expression according to whether the outer electrodes are reversible with respect to cations or anions.

Consider the connection of two Harned cells of the type considered above with HCl at molality $m_1 = 0.01\,\text{mol kg}^{-1}$ and $m_2 = 0.1\,\text{mol kg}^{-1}$ respectively and $E = 0.2225\,\text{V}$. Calculation of $\gamma_\pm$ for both cases via the extended Debye–Hückel equation yields $(a_\pm)_1 = 0.0090$ and $(a_\pm)_2 = 0.0755$. Individual cell emf values are, according to equation (6.38), $E_1 = 0.4643\,\text{V}$ and $E_2 = 0.3551\,\text{V}$.

Thus, by equation (6.39) $E_{\text{cell}} = 0.1092\,\text{V}$ whether the connection of the two cells is via the hydrogen or silver components: in both cases the extreme right-hand electrode is seen to be positive relative to the extreme left-hand electrode. In the former case the silver electrode on the extreme right adopts a potential of +0.4643 V while that at the extreme left adopts +0.3551 V; in the latter case the platinum contact on the extreme right adopts a potential of −0.3551 V while that at the extreme left adopts −0.4643 V. Calculations of E_{cell}, based upon individual cells, are seen to be consistent with the general expression (6.40) involving the ratio of the mean activities of HCl, i.e.

$$E_{\text{cell}} = 2 \times 0.02567 \ln \frac{0.0755}{0.0090} = 0.1092\,\text{V}$$

6.9 Concentration cells with liquid junctions

Cells within this category may be conveniently divided into two classes according to whether a liquid junction potential is present or eliminated by connection of the two half-cells by means of a salt bridge.

6.9.1 Cells with a liquid junction potential

Consider two half-cells having identical electrodes dipping into their respective solutions containing the same electrolyte but at different mean ion activities. Electrical contact between the half-cells is made by the two solutions meeting at a junction. Such a cell may be represented by

$$\begin{array}{cccccc} \mathrm{M} & | & \mathrm{MX} & \vdots & \mathrm{MX} & | & \mathrm{M} \\ (a_+)_1, & & (a_-)_1 & & (a_+)_2, & & (a_-)_2 \end{array}$$

where

$$(a_+)_2 > (a_+)_1, (a_-)_2 > (a_-)_1$$

with the electrodes reversible with respect to M^+ cations.

At the right-hand electrode, for the passage of 1 Faraday, 1 mole of M^+ ions will be deposited. However, migration of t_+ moles of M^+ across the junction will to some extent make good the loss of M^+ by the deposition process. Similarly, at the left-hand electrode, although 1 mole of M dissolves as M^+ ions, t_+ moles migrate out of the region towards the positive pole. This behaviour is summarized below.

Anode (−ve pole)			*Cathode* (+ve pole)
	$(a_+)_1, (a_-)_1$	$(a_+)_2, (a_-)_2$	
	$M \rightarrow M^+ + e$		$M^+ + e \rightarrow M$
	t_+ moles of M^+ migrate out	t_+ moles of M^+ migrate in	
	net gain of $(1 - t_+)$ moles of M^+ = t_- moles at $(a_+)_1$	net loss of $(1 - t_+)$ moles of M^+ = t_- moles at $(a_+)_2$	
	gain of t_- moles of X^- at $(a_-)_1$	loss of t_- moles of X^- at $(a_-)_2$	

t_+, t_- are the average transport numbers for the two activities of the electrolyte involved. It is clear that the overall process involves the transfer of material from the higher to the lower activity, viz.

$$\begin{array}{cccc} t_-\mathrm{M}^+ + t_-\mathrm{X}^- & \rightarrow & t_-\mathrm{M}^+ + t_-\mathrm{X}^- \\ (a_+)_2 \quad (a_-)_2 & & (a_+)_1 \quad (a_-)_1 \end{array}$$

For the process the free energy change per Faraday is

$$\Delta G = RT \ln \frac{(a_+)_1^{t_-} (a_-)_1^{t_-}}{(a_+)_2^{t_-} (a_-)_2^{t_-}} \tag{6.41}$$

since, by definition

$$a_+ a_- = (a_\pm)^2; a_+^{t_-} a_-^{t_-} = (a_\pm)^{2t_-}$$

therefore,

$$\Delta G = 2t_- RT \ln \frac{(a_\pm)_1}{(a_\pm)_2}$$

therefore

$$E_{\text{cell}} = 2t_- \frac{RT}{F} \ln \frac{(a_\pm)_2}{(a_\pm)_1} \tag{6.42}$$

It should be stressed that the transport number which appears in the equation for the cell emf is that of the ionic species with respect to which the electrodes are not reversible. For the general case where the electrolyte species provides ν ions of which there are ν_+ cations and ν_- anions, equations (5.31) takes the forms

$$E = t_- \left(\frac{\nu}{\nu_+}\right)\left(\frac{RT}{nF}\right) \ln \frac{(a_\pm)_2}{(a_\pm)_1} \tag{6.43}$$

or,

$$E = t_+ \left(\frac{\nu}{\nu_-}\right)\left(\frac{RT}{nF}\right) \ln \frac{(a_\pm)_2}{(a_\pm)_1} \tag{6.44}$$

according to whether the electrodes are reversible with respect to cations (equation (6.43)) or anions (equation (6.44)).

6.9.2 *Cells with eliminated liquid junction potentials*

Consider now the same half-cells as used in the previous section but joined via a salt bridge. This cell is represented by

$$\underset{(a_+)_1, (a_-)_1}{\text{M} \mid \text{MX}} \parallel \underset{(a_+)_2, (a_-)_2}{\text{MX} \mid \text{M}}$$

where

$$(a_+)_2 > (a_+)_1, \quad (a_-)_2 > (a_-)_1$$

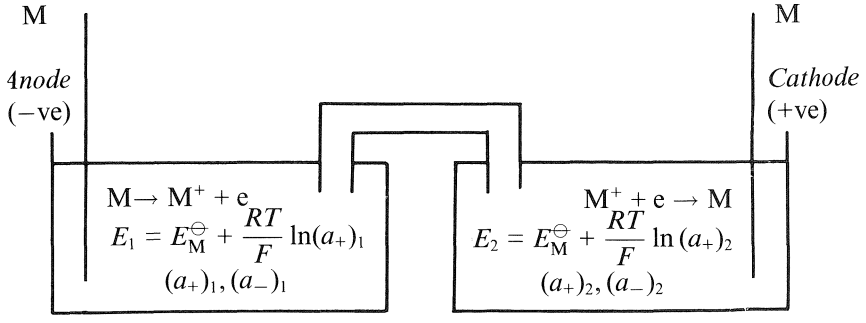

$$E_{\text{cell}} = E_2 - E_1 = \frac{RT}{F} \ln \frac{(a_+)_2}{(a_+)_1} \tag{6.45}$$

Now, since individual ion activity coefficients are inaccessible to measurement, the cell emf must be related to determinable mean ion activities. By definition,

$$\left(\frac{(a_{\pm})_2}{(a_{\pm})_1}\right)^2 = \frac{(a_+)_2(a_-)_2}{(a_+)_1(a_-)_1}$$

If it is assumed that

$$\frac{(a_+)_2}{(a_+)_1} \sim \frac{(a_-)_2}{(a_-)_1}$$

then

$$\frac{(a_{\pm})_2}{(a_{\pm})_1} \sim \frac{(a_+)_2}{(a_+)_1}$$

and

$$E = \frac{RT}{F} \ln \frac{(a_{\pm})_2}{(a_{\pm})_1} \tag{6.46}$$

6.9.3 *Calculation of liquid junction potentials*

It is apparent that the difference between the emf values of the cells considered in sections 6.9.1 and 6.9.2 gives the liquid junction potential (E_{lj}) involved in the former. Thus

$$E_{lj} = 2t_- \frac{RT}{F} \ln \frac{(a_{\pm})_2}{(a_{\pm})_1} - \frac{RT}{F} \ln \frac{(a_{\pm})_2}{(a_{\pm})_1} \tag{6.47}$$

Therefore,

$$E_{lj} = (2t_- - 1)\frac{RT}{F} \ln \frac{(a_{\pm})_2}{(a_{\pm})_1} \tag{6.48}$$

Now

$$t_+ + t_- = 1$$

Therefore,

$$(2t_- - 1) = t_- - t_+$$

Therefore,

$$E_{lj} = (t_+ - t_-)\left(\frac{RT}{F}\right) \ln \frac{(a_{\pm})_2}{(a_{\pm})_2} \tag{6.49}$$

The general form of equation (6.48) is

$$E_{lj} = \left(t_{\mp}\left(\frac{\nu}{\nu_{\pm}}\right) - 1\right) \frac{RT}{nF} \ln \frac{(a_{\pm})_2}{(a_{\pm})_1} \tag{6.50}$$

6.10 Membrane equilibria

When two solutions of the same salt at different concentrations are separated by a membrane which is permeable to both ion species, the potential across the membrane is identifiable with the junction potential between the solutions given by equation (6.50). If the membrane has a pore size that shows *restricted* permeability to one ion species, the transport number appearing in equation (6.50) is that of this species across the membrane.

Such phenomena are of great significance in biological cell membrane systems. Cell solutions usually contain a higher proportion of potassium salts than sodium salts while external solutions usually show the reverse. The cell surface may therefore be treated as a membrane separating solutions of potassium and sodium ions and which exhibits considerably lower permeability to sodium than to potassium ions. Potassium ions may therefore pass through the membrane from inside to outside the cell at a faster rate than sodium ions pass into the cell. The greater tendency for small, positively charged ions to pass to the outside of the cell leads to a charge distribution in which the interior tends to be negatively charged with respect to the exterior. Although a somewhat crude description, it does in fact summarize the essential condition at the membrane in nerve and muscle cells where electrical impulses are passed from one cell to another.

It is found that the above polarity may be reversed upon addition of species which may disturb the structure of the membrane and open it for transmission of larger ions. Such is the case if a quaternary ammonium salt is introduced near the membrane surface. It would appear that the organic cations are able to penetrate the membrane faster than the inorganic ions, so that they (temporarily at least) open the membrane structure and allow freer passage of inorganic ions. Such a mechanism has been postulated as a contributory factor in the control of the transmission of electrical impulse from one nerve cell to another and from nerve to muscle cells in an organism.

6.10.1 Membrane potentials

Consider two solutions with different concentrations of electrolyte and non-electrolyte species separated by a membrane. Suppose that the membrane allows passage of solvent molecules and at least one ionic species. After a time the concentrations of species in solutions either side of the membrane will reach equilibrium values. The concentration of any species which *cannot* pass through the membrane will remain constant.

When equilibrium is established, an *osmotic pressure difference* is set up across the boundary between the two solutions associated with an unequal distribution of diffusible material. Additionally, a *potential difference* (the membrane potential) is established across the membrane.

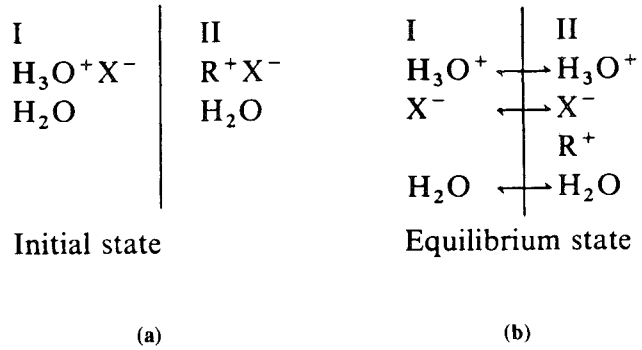

Figure 6.18 Distribution of ions within a system of solutions of electrolyte, RX, and acid, HX, separated by a membrane impermeable to R^+. (a) Initial state, (b) equilibrium state.

Consider the simple system in which an aqueous solution of a salt comprising R^+ and X^- ions is separated from an aqueous solution of the acid HX by a membrane which is *impermeable to* R^+. If the two solutions are labelled I and II, the initial and equilibrium situations may be represented by Figure 6.18.

It is assumed that R^+ on account of its size cannot diffuse through the membrane but that H_3O^+ and X^- will pass through until equilibrium is achieved. In this state the concentrations of H_3O^+ and X^- to the left of the membrane must be equal. In solution II to the right of the membrane X^- must electrically balance *both* R^+ and H_3O^+.

At equilibrium the following relationships must hold for electrochemical and chemical potentials of the three diffusible species.

$$\begin{aligned} {}^{\mathrm{I}}\tilde{\mu}_{H_3O^+} &= {}^{\mathrm{II}}\tilde{\mu}_{H_3O^+} \\ {}^{\mathrm{I}}\tilde{\mu}_{X^-} &= {}^{\mathrm{II}}\tilde{\mu}_{X^-} \\ {}^{\mathrm{I}}\mu_{H_2O} &= {}^{\mathrm{II}}\mu_{H_2O} \end{aligned} \tag{6.51}$$

Since the membrane is not permeable to R^+, the pressure of the two phases will differ and it is necessary to allow for the variation of chemical potential with pressure, $(\partial\mu_i/\partial P)_T = V_i$. The chemical potential of species i is related to its activity a_i by

$$\mu_i = \mu_i^{\ominus} + RT \ln a_i \tag{6.52}$$

Now, $\mu_i^{\ominus}$, which occurs in both electrochemical and chemical potentials, may be expressed as

$$\mu_i^{\ominus} = \mu_i^* + \int_0^P V^{\ominus} \mathrm{d}P \tag{6.53}$$

Where μ_i^*, is the value corresponding to $P = 0$ and $V^{\ominus}$ is the molar volume in the standard state. If, as an approximation we neglect the compressibility of the solution, we may write $V^{\ominus} = V$ = constant. Thus

$$\mu_i^{\ominus} = \mu_i^* + VP \tag{6.54}$$

and

$$\mu_i = \mu_i^* + VP + RT \ln a_i \tag{6.55}$$

Therefore, for water, acting as solvent in this case,

$${}^{I}\mu_{H_2O} = {}^{I}\mu^*_{H_2O} + V_{H_2O}P^{I} + RT \ln {}^{I}a_{H_2O} \tag{6.56}$$

and

$${}^{II}\mu_{H_2O} = {}^{II}\mu^*_{H_2O} + V_{H_2O}P^{II} + RT \ln {}^{II}a_{H_2O} \tag{6.57}$$

Therefore

$$V_{H_2O}(P^{I} - P^{II}) = RT \ln \frac{{}^{II}a_{H_2O}}{{}^{I}a_{H_2O}} \tag{6.58}$$

and since for charged species the following holds

$$\tilde{\mu}_i = \mu_i + z_i F\phi \qquad \text{(see equations (2.5), (5.2))}$$

it is possible to arrive at expressions for the ionic diffusible species which complement equation (6.58) viz.

$$(P^{I} - P^{II})V_{H_3O^+} = RT \ln \frac{{}^{II}a_{H_3O^+}}{{}^{I}a_{H_3O^+}} + F(\phi^{II} - \phi^{I}) \tag{6.59}$$

and

$$(P^{I} - P^{II})V_{X^-} = RT \ln \frac{{}^{II}a_{X^-}}{{}^{I}a_{X^-}} - F(\phi^{II} - \phi^{I}) \tag{6.60}$$

where $(\phi^{II} - \phi^{I}) = \Delta\phi$ (the membrane potential).

Elimination of $\Delta\phi$ between equations (6.59) and (6.60) gives

$$(P^{I} - P^{II}) = \left(\frac{RT}{V_{H_3O^+} + V_{X^-}}\right) \ln \left(\frac{{}^{II}a_{H_3O^+}{}^{II}a_{X^-}}{{}^{I}a_{H_3O^+}{}^{I}a_{X^-}}\right) \tag{6.61}$$

Elimination of $(P^{I} - P^{II})$ between equations (6.58) and (6.61) gives

$$\left(\frac{1}{V_{H_2O}}\right) \ln \left(\frac{{}^{II}a_{H_2O}}{{}^{I}a_{H_2O}}\right) = \left(\frac{1}{V_{H_3O^+} + V_{X^-}}\right) \ln \left(\frac{{}^{II}a_{\pm}^2}{{}^{I}a_{\pm}^2}\right) \tag{6.62}$$

or,

$$\frac{({}^{I}a_{\pm})^2}{({}^{I}a_{H_2O})^x} = \frac{({}^{II}a_{\pm})^2}{({}^{II}a_{H_2O})^x} \tag{6.63}$$

where

$$x = \frac{V_{H_3O^+} + V_{X^-}}{V_{H_2O}}$$

If $a_{H_2O} \sim 1$ in both phases, equation (6.63) becomes

$$^{I}a_{\pm} \sim {}^{II}a_{\pm} \tag{6.64}$$

The expression for $\Delta\phi$ may now be obtained by eliminating $(P^{I} - P^{II})$ between equation (6.58) and either equation (6.59) or equation (6.60)

$$\Delta\phi = \frac{RT}{F} \ln \left(\frac{{}^{II}a_{H_3O^+}}{{}^{I}a_{H_3O^+}} \right) \left(\frac{({}^{I}a_{H_2O})^{x+}}{({}^{II}a_{H_2O})^{x+}} \right) = \frac{RT}{F} \ln \left(\frac{{}^{I}a_{X^-}}{{}^{II}a_{X^-}} \right) \left(\frac{({}^{II}a_{H_2O})^{x-}}{({}^{I}a_{H_2O})^{x-}} \right) \tag{6.65}$$

where

$$x^+ = \frac{V_{H_3O^+}}{V_{H_2O}}; \quad x^- = \frac{V_{X^-}}{V_{H_2O}}$$

If again

$$^{I}a_{H_2O} \sim {}^{II}a_{H_2O}$$

$$\Delta\phi = \frac{RT}{F} \ln \left(\frac{{}^{II}a_{H_3O^+}}{{}^{I}a_{H_3O^+}} \right) = \frac{RT}{F} \ln \left(\frac{{}^{I}a_{X^-}}{{}^{II}a_{X^-}} \right) \tag{6.66}$$

The general expression for the membrane potential is

$$\Delta\phi = \frac{RT}{nF} \ln \frac{{}^{II}a_i}{{}^{I}a_i} = \frac{RT}{F} \ln \lambda \tag{6.67}$$

Here λ is known as the Donnan distribution coefficient, expressed by the membrane equilibrium condition in the presence of various ion types by

$$\left(\frac{{}^{II}a_{+}}{{}^{I}a_{+}} \right) = \left(\frac{{}^{II}a_{2+}}{{}^{I}a_{2+}} \right)^{1/2} = \left(\frac{{}^{II}a_{3+}}{{}^{I}a_{3+}} \right)^{1/3} = - - -$$

$$- - - = \left(\frac{{}^{I}a_{-}}{{}^{II}a_{-}} \right) = - - -$$

$$\left(\frac{{}^{I}a_{3-}}{{}^{II}a_{3-}} \right)^{1/3} = - - - = \lambda \tag{6.68}$$

Although the individual ion activities contained in λ cannot be measured, they may be replaced, for experimental purposes, by mean ion activities provided that solutions of such dilution are used that the Debye–Hückel limiting law holds.

The Donnan equilibrium has frequently been cited as controlling the movement of water and electrolytes into and out of biological cells. While chemical processes within the living cell can control the permeability of cell membranes to various species, explanations of the origin of steady natural cell membrane potentials cannot successfully be built on a *thermodynamic* equation. Expressions for such potentials of the *form* of the Donnan equation may be established from *kinetic* principles which involve *steady-state* concentration differences of species within and external to natural cells.

6.10.2 Dialysis

Membrane equilibria are made use of in the separation by dialysis of inorganic ions from solutions of biologically important polyelectrolytes such as nucleic acids and proteins. Dialysis is based on the principle that a membrane allows free passage of small particles in true solution through it while retaining particles of colloidal dimensions. If the solvent on the exit side of the membrane is continuously renewed, the particles escaping through the membrane are removed, further transference through the membrane encouraged and separation of the colloid species made feasible. In the technique of electrodialysis, removal of ions is made easier by an electric field. The solution containing the macroparticles is placed between two membranes with pure solvent on either side and an emf imposed between electrodes placed in the solvent compartments.

It is sometimes advantageous to take advantage of membrane hydrolysis and this is used to convert proteins into acidic forms without recourse to conventional chemical means which might interfere with the system. Consider dialysis into pure water of a salt NaR from a solution through a membrane which allows passage of Na^+ but is impermeable to R^-

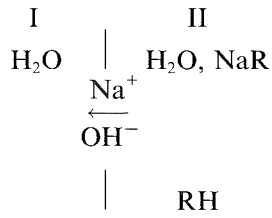

Sodium ions from II diffuse into I along with an equivalent number of hydroxyl ions. These latter arise from the dissociation of water which is necessary to maintain electroneutrality of I. The hydrogen ions produced by this process then associate with anions R^- to form the weak acid RH and maintain the electroneutrality of II. The initial and final equilibrium concentrations for the two solutions on either side of the membrane are as follows:

	I	II
Initial State	$[Na^+] = 0$	$[Na^+] = [R^-] = c$
Equilibrium condition	$[Na^+] = x = [OH^-]$	$[Na^+] = c - x$ $[R^-] = c$ $[H^+] = x$

At equilibrium, in accordance with equation (6.64)

$$({}^{I}a_{Na^+}{}^{I}a_{OH^-}) = ({}^{II}a_{Na^+}{}^{II}a_{OH^-})$$

therefore,

$$x^2 \sim (c - x)\left(\frac{K_w}{x}\right)$$

therefore,

$$x = (K_w c)^{\frac{1}{2}} \tag{6.69}$$

Although the number of sodium ions passing into I to meet the equilibrium conditions is not large, continuous replacement of solution I by pure water forces the process to continue by encouraging a continuous movement towards equilibrium. In this way hydrolysis of the species NaR may be effected to a significant extent.

6.10.3 Ion-exchange resins

Typical cation exchange resins possess open three-dimensional structures with sulphonic acid groups attached in a regular manner throughout the network. For electroneutrality, there are required to be cations contained within the network (e.g. hydrogen or sodium ions) equal in number to the acid groups. If such a resin is placed in an acid or salt solution, water enters the free space in the network and causes swelling. We now have the situation where anions and cations of the dissolved species can move between the external solution and that inside the resin. The sulphonic acid groups, however, are fixed—not in this case by a membrane impermeable to their motion through it, but by chemical bonding. The effect will nevertheless be the same as for the membrane system. The solution inside the resin will show a larger osmotic pressure and the resin will continue to swell until a balance is achieved with the restoring forces of the extended structure. There will be an unequal distribution of electrolyte ions between the resin solution and the external solution.

In the case of a hydrogen ion-exchange resin placed in a solution of a 1:1 acid HA, while the ratio $[H^+]/[A^-]$ in the external solution must be 1:1, the ratio internally will be found to be up to several orders of magnitude greater than this, i.e. the hydrogen ions are allowed ready access to the

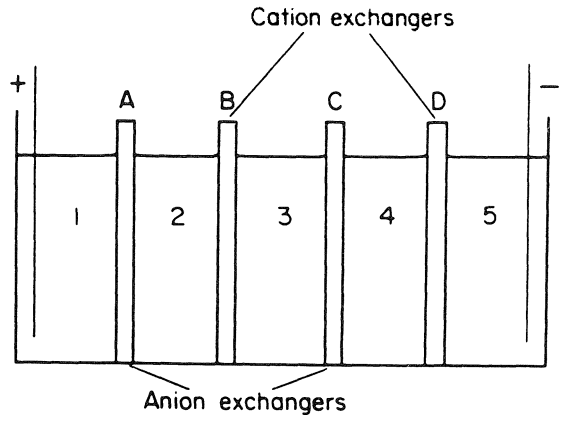

Figure 6.19 Schematic desalination plant.

interior of the resin—in fact they pass almost unhindered through the resin with a transport number very close to unity—while the resin presents an almost impermeable barrier to the A^- anions. Anion-exchange resins work on the same principle with cathodic groups distributed through the interior network of the resin. Free passage of anions is now possible with almost total restriction on the entry and passage of cations through the resin.

Combinations of cation- and anion-exchange resins are used in electrolytic desalination plants to produce fresh water from brackish water or even sea water. The salt water is placed in a series of compartments separated alternately by anion and cation exchangers (Figure 6.19).

An emf applied between electrodes placed in the extreme cells constrains the ions to move in opposite directions through the solution in the field produced. Free movement is not possible, since it is restricted by the ion exchangers. Thus the anion exchanger A allows free passage of anions from solution 2 to solution 1 but cations cannot pass from left to right through A to solution 2. Similarly, the cation exchanger B allows free passage of cations into solution 3 but does not allow anions through from 3 to 2. Thus, solution 1 becomes more concentrated in ions while solution 2 becomes more dilute. Similarly, solutions 3 and 5 become more concentrated and solution 4 more dilute. Such separation can continue until the desalination of solutions 2 and 4 is about 95% complete.

Problems

6.1 Write the half-cell and overall cell reactions for the following cells:

(i) $Zn|ZnSo_4(aq., 0.01 mol\,kg^{-1})||CuSO_4(aq., 0.001 mol\,kg^{-1})|Cu$;

(ii) $Pb|Pb(NO_3)_2$ (aq., 0.01 mol kg^{-1})$||KCl$ (aq., satd.), $Hg_2Cl_2(s)|Hg$;
(iii) $Zn|ZnSO_4$ (aq., 0.01 mol kg^{-1})$||FeSO_4$, $Fe_2(SO_4)_3$, H_2SO_4, aq.$|Pt$
(each species at 0.001 mol kg^{-1}).

Estimate the emf values of the cells at 298 K, using the Debye–Hückel equation to estimate activity coefficients and the $E^{\ominus}$ data from Tables 5.1 and 5.2.

6.2 Devise electrochemical cells suitable for studying the following equilibria and calculate their standard emf values at 298 K.

(i) $Ce^{4+} + Fe^{2+} \rightleftharpoons Fe^{3+} + Ce^{3+}$;
(ii) $Zn + 2AgCl \rightleftharpoons Zn^{2+} + 2Ag + 2Cl^-$.

(The standard potential of the silver/silver chloride electrode is +0.222 V.)

6.3 For the cell $Pt|H_2$(1 atm)$|HCl$(0.0256 mol kg^{-1})$|AgCl|Ag$, the emf at 298 K is 0.4182 V. Estimate the standard emf of the cell and the standard potential of the silver/silver chloride electrode.

6.4 For the following cell

$$Hg|Hg_2Cl_2(s), KCl\,(aq., satd.)||KCl\,(aq., 0.08\ mol\ kg^{-1}), AgCl(s)|Ag,$$

the emf was observed to be 0.051 V at 298 K. If the potential of the saturated calomel electrode at 298 K is 0.242 V, and the standard potential of the silver/silver chloride electrode is 0.222 V, obtain an estimate of the activity coefficient of the chloride ions in 0.08 mol kg^{-1} aqueous potassium chloride. Compare this value with those obtained from the Debye–Hückel limiting and extended laws.

6.5 Calculate the change in standard free energy at 298 K for the reaction

$$Sn(s) + Pb^{2+} = Sn^{2+} + Pb(s)$$

given that $E^{\ominus}_{Sn^{2+}/Sn} = -0.140$ V and $E^{\ominus}_{Pb^{2+}/Pb} = -0.126$ V.

6.6 The emf of the cell

$$Ag|AgNO_3\,(aq., 0.01\ mol\ kg^{-1})||AgNO_3\,(aq., 0.1\ mol\ kg^{-1}|Ag$$

is 0.054 V, while that of the cell

$$Ag|AgNO_3\,(aq., 0.01\ mol\ kg^{-1}) \vdots AgNO_3\,(aq., 0.1\ mol\ kg^{-1})|Ag$$

is 0.058 V. If the mean ion activity coefficients of aqueous 0.01 and 0.10 mol kg^{-1} silver nitrate are 0.898 and 0.735, respectively, obtain a mean value for the transport number of the silver ion.

6.7 Consider the situation where a solution of sodium chloride of initial concentration C_1 is brought into Donnan equilibrium with a solution of the sodium salt of a protein, NaR, at initial concentration C_2, the two solutions being separated by a membrane permeable to Na^+ and Cl^- ions but impermeable to R^-. Show that at equilibrium the number of moles, x, of NaCl which have entered the compartment containing the protein is given by $x = C_1^2/(C_2 + 2C_1)$.

6.8 A series of experiments was conducted in which 0.01 mol dm^{-3} aqueous solutions of colloidal electrolytes of general formula Na_yX were placed on one side of a membrane and equilibrated with an equal volume of 0.1 mol dm^{-3} sodium chloride solution on the other side. For the cases of y = 10, 15 and 20, calculate the fraction of sodium chloride which would have entered the colloid-containing section when Donnan equilibrium was established.

6.9 A cellophane bag containing 100 cm^3 of 0.1 mol dm^{-3} NaR solution was placed in 100 cm^3 of pure water and the whole system brought to equilibrium at 298 K. Calculate (i) the pH inside and outside the bag, and (ii) the potential difference across the bag wall. Assume that NaR is completely dissociated.

6.10 An approximately 250 cm^3 capacity rectangular perspex cell was divided into two equal compartments by a mechanically supported leak-proof membrane. In the left hand compartment were placed 100 cm^3 of very dilute hydrochloric acid containing 1.5 g of a completely dissociated monobasic colloidal acid. The membrane was impermeable to the anion of the acid. The right-hand compartment was filled with 100 cm^3 distilled water and the whole system was thermostated at 298 K and allowed to equilibrate. After equilibration, the pH of the solution to the right of the membrane was found to be 3.37 while that to the left was 2.72. Estimate the relative molecular mass of the colloidal acid.

6.11 Show that if, in the Donnan equilibration of the sodium salt of a protein Na_zR, the concentration of the protein is very much lower than that of other salts, the membrane potential may be expressed by

$$\Delta\phi \cong \left(\frac{RT}{2F}\right)\left(\frac{z^{\mathrm{I}}m_{\mathrm{R}^{z-}}}{^{\mathrm{II}}m}\right)$$

where $^{\mathrm{I}}m_{\mathrm{R}^{z-}}$ is the molality of the non-permeable protein solution and $^{\mathrm{II}}m$ is the molality of the electrolyte solution with which it is equilibrated.

6.12 The following values of membrane potential were obtained when the sodium salt of haemoglobin (Na_zHb) was equilibrated with sodium chloride, the pH of both solutions being maintained at 7.8 with phosphate buffer:

$^{\mathrm{I}}m_{\mathrm{Hb}^{z-}}$ (mol kg^{-1})	$\Delta\phi$(mV)
1.0×10^{-3}	−0.245
2.0×10^{-3}	−0.485
3.0×10^{-3}	−0.720
4.0×10^{-3}	−0.960
5.0×10^{-3}	−1.204

Calculate the average number of sodium ions combined with the haemoglobin molecule if $^{\mathrm{II}}m = 0.453$ mol kg^{-1}.

7 Electrode processes

7.1 Equilibrium and non-equilibrium electrode potentials

In Chapter 6 the reversible potential adopted by a metal electrode M when placed in a solution of ions M^+ was considered. The steady potential resulted from the rapid establishment of the equilibrium

$$M \rightleftharpoons M^+ + e \tag{7.1}$$

no net current flowing when the forward and backward rates of the reaction are equal. The further such an equilibrium lies to the *right* the more *negative* is the electrode potential.

If a potential rather more oxidizing or reducing than the equilibrium value is imposed upon such an electrode a small net current can be made to flow but with small disturbance of the electrode potential. This is because, although the applied excess potential causes a net reaction in one direction, the equilibrium re-asserts itself so rapidly that the electrode potential hardly alters. This process is of course used as the basis of the experimental determination of the electrode potential: exact balance of an applied potential from a potentiometer and that of the electrode system under study is recognized by zero net current in the galvanometer (see Figure 6.17).

7.1.1 Current–potential relationships for fast and slow systems

An idealized graph of current versus potential for a fast system takes the form shown in Figure 7.1. The small slope on the linear part of the curve is due to the effects of mass transfer processes which are slow relative to the electron exchange rate. The dashed regions represent the condition that these mass transfer processes control the overall rate of reaction.

It has been seen that some electrodes never show reversible potentials under experimental conditions because the rate of attainment of equilibrium is low: such processes are more realistically called *slow* rather than irreversible. In order for even a small cathodic or anodic current to flow a potential well in excess of the equilibrium value must be applied to the respectively negative or positive side of this value. For such cases a current voltage curve will take the form shown in Figure 7.2.

Chapter 6 introduced the equal and opposite currents flowing at E_{eq}. This *exchange current*, I_0, features importantly in electrode kinetics considered in the next section. It is, however, useful to introduce the concept here since

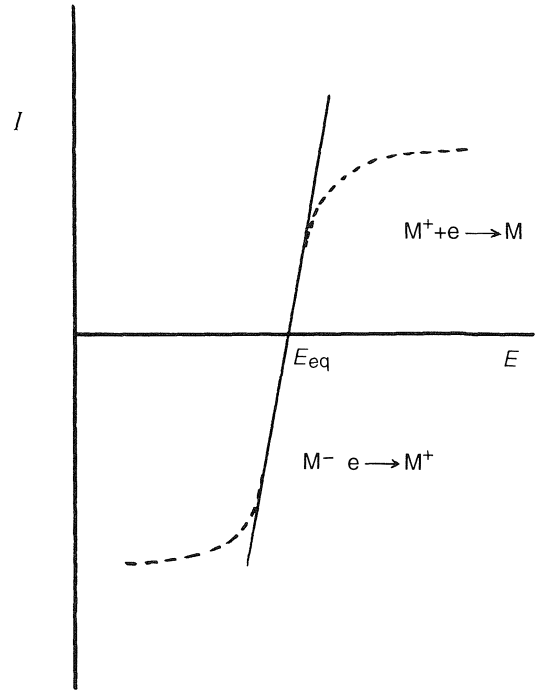

Figure 7.1 Idealized current-potential relationship for the system $M \rightleftharpoons M^+ + e$ in which equilibrium is established rapidly. The dashed regions correspond to the condition that mass transfer processes control the overall rate of the net anodic or cathodic reaction.

the values of *net* currents, consequent upon imposition of applied potentials, differ markedly relative to I_0 for reversible and irreversible systems. The two extremes of behaviour are contrasted in Figure 7.3.

For reversible systems I_0 is large: a small net change ΔI is sustainable without undue departure from reversibility (Figure 7.3(a)) and Nernstian conditions still apply. For irreversible processes (Figure 7.3(b)) ΔI is large with respect to I_0 (which is very small) and disturbance to the equilibrium is significant.

7.1.2 Mass transfer and electron-exchange processes

In considering electron-exchange reactions at electrodes, the layer of solution very close to the electrode surface comes under scrutiny. When conditions exist or are imposed such that the electronic levels in the electrode material and an electroactive solute material are compatible, electron transfer may take place. It will do so according to the Frank–Condon Principle

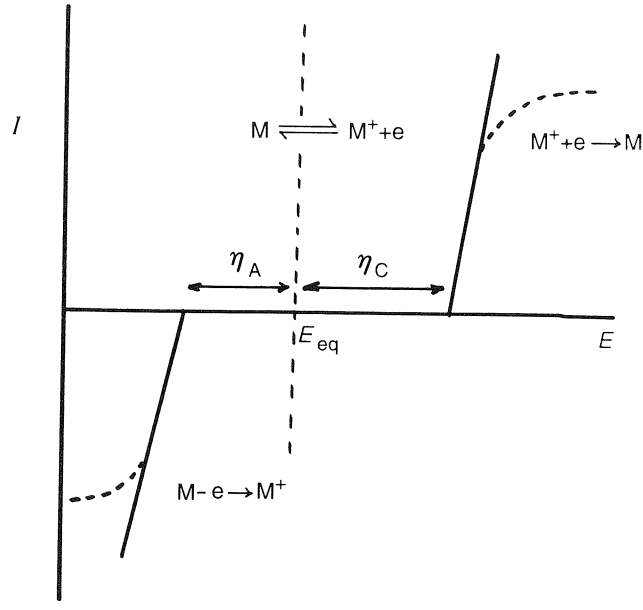

Figure 7.2 Idealized current–potential curve for a slow or irreversible system which requires an overvoltage, η_C, for the process $M^+ + e \rightarrow M$ and η_A for $M \rightarrow M^+ + e$. Here the equilibrium $M \rightleftharpoons M^+ + e$ is not established under the experimental conditions used and E_{eq} is not realizable. The dashed curves correspond to control of the rates of the net anodic and cathodic reactions by mass-transfer processes.

according to which the rates of electron transfer take place very much more rapidly than molecular rearrangements. The interplay of solvent interactions, applied potential and the very large field gradient within the double layer (of the order of 10^9 V m^{-1}) serves to produce a solute structure to (or from) which electrons may be transferred. When this happens a current flows through the electrode, through the external circuit and through the complementary electrode.

In order to sustain a current for a given potential it is necessary for the supply of material at the electrode surface to be sustained and the movement of ions through the solution will effectively constitute the *electrolytic current* which complements the *electronic current* flowing in the external circuit. Such movement cannot be increased indefinitely and a point must be reached where solute species react with the electrode as fast as they reach it. The current then approaches the limiting values indicated by the dashed curves in Figures 7.1 and 7.2. Before proceeding much further, the nature of the various mass transfer processes should be considered.

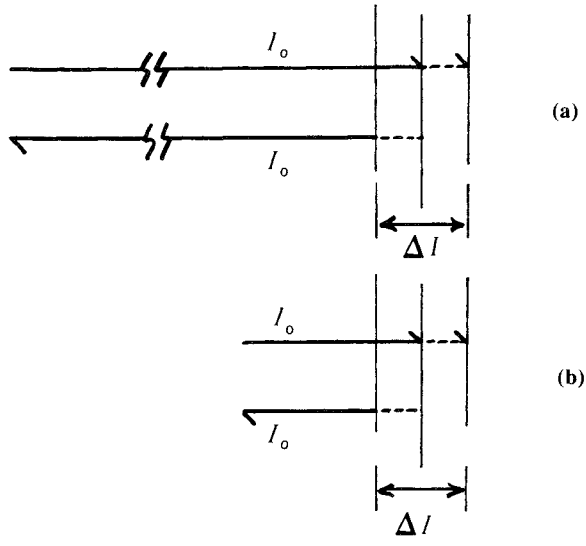

Figure 7.3 Diagrammatic representation of relative magnitudes of a net current ΔI and the exchange current I_0 for (a) a reversible system where $\Delta I \ll I_0$ and (b) an irreversible system where $\Delta I \sim I_0$ or $\Delta I > I_0$.

7.1.3 Types of mass transfer

There are three types of mass transfer.

1. *Migration.* The movement of cations and anions through a solution under the influence of an applied potential between electrodes placed in that solution. This phenomenon has been met with already and the significance of transport numbers has been discussed.
2. *Diffusion.* An electrode reaction depletes the concentration of oxidant or reductant at an electrode surface and produces a concentration gradient there. This gives rise to the movement of species from the higher to the lower concentration. Unlike migration, which only occurs for charged particles, diffusion occurs for both charged and uncharged species.
3. *Convection.* This includes thermal and stirring effects which can arise extraneously through vibration, shock and temperature gradients. More importantly, some electro-analytical methods are based upon controlled convection at electrodes. Considerable variation in the relative rates of mass transfer and electron-exchange processes is possible: the simplest interpretation of electrochemical reactions assumes that the rates of all processes occur rapidly.

7.2 The kinetics of electrode processes: the Butler–Volmer equation

The equilibrium

$$M \underset{v_c}{\overset{v_a}{\rightleftharpoons}} M^{n+} + ne \qquad \text{(see equation (7.1))}$$

may be considered from a kinetic viewpoint: v_a is the rate of the ionization (dissolution) or anodic process while v_c represents the rate of the discharge or cathodic process.

There will be an activation energy barrier to both processes which can be visualized as in Figure 7.4. Here the reaction profile involving the transition state (Figure 7.4(a)) may be seen as reflecting the intersection of reactant and use product energy parabolas (Figure 7.4(b)).

The rates for the processes may be expressed in terms of the Arrhenius equation, viz.

$$v_a = k_a e^{-\Delta G_a^{\ddagger}/RT} \tag{7.2}$$

and

$$v_c = k_c[M^{n+}]e^{-\Delta G_c^{\ddagger}/RT} \tag{7.3}$$

where k_a, k_c are corresponding rate constants and $[M^{n+}]$ is the concentration of metal ions (strictly the value at the electrode surface which, for present purposes, may be regarded as the outer Helmholtz plane).

At equilibrium $v_a = v_c$ so that

$$k_a \exp\left[-\frac{\Delta G_a^{\ddagger}}{RT}\right] = k_c[M^{n+}]\exp\left[-\frac{\Delta G_c^{\ddagger}}{RT}\right]$$

Therefore

$$\frac{\exp\left[-\Delta G_a^{\ddagger}/RT\right]}{\exp\left[-\Delta G_c^{\ddagger}/RT\right]} = \frac{k_c}{k_a}[M^{n+}]$$

so that, in terms of $\Delta G = \Delta G_c^{\ddagger} - \Delta G_a^{\ddagger}$

$$\exp\left[-\frac{\Delta G}{RT}\right] = \frac{k_c}{k_a}[M^{n+}] = \exp[nF\Delta\phi RT]$$

Therefore

$$\frac{nF\Delta\phi}{RT} = \ln\left(\frac{k_c}{k_a}\right) + \ln[M^{n+}]$$

or

$$\Delta\phi = \frac{RT}{nF}\ln\left(\frac{k_c}{k_a}\right) + \frac{RT}{nF}\ln[M^{n+}]$$

or

$$\Delta\phi = \Delta\phi^{\ominus} + \frac{RT}{nF}\ln[M^{n+}] \tag{7.4}$$

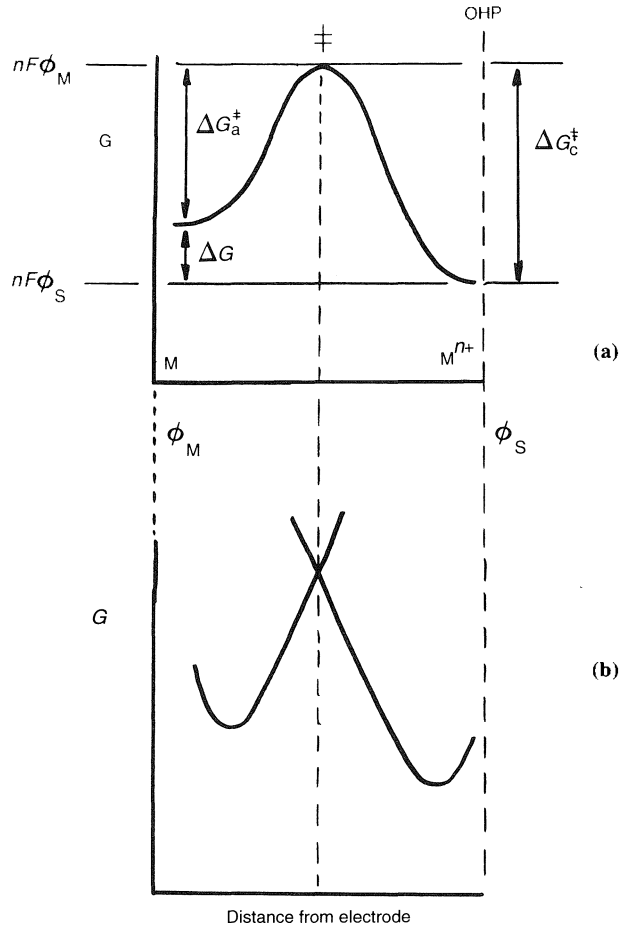

Figure 7.4 Electrode reaction free energy profile for a reversible process $M^{n+} + ne \rightleftharpoons M$. (a) Activation energy barriers and relative positions of reactant, product and activated complex with respect to distance from the electrode surface and outer Helmholtz plane (OHP). (b) Complementary free energy parabolas for reactant and product with crossing point at the transition state. Overall free energy change given by

$$\Delta G = \Delta G_c^{\ddagger} - \Delta G_a^{\ddagger} = n\Delta\phi F$$

$$\Delta\phi = \phi_M - \phi_S$$

which, in terms of the more commonly used symbols for electrode potentials becomes

$$E = E^{\ominus} + \frac{RT}{nF} \ln [M^{n+}] \tag{7.5}$$

Equation (7.5) clearly identifies with equation (6.20), i.e. the Nernst equation which has now been derived kinetically. A rather different insight is now given into $E^{\ominus}$ as a function of the rate constants of the two processes occurring at the electrode.

In irreversible systems no perceptible reaction occurs at E_{eq} or $\Delta\phi^{\ominus}$. The transition state can now only be formed by application of extra (cathodic or anodic) potential—the overvoltage, η. Thus to effect reduction of M^{n+} for this case the magnitudes of $\Delta G_c^{\ddagger}$ and $\Delta G_a^{\ddagger}$ become

$$\Delta G_c^{\ddagger} = (\Delta G_c^{\ominus})^{\ddagger} + \alpha nF\eta \tag{7.6}$$

and

$$\Delta G_a^{\ddagger} = (\Delta G_a^{\ominus})^{\ddagger} - (1 - \alpha)nF\eta \tag{7.7}$$

In this view η is seen as serving *two* functions: (i) part of it (a fraction α) assists the cathodic process; (ii) a fraction $(1 - \alpha)$ retards the anodic process. α is known as the *transfer coefficient*. This interpretation may be represented by Figure 7.5(a). Figure 7.5(b) shows a view of the effect of the overvoltage η imposed across the region between the electrode surface and the outer Helmholtz plane (OHP). Having reached the OHP a metal ion must then cross the interfacial region where it will experience increasing influence by η: if it reached as far as the surface proper it would experience the full value, but only a fraction of it, α, is required to produce the transition state which occurs at an intermediate distance.

It is seen that the idea is restricted in that it is not easy to represent both the cathodic and anodic functions on the same figure. However, the same argument as given above can be applied to the anodic overvoltage required to produce a net dissolution.

In terms of the new activation energies the rates of cathodic and anodic processes now become.

$$v_c' = k_c[M^{n+}] \exp\left[-\frac{\{(\Delta G_c^{\ominus})^{\ddagger} + \alpha nF\eta\}}{RT}\right] \tag{7.8}$$

and

$$v_a' = k_a \exp\left[-\frac{\{(\Delta G_a^{\ominus})^{\ddagger} - (1 - \alpha)nF\eta\}}{RT}\right] \tag{7.9}$$

Since for this case the condition of equal rates is not realized, a net cathodic or anodic reaction occurs for which the corresponding net current may be calculated. Respective rates may be expressed in terms of cathodic and anodic current densities as follows:

$$v_c' = \frac{i_c}{nF} \tag{7.10}$$

and

$$v_a' = \frac{i_a}{nF} \tag{7.11}$$

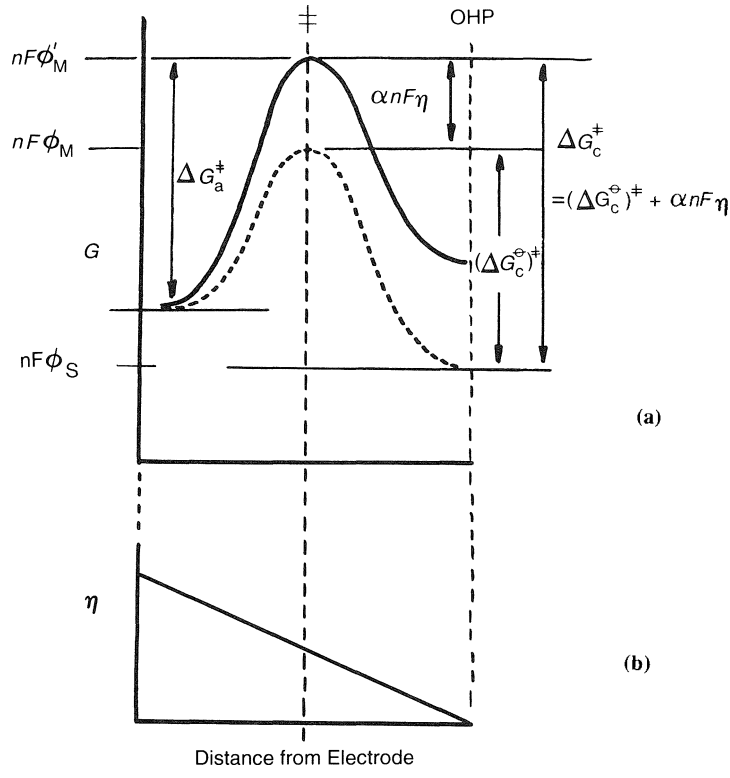

Figure 7.5 Electrode reaction free energy profile for an irreversible process. (a) Formation of transition state by imposition of cathodic overvoltage $\eta = \Delta\phi - \Delta\phi^{\ominus}$ where $\Delta\phi = \phi'_M - \phi_S$ and $\Delta\phi^{\ominus} = \phi'_M - \phi_S$. (b) Diagrammatic representation of the effect of the imposition of η across the region between electrode surface and outer Helmholtz plane.

Therefore,

$$i_c = nFk_c[M^{n+}]\exp\left[-\frac{(\Delta G_c^{\ominus})^{\ddagger}}{RT}\right]\exp\left[-\frac{\alpha nF\eta}{RT}\right] \tag{7.12}$$

and

$$i_a = nFk_a\exp\left[-\frac{(\Delta G_a^{\ominus})^{\ddagger}}{RT}\right]\exp\left[\frac{(1-\alpha)nF\eta}{RT}\right] \tag{7.13}$$

The forms of equations (7.12) and (7.13) may be simplified to

$$i_c = i_0\exp\left[-\frac{\alpha nF\eta}{RT}\right] \tag{7.14}$$

and

$$i_a = i_0 \exp\left[\frac{(1-\alpha)nF\eta}{RT}\right] \tag{7.15}$$

or, for currents I_c, I_a, I_0.

$$I_c = I_0 \exp\left[-\frac{\alpha nF\eta}{RT}\right] \tag{7.16}$$

and

$$I_a = I_0 \exp\left[\frac{(1-\alpha)nF\eta}{RT}\right] \tag{7.17}$$

i_0 and I_0 being the exchange current density and exchange current respectively.

It is seen that equations (7.16) and (7.17) are consistent with the condition

$$I_c = I_a = I_0 \text{ when } \eta = 0.$$

Clearly for the hypothetical reaction scheme proposed, a net cathodic current density $i = i_c - i_a$ is given by

$$i = i_0 \left\{\exp\left[-\frac{\alpha nF\eta}{RT}\right] - \exp\left[\frac{(1-\alpha)nF\eta}{RT}\right]\right\} \tag{7.18}$$

Equation (7.18) is known as the Butler–Volmer equation. This expression only strictly holds in the above form for processes involving a single electron. When electrochemical reactions involving more than one electron are considered it is more rigorous to replace α by α_c and to replace $(1-\alpha)$ by α_a since $\alpha_c + \alpha_a \neq 1$ except for $n = 1$, thus

$$i = i_0 \left\{\exp\left[-\frac{\alpha_c nF\eta}{RT}\right] - \exp\left[\frac{\alpha_a nF\eta}{RT}\right]\right\} \tag{7.19}$$

Application of equation (7.19) may be demonstrated by consideration of an electrode process with the following characteristics:

$$n = 1;\ \alpha_c = 0.65;\ \alpha_a = 0.35,\ I = 1\,\text{mA};\ A = 1\,\text{cm}^2$$

For a cathodic overvoltage $\eta = 0.1$ V a net cathodic current flows given by (noting that $F/RT = 38.95\,\text{C J}^{-1}$ at 298 K)

$$\begin{aligned}(I_c)_{net} &= \exp(-0.65 \times 38.95 \times (-0.1)) - \exp(0.35 \times 38.95 \times (-0.1)) \\ &= 12.575 - 0.256 \\ &= 12.319\,\text{mA}.\end{aligned}$$

If an anodic overvoltage $\eta = +0.1\,\text{V}$ is imposed the net anodic current is given by

$$\begin{aligned}(I_a)_{net} &= \exp(-0.65 \times 38.95 \times 0.1) - \exp(0.35 \times 38.95 \times 0.1)\\ &= 0.080 - 3.909\\ &= -3.829\,\text{mA}.\end{aligned}$$

Conversely, with an electrode process where α_a favours the anodic component (e.g. for the characteristics $n = 1$; $\alpha_c = 0.35$; $\alpha_a = 0.65$; $I_0 = 1\,\text{mA}$; $A = 1\,\text{cm}^2$), then for a cathodic overvoltage $\eta = -0.1\,\text{V}$, the net cathodic current is now given by

$$\begin{aligned}(I_c)_{net} &= \exp(-0.35 \times 38.95 \times (-0.1)) - \exp(0.65 \times 38.95 \times (-0.1))\\ &= 3.909 - 0.080\\ &= 3.829\,\text{mA}.\end{aligned}$$

While for an overvoltage $\eta = +0.1\,\text{V}$, the magnitude of the net anodic current is

$$\begin{aligned}(I_c)_{net} &= \exp(-0.35 \times 38.95 \times (0.1)) - \exp(0.65 \times 38.95 \times (0.1))\\ &= 0.256 - 12.575\\ &= -12.319\,\text{mA}.\end{aligned}$$

It has been common practice in the United Kingdom and the United States to represent current–voltage curves with cathodic currents increasing in the positive vertical direction and with voltages increasing negatively from left to right. This indeed has been the practice adopted here and the signs of the currents in the above calculations are consistent with this. However, many people consider it more logical to assign negative signs to cathodic currents deriving from a negative overvoltage and vice versa. It is a simple matter to rearrange signs in the above examples to conform with this alternative convention.

7.3 The relationship between current density and overvoltage: the Tafel equation

If the overvoltage is small, the exponential terms of equation (7.18) may be expanded and all terms except the first two neglected. The expression then reduces to

$$i = \frac{i_0 nF\eta}{RT} \tag{7.20}$$

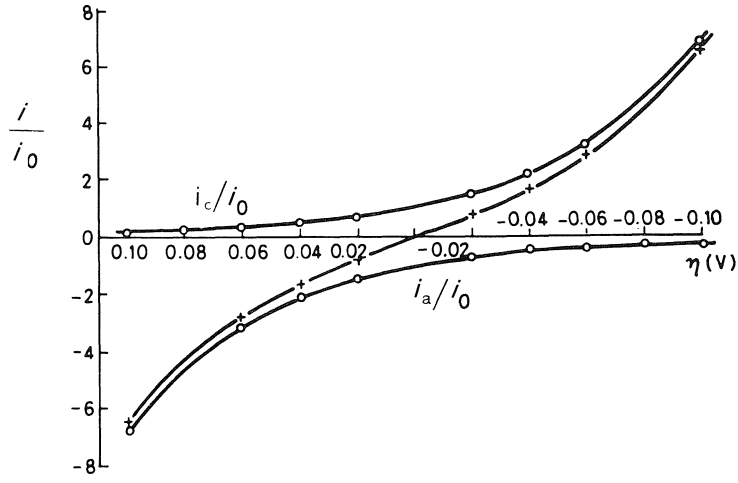

Figure 7.6 The ratio i/i_0 (calculated from equation (7.18)) plotted as a function of overvoltage η. i_c/i_0, i_a/i_0 are the partial cathodic and anodic ratios. $\alpha = 0.5$.

For higher overvoltages the full expression (7.18) must be used as has been demonstrated with the calculations given. In Figure 7.6 are shown calculated variations of i/i_0, i_c/i_0 and i_a/i_0 with overvoltage for $\alpha = 0.5$.

The asymmetrical variations of the same current ratios for $\alpha = 0.25$ and 0.75 are presented in Figure 7.7.

For a large overvoltage to the cathodic reaction, only the first exponential term in equation (7.18) is significant, the second being very small by comparison. The dependence of cathodic current density on overvoltage may then be given by

$$\ln i = \ln i_0 - \frac{\alpha nF\eta}{RT} \tag{7.21}$$

Explicitly, η is then given by

$$\eta = \frac{2.3RT}{\alpha nF} \log i_0 - \frac{2.3RT}{\alpha nF} \log i \tag{7.22}$$

Conversely, for a large overvoltage to the anodic reaction, only the second term of equation (7.18) is of significance and

$$\eta = -\frac{2.3RT}{(1-\alpha)nF} \log i_0 + \frac{2.3RT}{(1-\alpha)nF} \log i \tag{7.23}$$

Equations (7.22) and (7.23) are of identical form to an empirical equation proposed by Tafel, viz.

$$\eta = a + b \log i \tag{7.24}$$

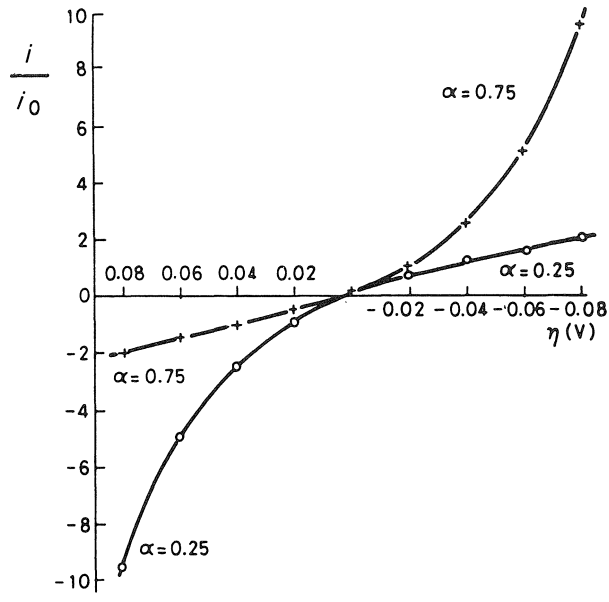

Figure 7.7 The ratio i/i_0 (calculated from equation (7.18)) plotted as a function of overvoltage η for $\alpha = 0.25$ and for $\alpha = 0.75$.

Graphs of η versus $\log i$ are known as Tafel plots, and examples are shown in Figure 7.8. The linear portions of the asymptotes correspond to the Tafel equation and have slopes (Tafel slopes) of magnitude b; $2.3RT/\alpha nF$ for the cathodic and $2.3RT/(1-\alpha)nF$ for the anodic process. An experimental line does not continue and cut the $\log i$ axis, since i refers to a *net* current density. This will approach zero as η approaches zero. The extrapolated asymptotes intersect on the line $\eta = 0$ at $\log i_0$.

7.4 The modern approach to the interpretation of electrode reactions

Strong hydration interaction between ions and water dipoles has been ignored in the above treatment of electrode reactions. However, it is clear that whether considering reactions such as

$$M^{3+} + e \rightleftharpoons M^{2+}$$

at electrodes or

$$M^{3+} + N^{2+} \rightleftharpoons M^{2+} + N^{3+}$$

in solution, changes in hydration shells must be an important part of any fuller theoretical model devised in attempting to explain the nature of electron-transfer reactions. The many attempts to cope with this problem

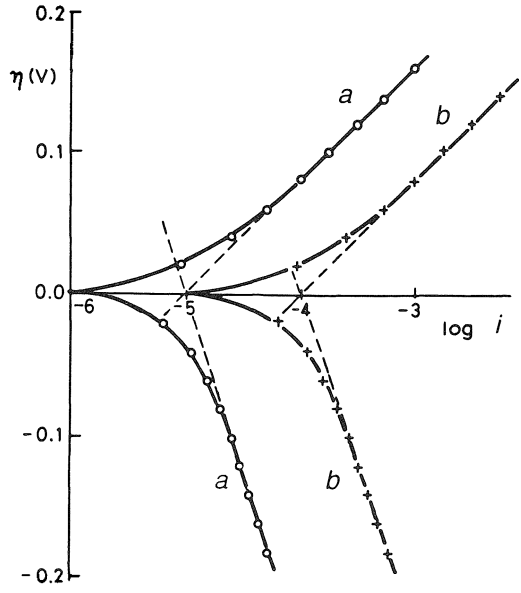

Figure 7.8 Tafel plots constructed using data from Figure 7.7. (a) $\alpha = 0.25$; $I = 10^{-5}$ A. (b) $\alpha = 0.25$; $I = 10^{-4}$ A.

have found some sort of culmination in the work of Marcus. This has been particularly successful in accounting for observed relationships between parameters characteristic of reactions occurring in a homogeneous manner in solution and those, essentially heterogeneous, occurring at electrodes.

In terms of the M^{3+} and M^{2+} energy parabolas shown in Figure 7.9, solvent redistribution may be represented by the function ΔG_s. ΔG_s, the reorganization energy, is a free-energy term representing the difference in hydration of reactants and products. The activation energy, $\Delta G^{\ddagger}$, is related to ΔG and ΔG_s by the following expression

$$\Delta G^{\ddagger} = \frac{(\Delta G + \Delta G_s)^2}{4\Delta G_s} \tag{7.25}$$

The contributing terms in the Butler–Volmer equation may be expressed in terms of rate constants as well as rates or currents. Thus, for a cathodic process

$$k_c = k_0 \exp\left[-\frac{\alpha n F \eta}{RT}\right] \tag{7.26}$$

which emphasizes the direct relationship between the transfer coefficient and

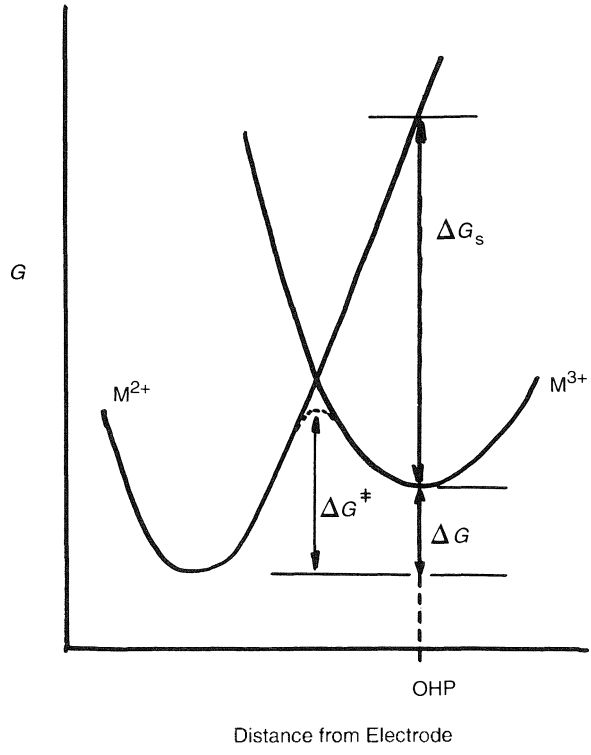

Figure 7.9 Intersecting free energy parabolas for oxidized and reduced species showing relationship between ΔG, $\Delta G^{\ddagger}$ and ΔG_S, the reorganization energy. OHP = outer Helmholtz plane.

the rate constant of the process to which it applies. Equation (7.26) may alternatively be written as

$$\ln k_c = \text{constant} - \frac{\alpha nFE}{RT}$$

Therefore

$$\alpha = -\left(\frac{\partial \ln k_c}{\partial E}\right) = \frac{\partial \Delta G^{\ddagger}}{\partial E} \tag{7.27}$$

which, in terms of equation (7.25) gives

$$\alpha = \frac{1}{2}\left(\frac{\Delta G}{\Delta G_s} + 1\right) \tag{7.28}$$

It is instructive to consider some of the implications of equation (7.28): its use makes predictions consistent with the kinetic treatment given so far and

introduces further insights into the nature of the energy profiles of electrode processes.

Firstly, if $\Delta G = 0$, corresponding to the reversible case where $\eta = 0, \alpha$ is seen to have the value 1/2. If $\Delta G_s \sim \Delta G, \alpha \sim 1$; this means that almost all the overvoltage η is being used in generation of the transition state (see Figure 7.5). The implication of this condition being established so close to the electrode surface is that the transition state has a structure much closer to the product than to the reactant. By contrast, if $\Delta G_s \sim -\Delta G, \alpha = 0$; the transition state is now formed near to the OHP and will resemble M^{n+}. These cases all imply a fairly *small* value for ΔG_s. If at the other extreme ΔG_s is large, and very much larger than ΔG, it is seen that α again has the value 1/2 but here the electrode process is *slow*. The wording of this last statement should be noted carefully: electron transfer as such occurs rapidly, in accordance with the Frank–Condon principle. Marcus has elaborated on the structural and environmental changes which are necessary to allow such adiabatic electron transfer. An important outcome of the Marcus model is that it predicts relationships which are experimentally verifiable. In particular, for a redox process which occurs both homogeneously in solution and at an electrode, the following relationship has been established between the two rate constants.

$$\frac{k_{\text{elec}}}{(k_{\text{hom}})^{1/2}} \sim 10^{-2}\,\text{m}^{1/2}\,\text{mol}^{1/2}\,\text{s}^{-1/2} \tag{7.29}$$

Thus for the process $V^{3+} \rightarrow V^{2+}$ for which $k_{\text{elec}} = 4 \times 10^{-5}\,\text{m}^2\,\text{s}^{-1}$ and $k_{\text{hom}} = 1.6 \times 10^{-5}\,\text{m}^3\,\text{mol}^{-1}\,\text{s}^{-1}$ equation (7.29) is seen to hold exactly. Many reactions show the ratio to have a value of the order given above but there are exceptions.

Electrode processes for which $n > 1$ take place in one-electron steps of which one is rate determining. For such cases the interpretation of an experimentally determined value of αn is not always clear: for what value of n should be used to calculate α if the contributing one-electron stages occur with very different values? For example, a known overall two-electron reduction may show an experimental value of $\alpha n = 1.4$ which might suggest $\alpha = 0.7$. But if the first transfer is fast with $\Delta G_s \sim \Delta G, \alpha_1 = 1$ so $\alpha_2 = 0.4$ and while 0.4 now reflects quite logically the position of the transition state on the distance axis, 0.7 does not.

7.5 Electrolysis and overvoltage

It is necessary now to consider a number of types of overvoltage, their source and control and the way in which they influence the course of an electrochemical reaction.

7.5.1 *Activation overvoltage* (η_A)

A slow electron transfer, such as that considered in previous sections, has a high activation energy. If such a reaction is to proceed at a reasonable rate and produce an efficient quantity of product, a significant increase of applied potential over the equilibrium value is necessary. This excess potential is known as activation overvoltage (η_A) This description emphasizes that the slow, rate-determining step in the process is the electron transfer due to the high activation-energy barrier which it must cross.

Two further types of overvoltage are of importance and may occur simultaneously with activation overvoltage.

7.5.2 *Resistance overvoltage* (η_R)

The most common form of resistance overvoltage arises from the passage of electric current through an electrolyte solution surrounding the electrode. Such a solution is not of infinite conductivity and shows resistance to the current flow, with the result that an ohmic (IR) drop in potential occurs between the working electrodes. This effect may be offset by insulating the solution of the reference electrode from the working solution by enclosing the former in a fine glass capillary, the open end of which is brought as close to the surface of the electrode under investigation as is compatible with uniform field force over the surface of this electrode (Figure 7.10)

The optimum position of this *Luggin capillary*, as it is called, is usually a matter of experiment.

A less common form of ohmic overvoltage is caused by the formation, on the surface of the electrode, of an adherent layer of reaction product which is a relatively poor conductor of electricity. Surface oxide films show such behaviour, their resistance being such that overvoltages of several hundred volts may be produced.

7.5.3 *Concentration overvoltage* (η_C)

This is a small, but important effect (particularly for some electroanalytical techniques) which arises due to concentration changes induced in the vicinity of electrodes by electrochemical reactions occurring there.

Consider the simplest of all cells in which two identical electrodes of metal M are placed in a solution of M^{n+} ions and let the electrode equilibria be established rapidly, i.e. if no potential is applied, but the cell is simply short-circuited, no current will flow since the potential of both electrodes is the same.

If even a small potential difference is applied between the electrodes, the balance is destroyed, one electrode becoming a cathode the other an anode. At the former M^{n+} ions are discharged at a faster rate than they dissolve

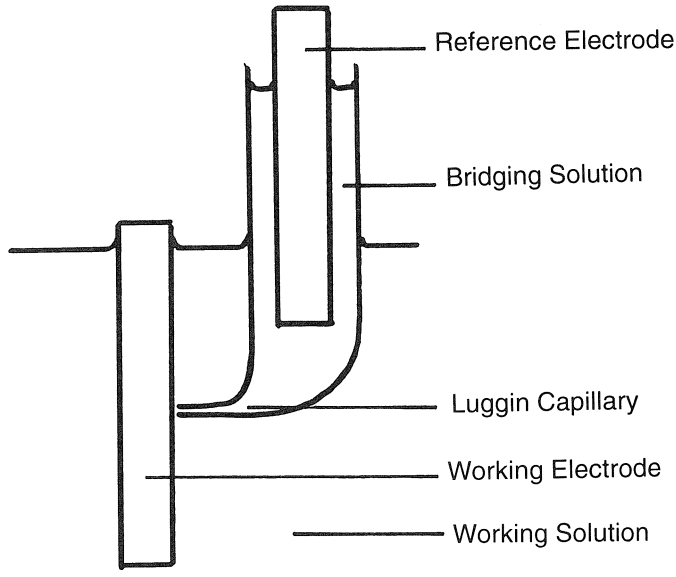

Figure 7.10 The principle of the Luggin capillary.

and at the anode M passes into solution more rapidly than M^{n+} ions are discharged.

The total amount of material discharged at the cathode or dissolved from the anode may be calculated from Faraday's laws, from a knowledge of the quantity of electricity passed. However, by reference to the Hittorf mechanism of electrolysis, we see that, at the cathode, only a fraction t_+ of the material deposited there has reached there by electrical migration. The remaining fraction must be made good from the layer of solution in the immediate vicinity of the electrode surface. From the moment that electrolysis starts, therefore, the solution close to the cathode surface shows a concentration decrease. For the same current to flow, and therefore the same rate of deposition of M^{n+}, a more negative potential will be required. Similarly, a more positive potential will be required at the anode since here only a fraction t_+ of the metal ions formed by dissolution are removed by migration so that the concentration of the anode solution increases. The effect is to produce a back emf, so that to maintain the current flow, the applied emf must be increased by this amount. An electrode whose potential deviates from its equilibrium value due to these causes is said to be *concentration polarized.* Stirring of the electrolyte solution or rotation or vibration of the electrodes can serve to reduce the extent of concentration polarization but does not eliminate it entirely.

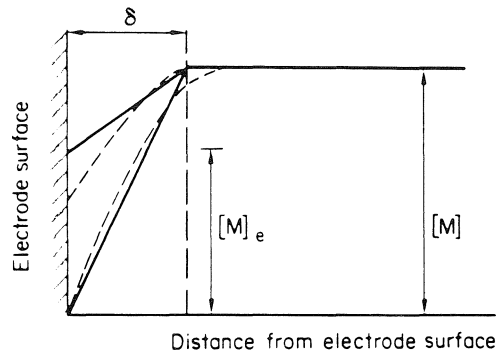

Figure 7.11 Representation of the concentration gradient in the vicinity of an electrode at which reduction is taking place.

At an electrode surface there is a diffusion layer across which there is a concentration variation from the surface to the edge of the layer. To a good approximation this variation may be regarded as uniformly linear as shown in Figure 7.11. The thickness of the layer, δ, has a magnitude of the order of 0.05 cm under static conditions, which becomes reduced to the region of 0.001 cm with rapid stirring.

For a steady current through the cell, the concentration of the surface layer of solution at the cathode falls and is made good by the diffusion of material from the bulk. A steady state is rapidly reached where M^{n+} ions removed by deposition are replaced by those arriving by both electrical migration and diffusion. The rate of arrival of M^{n+} ions by diffusion is given by

$$\frac{D([M^{n+}] - [M^{n+}]_e)}{\delta} \tag{7.30}$$

D is the diffusion coefficient of the species M^{n+}, and is defined as the amount of M^{n+} transported per unit area across unit diffusion layer thickness under unit concentration gradient in unit time.

The rate of arrival at the cathode of M^+ ions by migration is, for a current density i

$$\frac{t_+ i}{nF} \tag{7.31}$$

Since the total amount deposited is given by i/nF, it follows that, under steady-state conditions.

$$\frac{i}{nF} = \frac{t_+ i}{nF} + \frac{D([M^{n+}] - [M^{n+}]_e)}{\delta} \tag{7.32}$$

As the potential impressed between the electrodes is increased, the current density will increase so long as the concentration gradient across the diffusion layer can increase to maintain the supply of M^{n+}. A point will, however, be reached where M^{n+} becomes zero. Since the concentration gradient has now reached it maximum value, the rate of supply of $[M^{n+}]$ by diffusion has reached its maximum value and the electrode process can proceed no faster. Equation (7.32) now becomes

$$\frac{i_{\text{lim}}}{nF} = \frac{t_+ i_{\text{lim}}}{nF} + \frac{D[M^{n+}]}{\delta} \tag{7.33}$$

Comparing equations (7.32) and (7.33) it is seen that

$$\frac{i(1 - t_+)}{i_{\text{lim}}(1 - t_+)} = \frac{([M^{n+}] - [M^{n+}]_e)}{[M^{n+}]} \tag{7.34}$$

or

$$\frac{[M^{n+}]_e}{[M^{n+}]} = \frac{i_{\text{lim}}}{i_{\text{lim}} - i} \tag{7.35}$$

so that the concentration overvoltage, η_c, may be written

$$\eta_c = \frac{RT}{nF} \ln \frac{[M^{n+}]_e}{[M^{n+}]} = \frac{RT}{nF} \ln \frac{i_{\text{lim}}}{i_{\text{lim}} - i} \tag{7.36}$$

7.5.4 Summary of overvoltage phenomena and their distinguishing features

The overvoltage of an individual electrode may be expressed as the sum of contributions from activation, concentration and resistive film overvoltages:

$$\eta = \eta_A + \eta_C + \eta_R$$

the use of the Luggin capillary virtually eliminating the *IR* contribution. Hence, η_R is often absent.

There are a number of distinguishing features of the above three forms of overvoltage which allow the effects to be identified experimentally.

1. η_R unlike η_A and η_C, appears and disappears instantaneously when the polarizing circuit is made or broken.
2. η_A increases rapidly and exponentially after a polarizing current is caused to flow and decreases in a complementary way when the current flow is stopped. The exponential growth and decay are in accordance with the concept of η_A as a function of the activation energy of an electrode process. The magnitude of η_A is strongly affected by the physical and chemical nature of the electrode material.

3. η_C grows and decays slowly on application or interruption of the current flow at a rate characteristic of the diffusion coefficients of the species involved. η_C is unique in being the only form of overvoltage affected by stirring and is unaffected by the nature of the surface of the electrode material.

7.6 Hydrogen and oxygen overvoltage

The evolution of hydrogen and oxygen are well-known phenomena during electrolysis of dilute aqueous solutions of acids and bases between inert metal electrodes. If bright platinum electrodes are used for the electrolysis, it is found that in most cases the minimum potential difference which must be applied between them before gas bubbles appear is close to 1.7 V. That a similar value should usually be observed is hardly surprising since the same overall chemical process is occurring, viz. the decomposition of water, although the electrode reactions differ depending upon whether the solutions are acidic or alkaline.

In acid

$$\begin{aligned} \text{at the cathode} \quad & 2H^+ + 2e \rightarrow H_2 \\ \text{at the anode} \quad & H_2O \rightarrow \tfrac{1}{2}O_2 + 2H^+ + 2e \end{aligned}$$

In alkali

$$\begin{aligned} \text{at the cathode} \quad & 2H_2O + 2e \rightarrow H_2 + 2OH^- \\ \text{at the anode} \quad & 2OH^- \rightarrow \tfrac{1}{2}O_2 + H_2O + 2e \end{aligned}$$

7.6.1 Decomposition potentials and overvoltage

A graph of current, or current density, versus potential gives a decomposition curve and allows decomposition potentials to be determined (Figure 7.12). Decomposition potentials are never well-defined and can only be obtained approximately by extrapolation of the rising part of the curve to the potential axis. Nevertheless the value of approximately 1.7 V for the electrolysis of water is sufficiently different from the theoretical value for it to be apparent that there is a large cell overvoltage even when resistance and concentration effects are taken into account. The theoretical decomposition potential may be calculated as follows: the reaction occurring in the electrolysis cell is

$$H_2O(l) \rightarrow H_2(g) + \tfrac{1}{2}O_2(g)$$

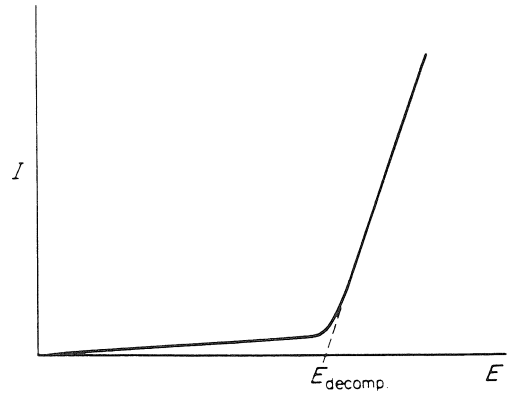

Figure 7.12 Decomposition curve. $E_{\text{decomp.}}$ is the minimum potential difference which must be applied between a pair of electrodes before decomposition occurs and a current flows. $E_{\text{decomp.}}$ has little theoretical significance since it is made up of two individual electrode potentials and their associated overvoltages.

for which $\Delta G^{\ominus} \sim 238\,140$ joules. Now $\Delta G^{\ominus} = -nFE^{\ominus}$ where, for the present case $E^{\ominus}$ is the standard emf of the hydrogen–oxygen cell; therefore,

$$E^{\ominus} = -\frac{238\,140}{2 \times 96\,500} = -1.23\,\text{V}$$

The cell overvoltage observed when using bright platinum electrodes is thus of the order of 0.5 V. An experimental decomposition voltage has no theoretical significance of its own, since a moment's consideration will show that it consists of two individual electrode potentials and the *IR* drop between them. These individual potentials will be made up of the thermodynamic values plus the overvoltages; the latter comprise contributions from activation, concentration and film resistance overvoltage.

7.6.2 *Individual electrode overvoltages*

Individual electrode overvoltages may be determined experimentally by means of the circuit in Figure 7.13. Here a constant electrolysis current density is maintained by a high-tension battery/series resistance combination to polarize the electrodes. Each electrode in turn is then combined with a reference electrode and the emf values of the two cells successively formed in this way measured via the potentiometer. Since the reference electrode potential is known, the potential of the anode and cathode may be determined at the current density imposed. The Luggin capillary, brought as close to the electrode surfaces as possible, largely removes the *IR* contribution to the

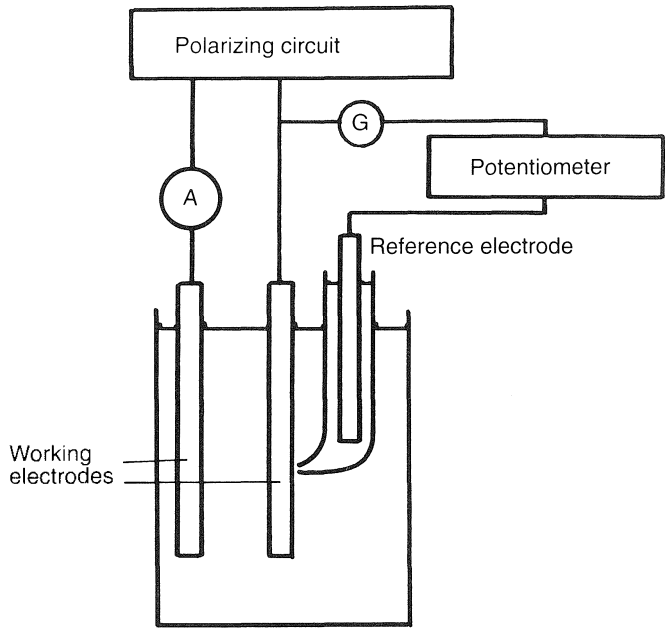

Figure 7.13 Determination of individual electrode overvoltages and elimination of the *IR* correction.

measured overpotential. By these means the cell overvoltage of about 0.5 V for the above case may be shown to comprise an overvoltage of about 0.1 V at the cathode and about 0.4 V at the anode. Table 7.1 shows approximate hydrogen overvoltages for various electrode materials in dilute sulphuric acid.

Table 7.1 Selected hydrogen overvoltages for various electrode materials in dilute sulphuric acid

Metal	η(V)
Hg	0.78
Zn	0.70
Sn	0.53
Cu	0.23
Ni	0.21
Pt (bright)	0.10
Pt (platinized)	0.005

7.7 Theories of hydrogen overvoltage

The essential stages in the overall process of hydrogen discharge and gas evolution at a cathode may be assumed to be as follows:

1. H_3O^+ ions diffuse from the bulk solution to the edge of the double layer.
2. H_3O^+ ions are transferred across the layer.
3. Dehydration of H_3O^+.
4. H^+ receives an electron from the electrode.

Stages (2), (3) and (4) constitute the discharge reaction which may be expressed as

$$M + H_3O^+ + e \rightarrow M\text{–}H + H_2O \tag{7.37}$$

(H atom adsorbed onto electrode surface)

5. Formation of hydrogen molecules from hydrogen atoms.
   This can occur in one of two possible ways, viz.

   (i) $M\text{–}H + M\text{–}H \rightarrow 2M + H_2$ (7.38)

   or

   (ii) $M\text{–}H + H_3O^+ + e \rightarrow M + H_2 + H_2O$ (7.39)

   (i.e. a new H_3O^+ ion interacts on the electrode surface—this is often called the electrochemical reaction)
6. Desorption of hydrogen molecules.
7. Formation of bubbles and evolution of gas.

The problem is to decide which stages are rate determining. If stage (1) were to be rate determining, then the process overall would be diffusion limited due to concentration polarization. Usually, one of the stages (2) to (5) is the slowest. Which one depends upon many factors such as the operating conditions and the nature of the cathode.

Tafel proposed that step 5(i), equation (7.38), of the above scheme is the slow stage. He was able, on the basis of this assumption, to derive a form of equation (7.24) in which the constant b takes the form $2.3RT/2F$, i.e. approximately 0.03 at 298 K. Such a value is rarely encountered in practice although it is observed with low overvoltage metals and with platinized platinum.

For many metals showing higher overvoltages, stages (2) to (4), producing the discharge reaction (7.37) would seem to contain the slow step. Again it is possible to derive an expression of the form of equation (7.24) but for which $b \sim 0.118$ at 298 K. This value is indeed observed for many of the higher overvoltage metals.

A form of equation (7.24), identfying constant b, but also predicting a dependency of overvoltage on the pH of the solution may be derived assuming that the slow step is the electrochemical reaction (7.39).

It is clear that no one theory can account for all classes of behaviour under all conditions. For low overvoltage metals, it seems probable that the catalytic process is rate determining, while for metals showing higher overvoltages, slow ion-discharge theories are more successful in explaining observed behaviour. In a smaller number of instances, the electrochemical theory is more successful, for example in explaining the behaviour of silver and nickel in alkaline solution where η is observed to be a function of the pH of the solution.

For electrode materials with high catalytic activity, it would appear that the slow stage in the hydrogen evolution process can be the removal of molecular hydrogen from the electrode surface by diffusion.

Problems

7.1 If the Tafel constants, a and b, have the values 1.54 V and 0.119 V respectively for the reduction of hydrogen ions at a lead cathode, calculate the values of the transfer coefficient α and the exchange current density.

7.2 When dilute sodium hydroxide was electrolysed using a nickel cathode, the overpotential was found to be 0.394 V to maintain a current density of 0.01 A cm^{-2} and 0.148 V to maintain a current density of 0.0001 A cm^{-2}. Calculate the transfer coefficient and exchange current density for the hydrogen/hydrogen ion equilibrium at a nickel cathode in the given medium.

7.3 At cathode overvoltages indicated, the following values of cathodic current were obtained at a platinum electrode of area 1.5 cm^2 immersed in a solution of Fe^{2+} and Fe^{3+} ions at 298 K. Use these data to calculate the transfer coefficient and the exchange current density.

η(V)	0.02	0.05	0.07	0.10	0.12	0.15	0.20
I(mA)	3.20	9.95	17.03	35.18	55.89	110.78	343.62

7.4 Given that the Tafel constants for the deposition of zinc on platinum are a = 0.280 V and b = 0.059 V, respectively, show why it is not possible to plate zinc on to platinum by electrolysis of a zinc salt at unit activity in neutral solution at a current density of 1 mA cm^{-2}.

7.5 Given the values of α and i_0 calculated in question 7.3, for a $Pt/Fe^{3+}/Fe^{2+}$ electrode, estimate the current density for an anodic overvoltage of 0.07 V.

7.6 For the discharge of hydrogen ions from dilute sulphuric acid at a platinum electrode at 298 K, the following current densities were observed for the range of cathodic overvoltages indicated

η(mV)	20	50	70	100	120	150	200	250
i(m A cm^{-2})	0.57	1.40	2.05	3.36	4.56	7.16	15.05	31.55

From the appropriate Tafel plot calculate the transfer coefficient, α, and the exchange current density, i_0.

7.7 For a $Pt/Ce^{4+}/Ce^{3+}$ electrode the exchange current density, i_0 has the value $4.0 \times 10^{-5}\,A\,cm^{-2}$ while the transfer coefficient is 0.75. Taking the standard potential of the electrode as +1.61 V and assuming unit activity for both ion species, calculate the currents flowing through an electrode of area $1\,cm^2$ at applied potentials of 1.30, 1.40, 1.50, 1.61, 1.70, 1.80 and 1.90 V.

7.8 If for the electrode equilibrium $Cu^{2+} + 2e \rightleftharpoons Cu$, the transfer coefficient is 0.5 and the exchange current density is $2.5 \times 10^{-5}\,A\,cm^{-2}$, calculate the Tafel constants at 298 K and estimate the overpotential to deposit copper from a solution of unit activity at this temperature at a current density of $5 \times 10^{-3}\,A\,cm^{-2}$.

PART II APPLICATIONS

8 Determination and investigation of physical parameters

8.1 Applications of the Debye–Hückel equation

The various forms of the equations resulting from the Debye-Hückel theory find practical application in the determination of activity coefficients and make possible the determination of thermodynamic data. Two important cases will be considered here.

8.1.1 Determination of thermodynamic equilibrium constants

Let us consider as an example the dissociation of a 1:1 weak electrolyte

$$AB \rightleftharpoons A^+ + B^-$$

The thermodynamic dissociation constant K_T is given by

$$K_T = \frac{[A^+][B^-]}{[AB]} \frac{\gamma_{A^+}\gamma_{B^-}}{\gamma_{AB}} = K\frac{\gamma_\pm^2}{\gamma_{AB}}$$

Therefore

$$K_T \sim K\gamma_\pm^2 \tag{8.1}$$

where K is the concentration, or conditional dissociation constant. For a weak electrolyte in dilute solution γ_{AB} for the undissociated, and therefore non-ionic, species is very nearly unity. Taking logarithms of equation (8.1) and substituting for $\gamma_\pm$ from the limiting law expression, we obtain

$$\log K = \log K_T + 2A\sqrt{I} \tag{8.2}$$

K_T may therefore be determined from measured values of K over a range of ionic strength values and extrapolating the K versus $\sqrt{I}$ plot to $\sqrt{I} = 0$. This is a general technique for the determination of all types of thermodynamic equilibrium constants, e.g. solubility, stability and acid dissociation constants.

8.1.2 Dependence of reaction rates on ionic strength

In the treatment of ionic reactions by Brønsted and Bjerrum an equilibrium is considered to exist between reactant ions and a 'critical complex', the

latter bearing close resemblance to the activated complex of the theory of absolute reaction rates. Thus, for the reaction scheme

$$A^{z_A} + B^{z_B} \rightleftharpoons \left(x^{(z_A+z_B)}\right)^{\ddagger} \longrightarrow \text{products} \tag{8.3}$$

we may write, for the pre-equilibrium

$$K = \frac{[x^{\ddagger}]}{[A][B]} \frac{\gamma_{\ddagger}}{\gamma_A \gamma_B} \tag{8.4}$$

(omitting charges for clarity) so that the rate, v with which A and B react may be expressed by

$$v = k[A][B] = k_0[A][B]\frac{\gamma_A \gamma_B}{\gamma_{\ddagger}} \tag{8.5}$$

where

$$k = k_0 \frac{\gamma_A \gamma_B}{\gamma_{\ddagger}} \tag{8.6}$$

k_0, k being the rate constants at infinite and finite dilution, respectively. In logarithmic form equation (8.6) becomes

$$\log k = \log k_0 + \log \gamma_A + \log \gamma_B - \log \gamma_{\ddagger} \tag{8.7}$$

in which activity coefficients may be expressed by equation (2.15) thus,

$$\log k = \log k_0 - \frac{A\sqrt{I}}{1 + Ba\sqrt{I}} [z_A^2 + z_B^2 - (z_A + z_B)^2]$$

Therefore

$$\log k = \log k_0 + \frac{2Az_A z_B \sqrt{I}}{1 + Ba\sqrt{I}} \tag{8.8}$$

or,

$$\log k \sim \log k_0 + 2Az_A z_B \sqrt{I} \tag{8.9}$$

in very dilute solution, or,

$$\log k \sim \log k_0 + 1.02 z_A z_B \sqrt{I} \tag{8.10}$$

for water as solvent at 298 K.

These last equations take account of the salt effect observed for reactions between ions, the slopes of graphs of $\log k/k_0$ versus $\sqrt{I}$ being very close to those predicted by equation (8.10) at low concentrations (Figure 8.1). At higher concentrations, deviations from linearity occur and these are particularly noticeable for reactions having $z_A z_B = 0$, e.g. for a reaction

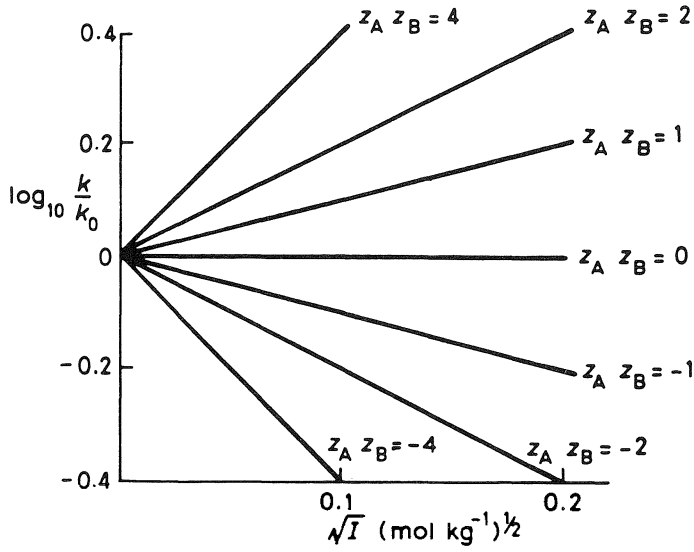

Figure 8.1 Theoretical variations of rate with $\sqrt{I}$ for reactions showing different values of the product $z_A z_B$.

between an ion and a neutral molecule. According to equation (8.10) such reactions should show no variation of rate with ionic strength and this is indeed the case up until about $I = 0.1$. Above this point, increasing ionic strength does cause the rate to vary. The reason for this is the bI term of the Hückel equation (2.19). In this case it may be readily shown that

$$\log k = \log k_0 + (b_A + b_B - b_{\pm})I \tag{8.11}$$

so that $\log k/k_0$ in this case becomes a linear function of I rather than of $\sqrt{I}$. This has been experimentally verified.

8.2 Determination of equilibrium constants by conductivity measurements

8.2.1 Solubilities of sparingly soluble salts

The conductivity of a saturated solution of a sparingly soluble salt may be found by subtracting from the observed value in water the conductivity of water itself. For such low concentrations of electrolyte the value for water, however pure, will now be significant, the small number of ions produced by the electrolyte giving a conductance of the same order of magnitude as water; for example, κ for an aqueous AgCl solution saturated at 298 K

was found to be $3.42 \times 10^{-4}\,\Omega^{-1}\,m^{-1}$. κ for the water used was $1.60 \times 10^{-4}\,\Omega^{-1}\,m^{-1}$.

Therefore
$$\kappa(AgCl) = (3.42 - 1.60) \times 10^{-4}\,\Omega^{-1}\,m^{-1}$$
$$= 1.82 \times 10^{-4}\,\Omega^{-1}\,m^{-1}$$

The molar conductivity, Λ_s, for a saturated solution of such an insoluble electrolyte may be taken as approximating closely to Λ_0. This quantity may be calculated, from values of λ_0^+ and λ_0^- derived from measurements on more soluble electrolytes, to be $1.38 \times 10^{-2}\,\Omega^{-1}\,mol^{-1}$. Thus equation (4.4a) may be used to calculate C which now becomes the solubility:

$$C \sim \frac{\kappa}{\Lambda_0} = \frac{1.82 \times 10^{-4}}{1.38 \times 10^{-2}}$$
$$= 1.32 \times 10^{-5}\,mol\,dm^{-3}$$

From this the solubility product, K_s, may be obtained as

$$K_s \sim [Ag^+][Cl^-] = 1.74 \times 10^{-10}$$

8.2.2 The ionic product of self-ionizing solvents

For water, which we have seen ionizes according to $H_2O + H_2O \rightleftharpoons H_3O^+ + OH^-$,

$$K_w = [H_3O^+][OH^-]$$

It is necessary to determine κ for very pure water. Then, knowing the ion conductivities for water at infinite dilution

$$C = [H_3O^+] = [OH^-] = \frac{\kappa}{(\lambda_{H^+})^0 + (\lambda_{OH^-})^0} \tag{8.12}$$

Hence C may be found and $K_w = C^2$.

8.2.3 Dissociation constants of weak electrolytes, e.g. weak acids

Dissociation constants may be determined from conductance data by use of equation (4.8) which, on rearrangement, gives

$$C\Lambda_C = K_a \frac{\Lambda_0^2}{\Lambda_C}\left(1 - \frac{\Lambda_C}{\Lambda_0}\right)$$
$$= K_a\left(\frac{\Lambda_0^2}{\Lambda_C} - \Lambda_0\right)$$

A plot of $C\Lambda_C$ versus $1/\Lambda_c$ gives a straight line of slope $K_a\Lambda_0^2$ and intercept $-K_a\Lambda_0$ from both of which K_a is determinable.

In order to determine the thermodynamic constant K_a^T it is necessary to determine K_a at different low concentrations and to obtain corresponding values of the degree of dissociation, α. From equation (8.1)

$$\log K_a^T = \log K_a - 2A\sqrt{I}$$

A being the Debye–Hückel constant for water as solvent, and for a weak acid, HA

$$I = \tfrac{1}{2}([H^+] + [A^-]) \quad \text{and} \quad [H^+] = [A^-] = \alpha C$$

therefore

$$I = \alpha C$$

therefore,

$$\log K_a^T = \log K_a - 2A\sqrt{(\alpha C)} \tag{8.13}$$

where K_a^T is the true thermodynamic dissociation constant of the acid, a plot of $\log K_a$ versus $\sqrt{(\alpha C)}$ giving a straight line of intercept $\log K_a^T$.

8.3 Thermodynamics of cell reactions

Measurement of the emf of a reversibly operating cell as well as its temperature coefficient enable ΔG,ΔH and ΔS for the cell reaction to be determined. ΔG at a given temperature follows directly from the cell emf E, by application of the equation

$$\Delta G = -nFE \tag{8.14}$$

ΔH may be expressed in terms of ΔG in the form of the Gibbs–Helmholtz equation

$$\Delta H = \Delta G - T\left[\frac{\partial(\Delta G)}{\partial T}\right]_P \tag{8.15}$$

which, in terms of the cell emf, takes the form

$$\Delta H = -nFE - T\left[\frac{\partial(-nFE)}{\partial T}\right]_P \tag{8.16}$$

or,

$$\Delta H = -nFE + nFT\left(\frac{\partial E}{\partial T}\right)_P \tag{8.17}$$

$(\partial E/\partial T)_P$ being the temperature coefficient of the cell emf at constant pressure. In practice this has to be determined very carefully by determining E for the cell over a wide range of temperature so that the tangent to the E–T plot at a given temperature may be drawn and its slope measured.

Once ΔG and ΔH have been found, ΔS may be calculated from

$$\Delta G = \Delta H - T\Delta S \tag{8.18}$$

or

$$\Delta S = \frac{(\Delta H - \Delta G)}{T}$$

therefore,

$$\Delta S = nF\left(\frac{\partial E}{\partial T}\right)_{\mathrm{P}} \tag{8.19}$$

Since cell emf values are measured in volts, the units of ΔH and ΔG are joules and those of ΔS, joules deg^{-1}. Positive, negative and almost zero temperature coefficients have been observed, although negative coefficients are the most usual, signifying that for most cells the electrical energy obtainable from them is less than ΔH because some heat is produced as the cell operates. For positive coefficients the energy obtainable is greater than ΔH and in this case heat must be absorbed from the surroundings when the cell operates and unless a supply of heat is maintained the temperature of such a cell will fall. For a cell with a near zero temperature coefficient, the electrical energy is almost identical with the enthalpy change and this is found, for example, with the Daniell cell. It was somewhat unfortunate that early work with a Daniell cell appeared to confirm the erroneous belief that the electrical energy of a reversible cell was always equal to $-\Delta H$ of the cell reaction.

In principle, electrochemical measurements provide a most sophisticated means of determining such data particularly in the light of the precision with which potentials may be measured when due experimental precautions are taken. It is essential, however, that the reaction under study does actually occur in the cell to the exclusion of all others. It is also vital, of course, that both the electrodes used in the cell behave reversibly.

8.4 Determination of standard potentials and mean ion activity coefficients

Of particular use in such determinations are cells of the Harned type of which the simplest is represented by

$$\mathrm{H_2(1\ atm),\ Pt|HCl|AgCl(s),Ag}$$
$$m$$

m being the molality of the hydrochloric acid. Since the overall cell reaction is

$$\tfrac{1}{2}\mathrm{H_2} + \mathrm{AgCl(s)} \longrightarrow \mathrm{Ag(s)} + \mathrm{H^+} + \mathrm{Cl^-} \tag{8.20}$$

$$-\Delta G = \underset{(n=1)}{nFE} = RT \ln K - RT \ln \frac{a_{Ag} a_{H^+} a_{Cl^-}}{a_{H_2}^{1/2} a_{AgCl}} \tag{8.21}$$

or

$$E = E^{\ominus} - \frac{RT}{F} \ln a_{H^+} a_{Cl^-} = E^{\ominus} - \frac{2RT}{F} \ln a_{\pm} \tag{8.22}$$

In terms of the molality of the hydrocholoric acid equation (8.22) becomes

$$E = E^{\ominus} - \frac{2RT}{F} \ln m - \frac{2RT}{F} \ln \gamma_{\pm} \tag{8.23}$$

$\gamma_{\pm}$ being the mean ion activity coefficient of the acid. Equation (8.23) may more usefully be expressed in the form

$$\left(E + \frac{2RT}{F} \ln m\right) = E^{\ominus} - \frac{2RT}{F} \ln \gamma_{\pm} \tag{8.24}$$

It is seen that this equation provides a valuable route to the determination of $\gamma_{\pm}$ but that in order to do this it is necessary to know $E^{\ominus}$. If a number of measurements of E are made for a range of values of m extending into the region where the Debye–Hückel limiting law holds, i.e. where $\ln \gamma_{\pm} \propto m^{\frac{1}{2}}$, $E^{\ominus}$ may be obtained by plotting the left hand side of equation (8.24) versus $m^{\frac{1}{2}}$. As $m \to 0, \gamma_{\pm} \to 1$ so that extrapolation of the line to $m^{\frac{1}{2}} = 0$ gives $E^{\ominus}$ as intercept.

It is normally better, however, to use forms of the Hückel equation, e.g.

$$-\ln \gamma_{\pm} = A\left(\frac{\sqrt{m}}{1+\sqrt{m}} - Bm\right) \tag{8.25}$$

so that

$$\left[E + \frac{2RT}{F} \ln m - \frac{A\sqrt{m}}{1+\sqrt{m}}\right] = E^{\ominus} - ABm \tag{8.26}$$

A graph of the left-hand side of equation (8.26) versus m may be extrapolated to the condition $m = 0$ to give an intercept of $E^{\ominus}$.

Once $E^{\ominus}$ is known, equation (8.26) may be used to calculate $\gamma_{\pm}$ for any molality of acid. The general principle of the technique may be extended to other electrolytes provided that the cell can be devised so that each electrode is reversible with respect to one of the ions.

Another possibility is to combine two cells of the above type back-to-back in the form of a cell without transference. The emf of such a cell is given by

$$E = \frac{2RT}{F} \ln \frac{m_2(\gamma_{\pm})_2}{m_1(\gamma_{\pm})_1} \tag{8.27}$$

If $(\gamma_{\pm})_1$ is known at molality m_1, $(\gamma_{\pm})_2$ at molality m_2 (or any other molality) may be determined by using equation (8.27) in the form

$$\frac{EF}{2 \times 2.3RT} = \log \frac{m_2}{m_1} + \log \frac{(\gamma_{\pm})_2}{(\gamma_{\pm})_1} \tag{8.28}$$

or,

$$\log(\gamma_{\pm})_2 = \frac{EF}{4.6RT} + \log(\gamma_{\pm})_1 - \log\frac{m_2}{m_1} \tag{8.29}$$

$(\gamma_{\pm})$ may be determined by the Debye–Hückel relation in dilute solution, i.e.

$$-\log\gamma_{\pm} = \frac{A\sqrt{m}}{1 + Ba\sqrt{m}} \tag{8.30}$$

(for a 1:1 electrolyte). Rearrangement and expansion of equation (8.30) gives

$$\begin{aligned} -\log\gamma_{\pm} &= A\sqrt{m}(1 + Ba\sqrt{m})^{-1} \\ &= A\sqrt{m}(1 - Ba\sqrt{m} + \cdots) \\ &= A\sqrt{m} - ABam \end{aligned} \tag{8.31}$$

It was shown by Hitchcock that $\log\gamma_{\pm}$ may also be given by

$$\log\gamma_{\pm} = B' - \log\frac{(\gamma_{\pm})_1}{(\gamma_{\pm})_2} \tag{8.32}$$

where B' is a further constant. Combining equation (8.32) with equation (8.31) gives

$$\log\frac{(\gamma_{\pm})_1}{(\gamma_{\pm})_2} - A\sqrt{m} = B'(ABa)m \tag{8.33}$$

If the left-hand side of equation (8.33) is plotted against m, a linear plot is obtained of slope (ABa) and intercept B'. When B' is known, the value of $\log\gamma_{\pm}$ at any molality may be calculated by means of equation (8.32)

If transport numbers for electrolyte ions are known reliably over the concentration range used in a cell, it is possible to determine $\gamma_{\pm}$ values from cells with transference. This, however, is a less usual practice.

Amalgam electrodes have proved useful in the determination of values for alkali chlorides and hydroxides using cells such as

$$\mathrm{M(Hg)|MCl|AgCl(s), Ag}$$

or

$$\mathrm{H_2, Pt|MOH|M(Hg)}$$

8.5 The determination of transport numbers

The concept of transport number was introduced in Chapter 4 where it was seen that the complementary movement of cations and anions under the

influence of an applied electric field could be used to identify the behaviour of individual ion species.

There are essentially three approaches to the determination of transport numbers: the method due to Hittorf (of which there are several modifications), the moving boundary method (of which there are several forms) and methods based on measurements of cell emf.

8.5.1 Determination by the Hittorf method

In this method the cathode, anode and central portions of an electrolysis cell are made physically distinct and solutions contained within them (catholyte, anolyte and central) are analysed after controlled electrolysis for a known period of time.

Figure 8.2 shows the Hittorf mechanism of electrolysis when using electrodes made of the metal whose cations are those of the electrolyte in solution and when Q coulombs are passed. It is seen that the concentration of the electrolyte in the central portion of the cell remains unchanged at the end of the electrolysis.

Consider an electrolyte, represented by MX, whose constituent ions are M^{z+} and X^{z-} where $|z_+| = |z_-|$ (an example would be copper sulphate giving Cu^{2+} and SO_4^{2-}).

At the cathode M^{z+} ions are discharged according to

$$M^{z+} + ze \longrightarrow M$$

while at the anode M dissolves,

$$M \longrightarrow M^{z-} + ze$$

As a consequence of Faraday's laws (Chapter 1), after the passage of Q coulombs, $Q/|z_+|F$ moles of M have been deposited on the cathode surface. Of these $Q/|z_+|F$ moles only an amount $t_+Q|z_+|F$ is provided by the migration process. The remainder must be provided by electrolyte close to the cathode surface. Most of the species M^{z+} will thus be stripped out of the immediate vicinity of the cathode soon after electrolysis is started.

A concentration gradient will now be set up between the solution at the surface of the cathode and regions of the solution further away. Across this gradient M^{z+} and X^{z-} ions will diffuse and by the time Q coulombs have passed, $t_-Q/|z_+|F$ moles of M^{z+} will have been provided by diffusion, and discharged as M, to make up the total of $Q/|z_+|F$ moles of M deposited.

When a steady current flows, the concentration gradient at the electrode surface automatically adjusts itself to maintain just the correct rate of diffusion. Diffusion of both ion species of the electrolyte ensures that there is always sufficient of the anion being provided in this region so that the rate

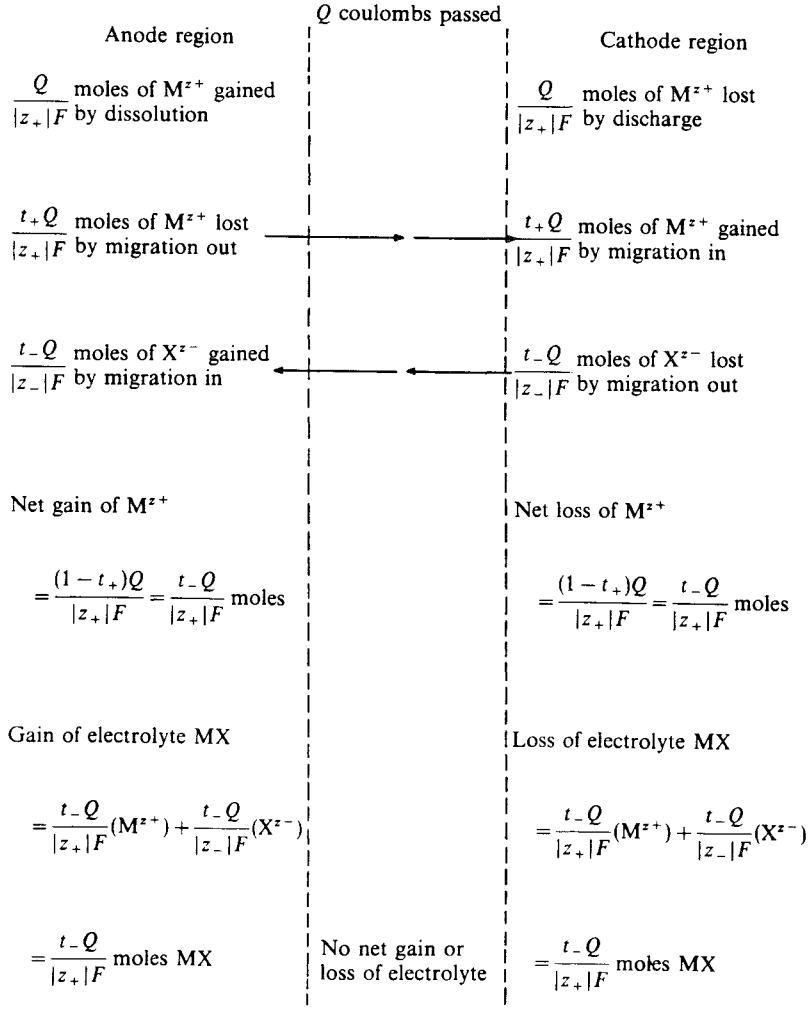

Figure 8.2 Hittorf electrolysis mechanism for the case where the electrodes are of the metal whose cation is that of the electrolyte in solution.

of migration of the anion away from the cathode is maintained. It is seen from Figure 8.2 that a net loss of $t_-Q/|z_+|F$ moles of electrolyte occurs in the catholyte solution.

Similar arguments apply to the anode region. After the passage of Q coulombs, $Q/|z_+|F$ moles of M^{z+} have dissolved from the anode of which $t_+Q/|z_+|F$ migrate out, leaving a net gain of $t_-Q/|z_+|F$ moles of M^{z+} in the anolyte. This is complemented by the migration into the anolyte of $t_-Q/|z_-|F$ moles of X^{z-}. Thus a net gain of $t_-Q/|z_+|F$ moles of electrolyte occurs in the anolyte solution.

As to the central portion, whatever it has gained from the anode region it has donated to the cathode region and vice versa. It thus experiences neither a net gain nor a net loss of electrolyte during the course of the electrolysis unless this is so prolonged that the diffusion processes, referred to above, extend so far out from the electrode surfaces that they become significant here and invalidate the calculations.

It is important to note that for the above case, in which it is the cations which react at the electrodes, the losses and gains in both electrode regions are functions of the transport number of the anion. It is evident that the transport number of the cation cannot be determined independently but must be calculated from the expression

$$t_+ + t_- = 1$$

For the case where the electrolyte is of a more general type whose ions are dispersed in solution according to

$$M_{\nu+}X_{\nu-} \longrightarrow \nu_+ M^{z+} + \nu_- X^{z-}$$

then the respective gain and loss of electrolyte in anolyte and catholyte is again given by,

$$\frac{t_- Q}{|z_+|F}(M^{z+}) + \frac{t_- Q}{|z_-|F}(X^{z-})$$

Here, however,

$$z_+ \neq z_-$$

but rather

$$\nu_+ z_+ = \nu_- z_-$$

i.e. the gain and loss become

$$\frac{t_- Q}{|z_+|F}(M^{z+}) + \left(\frac{\nu_-}{\nu_+}\right)\left(\frac{t_- Q}{|z_+|F}\right) = \frac{t_- Q}{|z_+|F} \text{ moles of } M_{\nu+}X_{\nu-}$$

For example, in the case of a copper(II) halide, CuX_2, for which $z_+ = 2$ and $z_- = 1, \nu_+ = 1$ and $\nu_- = 2$, the gain and loss are

$$\frac{t_- Q}{2F}(Cu^{2+}) + \frac{2t_- Q}{2F}(X^-) = \frac{t_- Q}{2F}(CuX_2)$$

Electrolysis processes may not always be as simple as this and caution must be exercised in calculating transport numbers in that it is necessary to have firm prior knowledge of precisely what electrode reactions occur. For instance, for the electrolysis of metal salts with inert electrodes, such as platinum, hydrogen and not the metal cation may be discharged; similarly, oxygen may be discharged in preference to the anion. Even if the electrolyte

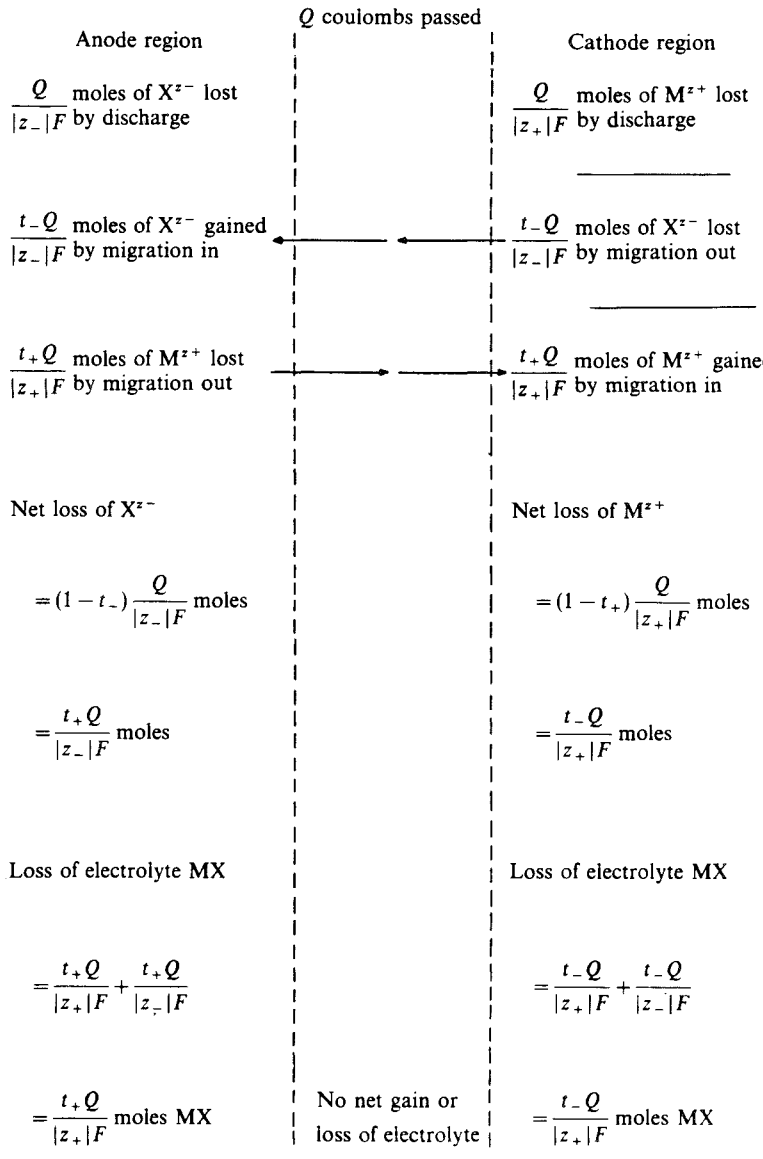

Figure 8.3 Hittorf electrolysis mechanism for the case in which anion and cation are discharged at inert electrodes.

anion and cation are discharged, the net result using inert electrodes will be quite different from the case considered above. The mechanism in this case is shown in Figure 8.3. Here it is seen that there is a net loss of electrolyte

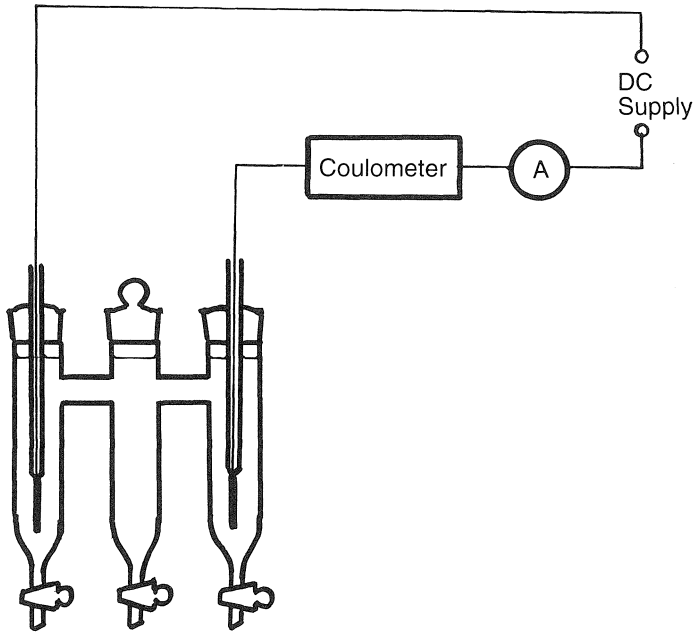

Figure 8.4 Experimental circuit for Hittorf determination of transport numbers.

from both anode and cathode regions. Again, however, no gain or loss occurs in the central region.

For this case at the cathode M^{z+} cations are discharged,

$$M^{z+} + ze \longrightarrow M$$

while at the anode X^{z-} anions are discharged

$$X^{z-} \longrightarrow X + ze$$

The essential experimental circuit for Hittorf's method is shown in Figure 8.4.

A current of 10–20 mA is passed for 1–2 hours. Smaller currents passed for longer times encourage the undesirable diffusion into the central compartment. After electrolysis, samples of solution from anode and/or cathode compartment are withdrawn and analysed. It is also advisable to analyse a sample of solution from the central compartment to check that the composition in this region has, in fact, remained unchanged.

It is most important that concentrations of the compartments be referred to a given weight of solvent, since concentration changes in the electrolyte solution are associated with volume changes. This is due to the fact that ionic species are hydrated and carry their hydration shells with them during their movements through a solution during electrolysis. Suppose that a

given weight of solvent contains n_0 moles of a cation species initially and n after electrolysis. If n_e is the number of moles deposited cathodically (determined by the series coulometer), $t_+ n_e$ is the number added to the cathode region by migration. Thus,

$$n - n_0 = n_e - t_+ n_e$$

and therefore,

$$t_+ = \frac{n_e + n_0 - n}{n_e} \tag{8.34}$$

Hittorf's method provides an excellent demonstration of the nature of electrolysis processes. On the practical level, however, it has obvious drawbacks, not least of which is the usually low precision with which the small concentration changes may be determined.

8.5.2 Determination by moving boundary methods

Such methods represent direct applications of equations (4.54) and (4.55) whereby transport numbers are related to the speeds with which ions move. Moving boundary techniques are based upon the observed rate of movement, under the influence of an applied emf, of a sharp boundary between solutions of two different electrolytes having an anion or cation in common. Measurement of the rate of movement of a sharp boundary presents few problems, since, even if the solutions do not differ in colour, the difference in their refractive indices makes the boundary between them easily distinguishable. A schematic diagram of the relation between two such solutions is shown in Figure 8.5 for the determination of the transport number of a cation. For anion transport numbers, two electrolytes with a common cation are used. If the transport number of M_1^+ is required, $M_2^+X^-$ is referred to as the indicator electrolyte, M_1^+ being sometimes referred to as the leading ion. It is necessary for this latter ion to have higher conductivity than M_2^+.

Let us suppose that the boundary moves from AB to CD when a quantity It coulombs of electricity is passed; let the volume swept out by the boundary be V. Thus, in the volume bounded by AB and CD, the $M_1^+X^-$ initially present is completely replaced by $M_2^+X^-$ after the passage of It coulombs. Or, C_1VF charges pass through a section of the tube in time t. This in turn must be equal to the fraction t_1^+It of the quantity of electricity passed.

Therefore

$$t_1^+ = \frac{C_1 VF}{It} \tag{8.35}$$

Apart from the density and conductivity conditions indicated in Figure 8.5 there is a particular value of the ratio C_1/C_2 necessary for the boundary to

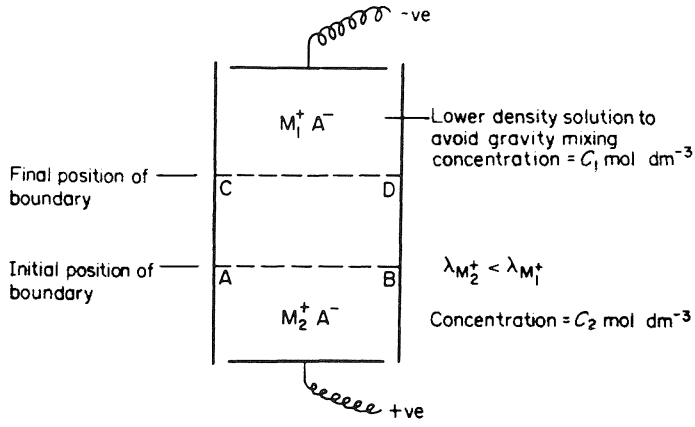

Figure 8.5 Principle of the moving boundary method.

remain sharp. This may be shown as follows: suppose that the boundary moves from AB to CD on the passage of 1 Faraday, so that the quantity of M_1^+ transported across the boundary is t_1^+ moles. Since this was originally contained in a volume V, it follows that

$$t_1^+ = C_1 V \tag{8.36}$$

Similarly, for the indicator electrolyte,

$$t_2^+ = C_2 V \tag{8.37}$$

Or, combining equations (8.36) and (8.37)

$$\frac{C_2}{C_1} = \frac{t_2^+}{t_1^+} \tag{8.38}$$

It appears from this last equation that only by accurate fore-knowledge of t_2^+/t_1^+ could the correct value of C_2 be decided. In practice it is only found necessary for equation (8.38) to hold within about 10%. Since the indicator solution is chosen to have a lower conductivity than that of the electrolyte under study, the field gradients must differ in the two solutions if the ions M_1^+ and M_2^+ are to move at the same speed and maintain a sharp boundary.

Since $\lambda_{M_2^+} < \lambda_{M_1^+}$, the potential gradient (for a given current) is steeper in the indicator solution than in the leading solution. If M_1^+ ions tended to lag behind the boundary into the indicator solution, they would immediately be accelerated by the steeper potential gradient towards the boundary. Similarly, if M_2^+ ions tended to move in front of the boundary, the smaller potential gradient would serve to slow them down (Figure 8.6)

The simplest use of the moving boundary method is that in which an autogenic boundary is formed, i.e. one formed spontaneously at the start of an electrolysis.

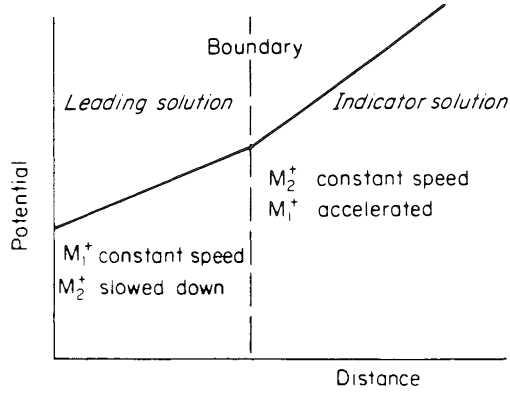

Figure 8.6 Conditions for maintenance of a sharp boundary.

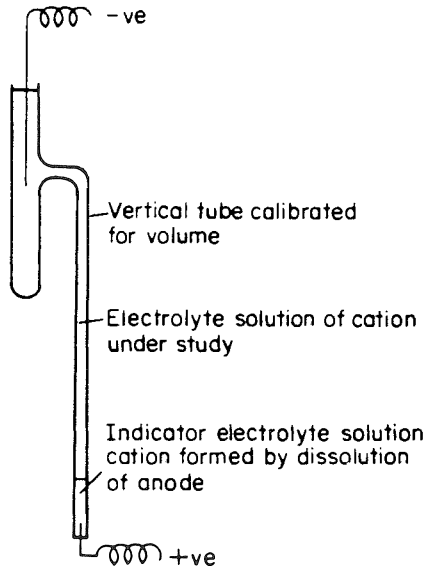

Figure 8.7 The formation of an autogenic boundary.

The principles are shown in Figure 8.7. The cathode is chosen as appropriate to the electrolyte used: if the transport number of metal ion M^+ is to be determined, an electrolyte MX is used, using a cathode of metal M. The anode might be copper or cadmium.

On application of a potential the anode dissolves and a solution of CuX_2 or CdX_2 is formed near to its surface. This is the indicator solution; the boundary between MX and CuX_2 or CdX_2 is followed in order to obtain a value of the transport number of M^+ by application of equation (8.35).

8.5.3 Determination using cell emf

Comparison of the expressions for the emf values of cells with and without transport, for example for the cells

$$\begin{array}{c} \mathrm{Zn|ZnSO_4 \vdots ZnSO_4|Zn} \\ (a_\pm)_1 \quad (a_\pm)_2 \qquad\qquad \text{emf } E_1 \end{array}$$

and

$$\begin{array}{c} \mathrm{Zn|ZnSO_4,\ Hg_2SO_4|Hg|Hg_2SO_4,\ ZnSO_4|Zn} \\ (a_\pm)_1 \qquad\qquad\qquad\qquad (a_\pm)_2 \qquad\qquad \text{emf } E_2 \end{array}$$

shows that the first involves the transport number, t_-, of the sulphate anion, whilst the second does not: thus

$$E_1 = t_- \frac{RT}{F} \ln \frac{(a_\pm)_2}{(a_\pm)_1} \tag{8.39}$$

and

$$E_2 = \frac{RT}{F} \ln \frac{(a_\pm)_2}{(a_\pm)_1} \tag{8.40}$$

and

$$\frac{E_1}{E_2} = t_- \tag{8.41}$$

It must be borne in mind that t_- represents the average value of the transport number for the two solutions of mean ion activities $(a_\pm)_1$ and $(a_\pm)_2$. The values of these latter quantities should therefore in practice be as close to one another as is compatible with sufficiently large emf values to be precisely measured.

8.5.4 Interpretation and application of transport numbers

In section 8.5.1 it was pointed out how necessary it is to know and understand the electrode process which occurs at the anode and cathode during transport number measurements so that one is quite sure which ion it is for which a certain value is determined. One must also pay strict attention to the way in which an electrolyte may ionize and the forms in which the ions are present in solution under given conditions. In this way experimental results which appear unrealistic may be explained rationally. The cadmium ion shows a transport number of about 0.4 in very dilute solutions of cadmium iodide. With progressively higher electrolyte concentrations, however, the value drops sharply below 0.4, passes through zero and finally

attains negative values. At the same time the transport number of the iodide ion apparently increases beyond 0.6, passes through, and eventually exceeds, unity.

The above observations are easily explained when the nature of the ions present in more concentrated solutions of cadmium iodide is understood. In such solutions this electrolyte exists largely as Cd^{2+}, and CdI_4^{2-}, i.e. as the simple cadmium ion with a double charge and as a doubly charged anionic complex ion. This latter will obviously migrate in a direction opposite to that of the simple ion. The fact that measured cadmium transport numbers approach negative values indicates that the conductivity of the complexed form is greater than that of the uncomplexed (aquo) form so that a net loss of cadmium occurs at the cathode.

A more fundamental use of transport numbers is in the determination of ion conductivities from measurements of conductivities of electrolytes; an ion conductivity being a fraction t_+ of the observed value for the electrolyte. In order to obtain infinite dilution values of ion conductivities, molar conductivities and transport numbers also have to be obtained by extrapolation to these conditions. In some cases this process may be unreliable. Once, however, the conductivity of a given ion is reliably obtained it is possible to obtain those of any oppositely charged partner in a variety of electrolytes by subtraction.

8.6 Determination of equilibrium constants by measurements of potential

8.6.1 Dissociation constants of weak acids

Such constants may be determined approximately by application of the Henderson–Hasselbalch equation (see equation (3.50)), viz.

$$\mathrm{pH} \sim \mathrm{p}K_\mathrm{a} + \log \frac{b}{a-b} \tag{8.42}$$

where a is the number of moles of a weak monobasic acid in solution and b the number of moles of a strong base added to it so that some of the acid is converted to the salt of the base. It is clear that if $b = a/2$ then $\mathrm{pH} = \mathrm{p}K_\mathrm{a}$, so that, if half the equivalent amount of strong base is added to the weak acid, the pH of the resulting solution is approximately the $\mathrm{p}K_\mathrm{a}$ value.

Figure 8.8 shows the experimental curve for the titration of $25\,\mathrm{cm}^3$ of $0.1\,\mathrm{mol\,dm}^{-3}$ ethanoic acid with $0.1\,\mathrm{mol\,dm}^{-3}$ sodium hydroxide at 298 K. At the half-equivalence point, pH = 4.74, i.e.

$$\mathrm{p}K_\mathrm{a} = 4.74 \text{ and } K_\mathrm{a} = 1.82 \times 10^{-5}$$

At the equivalence point equation (3.41) predicts that the pH should be given by

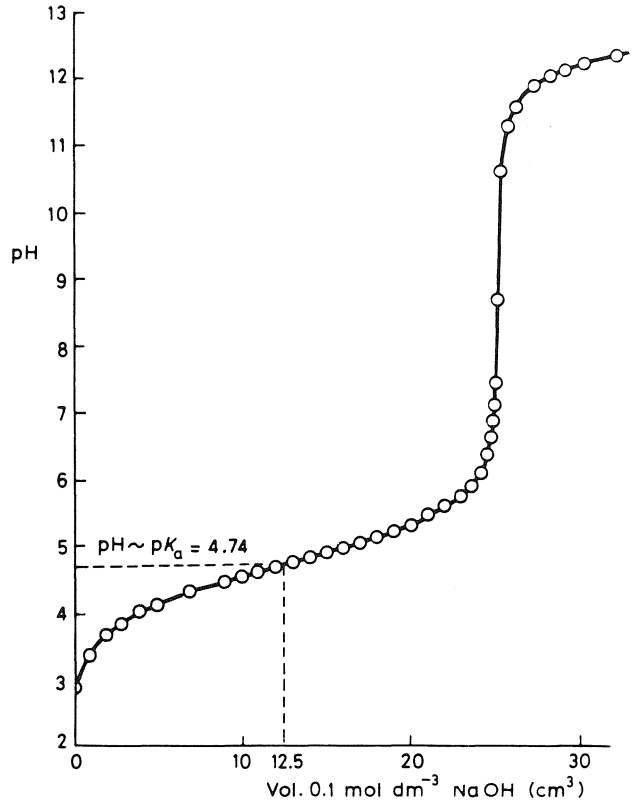

Figure 8.8 Variation of pH with volume of added 0.1 mol dm^{-3} sodium hydroxide during titration of 25 cm^3 0.1 mol dm^{-3} ethanoic acid.

$$\begin{aligned} \text{pH} &= \tfrac{1}{2}(\text{p}K_\text{w} + \text{p}K_\text{a} + \log C) \\ &= \tfrac{1}{2}(14 + 4.74 + (-1.30)) \\ &= 8.72 \end{aligned}$$

This value agrees closely with the value in Figure 8.8.

More accurate determinations are based on emf measurements of Harned cells in which the central compartment is occupied by a solution of the weak acid, one of its salts formed with a strong base, and a strong electrolyte with its cation derived from the strong base and its anion common with that of the electrode anion, e.g.

$$\text{Pt, H}_2(1\text{ atm})|\text{HA}(m_1), \text{NaA}(m_2), \text{NaCl}(m_3), \text{AgCl(s)}|\text{Ag}$$

The emf of this cell if given by

$$E_{\text{cell}} = E_{\text{AgCl}} - E_{\text{H}_2} \tag{8.43}$$

therefore,

$$E_{\text{cell}} = E^{\ominus}_{\text{AgCl}} - \frac{RT}{F} \ln a_{\text{Cl}^-} - \frac{RT}{F} \ln a_{\text{H}^+} \tag{8.44}$$

or,

$$E_{\text{cell}} = E^{\ominus}_{\text{AgCl}} - \frac{RT}{F} \ln a_{\text{H}^+} a_{\text{Cl}^-} \tag{8.45}$$

therefore,

$$\frac{F(E_{\text{cell}} - E^{\ominus}_{\text{AgCl}})}{RT} = -\ln m_{\text{H}^+} m_{\text{Cl}^-} - \ln \gamma_{\text{H}^+} \gamma_{\text{Cl}^-} \tag{8.46}$$

Now

$$K_{\text{a}} = \left(\frac{m_{\text{H}^+} m_{\text{A}^-}}{m_{\text{HA}}} \right) \left(\frac{\gamma_{\text{H}^+} \gamma_{\text{A}^-}}{\gamma_{\text{HA}}} \right)$$

Therefore,

$$\ln K_{\text{a}} = \ln \frac{m_{\text{H}^+} m_{\text{A}^-}}{m_{\text{HA}}} \ln \frac{\gamma_{\text{H}^+} \gamma_{\text{A}^-}}{\gamma_{\text{HA}}} \tag{8.47}$$

If the right-hand side of equation (8.47) is added to the right-hand side of equation (8.46) while the left-hand side of equation (8.47) is subtracted from it, the equality in equation (8.46) is in no way affected, thus

$$\frac{F(E_{\text{cell}} - E^{\ominus}_{\text{AgCl}})}{RT} = -\ln \frac{m_{\text{HA}} m_{\text{Cl}^-}}{m_{\text{A}^-}} - \ln \frac{\gamma_{\text{HA}} \gamma_{\text{Cl}^-}}{\gamma_{\text{A}^-}} - \ln K_{\text{a}}$$

or

$$\left[\frac{F(E_{\text{cell}} - E^{\ominus}_{\text{AgCl}})}{2.3RT} + \log \frac{m_{\text{HA}} m_{\text{Cl}^-}}{m_{\text{A}^-}} \right] = -\log \frac{\gamma_{\text{HA}} \gamma_{\text{Cl}^-}}{\gamma_{\text{A}^-}} - \log K_{\text{a}} \tag{8.48}$$

The emf of the cell is measured at various values of m_1, m_2 and m_3 and the left-hand side of equation (8.48) plotted as a function of the ionic strength of the solution. At the condition $\text{I} \rightarrow 0$, each $\gamma \rightarrow 1$ and the right-hand side of the equation approaches $-\log K_{\text{a}}$.

Since the sodium chloride is completely dissociated, $m_{\text{Cl}^-} = m_3$. HA is partly dissociated into H_3O^+ and A^- so that $m_{\text{HA}} = m_1 - m_{\text{H}_3\text{O}^+} \sim m_1$ if $m_{\text{H}_3\text{O}^+}$ is small. Also, the A^- ions originate partly from NaA and partly from HA so that $m_{\text{A}^-} = m_2 + m_{\text{H}_3\text{O}^+} \sim m_2$ if $m_{\text{H}_3\text{O}^+}$ is small. Thus equation (8.48) may be reasonably approximated to

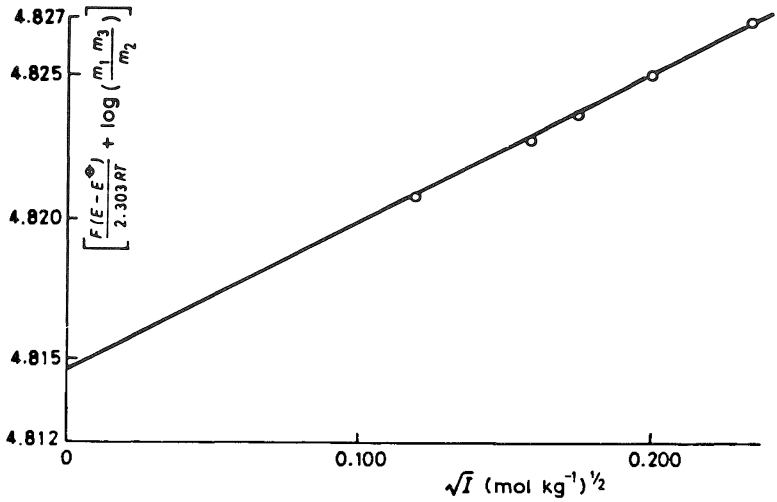

Figure 8.9 Determination of the dissociation constant of n-butyric acid in aqueous solution according to equation (8.48). $-\log K_a = 4.8147$; $K_a = 1.52 \times 10^{-5}$.

$$\left[\frac{F(E_{cell} - E^{\ominus}_{AgCl})}{2.3RT} + \log\left(\frac{m_1 m_3}{m_2}\right)\right] = -\log\frac{\gamma_{HA}\gamma_{Cl^-}}{\gamma_{A^-}} - \log K_a \qquad (8.49)$$

Figure 8.9 shows the appropriate plot for the system

Pt, H_2|butyric acid (m_1), sodium butyrate (m_2), NaCl(m_3), AgCl(s)|Ag

Use of equation (8.49) is restricted to acids with pK_a values in the region of 4–5; $m_{H_3O^+}$ must be calculated in the case of stronger acids and the effects of hydrolysis must be taken into account for weaker acids. The important feature of the method is that it is independent of pH measurements. pK_a values determined in this way may be used to standardize the practical pH scale which will be discussed in section 8.7.

A further method involves forming a half-cell by immersing a hydrogen electrode in the solution of the acid whose dissociation constant is required. A complete cell is made by coupling this half-cell with a suitable reference electrode via a salt bridge. The acid is titrated with a strong base, the pH of the solution being measured potentiometrically after each addition of base.

It is necessary to calibrate the reference electrode and salt bridge with standard buffers if agreement is to be obtained between values of dissociation constants obtained by this method and those resulting from Harned cell measurements, which are independent of pH.

We require a formal expression for $a_{H_3O^+}$ which is provided by the equation for the thermodynamic dissociation constant of the acid, viz.

$$\begin{aligned} a_{H_3O^+} &= \frac{K_a a_{HA}}{a_{A^-}} \\ &= K_a \left(\frac{m_{HA}}{m_{A^-}}\right)\left(\frac{\gamma_{HA}}{\gamma_{A^-}}\right) \end{aligned} \tag{8.50}$$

Let the overall concentration of the acid be m_a; during the course of the titration m_{HA} will decrease as A^- is formed and m_{A^-} increases. At all stages, however,

$$m_a = m_{HA} + m_{A^-} \tag{8.51}$$

If m_b represents the varying concentration of base added during the titration, it is seen that

$$m_b + m_{H^+} = m_{A^-} + m_{OH^-} \tag{8.52}$$

i.e.

$$m_b = m_{A^-} + m_{OH^-} - m_{H^+}$$

Substitution for m_{HA} from equation (8.51) and for m_{A^-} from equation (8.52) into equation (8.50) gives

$$\begin{aligned} a_{H_3O^+} &= K_a \left[\frac{m_a - m_{A^-}}{m_b - m_{OH^-} + m_{H^+}}\right]\left(\frac{\gamma_{HA}}{\gamma_{A^-}}\right) \\ &= K_a \left[\frac{m_a - m_b + m_{OH^-} - m_{H^+}}{m_b - m_{OH^-} + m_{H^+}}\right]\left(\frac{\gamma_{HA}}{\gamma_{A^-}}\right) \\ &= K_a \left(\frac{m_a - B}{B}\right)\left(\frac{\gamma_{HA}}{\gamma_{A^-}}\right) \end{aligned} \tag{8.53}$$

where $B = m_b - m_{OH^-} + m_{H^+}$ or,

$$\mathrm{pH} = \mathrm{p}K_a + \log \frac{B}{m_a - B} + \log \frac{\gamma_{A^-}}{\gamma_{HA}} \tag{8.54}$$

The last term on the right-hand side of equation (8.54) may be expressed in terms of the Debye–Hückel theory i.e.,

$$\log \frac{\gamma_{A^-}}{\gamma_{HA}} = -A\sqrt{I} + bI \tag{8.55}$$

so that equation (8.54) becomes

$$A\sqrt{I} - \log \frac{B}{m_a - B} + \text{pH} = \text{p}K_a + bI \tag{8.56}$$

pK_a may now be determined by plotting the left-hand side of equation (8.56) for each point of the titration curve, against ionic strength. The value is obtained, by extrapolation to zero ionic strength, as the intercept on the ordinate axis. Calculation of B is facilitated by the application of similar approximations to those used in the Harned method.

In order for the values of pK_a to be in agreement with those obtained by the Harned method, it is vital that the potential of the reference electrode/salt bridge combination is given a value such that the pH values determined during the titration agree with those obtained by calculation from true dissociation constants given by the Harned method.

8.6.2 The ionization constant of water

Again, a cell without a liquid junction is used, e.g.

$$\text{Pt}, H_2|\text{MOH}(m_1),\ \text{MCl}(m_2)|\text{AgCl(s)}, \text{Ag}$$

for which

$$E = E^{\ominus} - \frac{RT}{F} \ln m_{H^+} m_{Cl^-} \gamma_{H^+} \gamma_{Cl^-} \tag{8.57}$$

Now

$$\begin{aligned} K_w &= \frac{a_{H^+} a_{OH^-}}{a_{H_2O}} \\ &= \frac{\gamma_{H^+} \gamma_{OH^-} m_{H^+} m_{OH^-}}{a_{H_2O}} \end{aligned} \tag{8.58}$$

Combining equations (8.57) and (8.58) and noting that $a_{H_2O} = 1$, we obtain

$$\begin{aligned} E &= E^{\ominus} - \frac{RT}{F} \ln \frac{m_{Cl^-} \gamma_{Cl^-} K_w}{m_{OH^-} \gamma_{OH^-}} \\ &= E^{\ominus} - \frac{RT}{F} \ln K_w - \frac{RT}{F} \ln \frac{m_{Cl^-}}{m_{OH^-}} - \frac{RT}{F} \ln \frac{\gamma_{Cl^-}}{\gamma_{OH^-}} \end{aligned} \tag{8.59}$$

or,

$$\left[E - E^{\ominus} + \frac{RT}{F} \ln \frac{m_2}{m_1}\right] = -\frac{RT}{F} \ln K_w - \frac{RT}{F} \ln \frac{\gamma_{Cl^-}}{\gamma_{OH^-}} \qquad (8.60)$$

As before, the left-hand side of equation (8.60) is plotted as a function of ionic strength (or $\sqrt{}$ (ionic strength), which gives a rather better plot) and $-\ln K_w$ is determined as the intercept at $I = 0$ when $\gamma_{Cl^-}/\gamma_{OH^-} = 1$.

8.6.3 Solubility products

The problem with such determinations is to devise suitable electrodes and cells. One method is to use the sparingly soluble material as part of an electrode, e.g. to determine K_{AgCl} one could employ a silver–silver chloride electrode. K_{AgCl} may then be measured approximately by coupling the electrode with a reference electrode and determining its potential.

The potential of the silver electrode is given by

$$E = E^{\ominus}_{Ag} + \frac{RT}{F} \ln a_{Ag^+} \qquad (8.61)$$

therefore,

$$E = E^{\ominus}_{Ag} + \frac{RT}{F} \ln K_{AgCl} - \frac{RT}{F} \ln a_{Cl^-} \qquad (8.62)$$

since

$$\left(a_{Ag^+} = \frac{K_{AgCl}}{a_{Cl^-}}\right)$$

and

$$\ln K_{AgCl} = (E - E^{\ominus}_{Ag})\frac{F}{RT} + \ln a_{Cl^-} \qquad (8.63)$$

In order for equation (8.63) to be used it is required to know $E^{\ominus}_{Ag}$ and a_{Cl^-} the former may be determined, the latter assumed approximately equal to $a_{\pm}$ of KCl. Since suitable electrode systems can usually be devised the method is used fairly widely even through it is not particularly accurate.

An alternative method can present serious problems in that is not always easy to devise a suitable cell. For the determination of K_{AgCl} the following cell could be used

$$\begin{array}{c} \text{Ag, AgCl(s), HCl}|\text{Cl}_2\text{, Pt} \\ \qquad\qquad\quad 1\text{ atm} \end{array}$$

This cell has also the further disadvantages that chlorine electrodes are difficult to use since chlorine attacks platinum while formation of HCl and

HClO can alter the composition of the solution. The emf of the cell is given by

$$E = E_{Cl_2} - E_{Ag}$$

therefore

$$E = E^{\ominus}_{Cl_2} - \frac{RT}{F} \ln a_{Cl^-} - E^{\ominus}_{Ag} - \frac{RT}{F} \ln K_{AgCl} + \frac{RT}{F} \ln a_{Cl^-} \tag{8.64}$$

therefore

$$E = \left(E^{\ominus}_{Cl_2} - E^{\ominus}_{Ag}\right) - \frac{RT}{F} \ln K_{AgCl} \tag{8.65}$$

from which K_{AgCl} may be found when the standard potential of the silver and of the chlorine electrode are known.

8.6.4 Equilibrium constants of redox reactions

Standard redox potentials may be used to determine whether reactions proceed quantitatively and whether, therefore, they may be usefully employed analytically. It is well known, for example, that Ce^{4+} ions oxidize Fe^{2+} ions and that this reaction is used for the titrimetric determination of Fe(II). The usefulness of such reactions may be assessed by considering the redox potentials for the individual redox systems. Thus, we have

$$E_{Fe^{3+}|Fe^{2+}} = E^{\ominus}_{Fe^{3+}|Fe^{2+}} + \frac{RT}{F} \ln \frac{a_{Fe_{3+}}}{a_{Fe^{2+}}}$$

$$(= +0.76\,\text{V})$$

and

$$E_{Ce^{4+}|Ce^{3+}} = E^{\ominus}_{Ce^{4+}|Ce^{3+}} + \frac{RT}{F} \ln \frac{a_{Ce^{4+}}}{a_{Ce^{3+}}}$$

The reaction for the cell obtained by combining the two electrodes is

$$Ce^{4+} + Fe^{2+} \longrightarrow Fe^{3+} + Ce^{3+} \tag{8.66}$$

If two such half-cells are coupled, the activity of Fe^{3+}ions increases while that of Fe^{2+}ions decreases, causing an increase of the ratio $a_{Fe^{3+}}/a_{Fe^{2+}}$. At the same time, a decrease in $a_{Ce^{4+}}$ and an increase in $a_{Ce^{3+}}$ leads to a decrease in the ratio $a_{Ce^{4+}}/a_{Ce^{3+}}$. Thus, it is seen that the potentials approach each other and meet at the condition of equilibrium when we may write

$$E^{\ominus}_{Fe^{3+}/Fe^{2+}} + \frac{RT}{F} \ln \left(\frac{a_{Fe^{3+}}}{a_{Fe^{2+}}}\right)_{eq} = E^{\ominus}_{Ce^{4+}/Ce^{3+}} + \frac{RT}{F} \ln \left(\frac{a_{Ce^{4+}}}{a_{Ce^{3+}}}\right)_{eq} \tag{8.67}$$

therefore,

$$E^{\ominus}_{Ce^{4+}/Ce^{3+}} - E^{\ominus}_{Fe^{3+}/Fe^{2+}} = \frac{RT}{F}\ln\left(\frac{a_{Fe^{3+}}}{a_{Fe^{2+}}}\right)_{eq} - \frac{RT}{F}\ln\left(\frac{a_{Ce^{4+}}}{a_{Ce^{3+}}}\right)_{eq}$$
$$= \frac{RT}{F}\ln\left(\frac{a_{Fe^{3+}}a_{Ce^{3+}}}{a_{Fe^{2+}}a_{Ce^{4+}}}\right)_{eq} \qquad (8.68)$$

therefore,

$$1.61 - 0.76 = \frac{RT}{F}\ln K$$

K being the equilibrium constant for the redox process. For the case K is seen to be large ($\sim 2.39\times10^{14}$ at 298 K) so that the reaction is quantitatively useful since the equilibrium is also established *rapidly*.

8.6.5 Formation (stability) constants of metal complexes

In a cell of the type

$$\underset{1}{M|MX}\|\underset{2}{MX|M}$$

considered in section 6.9.2, the emf will be given approximately by a form of equation (6.45) written in terms of concentrations, viz.

$$E \sim \frac{RT}{F}\ln\frac{[M^+]_2}{[M^+]_1}$$

If a complexing agent is added to the left-hand solution, $[M^+]_1$, is reduced and the emf is altered.

For example, if a concentration cell based on silver electrodes placed in different concentrations of silver nitrate is used, the value of E will be different in the absence and presence of a measured concentration of ammonia added to the left-hand half-cell solution. The reason for this is the formation of the complex $Ag(NH_3)_2^+$ by the reaction

$$Ag^+ + 2NH_3 \rightleftharpoons Ag(NH_3)_2^+$$

characterized by the formation constant

$$\beta_2 = \frac{[Ag(NH_3)_2]^+}{[Ag^+][NH_3]^2} \qquad (8.69)$$

From the observed emf it is possible to calculate the concentration of free uncomplexed Ag^+ in the solution containing the complex. This in turn

leads to the concentration of the complex and of unbound ammonia so that substitution of these values in equation (8.69) yields a value of β_2.

A frequently used method to investigate such systems is based on pH titrations. The shape of the titration curve of a complexing agent, with acidic or basic properties with an appropriate base or acid respectively will be modified in the presence of a metal ion. Analysis of the difference can yield formation constant data for both single and consecutively formed complex species.

Polarographic half-wave potentials (Chapter 9) and molar ion conductivities or diffusion coefficients have been effectively used for the determination of consecutive overall and stepwise formation constants.

8.7 The experimental determination of pH

8.7.1 The hydrogen electrode

From a consideration of the formal definition of pH, viz.

$$\mathrm{pH} = -\log a_{\mathrm{H}^+}$$

it is clear that an electrode in equilibrium with a solution containing hydrogen ions will adopt a potential which is a function of the concentration of hydrogen ions and therefore of the pH of the solution. Since the equilibrium at the electrode is

$$\mathrm{H}^+ + \mathrm{e} \rightleftharpoons \tfrac{1}{2}\mathrm{H}_2$$

the potential adopted is given by

$$E = E^{\ominus} + \frac{RT}{F} \ln \frac{a_{\mathrm{H}^+}}{(a_{\mathrm{H}_2})^{\frac{1}{2}}}$$

or

$$E = \frac{RT}{F} \ln a_{\mathrm{H}^+} - \frac{RT}{2F} \ln P_{\mathrm{H}_2}$$

since $E^{\ominus} = 0$ by definition for this electrode as the primary standard. Further, if the partial pressure of hydrogen is 1 atmosphere.

$$E = \frac{RT}{F} \ln a_{\mathrm{H}^+} \tag{8.70}$$

Exact potentiometric determination of pH using the hydrogen electrode is not as easy as it might at first appear. In principle, it could be coupled with a suitable reference electrode to form the cell

$$\text{reference electrode}||H_3O^+|H_2, Pt$$

for which the emf may be written

$$E = E_{H_2|H_3O^+} - E_{ref} = \frac{2.3RT}{F} \log a_{H_3O^+} - E_{ref} \tag{8.71}$$

assuming that the liquid junction potential is eliminated. Or, in terms of pH,

$$pH = -\frac{(E + E_{ref})F}{2.3RT} \tag{8.72}$$

However, even if the liquid junction potential is eliminated it is required to know E_{ref}, since the value of pH obtained will be strongly influenced by its value. The value of E_{ref} is calculated assuming that ionic activity coefficients are determined only by the total ionic strength and not by the individual chemical properties of the species.

All that one can hope to do by such a method is to determine pH values which are consistent with those calculated from thermodynamic constants using equation (8.56). Thus, it is necessary to reassess the values of potential adopted by reference electrodes used for this purpose and also to take appropriate account of liquid junction potentials.

If the pH value determined by using equation (8.72) is to identify with that used in equation (8.56) to give the thermodynamic dissociation constant of an acid, then the following equality is necessary

$$-\frac{(E + E_{ref})F}{2.3RT} = pK_a + \log \frac{B}{m_a - B} - A\sqrt{I} + bI \tag{8.73}$$

or,

$$E + \frac{2.3RT}{F}\left(pK_a + \log \frac{B}{m_a - B} - A\sqrt{I}\right) = -E_{ref} - \frac{2.3RT}{F} bI \tag{8.74}$$

Experimentally, the hydrogen electrode is immersed in a series of solutions containing weak acids and their salts, the true dissociation constants of the acids being known. Connection of the chosen reference electrode to this solution is achieved by a means of a saturated potassium chloride salt bridge. When the left-hand side of equation (8.74) is plotted as a function of ionic strength, a reassessed value of E_{ref} is obtained as intercept on the I axis. No account has been taken of the liquid junction potential which exists between the salt bridge and the electrolyte solution and whose value varies with both the nature of the buffer used and its concentration. Such variations only produce uncertainities of the order of tenths of millivolts in the value of E_{ref} obtained and the scale of pH values thus obtained constitutes the conventional pH scale.

In practice, the use of the hydrogen electrode for pH determinations is severely limited in that is may not be used in solutions containing reducible materials and is easily poisoned by catalytic poisons.

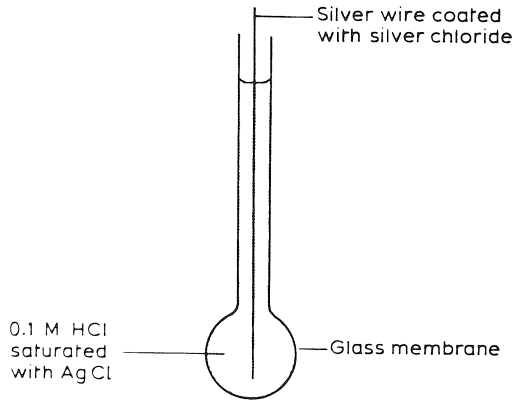

Figure 8.10 Components of the glass electrode.

8.7.2 The glass electrode

The glass electrode is the most widely used indicator electrode for pH determinations used in the laboratory. It operates on the principle that the potential difference between the surface of a glass membrane and a solution is a linear function of pH. A standard solution of know pH must be in contact with the other side of the membrane and in this is immersed a reference electrode (silver/silver chloride or calomel). The construction is shown schematically in Figure 8.10.

The arrangement may be represented as

$$\text{Ag, AgCl(s)|0.1 M HCl|glass|solution}$$

When used in practice it must be coupled with a further reference electrode also dipping into the working solution, e.g.

$$\text{Ag, AgCl(s)|0.1 M HCl|glass|solution||KCl (saturated), } Hg_2Cl_2(s), \text{Hg}$$

Since the potential of the silver/silver chloride electrode is constant and the potential difference between the inner surface of the glass membrane and the hydrochloric acid solution is constant, the only potential difference which can vary is that between the outer surface of the membrane and the working solution. The overall potential of the system is thus a function of the pH of the working solution only.

The above cell forms the basis for the practical pH scale which may be defined by

$$pH_X = pH_S - \frac{(E_X - E_S)F}{2.3RT} \tag{8.75}$$

Here, pH_S, represents the value for a standard buffer solution while E_S is the emf of the cell when this buffer is present. pH_X and E_X represent the pH value and cell emf respectively when the buffer solution is replaced by the solution under study. pH_S values are obtained initially by the methods previously described whereby reference electrodes are recalibrated by the use of equation (8.74).

The mode of action of the glass electrode is very complex and, of all the theories put forward, no single one can account for all the observed properties. It is very likely, however, that an important stage involves the absorption of hydrogen ions into the lattice of the glass membrane. The potential of the glass electrode/calomel cell may be expressed as

$$E = K + \frac{RT}{F} \ln a_{H^+} \tag{8.76}$$

Here K is not a true constant but varies on a day-to-day basis for any electrode. It is for this reason that a glass electrode must always be standardized at regular intervals with buffer solutions of know pH. At least two such solutions should be used covering a range of pH values to ensure the constancy of K over this selected range. The variation of K is a function of the asymmetry potential of the glass electrode which is determined by the differing responses to pH of the inner and outer surfaces of the membrane. This difference may well originate in the different conditions of strain in the two surfaces.

The glass electrode works reliably in the range pH 1–9 and it is unaffected by poisoning and oxidizing and reducing agents. In alkaline solutions, at pH > 9, particularly when sodium ions are present, the pH values recorded tend to be lower than the true values and this is due to the infiltration of sodium ions into the glass lattice. Such 'alkaline errors' are minimized by the use of special glasses; lithium glasses, for instance, extend the range reliably to pH 12. At the acid extreme of the scale, reliability is again questionable for pH < 1, where it appears that interference from anion surface adsorption occurs.

Problems

8.1 The dissociation constant of 2,4-dinitrophenol at 298 K has been observed to have the following values in varying concentrations of sodium chloride

$K \times 10^5$	8.344	8.424	8.541	8.630	8.776	8.923	9.162
m (NaCl)	0.0001	0.0002	0.0004	0.0006	0.0010	0.0015	0.0025

Use these data to determine the thermodynamic dissociation constant of 2,4-dinitrophenol at 298 K. (It may be assumed that the ionization of 2,4-dinitrophenol itself makes negligible contribution to the ionic strength of the solutions.)

8.2 The effect of ionic strength upon the rate constant for the reaction between the persulphate ion and the iodide ion has been reported by C.V. King and M.B. Jacobs (1931) *J. Am.*

Chem. Soc., **53**, 1704. The following table collects selected rate constant data, one set in which the ionic strength is maintained by the addition of KCl, the other in which KI is used for this purpose.

$-\log k$	$\sqrt{I}$ (KCl used)	$-\log k$	$\sqrt{I}$ (KI used)
0.987	0.0452	0.996	0.0336
0.979	0.0495	0.983	0.0524
0.951	0.0604	0.943	0.0675
0.935	0.0667	0.917	0.0797
0.928	0.0803	0.893	0.0903
0.900	0.0919	0.889	0.0998
0.876	0.1022	0.860	0.1138
0.854	0.1116	0.836	0.1239
0.801	0.1358	0.801	0.1376
0.772	0.1564	0.770	0.1580

What information may be obtained from these data?

8.3 A saturated solution of silver chloride at 298 K was found to have a conductivity of $2.733 \times 10^{-6}\,\Omega^{-1}\,cm^{-1}$. The conductivity of the water used for preparing the solution was $0.880 \times 10^{-6}\,\Omega^{-1}\,cm^{-1}$. The limiting molar conductivities at infinite dilution at 298 K for silver nitrate, hydrochloric acid and nitric acid are 133.36, 426.15 and $421.26\,\Omega^{-1}\,cm^2\,mol^{-1}$ respectively. Calculate the solubility of silver chloride at 298 K and its thermodynamic solubility product.

8.4 The ion conductivities for H_3O^+ and OH^- ions at infinite dilution at 298 K are $3.4981\,\Omega^{-1}\,m^2\,mol^{-1}$ and $1.9830\,\Omega^{-1}\,m^2\,mol^{-1}$ respectively. The conductivity of very pure water at 298 K is $5.498 \times 10^{-6}\,\Omega^{-1}\,m^{-1}$. Calculate a value for the ionic product of water K_w at 298 K.

8.5 The following values of the molar conductivity of ethanoic acid were obtained at 298 K. By an appropriate graphical method obtain an approximate value for the dissociation constant of the acid. Why must values obtained by such means be regarded as approximate?

C (mol dm^{-3})	0	0.0005	0.001	0.002	0.005	0.01	0.02
Λ (Ω^{-1} cm^2 mol^{-1})	390.7	66.5	48.5	35.5	23.8	16.2	10.7

8.6 The Clark cell,

$$\mathrm{Zn(10\%\ amalgam\ in\ Hg)|ZnSO_4.7H_2O(s), Hg_2SO_4(s)|Hg}$$
$$\text{(satd. aq. soln.)}$$

has the following values of emf for the temperatures shown

T (K)	293	298	308	318	328
E (V)	1.4267	1.4202	1.4062	1.3908	1.3740

Estimate the Gibbs free energy change, the entropy change and the enthalpy change for the cell reaction at 308 K.

8.7 The standard emf of the cell Ag|AgBr(s)|AgBr(aq)|Ag is 0.726 V at 298 K. Use this information to calculate the solubility product and solubility of silver bromide in water.

8.8 The cell H_2(1 atm) Pt|HCl aq. (m)|AgCl|Ag was found, at 298 K, to have the following values of emf for various molalities of hydrochloric acid.

m (mol kg^{-1})	0.0004	0.0036	0.0100	0.0400	0.0900
E (V)	0.6266	0.5160	0.4656	0.3974	0.3577

Determine the standard emf of the cell and calculate the activity coefficient of hydrochloric acid in the most concentrated of the five solutions.

8.9 In a Hittorf experiment the anode compartment of the apparatus contained 0.0758 g of silver nitrate plus 10 g water. After electrolysis, the solution had the composition of 0.2701 g silver nitrate and 28.755 g water. In the time of the electrolysis 0.01857 g of copper were deposited in a series copper coulometer. Estimate the transport numbers of the silver and nitrate ions.

8.10 The boundary formed between an aqueous solution of hydrochloric acid (0.01 mol dm^{-3}) and sodium chloride contained in a vertically mounted tube of internal diameter 5 mm, moved a distance of 7.2 mm in 5 min with a constant current flow of 5.5 mA. Estimate the transport number of the hydrogen ion.

8.11 The emf of the cell Pt, H_2(1 atm)|HCl(aq. 0.025 mol kg^{-1}, AgCl(s)|Ag is 0.4196 V at 298 K. Calculate the pH of the hydrochloric acid in the cell if the standard potential of the silver/silver chloride reference electrode is 0.2225 V at 298 K. Compare the value obtained using the Debye–Hückel limiting law.

8.12 The emf of the cell

Pt, H_2(1 atm)|ethanoic acid (aq. 0.0082 mol kg^{-1}),
sodium ethanoate, (aq. 0.0075 mol kg^{-1}),
sodium chloride, (aq.0.0079 mol kg^{-1}), AgCl(s)| Ag

is 0.6253 V at 298 K. The standard potential of the silver/silver chloride electrode is 0.2225 V. Calculate an approximate value for the dissociation constant of ethanoic acid.

8.13 The variation of the ionic product of water (K_w) with temperature was reported by H.S. Harned and W.J. Hamer (1933) *J. Am. Chem. Soc.*, **55**, 2194. Some of their results are tabulated below; use them to estimate the heat of ionization of water at 288, 298 and 308 K. Hence, calculate the heat of neutralization of a strong monobasic acid by a strong base in dilute aqueous solution at 298 K.

T(K)	278	288	298	308	318	328
K_w ($\times 10^{14}$)	0.186	0.452	1.008	2.088	4.016	7.297

9 Electroanalytical techniques

9.1 What constitutes electroanalysis?

Much of this chapter is concerned with the analytical applications of current–voltage relationships which form the basis of the wide range of voltammetric methods. These have their foundation in the understanding of electrode processes considered in Chapter 7 and to some extent in the electrochemical thermodynamics of Chapter 6. This link with mechanistic aspects of electrochemistry has led to the inclusion here of a small amount of material on the elucidation of mechanism. Such analysis of *behaviour* rather than of *quantity* may offend a purist view of analysis, but contextually seems appropriate for the present coverage.

A further link with material presented earlier derives from the distinctive range of electrometric titrations. All concentration-dependent electrochemical parameters may, in principle, be made the basis of a titration method. This is no less true of the use of diffusion currents in voltammetry to produce the range of amperometric techniques, than it is of the similar exploitation of conductivities and electrode potentials in the respective techniques of conductimetric and potentiometric titration. Quantitative electrochemical generation of a titrant—a direct application of Faraday's laws—makes possible the design of coulometric titrations.

9.2 Conductimetric titrations

Variations of conductivity may be used to follow the courses of acid–base and precipitation reactions. A drawback of the latter is the possible contamination of the electrodes by the precipitate formed. A grave disadvantage of any conductivity-based titration is its non-applicability in the presence of high concentrations of electrolyte species other than those required to be determined. This is in contrast to many other electroanalytical techniques where such electrolytes not only do not interfere, but offer distinct advantages.

Conductimetric titration curves for acid–base reactions depend upon the relative strengths of the acids and bases used. In order to maintain straight-line variations of conductivity, it is best to use a titrant concentration considerably greater than that of titrand.

1. *Titration of strong acid by strong base.* The titration graph will have

the form shown in Figure 9.1(a). Rounding of the graph near the equivalence point is due to water dissociation. This latter is immaterial since it is only necessary to take a number of points well to either side of the equivalence point and to extrapolate the two linear segments accordingly. The explanation of the shape of the graph is very simple: over the region AB the fast-moving hydrogen ions of the acid are replaced by the more slowly moving base cations with a consequent fall in conductivity. After all the hydrogen ions are removed, the conductivity rises between B and C as an excess of hydroxyl ions is added to the solution.

2. *Titration of weak acid by strong base.* The type of titration graph obtained in this case is shown in Figure 9.1(b). The conductivity initially rises from A to B as the salt, e.g. sodium ethanoate is formed. Any contribution to the overall conductivity by that of hydrogen ions is largely suppressed by the buffering action of the ethanoate ion. Beyond the equivalence point, the conductivity increases from B to C due to the increasing concentration of hydroxyl ions.

3. *Titration of strong acid by weak base.* The titration plot will take the form shown in Figure 9.1(c). An initial rapid decline over the region AB is due to the replacement of the mobile hydrogen ions by cations of the weak base. From B to C the weak base is added in excess to a solution of its salt so that its ionization is suppressed. Consequently, the conductivity of the excess hydroxyl ions is neglible.

4. *Titration of weak acid by weak base.* In such cases, titration curves of the type shown in Figure 9.1(d) are obtained. Over the region AB, corresponding to the initial addition of weak base, the ionization of the weak acid is suppressed by the buffer action so that the conductivity falls. As the salt is progressively formed, the number of ions in solution rises with consequent increase in conductivity over BC. In the region CD, addition of the weakly ionized base to a solution of its salt causes the conductivity to almost level off.

9.3 Potentiometric titrations

Potentiometric techniques use measurement of electrode potentials and their variation with the changing chemical environment induced by the progressive interaction of a titrant and a titrand. Such methods should be distinguished from those where an electrode potential is used for direct measurements of concentration of an analyte as is the case with a potentiometric sensor.

9.3.1 Zero current potentiometry

For this technique it is simply required to have access to an indicator electrode whose potential is a function of the activity of the species to be

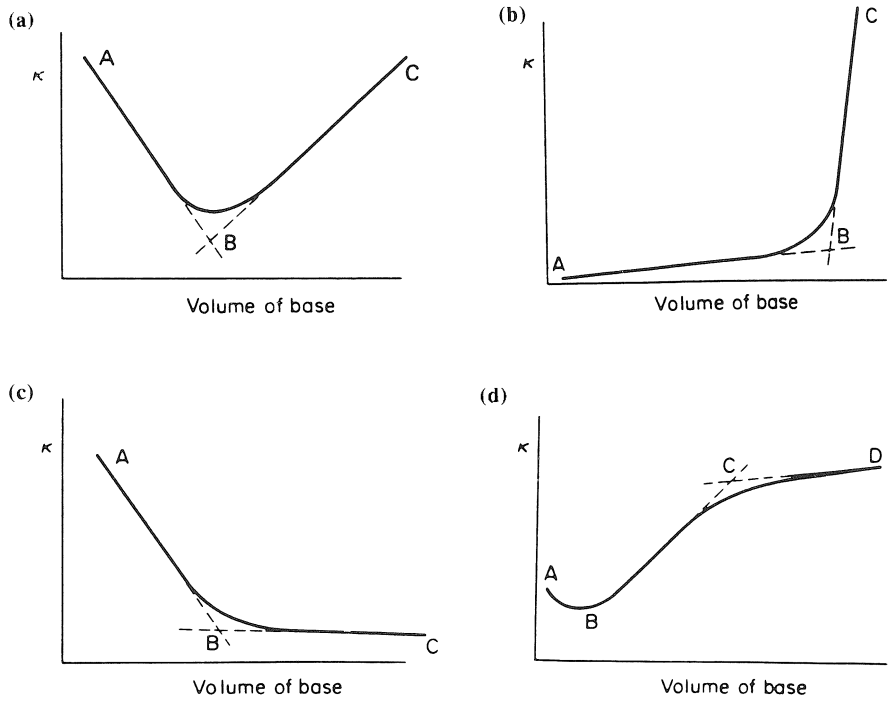

Figure 9.1 Shapes of conductimetric titration graphs for titration of: (a) strong acid by strong base; (b) weak acid by strong base; (c) strong acid by weak base; (d) weak acid by weak base (for this case the equivalence point is insufficiently clear to be exploited).

titrated. A cell is made by placing this component with a suitable reference electrode in the solution to be titrated. The cell is connected within the circuit shown schematically in Figure 9.2, its emf being measured after each addition of titrant: zero current is maintained through the indicating galvanometer by balancing the cell emf against the potentiometer voltage.

The equivalence point of the titration may be determined either from the inflexion point of the graph of indicator electrode potential versus titrant volume (Figure 9.3(a)) or, with appropriate instrumentation, from the derivative plot of dE/dv versus v (Figure 9.3(b)).

Although the potential–volume plot is always of the same essential shape, its definition is dependent upon the equilibrium constant of the titration reaction and its stoichiometry. The equivalence point may be identified with the inflexion point for a 1:1 reaction with a large equilibrium constant and may be satisfactorily determined for a large number of acid–base, precipitation, redox and, in particular, complexometric titrations.

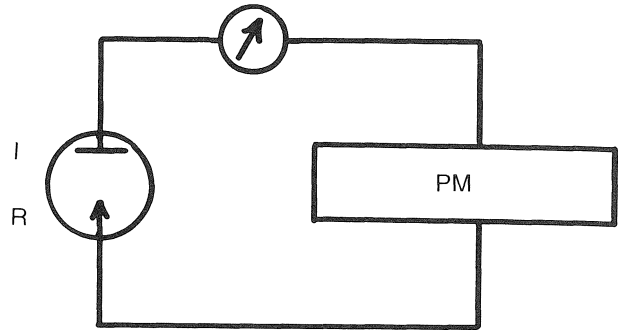

Figure 9.2 Basic circuit for classical potentiometry. I = indicator electrode; R = reference electrode; PM = potentiometer device.

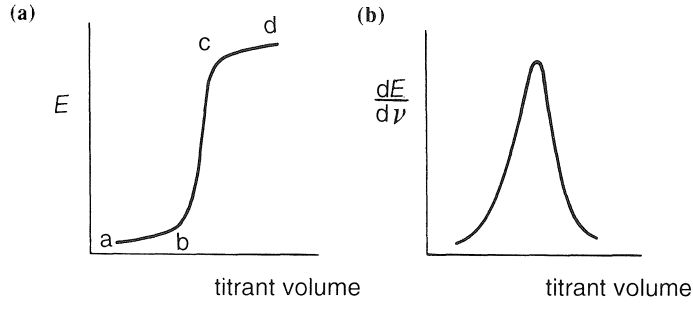

Figure 9.3 Potentiometric titration curves. See text for explanation.

Electrode reactions need not proceed reversibly for a satisfactory potentiometric end-point to to be determined. What is essential is that there shall be a large well-defined potential change in the region of the end-point.

Consider the oxidation of Fe^{2+} ions by Ce^{4+} ions, a reaction already considered in section 8.6.4 where it was seen that the redox potential of the Fe^{3+}/ Fe^{2+} couple (+0.76 V) is significantly different from that of the Ce^{4+}/Ce^{3+} couple (+1.61 V). With a solution of Fe^{2+} ions placed in the cell fitted with a platinum indicator and a calomel reference electrode and a burette delivering a solution of Ce^{4+} ions, a titration curve of the form shown in Figure 9.3(a) may be obtained. As soon as a small amount of Ce^{4+} solution is added to the solution of Fe^{2+} ions, some oxidation takes place, i.e.

$$Fe^{2+} + Ce^{4+} \rightarrow Fe^{3+} + Ce^{3+}$$

The indicator and reference electrodes are now dipping into a solution containing mainly Fe^{2+} ions but a small amount of Fe^{3+} ions as well. The potential of the platinum electrode will now adopt a characteristic value which is a function of the activity ratio of Fe^{3+} to Fe^{2+} ions as expressed in the Nernst equation,

$$E_{Fe^{3+}/Fe^{2+}} = E^{\ominus}_{Fe^{3+}/Fe^{2+}} + \frac{RT}{F} \ln \frac{a_{Fe^{3+}}}{a_{Fe^{2+}}}$$

As more Ce^{4+} ions are added the ratio of Fe^{3+} to Fe^{2+} ions increases. The potential adopted by the indicator electrode does not, however, vary greatly. Its value increases only slowly over the range a–b in accordance with the Nernst equation. A point will be reached where all the Fe^{2+} ions have been removed by oxidation and a small excess of Ce^{4+} ions has been added. The potential of the indicator electrode will now be a function of the ratio of activities of Ce^{4+} and Ce^{3+} ions according to

$$E_{Ce^{4+}/Ce^{3+}} = E^{\ominus}_{Ce^{4+}/Ce^{3+}} + \frac{RT}{F} \ln \frac{a_{Ce^{4+}}}{a_{Ce^{3+}}}$$

The region c–d shows similar slight variation of potential with titrant volume as is seen over the region a–b. The regions a–b and c–d are separated widely because of the large difference in standard potentials of the two redox systems. It is seen that in the region of the equivalence point, the potential of the two couples is the same—a fact already used in section 8.6.4 to calculate the equilibrium constant of the redox reaction. Between the two, virtually plateau, regions the potential shows a sharp increase.

9.3.2 Constant current potentiometry

Constant current techniques often prove to be useful for redox titrations involving couples of which at least one behaves in an irreversible manner, i.e. equilibrium is not established instantaneously at the electrode surface. As a result of this, the potential jump in the region of the end-point is too small to be useful. The potentials of electrodes which behave irreversibly show considerable variation in value when they pass a current. The constant current required for such titrations has to be determined in a separate experiment prior to the titration itself. In Figure 9.4 are shown current–voltage curves for two redox couples one of which behaves reversibly, the other irreversibly. It is seen that at zero current the potentials are very close whereas, with increasing current, they begin to diverge considerably. In some cases the divergence can be so large that, when the titration is subsequently performed, there is no need to plot the titration graph since

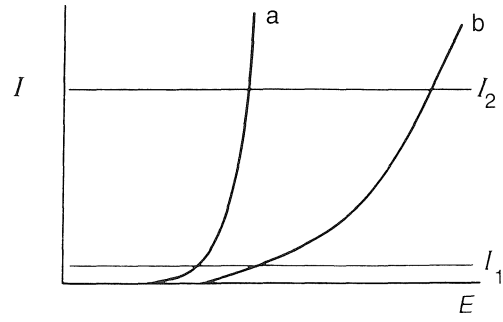

Figure 9.4 Current–potential curves for titrant, (a) (reversible) and titrand, (b) (irreversible): constant current I_2 gives better separation of potentials than does I_1.

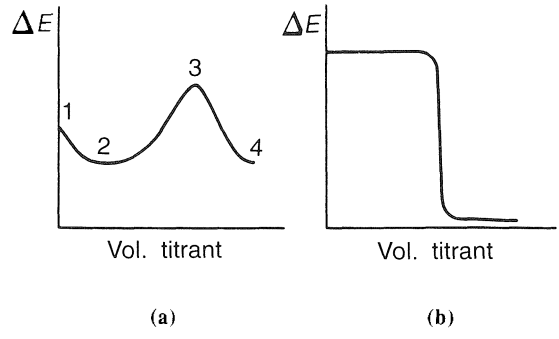

Figure 9.5 Potentiometric titration curves using two indicator electrodes. (a) Both redox couples reversible. (b) One couple reversible, the other irreversible. See text for explanation.

the end-point is directly determinable by a large change in electrode potential.

9.3.3 Potentiometry with two indicator electrodes

When two indicator electrodes are used the potential difference between them is plotted as a function of titrant concentration. The shapes of the individual titration curves vary with the degree of irreversibility of the couples as shown in Figure 9.5. Titration of Fe(II) by Ce(IV) gives a curve of the type shown in Figure 9.5(a) and the reactions occurring at various points on the curve will be considered briefly. The most important stages of the titration occur at the points on the curve labelled 1–4.

1. The only electroactive species present are Fe^{2+} and H_3O^+ so that the only reactions possible are

$$H_3O^+ + e \rightarrow \tfrac{1}{2}H_2 + H_2O \quad \text{at the cathode}$$

and

$$Fe^{2+} \rightarrow Fe^{3+} + e \quad \text{at the anode}$$

Since these two reactions occur at well-separated potentials, ΔE is large.

2. At this point the titration reaction is half completed, so that $[Fe^{2+}] = [Fe^{3+}] = [Ce^{3+}]$. Possible reactions are now

$$Fe^{3+} + e \rightarrow Fe^{2+} \quad \text{at the cathode}$$

and

$$\left.\begin{array}{l} Fe^{2+} \rightarrow Fe^{3+} + e \\ \text{or} \\ Ce^{3+} \rightarrow Ce^{4+} + e \end{array}\right\} \text{at the anode}$$

Since the second suggested anode reaction only occurs at a very positive potential it is an unlikely contribution. ΔE is now small since the cathode and anode reactions occur at almost the same potential (the Fe^{3+}/Fe^{2+} couple is fairly reversible)

3. Here the end-point has been reached; all the Fe^{2+} has been oxidized to the Fe^{3+} state and all the Ce^{4+}has been reduced to Ce^{3+}. The electrode reactions are thus

$$Fe^{3+} + e \rightarrow Fe^{2+} \quad \text{at the cathode}$$

and

$$Ce^{3+} \rightarrow Ce^{4+} + e \quad \text{at the anode}$$

ΔE is again very large, since the latter reactions occur at widely differing potentials.

4. As more and more Ce^{4+} ions enter the solution beyond the end-point, the reactions are likely to be

$$Ce^{4+} + e \rightarrow Ce^{3+} \quad \text{at the cathode}$$

and

$$Ce^{3+} \rightarrow Ce^{4+} + e \quad \text{at the anode}$$

ΔE drops rapidly from the end-point to a very small value consistent with the high degree of reversibility of the Ce^{4+}/Ce^{3+} system.

In the case of titration of an irreversible titrand by a reversible titrant, the change of ΔE in the region of the equivalence point is shown in Figure 9.5(b).

9.4 Classical voltammetric techniques

Voltammetry is the generic term for techniques which make use of current–voltage curves under conditions of concentration polarization of an indicator electrode.

The total rate of deposition of a metal ion, M, in terms of the rates of the mass-transfer processes migration and diffusion has been expressed by

$$\frac{i}{nF} = \frac{t_+ i}{nF} + \frac{D([\mathrm{M}^{n+}] - [\mathrm{M}^{n+}]_e)}{\delta} \qquad \text{(see equation (7.32))}$$

or

$$\frac{i_{\lim}}{nF} = \frac{t_+ i_{\lim}}{nF} + \frac{D}{\delta}[\mathrm{M}^{n+}] \qquad \text{(see equation (7.33))}$$

The last expression holds under conditions of maximum diffusion rate when the surface concentration of the cation is zero.

Equation (7.33) relates the limiting current density to the concentration of the species M^{n+}. Unfortunately it also involves its transport number: since this varies with conditions and concentration, the equation as it stands does not hold very promising analytical possibilities. However, there is a very simple way of almost completely eliminating the electrical migration effect.

It has been seen earlier that t_+ for a given ion species is diminished in the presence of other ions: it then serves to carry a *smaller fraction* of the total current. Addition of a sufficient excess of another electrolyte, showing no electrochemical reactions which interfere with M^{n+}, causes t_+ to become vanishingly small. The rate of arrival of M^{n+} at the cathode is then controlled solely by diffusion. The added species is known as an indifferent, base, or supporting electrolyte: potassium chloride is useful in this role and is commonly used. Thus equation (7.33) becomes

$$\frac{i_{\lim}}{nF} = \frac{D}{\delta}[\mathrm{M}^{n+}] = \frac{I_{\lim}}{AnF}$$

A being the surface area of the electrode and $I_{\lim}$ the limiting diffusion-controlled current, explicitly given by

$$I_{\lim} = \frac{nFAD[\mathrm{M}^{n+}]}{\delta} \qquad (9.1)$$

It has not always been easy to exploit equation (9.1) for quantitative analysis: this is because the prime requirement for quantitative analysis—reproducibility—is not always easily obtained with solid electrodes due to contamination by the products of electrolysis. However, partly due to improved methods of pretreatment and partly because of the speed of voltage

scans with modern techniques, solid electrodes are now quite as important as the classical voltammetric electrode material, viz. mercury.

9.4.1 Polarography

This is the particular form of voltammetry based on the use of a dropping mercury (micro-)electrode (DME). This consists of mercury in the form of small drops issuing from the end of a fine-bore capillary.

Mercury in contact with a solution of an electrolyte such as potassium chloride approaches very closely in its behaviour to that required of an ideal polarized electrode (see Chapter 5). Within a certain fairly wide range of potentials, no ions are discharged at its surface, nor are they dissolved from it. This means that the potential applied to it may be varied at will without the establishment of electrochemical equilibria. In practice, *a near-ideal polarized electrode* may be recognized by the fact that, over a range of applied potential, no current flows. A *polarized* electrode shows *no current change* over a range of applied potential.

Despite the obvious practical complication of working with a dynamic rather than a static electrode, the DME shows a number of advantages.

1. Drops are reproducibly formed so that currents, although varying with drop growth and detachment from the capillary, are also reproducible.
2. A fresh surface of electrode is continuously presented to the electrolyte solution, eliminating chemical contamination and an 'electrode history'.
3. Since the DME is a micro-electrode, solutions may be partially electrolysed very many times without measurable reduction in concentration.
4. The hydrogen overvoltage for mercury as an electrode material is, as discussed in Chapter 7, extremely high. In fact, the cathodic polarization limit is caused by discharge of electrolyte cations rather than of hydrogen ions. The current–voltage characteristics of the DME in potassium chloride solution are shown in Figure 9.6.
5. Since so many electro-active species undergo electron exchange processes on mercury in the near-ideal polarized range of 0 to -1.8 V, they show analytically exploitable signals superimposed on the charging current baseline shown in Figure 9.6.

Advantages of the DME are tempered by a number of disadvantages:

1. The cathodic versatility of mercury is not matched by its anodic behaviour. Dissolution sets in at about $+0.4$ V vs. the saturated calomel electrode potential. So far as most metal ions are concerned, this is of little importance since most of them are reduced at potentials considerably more negative than this although copper and silver are exceptions.
2. Oxygen is reduced in a two-stage process as follows:

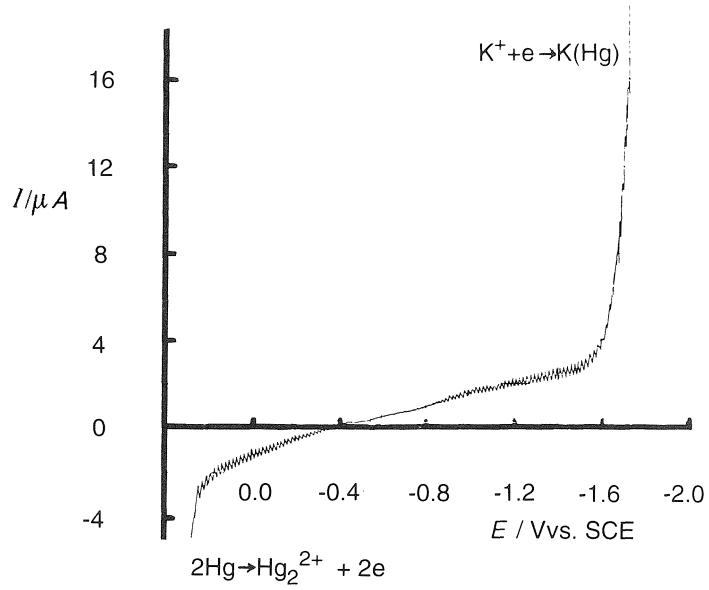

Figure 9.6 Current–voltage curve for 0.1 mol dm^{-3} potassium chloride at a dropping mercury electrode.

In acidic media.

$$\begin{array}{ll} \textit{Stage 1.} & O_2 + 2H^+ + 2e \rightarrow H_2O_2 \\ \textit{Stage 2.} & H_2O_2 + 2H^+ + 2e \rightarrow 2H_2O \\ \hline \textit{Overall} & O_2 + 4H^+ + 4e \rightarrow 2H_2O \end{array}$$

In neutral and alkaline media.

$$\begin{array}{ll} \textit{Stage 1.} & O_2 + 2H_2O + 2e \rightarrow H_2O_2 + 2OH^- \\ \textit{Stage 2.} & H_2O_2 + 2e \rightarrow 2OH^- \\ \hline \textit{Overall} & O_2 + 2H_2O + 4e \rightarrow 4OH^- \end{array}$$

These reactions are seen to identify with the reverse of the anodic processes occurring in the electrolysis of water considered in section 7.6.

The current–voltage curve for oxygen extends over most of the cathodic working range. Dissolved oxygen must therefore be removed from a working solution by flushing with some inert gas, such as nitrogen, before electrolysis is attempted.

3. Mercury is toxic, but sensible precautions make its use safe.

Schematic circuits for voltammetry generally and for classical d.c. polarography in particular are shown in Figure 9.7. The essential features of a

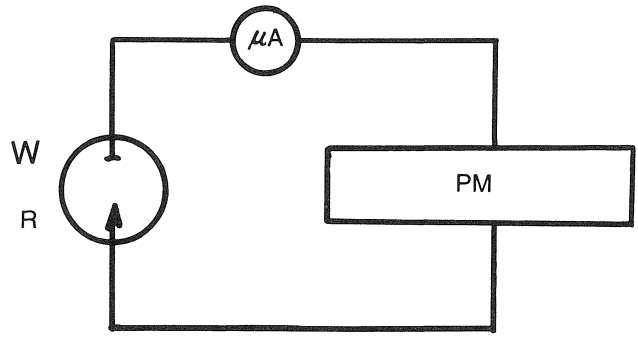

(a)

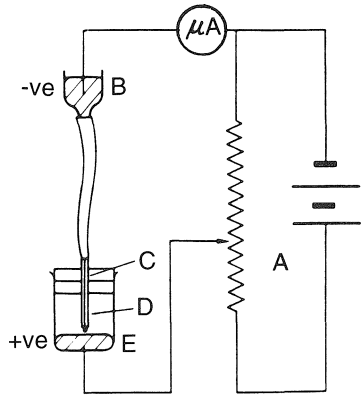

(b)

Figure 9.7 (a) Schematic circuit for classical (two-electrode) voltammetry. The circuit is similar to that for potentiometry except that a *controlled* microscopic electrolytic process is induced and the current measured by a microammeter. W = working microelectrode; R = reference electrode; PM = potentiometer device. (b) Basic polarographic circuit. A = potentiometer for variation of applied potential between C and E; B = mercury reservoir; C = dropping mercury electrode; D = working solution containing depolarizer(s) and supporting electrolyte; E = mercury pool anode (in precise measurements of potential this is replaced by a true reference electrode such as a saturated calomel electrode).

polarographic current–voltage curve are shown in Figure 9.8. Such curves are known as polarograms or 'polarographic waves'. They show development of a *faradaic* current signal superimposed on the residual *non-faradaic* (charging) current. It is seen that this residual current cuts the voltage axis, usually at about −0.4 or −0.5 V vs. SCE, and corresponds to the potential of zero charge (Chapter 5).

The current plateau corresponds to the condition that metal ions are reduced as fast as they reach the electrode by natural diffusion. In the range of applied potential where this constant diffusion current flows, the

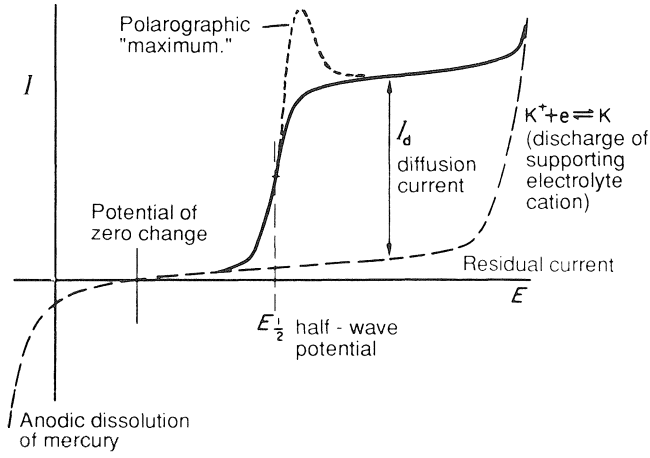

Figure 9.8 Essential features of a polarographic current–voltage curve or wave (polarogram). The polarogram corresponding to reduction of a depolarizer is superimposed on the supporting electrolyte curve in the region of the 'residual current'.

DME is clearly polarized—it is in fact described as *concentration polarized.* Reducible and oxidizable species which show such characteristics are often described as *depolarizers*: reference to the polarogram in Figure 9.8 makes this terminology clear. The 'polarographic maximum' indicated on the main wave profile derives from unusual (tangential rather than radial) mass transfer. Such behaviour seems to originate in a charge distribution between the capillary and the solution end of a mercury drop. The effect may be eliminated by the addition to the solution of a 'maximum suppressor' such as gelatin or (better) Triton-X-100. Such species function in this context through their surface activity: they are added at very low levels (< 1%) since too much can distort the profile and lower the limiting currents of polarographic waves.

9.4.2 *Characteristics of diffusion-controlled polarographic waves*

Mean diffusion currents are expressed in the Ilkovic equation

$$\bar{I}_d = 607nD^{\frac{1}{2}}m^{\frac{2}{3}}t^{\frac{1}{6}}C \qquad (9.2)$$

Here n is the number of electrons transferred in the electrode reaction, D is the diffusion coefficient of the depolarizer ($cm^2\,s^{-1}$), m is the rate of flow of mercury ($mg\,s^{-1}$), t is the drop time (s) and C is the depolarizer concentration ($mmol\,dm^{-3}$). With these units and the numerical constant given in equation (9.2) $\bar{I}_d$ is given in microamps. The potential at the midpoint of the wave, where $\bar{I} = \bar{I}_d/2$, known as the *half-wave potential* ($E_{\frac{1}{2}}$), is

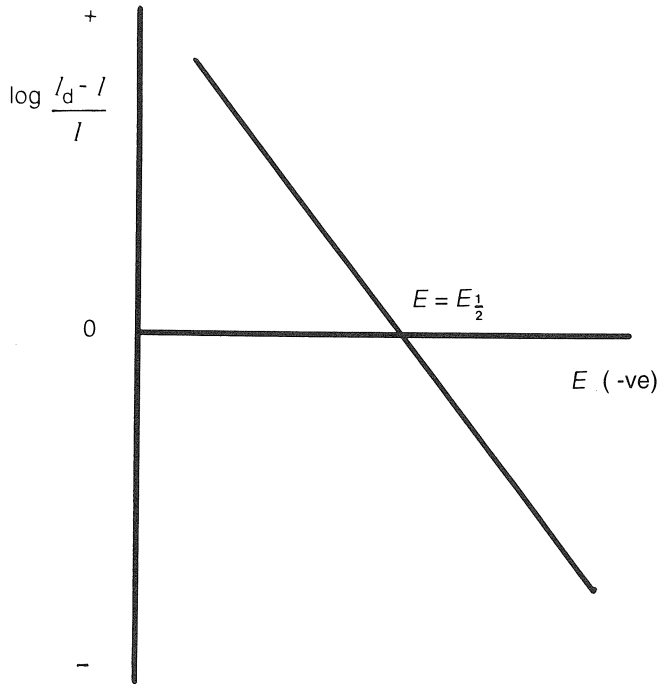

Figure 9.9 Logarithmic analysis of a reversible polarographic wave. Slope = $nF/2.3RT$.

characteristic of a given depolarizer for fixed solution conditions. As such, half-wave potentials may be used to identify qualitatively components in a mixture of depolarizers. Values are, however, extremely sensitive to the presence of different complexing species, including supporting electrolyte anions, and $E_{\frac{1}{2}}$ values should be used for 'fingerprinting' only with extreme caution. Provided that the reduction process occurs reversibly the currents and corresponding potentials on the rising portions of waves are related through the Heyrovsky–Ilkovic equation

$$E = E_{\frac{1}{2}} + \frac{RT}{nF} \ln (\bar{I}_d - \bar{I})/\bar{I} \qquad (9.3a)$$

Equation (9.3a) is seen to be very similar to the Nernst equation and may be regarded as its polarographic equivalent. A plot of $\ln [(\bar{I}_d - \bar{I})/\bar{I}]$ versus E may be used to identify both n and $E_{\frac{1}{2}}$ (Figure 9.9).

The sensitivity of $E_{\frac{1}{2}}$ values to complexation has two significant applications. The separation of otherwise overlapping and interfering polarographic signals may be effected by the addition of an appropriate ligand to a working solution. Modern techniques with improved signal resolution have obviated the necessity for such procedures to some extent, but multiple ion analysis (a distinct advantage of polarography) is usually effected

by working in several complexing media to spread the waves in differing patterns. A separation of 0.2 V between the $E_{\frac{1}{2}}$ values of following waves is regarded as the minimum for satisfactory analysis. Additionally, accurate measurement of the shift in $E_{\frac{1}{2}}$ with ligand concentration has formed the basis of a range of methods for determining formation (or stability) constants. It is usually necessary for the reduction of both aqua and otherwise complexed ions to take place reversibly. Under these conditions it may be shown that for a complexing reaction

$$\mathrm{M} + N\mathrm{X} \rightleftharpoons \mathrm{MX}$$

the shift in half-wave potential, $\Delta E_{\frac{1}{2}}$, is given by

$$\frac{0.4343nF}{RT} \cdot \Delta E_{\frac{1}{2}} \sim \log \beta_N + N \log [\mathrm{X}] \tag{9.4}$$

where β_N is the formation constant of MX_N and [X] is the free ligand concentration.

For irreversible reductions a wave has less than the theoretical slope for the number of electrons transferred and equation (9.3a) must be modified to

$$E = E_{\frac{1}{2}} + \frac{RT}{\alpha nF} \ln \frac{\bar{I}_{\mathrm{d}} - \bar{I}}{\bar{I}} \tag{9.3b}$$

α being the transfer coefficient. It is instructive to compare the expected shapes for two reductions having the same value for n, one involving a rapid electron transfer (reversible), the other a slow one (irreversible) as shown in Figure 9.10. For wave (a), diffusion is rate determining over the entire wave profile, the mass-transfer process being always slower than the electron-exchange rate. For wave (b), the electron transfer process is rate determining over lower parts of the wave, even these small currents requiring large (activation) overvoltage to sustain them. It is not until the later part of the wave, where even more overvoltage is applied, that the electron-transfer rate becomes of such a magnitude that this process gives way to the diffusion process in determining the rate. Thus, it is important to realize that, even for slow processes, the limiting currents are subject to diffusion control and as such are given by the Ilkovic equation. It follows that both reversible and irreversible diffusion controlled waves may be exploited analytically. For analysis it is possible to draw a calibration graph of diffusion current versus concentration and to read 'unknown' concentrations from this. Sometimes it may be more convenient to employ standard addition techniques, whereby the increase in a current signal caused by the addition of a known concentration of the depolarizer to be determined, enables the concentration producing the original signal to be calculated by simple proportion.

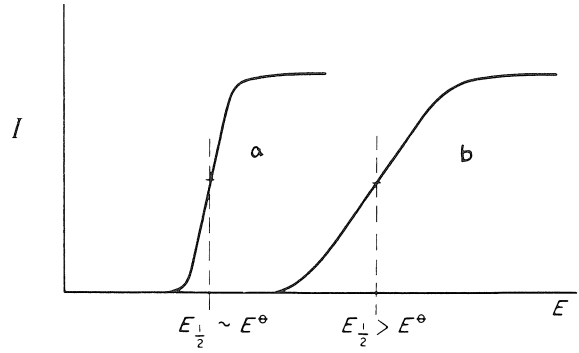

Figure 9.10 Comparison of polarograms for (a) a reversible and (b) an irreversible reduction. The limiting currents in both cases being diffusion controlled and the number of electrons transferred equal.

In order to base analytical methods upon the application of the Ilkovic equation, it is essential to establish that limiting currents produced by depolarizers are diffusion controlled. This is by no means always the case. Rearrangement of equation (9.2) in the form

$$\bar{I}_d = (607nD^{1/2}C)(m^{2/3}t^{1/6})$$

emphasizes the presence of two types of variable in the Ilkovic equation—those concerned with the solution and those concerned with the electrode. When electrode factors are maintained constant, a linear relationship between $\bar{I}_d$ and concentration is maintained. If solution factors are kept constant, $\bar{I}_d \propto m^{2/3}t^{1/6}$. By Poiseuille's equation, the rate of flow of a liquid (v) through a capillary under a head of liquid is directly proportional to the height of the column, h. Therefore $v \propto m \propto h$, and since also $v \propto 1/t, \bar{I}_d \propto h^{2/3}h^{-1/6} = h^{1/2}$. Thus, a diffusion- controlled wave shows a linear relationship between $\bar{I}_d$ and the square root of the height of the mercury reservoir.

The simplest experimental arrangement may be used for concentration determinations in the range 10^{-5} mol dm^{-3} to 10^{-2} mol dm^{-3}. Below about 10^{-4} mol dm^{-3}, however, the ratio of faradaic current to the concentration-independent non-faradaic current becomes progressively smaller until the latter predominates. All modern instrumental refinements of the polarographic method are aimed at improving this ratio: these are considered in section 9.6.

Solid electrodes offer some advantage in this regard: if suitable pretreatment can be devised and implemented to obtain reproducible results, the problem of residual currents does not arise. Additionally, they allow probing of the anodic potential range which mercury does not.

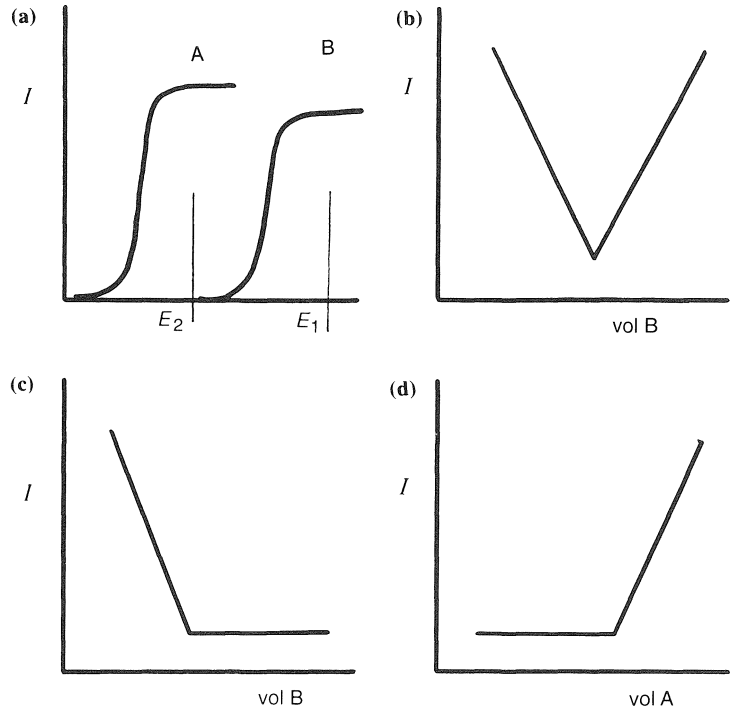

Figure 9.11 (a) Selected polarographic characteristics of titrant A and titrand B for amperometry; (b) titration of A by B at applied potential E_1; (c) titration of A by B at applied potential E_2; (d) titration of B by A at potential E_2.

9.4.3 Amperometric titrations

Because of the direct proportionality of diffusion current and bulk depolarizer concentration, titration of such species by following the diffusion current which they generate at a fixed potential can be particularly convenient. It is not necessary for both titrant and titrand to be electro-active although the more conventional form of titration curve is obtained when this situation obtains. A number of commonly encountered circumstances are summarized in Figure 9.11.

Titration of species B as titrand by A as titrant (or indeed of A by B) with an applied potential E_1 (Figure 9.11(a)) yields the titration curve shown in Figure 9.11(b).

Titration of A by B at an applied potential E_2 where only A is electroactive produces the curve of Figure 9.11(c), while titration of B by A at this same potential yields Figure 9.11(d). Curves of the type shown in Figure 9.11(c) and 9.11(d) are also obtained when either titrant or titrand are electro-inactive and are particularly common with analysis based on quanti-

tative complexation. The DME may be used successfully for amperometry, the electrode even functioning satisfactorily in stirred solutions which are heavily loaded with the precipitated products of a titration reaction. Solid electrodes are, however, particularly useful in this context even though these may have their current responses affected by an electrochemical history. Identification of a titration end-point is not affected by what would be a distinct disadvantage in direct volumetric analysis. This allows full advantage to be taken of controlled forced convection in the form of rotated electrodes to enhance measured current signals. A singular advantage of the techniques of amperometry is the extreme simplicity of the apparatus which may be used for accurate analysis. The modification whereby a constant small voltage is applied between a pair of identical indicator electrodes and the resultant current measured directly during the course of the titration complements the similar variation used in potentiometry and allows the use of 'dead-stop' techniques.

9.4.4 Wave characteristics and the mechanism of electrochemical processes

The profile of a current–voltage curve can reflect a more or less complex interplay of sequential electron-transfer processes further complicated by the involvement of associated chemical reactions. Analysis of polarographic and other voltammetric signals has led to much insight into the nature of electrode processes and has contributed to the development of industrial processes and to the identification of the controlled parameters required for their efficient exploitation.

Consider first a few possibilities arising from sequential electron transfer: these may be understood in terms of the scheme

$$M^{2+} \xrightarrow{e} M^{+}$$

$$M^{+} \xrightarrow{e} M^{0}$$

When both electrons are transferred rapidly the reaction may be expressed as

$$M^{2+} \xrightarrow{2e} M^{0}$$

and the polarogram will have the profile characteristic of a reversible two-electron reduction (Figure 9.12(a)). For example Cu^{2+} in non-complexing supporting electrolytes shows such a wave: in reality it is somewhat obscured by the fact that the half-wave potential is close to 0.0 V vs. SCE so that the foot of the polarogram is overtaken by the anodic curve corresponding to the dissolution of mercury. However, in complexing media, such as ammonia, the lower oxidation state is sufficiently stabilized relative to the higher one that it shows separate reduction. Two one-electron reversible waves are now observed (Figure 9.12(b)).

If the first step is slower than the second, i.e.

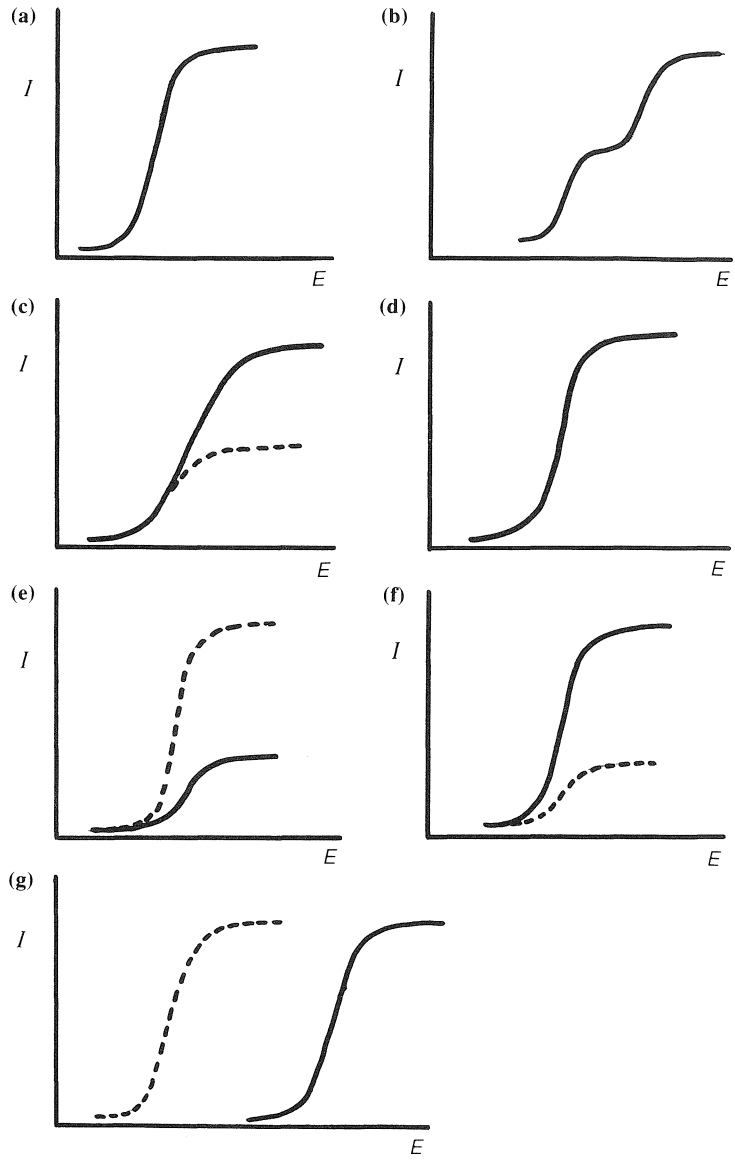

Figure 9.12 (a) Reversible 2-electron reduction wave, both electrons transferred rapidly. (b) Separation into equal one-electron stages through complexation producing a relatively more stable lower oxidation state intermediate. (c) Slope of overall two-electron wave controlled by slow first electron transfer. (d) Slope of overall two-electron wave controlled by fast first electron transfer. (e) Formation of 'kinetic' wave smaller than the hypothetical profile based on a diffusion-controlled current. The CE mechanism. (f) Formation of a 'catalytic' wave by regeneration of depolarizer at electrode surface. The EC' mechanism. (g) Shift of wave profile to more negative potentials where reduction product undergoes subsequent chemical reaction. The EC mechanism.

$$M^{2+} \xrightarrow{e(slow)} M^{+}$$

$$M^{+} \xrightarrow{e(fast)} M^{0}$$

the shape and slope of the wave will be dominated by this slow rate-determining step whose wave profile cannot be seen in isolation but is indicated by the dashed curve in Figure 9.12(c). The overall two-electron wave will have the slope of this first stage but an overall height the same as in Figure 9.12(a).

If the second step is slower than the first, i.e.

$$M^{2+} \xrightarrow{e(fast)} M^{+}$$

$$M^{+} \xrightarrow{e(slow)} M^{0}$$

the ready supply of M^{+} via the first stage means that, although the overall height of the wave remains the same as in the previous case, the overall profile is much steeper (Figure 9.12(d)).

One of the earliest types of polarographic behaviour recognized as different to the diffusion-controlled situation characterized by the Ilkovic equation is that in which a *kinetic* wave is formed. In the more modern classification of coupled electrode and homogeneous reactions these are said to proceed by the CE mechanism, i.e. a chemical followed by an electrochemical reaction. The general scheme may be expressed as

$$A \underset{k_{-1}}{\overset{k_1}{\rightleftharpoons}} B \xrightarrow{\pm ne} C$$

and is exemplified by the behaviour of formaldehyde viz.

$$(HO)_2CH_2 \underset{k_{-1}}{\overset{k_1}{\rightleftharpoons}} H_2O + CH_2O \xrightarrow[+2e]{2H^{+}} CH_3OH \qquad (9.5)$$

Formaldehyde exists in aqueous solution largely as the electro-inactive hydrate. The reducible anhydrous molecule is formed from the hydrate only slowly and a wave is produced which is smaller than would be expected for diffusion control (Figure 9.12(e)). A further distinguishing feature is that the height of the wave is not influenced by the mercury reservoir height.

A further type of behaviour is in polarographic terminology known as a *catalytic* wave: it is often significantly higher than the expected diffusion-controlled wave (Figure 9.12(f)) and originates in the regeneration of the depolarizer at the electrode surface by chemical reaction with some solute species. Such behaviour is frequently represented by the scheme

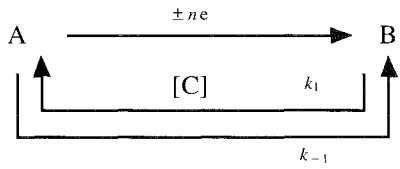

and is shown by the Fe^{3+}/Fe^{2+} system in the presence of hydrogen peroxide to oxidize the lower valency–state product. In general terminology this is known as an *EC′* mechanism. In a modification termed an EC mechanism, viz.

$$A \xrightarrow{\pm ne} B \underset{k_{-1}}{\overset{k_1}{\rightleftharpoons}} C$$

the product of an electrochemical reaction has its concentration reduced by a subsequent chemical reaction which produces a secondary product. The effect is to shift the position of the reduction or oxidation wave—to more negative potentials for the former and to more positive potentials for the latter case—although the height remains unaltered (Figure 9.12(g)). The oxidation of *p*-aminophenol on a platinum electrode shows such behaviour, viz.

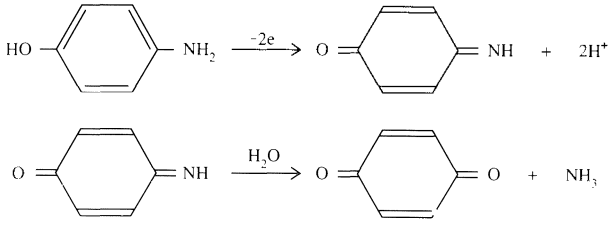

(9.6)

The sequence of behaviour represented in Figure 9.12 more or less exhausts the capabilities of electrochemical techniques themselves to *imply* mechanisms. Analysis of electrochemical behaviour can only *indirectly* lead to the elucidation of mechanisms: this is particularly the case in respect of intermediates formed at an electrode surface.

Predictions of expected experimental characteristics can be made to some extent on the basis of theoretical models. Matching the predictions of a model with what is actually seen has proved to be a powerful approach but may lead to only qualified support for a particular mechanism. Differences in electrochemical parameters reflecting different mechanisms may be very small: in some instances different proposed routes lead to identical experimental behaviour. Thus, while it is possible from current–voltage curves to *infer* an ECE mechanism with the scheme

$$A \xrightarrow{\pm ne} B$$

$$B \xrightarrow{k_1} C$$

$$C \xrightarrow{\pm n'e} D$$

the experimental behaviour could, in fact, equally well be accounted for by the following disproportionation (DISP) sequence

$$A \xrightarrow{\pm ne} B$$

$$B \xrightarrow{k_1} C$$

$$B + C \longrightarrow A + D$$

Such problems have led to the harnessing of various spectroscopic techniques to voltammetric investigations to allow direct identification of short-lived intermediates. These approaches are complemented by more modern electrochemical methods based on cyclic voltammetry (section 9.7) and the ring–disc electrode (section 9.6)

9.5 Modern polarographic methods

Modern techniques use a three-electrode rather than a two-electrode system of the sort shown in Figure 9.2. Figure 9.13 shows the essential features of the circuit which is aimed at overcoming the disadvantage of the *IR* drop which can distort classical polarograms. In order to minimize such effects before the introduction of potentiostats it was necessary to use very high concentrations of supporting electrolytes. These often needed to be higher even than those required for the suppression of the migration effect and introduced the further complication of requiring very high purity electrolytes for trace analysis of depolarizers.

With the three-electrode arrangement current only flows between indicator and counter electrodes: the potentiostat probes the potential difference between indicator and reference electrodes. If the *IR* drop causes a *difference* between the potential difference probed and that required, the potentiostat responds by increasing the potential applied to the indicator electrode.

9.5.1 Variation of current during the life of mercury drops

At applied potentials corresponding to electrochemical processes taking place, the faradaic current varies in the manner shown in Figure 9.14.

In the short period just before detachment, the current remains virtually constant. If this may be instrumentally sampled, a *net* current, free

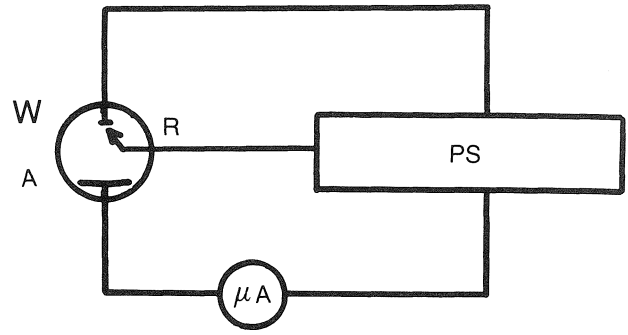

Figure 9.13 Circuit for three-electrode voltammetry. The microammeter responds to current flowing between the working and auxiliary/counter electrodes. W = working electrode; R = reference electrode; A = auxiliary or counterelectrode; PS = potentiostat (this probes the potential difference between W and R).

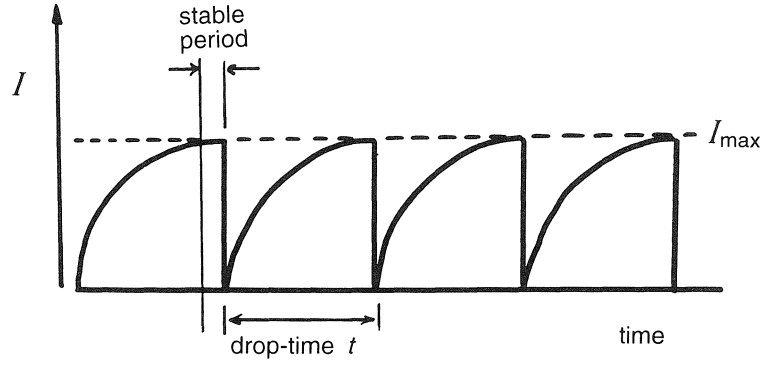

Figure 9.14 Variation of faradaic current in a sequence of drops during an electrode process sensed by the DME.

of oscillations, may be recorded during a synchronized potential scan and some improvement in sensitivity gained from the resulting (stepped) polarogram. Although such sampled (or Tast) d.c. polarography now has limited analytical application it occupies an important place in developments leading towards modern pulse techniques. These evolved via methods based upon the superimposition of square-wave voltage profiles on a conventional d.c. voltage scan.

At the end of each square-wave voltage half-cycle the a.c. component of the cell current contains an improved faradaic to non-faradaic ratio compared to its value at the start. While both components will have decayed during the period in question they do so to different extents (Figure 9.15).

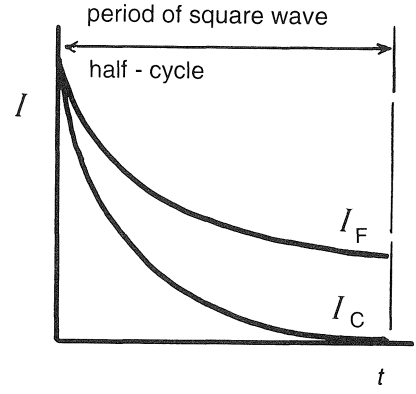

Figure 9.15 Decay of faradaic (I_F) and capacitance (I_C) a.c. components during a square/rectangular wave voltage half-cycle.

9.5.2 *Pulse polarography*

Pulse techniques combine the use of rectangular potential waveforms with synchronization of their application during the stable condition close to the end of the life of a mercury drop. It is usual to control the drop-life to 1/2, 1 or 2 s by electromechanical detachment of drops from a DME system with a long (12–15 s) natural period. More recently, the static mercury dropping electrode has been developed which eliminates the gravitational reservoir generation of electrode material. In this device a solenoid-operated plunger system supplies mercury drops from a low-level reservoir. This system is safer than the traditional one, allows rapid formation of stable drops and uses wider-bore capillaries less susceptible to blockage. Voltage pulses of increasing magnitude are applied in synchronization near to the end of each drop-life of a succession of drops. Resultant net faradaic current components are recorded instrumentally and displayed as a function of applied potential. The pulse profile and consequent polarogram are shown in Figure 9.16.

The pulse polarogram is seen to have the essential shape of a conventional polarographic wave but generated in a sequence of steps rather than continuous output oscillations. Such changes improve the detection limits of the classical technique by approximately an order of magnitude, i.e. to about 10^{-6} mol dm^{-3}.

9.5.3 *Differential pulse polarography*

This technique is based on the effects of superimposing a series of equal square-wave impulses (5–100 mV) on a linearly increasing d.c. voltage.

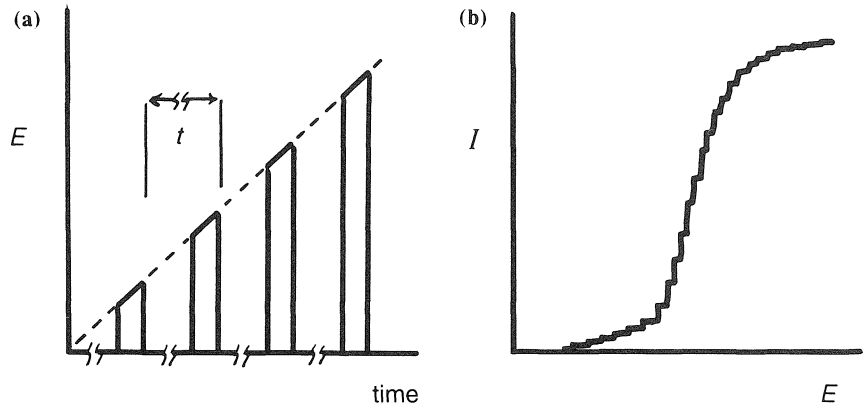

Figure 9.16 (a) Potential pulse-time profile for pulse polarography; (b) stepped (sampled) pulse polarogram.

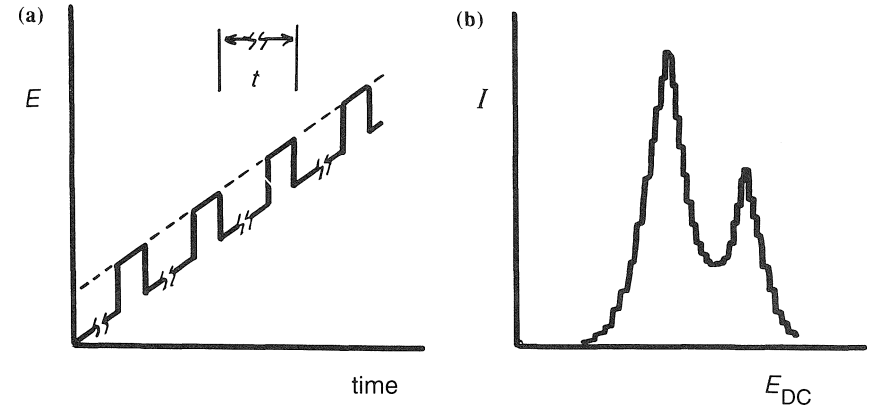

Figure 9.17 (a) Potential pulse-time profile superimposed on linear potential ramp for differential pulse polarography; (b) Sequential differential pulse polarogram with peaked form giving improved resolution between following signals.

Synchronization is effected such that a pulse is applied once during the last stages of the life of each drop. The current signal recorded in this case is the difference between the current flowing just before the imposition of a pulse and that flowing during its last few milliseconds. The combined potential profile and a resultant polarogram are shown in Figure 9.17. Sharply peaked, stepped signals allow analysis at depolarizer concentrations of the order of 10^{-8} mol dm^{-3} and significantly improve resolution between adjacent polarograms.

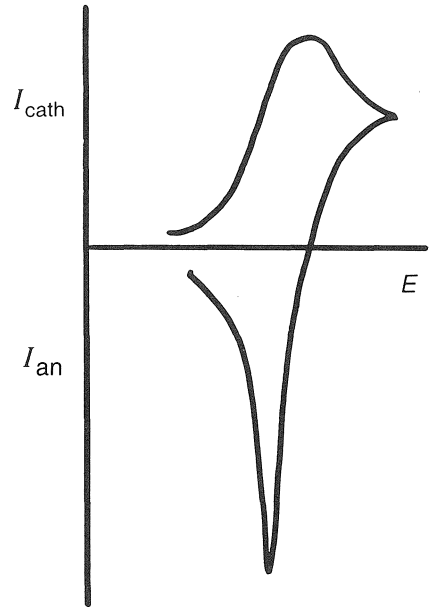

Figure 9.18 Current–voltage pattern for slow cathodic deposition followed by anodic stripping.

9.5.4 Stripping voltammetry

If a solution of a silver ions is subject to voltammetric analysis at a carbon electrode with a slowly varying potential whose direction is reversed, after the diffusion limit is reached, and restored to its original value, a current–voltage curve of the type shown in Figure 9.18 is obtained.

The enhanced anodic signal is caused by the accumulation of silver on the electrode during the slow forward sweep. This principle may be used in anodic stripping analysis which amounts to a convenient preconcentration technique. A stationary hanging mercury drop may be used when the metal forms an amalgam.

9.6 Voltammetry based on forced controlled convection

Controlled hydrodynamic conditions referred to when considering amperometry have also been used in direct analysis.

Any technique which is based on controlled convection, whether this is by controlled stirring of the working solution, by rotation or vibration of an electrode within such a solution, or by the flow of solution past stationary electrodes (as used in some high-performance liquid chromatography detector systems) may be classed under the heading of *hydrodynamic voltammetry*. Two cases will be considered briefly here.

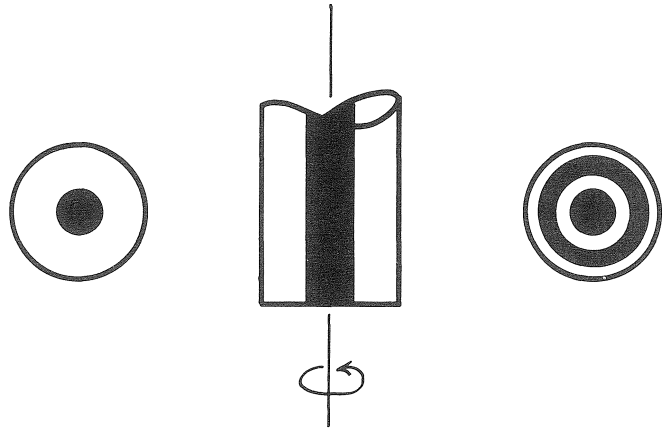

Figure 9.19 (a) Section through rotating disc electrode: conducting electrode material is surrounded co-axially by insulating support. (b) Orientation of electrode during rotation when exposed disc is presented to a solution. (c) Section through ring–disc electrode. The materials of ring and disc may be the same or different and are separated coaxially by the insulating support.

9.6.1 Rotating disc voltammetry

A disc electrode, typically rotated at a rate of 20 rotations per second, which is precisely controllable, is capable of generating equally controllable currents. The structure of such a probe is shown in Figure 9.19(a), (b). The magnitude of the current signals generated is expressible in terms of an equation similar in form to equation (9.1) except that the diffusion layer thickness, δ, is now expressed in terms of hydrodynamic parameters, viz.

$$\delta = \frac{1.62D^{1/3}\nu^{1/6}}{\omega^{1/2}} \tag{9.7}$$

Here ω is the angular velocity of rotation and ν is the kinetic viscosity of the solution. Substitution of equation (9.7) into equation (9.1) yields the Levich equation,

$$I_{\text{lim}} = \frac{nFAD^{2/3}\omega^{1/2}[\text{M}^{n+}]}{1.62\nu^{1/6}} \tag{9.8}$$

9.6.2 The ring–disc electrode

In this device an additional ring surrounds the central disc and is separated from it by a narrow ring of insulating material (Figure 9.19(c)). In some modifications the disc and ring are made of different materials.

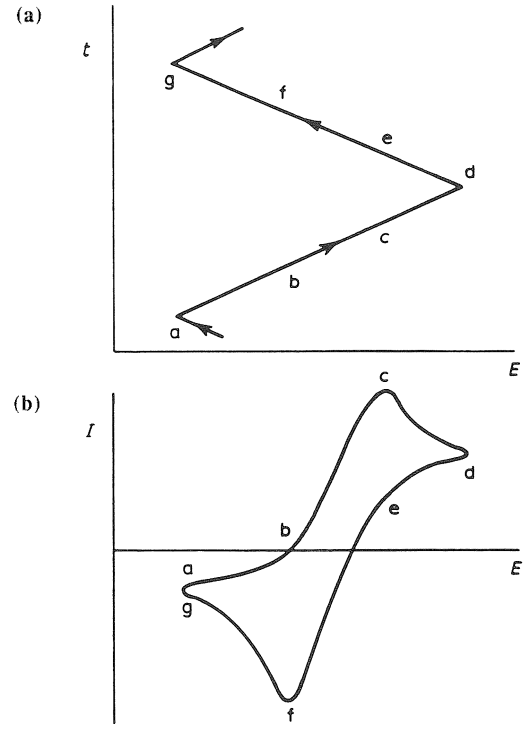

Figure 9.20 (a) Symmetrical saw-tooth potential–time signal used in cyclic voltammetry. (b) Corresponding cyclic voltammogram for a near-reversible system.

The system has found particular application in mechanistic/kinetic studies since it allows detection of unstable products formed by electrode reactions at the disc region. This may be achieved by subjecting the latter to a conventional linear potential scan while maintaining a constant potential applied to the ring at a value characteristic of the limiting current region of the species generated at the disc.

A modification using impingement of electrolyte solution on a small-scale ring–disc system has allowed realization of the wall-jet ring–disc electrode considered in Chapter 10.

9.7 Cyclic voltammetry

In this technique the applied potential is varied with time in a symmetrical saw-tooth wave form as shown in Figure 9.20(a), while the resulting current is detected and recorded over the entire cycle of forward and reverse sweeps (Figure 9.20(b)).

It is usual for solid microelectrodes to be used and glassy or pyrolytic carbon or carbon-paste probes have proved to be convenient. Species which are reduced and deposited in the forward scan of each cycle are re-oxidized in the reverse scan. The technique is useful in the elucidation of mechanism particularly in respect of the identification of intermediates. With the very high sweep rates which may be generated by modern electronic techniques it has proved possible to identify short-lived intermediates which decompose within the time scale of conventional voltage scan frequencies. In Figure 9.20(b) is shown the form of a cyclic voltammogram expected for a near-reversible system. The greater the separation between the peaks for forward and reverse scans, the more irreversible is the electrode process.

9.8 Ultramicroelectrodes

A very small plane electrode surface with a diameter less than about 50 μm offers particular features in respect of the establishment of steady-state diffusion-controlled currents. Such currents, because of such a small electrode area, will be extremely small; the nanoamp scale now replaces that of the microamp.

Although *currents* are so small, *current densities* are very high and have a quite different distribution at the very small plane surface to that at a larger one. The comparative distributions are shown in Figure 9.21. The predominating influence of edge effects shown in Figure 9.21(b) produces an essentially hemispherical charge density distribution. The electrode thus behaves as though it were hemispherical (Figure 9.21(c)): this offers some theoretical advantage in that it is significantly easier to solve current equations for such a profile than it is for a plane. Three practical advantages are important:

1. A supporting electrolyte need not be used since steady-state currents are established in their absence.
2. A three-electrode, potentiostatic polarizing system is not required. Currents are so small that reference electrodes can now sustain them without associated *IR* problems.
3. Such electrodes offer some promise as *in vivo* analytical probes, although there can be disadvantages arising from the insulating effects of antibodies resulting from rejection of electrode material.

The steady-state diffusion-limited currents may be expressed by equations of elegant simplicity, viz.

$$I_d = knFDrC \tag{9.9}$$

where k is a numerical constant of value 4 or 2π, according as to whether

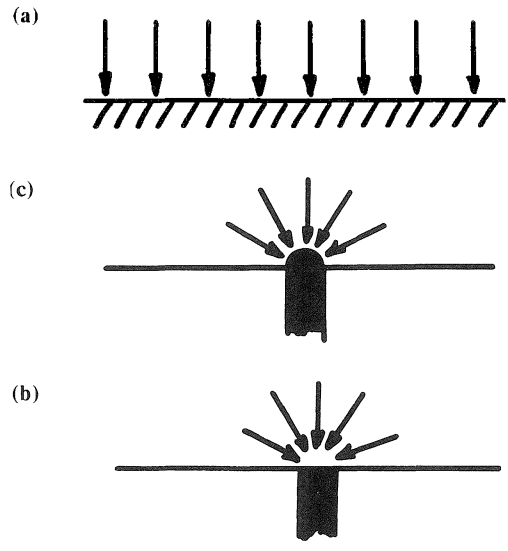

Figure 9.21 (a) Current density distribution at a large planar electrode where edge effects are insignificant. (b) Near-hemispherical current density distribution at a very small planar electrode where edge effects are significant: (c) Current density distribution at a hemispherical ultramicroelectrode.

the electrode is planar (Figure 9.21(b)) or hemispherical (Figure 9.21(c)) relative to its insulating support.

9.9 Electrogravimetry

As the name implies, methods under this heading combine electrodeposition and weighing, i.e. total electrolytic removal of a species from solution followed by measurement of the change in weight of a suitable cathode.

A restricting feature is the obvious requirement that only *one* species must react with the working electrode: in the earliest constant-current methods, a progressive increase in applied voltage is required to sustain that current during the electrolysis. This increases the possibility of interference from other metal depositions or even hydrogen evolution. Controlled potential gravimetry (Figure 9.22) ensures deposition well removed from other processes: however, this means that a long time may be required for the electrolysis to reach completion recognized by a condition of zero current.

9.10 Coulometric methods

The circuit required for controlled potential coulometry is shown in Figure 9.23. Here the electronic integrator provides direct measurement of the

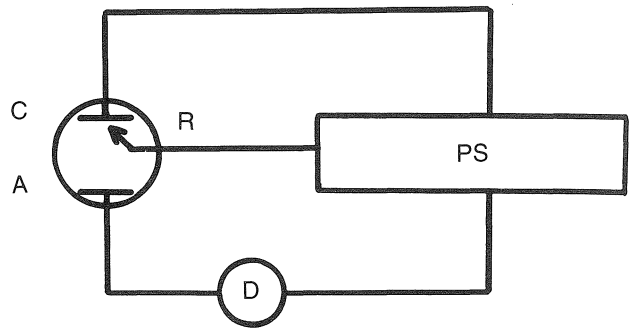

Figure 9.22 Schematic circuit for controlled potential electrogravimetry. PS = potentiostat; C = cathode (large-area mercury pool or platinum mesh); R = reference electrode; A = auxiliary electrode; D = current detector.

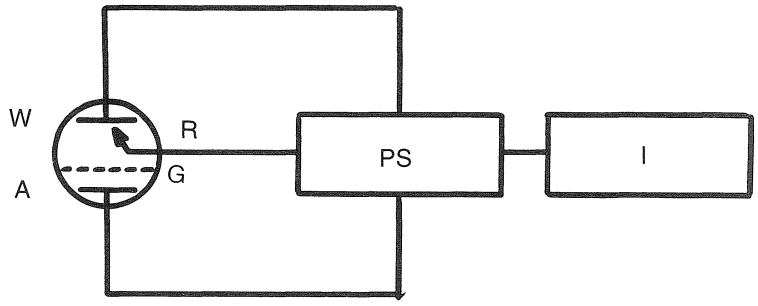

Figure 9.23 Schematic circuit for controlled potential coulometry. W = working electrode; A = auxiliary electrode; R = reference electrode; PS = potentiostat; I = electronic integrator to measure directly the quantity of electricity passed during electrolysis; G = separator between working and auxiliary electrode compartments.

quantity of electricity passed during electrolysis of a required analyte. A contributing feature to the high precision and accuracy achievable is the physical separation of working and counterelectrode compartments. The range of potentials available for such analysis is defined by the most frequently used electrode materials, namely mercury and platinum.

Coulometric methods require large area electrodes (mercury pool or platinum mesh) combined with rapid stirring to encourage rapid completion of electrolysis. This is in sharp contrast to voltammetry where microelectrodes are used in either quiet solutions or with carefully controlled convection. Coulometry is essentially destructive while voltammetry involves such a small amount of actual decomposition that in practical terms its techniques are non-destructive.

The most efficient analyses will be those based on reversible electrode reactions since applied potentials near to a realizable $E^{\ominus}$ will ensure efficient electrolysis. Irreversible processes are more problematic in that applied potentials often well removed from $E^{\ominus}$, to ensure a practicable electrolysis rate, introduce difficulties associated with interference from other electroactive species, secondary reactions and low current efficiencies.

Coulometric *titrations* are based on the generation of a titrant by electrolytic means: conventional standardization of titrant is thus obviated although it is, of course, imperative that the generation occurs with 100% efficiency. A particular advantage is that it is sometimes possible to use unstable titrants which would be unusable by conventional volumetric means. This makes available some quantitatively useful analytical reactions which find no place with other titration methods.

Problems

9.1 Calculate the limiting current density for an electrode at which silver is deposited from an aqueous solution containing silver ions at a concentration of 0.1 mol dm^{-3}, in the presence of excess indifferent electrolyte, if the diffusion layer thickness is 0.05 cm. Estimate the effect on the magnitude of the limiting current if the solution is stirred rapidly.

9.2 The following mean currents, for the applied potentials indicated, were obtained for a reversible, diffusion-controlled reduction of a metal ion M^{n+} to metal M at a dropping mercury electrode at 298 K (all mean current values have been corrected for the appropriate residual current in the presence of excess KCl at 298 K).

E (V) vs. SCE	0.97	0.98	0.99	1.01	1.02	1.03	1.04	1.05
$\bar{I}$ (μA)	2.134	4.255	7.718	17.100	20.644	22.831	25.000	25.000

By means of an appropriate graph, determine the half-wave potential ($E_{1/2}$) and the number of electrons (n) transferred per metal ion during the reduction process.

Given that the concentration of M^{n+} was 2.98×10^{-3} mol dm^{-3}, that the rate of flow of mercury (m) was 3.299 mg s^{-1} and that the drop-time (t) was 2.47 s, estimate the value of the diffusion coefficient (D) of the hydrated M^{n+} cation.

9.3 For a metal ion M^{n+} at a concentration of 3.06×10^{-3} mol dm^{-3} and in the presence of excess inert electrolyte, the following data were obtained using the same dropping mercury electrode system as used in Question (9.2).

E (V) vs. SCE	1.00	1.02	1.03	1.05	1.07	1.09	1.10	1.15
$\bar{I}$(μA)	3.809	7.025	9.207	13.733	17.881	20.678	23.800	23.800

(Current values have again been corrected for the residual, capacitance effect.)

It was found that the plot of $\bar{I}_d$ versus square root of mercury reservoir height was linear and passed through the origin of the graph. Determine the half-wave potential ($E_{1/2}$) and assess the nature of the electrode process.

9.4 The method of standard addition has been used to determine traces of nickel impurity in cobalt salts by various polarographic techniques.

Reagent grade $CoSO_4.7H_2O$(300 g) was dissolved in about 50 cm^3 water in a 100 cm^3 volumetric flask; after addition of 2 cm^3 conc. HCl and 5 cm^3 pure pyridine plus 5 cm^3 of 0.2% gelatin, the solution was diluted to the mark.

Exactly 75 cm^3 of this solution were transferred to a polarographic cell and a d.c. polarogram with I_d = 1.97 μA was obtained for the conditions used. After adding 4 cm^3 of a 9.24 × 10^{-3} mol dm^{-3} solution of AnalaR $NiCl_2$, a polarogram with I_d = 3.95 μA was obtained.

Explain the principles behind the observations and estimate the percentage of nickel in the original sample as both Ni and $NiSO_4.7H_2O$. Derive any equation required for the estimation.

9.5 Two metal ion species M^{2+} and N^{2+} in non-complexing supporting electrolytes show almost coincident polarographic waves so that analysis for M^{2+} in the presence of N^{2+} is not possible.

In the search for some ligand species, X, which complexes with N^{2+} rather than with M^{2+}, estimate the approximate stability constant required, at a ligand concentration of 0.2 mol dm^{-3}, to induce the required wave separation of about 0.2 V for d.c. polarography.

Make clear any assumptions underlying the calculation.

10 Electrochemical sensors

10.1 Ion-selective electrodes

Although a number of devices, which offer analysis via a direct relationship between an electrochemical parameter and an analyte concentration, may be broadly described as sensors, the term tends to be used in relation to a number of features of experimental convenience. These concern the size, exclusivity of response to particular species, robustness and the ease and speed of practical application.

The glass electrode, considered in Chapter 8 in the context of pH measurement, is the best known example of an ion-selective electrode (ISE). Its operation depends on the modification of a half-cell potential by the response to hydrogen ions of a glass membrane separating the half-cell from a solution whose pH is required. Many ion-selective membrane materials have been developed, the response probed by all of them being a function of ion-exchange reactions at their surface and ion-conduction inside them. They fall into three categories, viz. glass, solid state and liquid.

10.1.1 Glass membrane electrodes

It is well known that glass electrodes require soaking before use to allow certain components of the glass and the solution to exchange and produce an 'ion-exchanging layer' on the membrane surface. The condition of the electrode after this operation is completed is summarized in Figure 10.1. Water molecules become associated with part of the membrane and play a part in the ion-exchange process. Glass is unique in that, while it is an ionic conductor for small ions such as sodium, it is hydrogen ions which are involved most exclusively in the ion-exchange process even at high pH values and when the activity of ions such as Na^+ is high. In the latter condition, the membrane shows response to these ions as evidenced by the 'alkaline error'.

Electrodes specifically designed for the determination of Na^+ or K^+ have had the composition of the glass membrane so devised to show an enhanced alkaline error while at the same time having the preference for hydrogen ions in the exchange process suppressed.

By analogy with the expression representing the formal definition of pH it is possible to define the quantity pX by

$$pX = -\log a_X \tag{10.1}$$

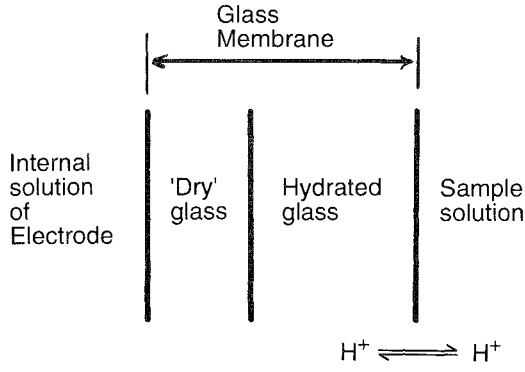

Figure 10.1 Arrangement of a glass membrane electrode. Compare with the glass electrode structure shown in Figure 8.10.

for an electrode responsive to ion X, whose activity a_X is related to the potential adopted by the electrode by

$$E = K + \frac{2.3RT}{nF} \log a_X \tag{10.2}$$

so that

$$E = K - \frac{2.3RT}{nF} \mathrm{pX} \tag{10.3}$$

K representing the proportion of sensed potential due to constants of the system.

10.1.2 Solid-state electrodes

Here the membrane is either a single crystal or a solid ion-exchanging material. For instance, for halide ion-sensitive electrodes the membrane may be a solid silver salt, the potential of the electrode being given by

$$E = E^{\ominus} + \frac{2.3RT}{F} \log a_{Ag^+} \tag{10.4}$$

At the surface of the membrane there is a certain activity of silver ions which is a function of the halide activity of the solution into which the electrode dips (Figure 10.2).

The activity of silver ions may be expressed in terms of the solubility product of the silver halide by

$$a_{Ag^+} = \frac{K_{AgX}}{a_{X^-}} \tag{10.5}$$

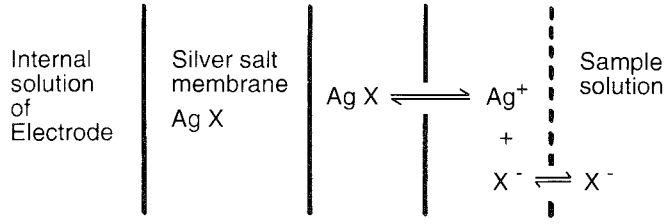

Figure 10.2 Arrangement of components and interactions in a solid-state halide ion-sensitive electrode.

therefore,

$$E = E^{\ominus} + \frac{2.3RT}{F}(\log K_{AgX} - \log a_{X^-})$$

$$E = K - \frac{2.3RT}{F}\log a_{X^-} \tag{10.6}$$

10.1.3 Liquid membrane electrodes

A liquid membrane comprises a thin, porous inert support impregnated with an ion-exchanging material in the liquid phase. This material is often an organic species dissolved in some organic solvent, in which case use in non-aqueous solutions may be restricted. There are two types of liquid membranes: (a) charged liquid membranes which usually contain the ion for which the electrode is sensitive (the operation here is very similar to the solid state case), and (b) neutral liquid membranes which do not contain the ion to be detected but a polymeric species whose geometry offers selectivity to particular ion species by allowing encapsulation within a cavity of appropriate size. The antibiotic valinomycin, incorporated into a polyvinyl chloride matrix or dissolved in diphenylether operates very effectively in this way with K^+ ion-selective electrodes. The situation across the membrane is shown in Figure 10.3.

The principle has been widely and effectively used in electrodes based on exploitation of the tailor-made cavities available within cryptands and crown ethers.

10.2 Problems with ion-selective electrodes

The most important practical difficulty with ion-sensitive electrodes is the interference from ion species in solution other than the one required. Such electrodes must therefore be devised so that their *selectivity* for the ion in

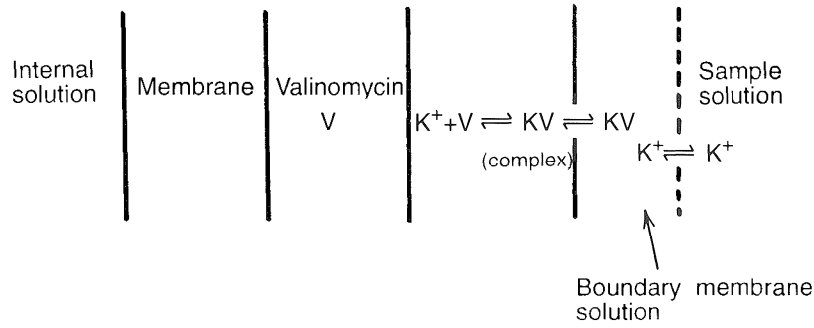

Figure 10.3 Arrangement of components and interactions in the K^+-sensitive valinomycin electrode.

question is as high as possible. Glass electrodes for pH determination are the most selective of all ion-sensitive electrodes but it has been seen that, even here, serious interferences may occur. When other ions interfere the equation for the potential adopted by the electrode must be modified to

$$E = K + \frac{2.3RT}{nF} \log (a_i + K_{ij}a_j + K_{ik}a_k + K_{il}a_l \ldots) \qquad (10.7)$$

where a_i = activity of ion to be determined; a_j, a_k, a_l, ... = activities of interfering ions; and K_{ij}, K_{ik}, K_{il} ... = 'selectivity constants' of the electrode towards particular ions. These selectivity constants are defined as follows

$$K_{ij} = \frac{u_j}{u_i}({}_eK_{ij}) \qquad (10.8)$$

where u_i, u_j are ion mobilities and ${}_eK_{ij}$ is the equilibrium constant for the reaction:

$$j_{solution} + i_{membrane} \rightleftharpoons j_{membrane} + i_{solution}.$$

In cases where neutral membranes are used, the mobilities used are those of the complexes of the membrane material formed by the determined and interfering ions.

The Nernstian basis of all such potentiometric sensor devices carries with it a more fundamental disadvantage. The signal–activity relationship is a *logarithmic* one, small errors in measurement of potential generating large errors in analysis unless care is taken. A matter sometimes overlooked is that such probes respond to *activity* rather than concentration.

Other disadvantages can be the comparatively short lives of some devices and interference from electronic noise: matters addressed by the significant industry which has developed around this major feature of modern analytical chemistry.

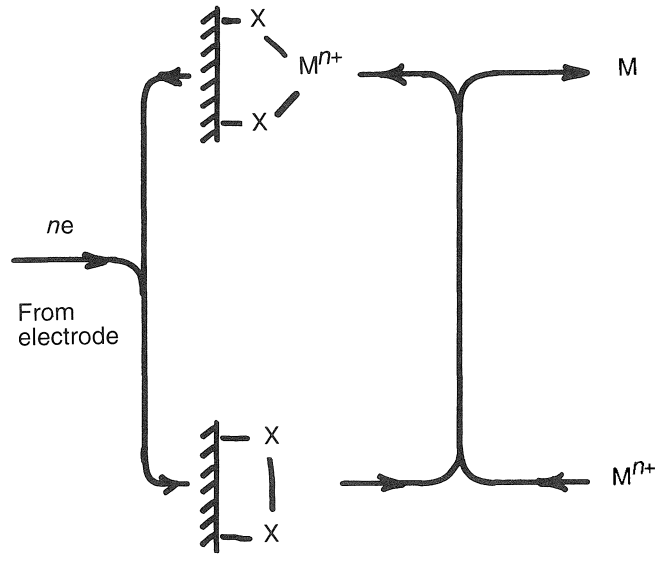

Figure 10.4 Scheme for chemically modified electrode based on interaction of metal ion M^{n+} with adsorbed analyte-specific ligand species X_2.

10.3 Chemically modified electrodes

A chemically modified electrode (CME) is one whose surface is purposely contaminated with material which reacts selectively and reversibly with a chosen analyte. Such a material might be an adsorbed ligand with which a metal ion binds (Figure 10.4).

Although a simple idea, there are significant difficulties to be overcome in the construction of such probes. There must be effective adsorption of the analyte-specific species (represented by X_2 in Figure 10.4) onto the otherwise inert conductor. Interaction of this adsorbed material with the studied analyte must be rapid and strong in comparison with that of competing species: it must not be so strong, however, that the interaction process cannot be reversed and the probe used repeatedly with X_2 in position for further analyses. It is also necessary for there to be an electron transfer between the complexed analyte and conductor.

Operation of such *amperometric* sensors depends upon measurement of the steady-state current flowing in consequence of a constant potential maintained between the conductor and a suitable reference electrode. The latter would invariably be built into the—often significantly miniaturized—probe. The easier and more accurate measurement of currents compared

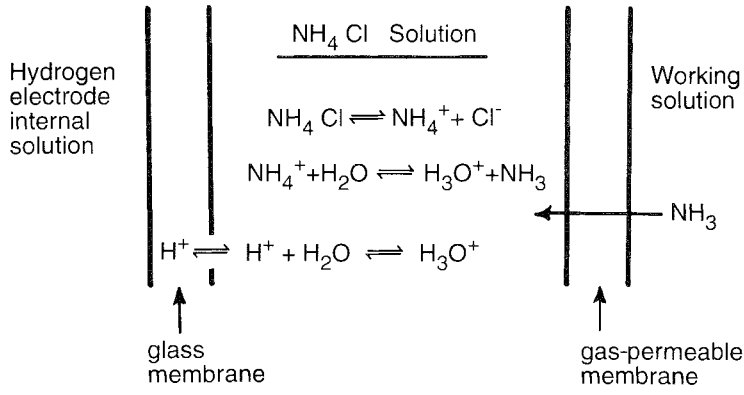

Figure 10.5 Components and interactions in an ammonia-sensing electrode.

with potentials, combined with the direct proportionality of signal and concentration, has attracted considerable commercial investment in the development of amperometric sensors.

10.4 Gas-sensing electrodes

These may be of potentiometric or amperometric type. The former are based on a conventional potentiometric sensor whose response to its specific analyte is modified by quantitative interaction of dissolved gas with this species. An example is an ammonia-sensing electrode based on a hydrogen electrode operating in a solution of ammonium chloride (Figure 10.5). This is combined with a thin layer at the glass interface enclosed by a gas-permeable polymer membrane. Diffusion of NH_3 molecules from the working solution disturbs the electrolyte equilibrium of the internal solution and thus its pH as sensed by the glass electrode. The difference in potential caused is a function of the logarithm of NH_3 concentration.

Amperometric gas-sensing electrodes have a similar construction but they function by responding to the steady-state diffusion-controlled electrochemical reactions of dissolved gases. This may be understood by reference to the schematic arrangement of an oxygen sensor shown in Figure 10.6.

The steady-state diffusion of O_2 molecules through both the separating membrane and the electrolyte solution of the sensing region results in a steady current signal (I) if the potential of the indicator electrode (E) is suitably poised with respect to the reference (R).

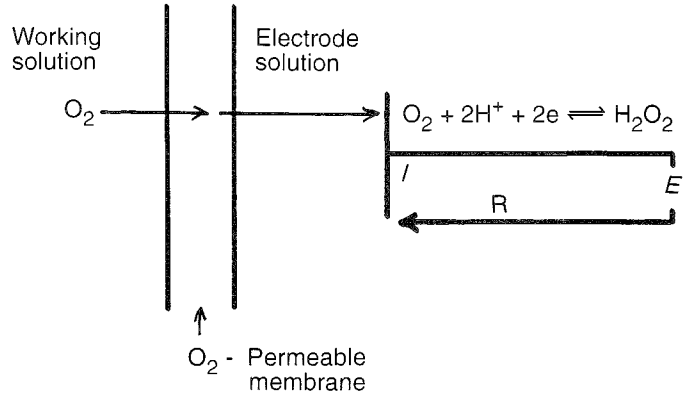

Figure 10.6 Scheme for an amperometric oxygen-sensing electrode.

10.5 Enzyme electrodes

The chemical specificity of enzymes has been made the basis of both potentiometric and amperometric devices. As with chemically modified electrodes, the principle is simple but the problems of immobilizing an enzyme onto an appropriate probe, controlling containment of solutions by means of membranes and ensuring reproducibility are formidable ones. Nevertheless there have been some notable successes and a great deal of effort and funding is currently directed towards the development of such sensors. Urease has been successfully used in a urea probe, shown schematically in Figure 10.7, a device based on a modified ammonium ion selective electrode.

Difficulties have sometimes been encountered in establishing equilibria and steady potentials for such systems and it is more usual for enzyme electrodes to be of the amperometric type.

The enzyme glucose oxidase (GOD) has been used in a variety of electrode systems to detect glucose. Hydrogen peroxide, produced by reoxidation of the reduced enzyme ($GODH_2$) may be detected via its anodic reaction.

$$\underset{(G)}{\text{glucose}} + \underset{(GOD)}{\text{glucose oxidase}} \longrightarrow \underset{(GODH_2)}{\text{reduced enzyme}} + \underset{(GL)}{\text{gluconolactone}}$$

$$GODH_2 + O_2 \longrightarrow H_2O_2 + GOD$$

$$H_2O_2 - 2e \rightleftharpoons O_2 + 2H^+$$

The amperometric signal is directly proportional to the concentration of glucose in the medium to be analysed and may be measured by connec-

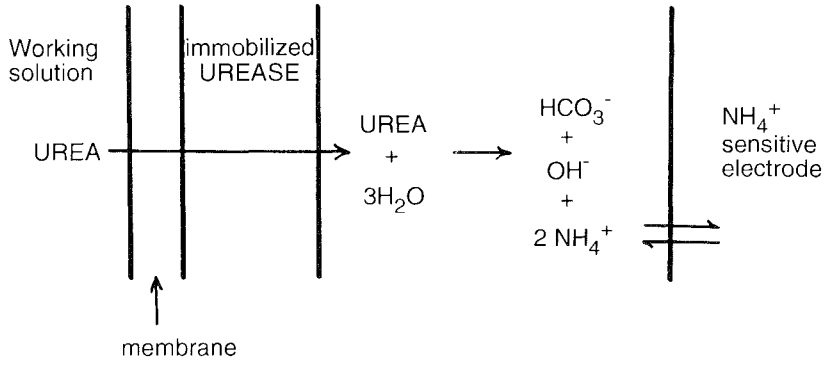

Figure 10.7 Scheme for a potentiometric enzyme electrode.

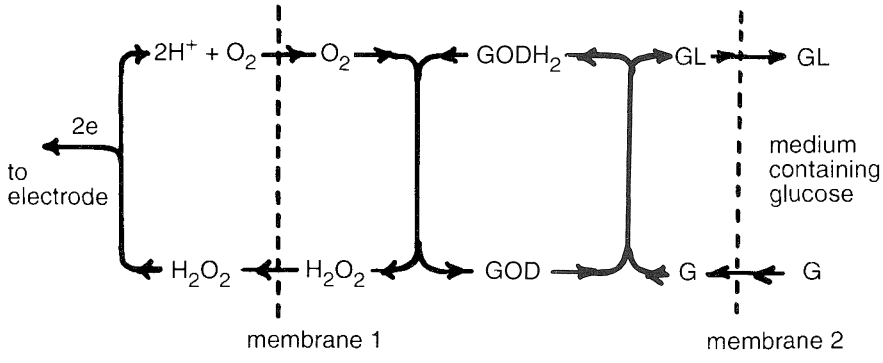

Figure 10.8 Arrangement for an amperometric glucose sensor based on glucose oxidase with hydrogen peroxide as electron mediator.

tion with a reference electrode. The sequence of reactant–product cycles is shown in relation to the schematic probe structure in Figure 10.8.

A major disadvantage of this system is the necessity for two membranes to contain the two chemical cycles and to separate them from the electrochemical step. Further, the performance of the probe is somewhat affected by changes in the prevailing concentration of oxygen.

It has been found possible to use single membrane systems in conjunction with electron mediators based upon ferrocene derivatives. The sequence of chemical–electrochemical cycles now becomes simplified to that shown in Figure 10.9. Re-oxidation of reduced enzyme is effected by, for instance, the ferrocenium ion, $FcCO_2H^+$, formed by oxidation of ferrocene

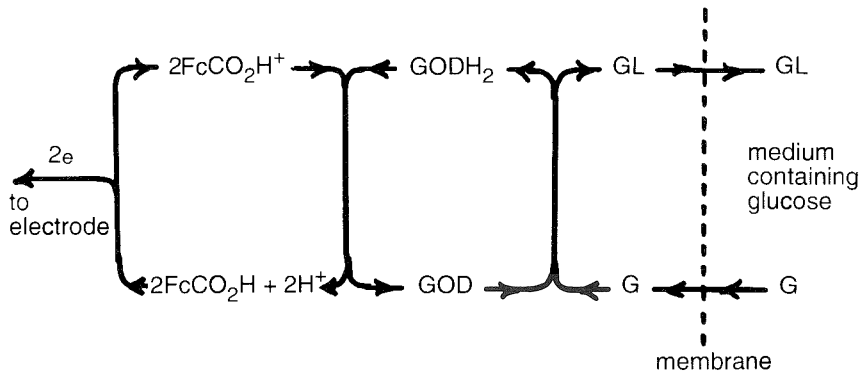

Figure 10.9 Scheme of chemical–electrochemical cycles for a ferrocene-mediated enzyme electrode.

carboxylic acid, $FcCO_2H$

$$GODH_2 + 2FcCO_2H^+ \longrightarrow GOD + 2FcCO_2H + 2H^+$$

followed by the amperometric signalling reaction

$$2FcCO_2H - 2e \rightleftharpoons 2FcCO_2H^+$$

A glucose concentration-dependent current is generated when the potential of the working electrode is made positive to the correct extent with respect to the reference (usually SCE). This requires potentiostatic control to a value which is dependent upon the ferrocene derivative used.

An even simpler system, at least superficially, is based upon the initially reduced form of the enzyme becoming re-oxidized directly at the electrode surface due to the modification of the latter. This has usually involved incorporation of a conducting organic salt which both allows strong adsorption of both forms of the enzyme and aids electron transfer. The arrangement now becomes simplified to that in Figure 10.10.

10.6 Sensors based on modified metal oxide field effect transistors (MOSFETs)

Introduction of such transistor devices brings a quite new dimension to sensor systems. Their effectiveness, coupled with the capability of miniaturization and stacking into multiple probes leads on to the possibility of making systems capable of sensing several analytes. The essential features

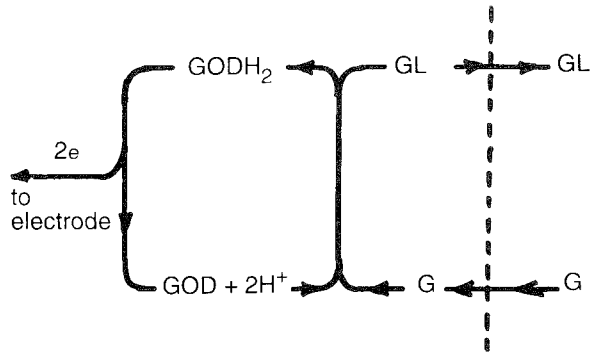

Figure 10.10 Unmediated enzyme electrode reactions.

of a MOSFET are shown in Figure 10.11, the significant property for exploitation in analysis being the modulation of the current, I_{SD}, by the gate voltage, E_G. In its application as a sensor the device is modified to what is known as a ChemFET—a Chemically Sensitive Field Effect Transistor. This involves replacement of the gate electrode by some kind of analyte sensor together with a reference electrode and solution of species to be determined. In essence the device operates on both potentiometric and amperometric characteristics. The primary analytical interaction of analyte with sensor produces a response in E_G. This, in turn, affects the value of I_{SD} which is the quantity measured as a concentration indicator.

10.7 The wall-jet ring–disc electrode (WJRDE)

A modification of the ring–disc electrode (Chapter 9) is directed at analytical application. The ring–disc system is held stationary while a jet of analyte-containing solution is made to impinge on the disc component. This can be effected on a very small scale and the usual arrangement is shown in Figure 10.12.

The jet can be so controlled that its scattering at the disc (Figure 10.12, inset) produces a reproducible pattern leading to a controllable mass-transfer profile not unlike that considered briefly in section 9.6.

The device has been successfully used in the determination of protein concentrations by microtitration with electrolytically generated bromine. The potential difference between ring and disc may be poised such that Br_2 is generated at the disc and reduced at the ring. Under such circumstances a plot of ring current versus disc current is linear as shown in Figure 10.13, curve (a).

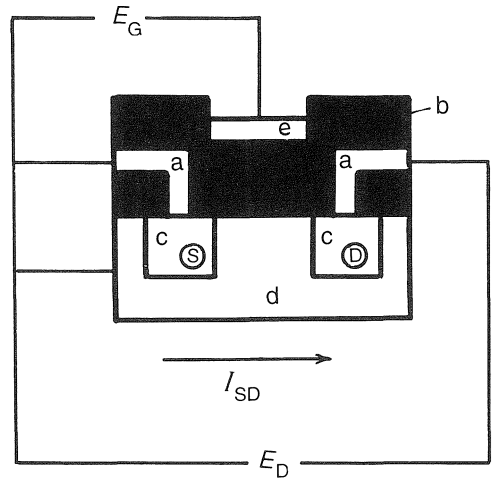

Figure 10.11 The features of a MOSFET. In conversion to an analytical sensor as a ChemFET, the gate electrode is replaced by an analyte sensor plus reference electrode and incorporates a cell to contain the solution to be analysed. (a) conductor, (b) insulator, (c) n-type semiconductors (S = source, D = drain), (d) p-type semiconductor, (e) gate electrode. E_G = gate voltage, I = current. E_D = drain voltage.

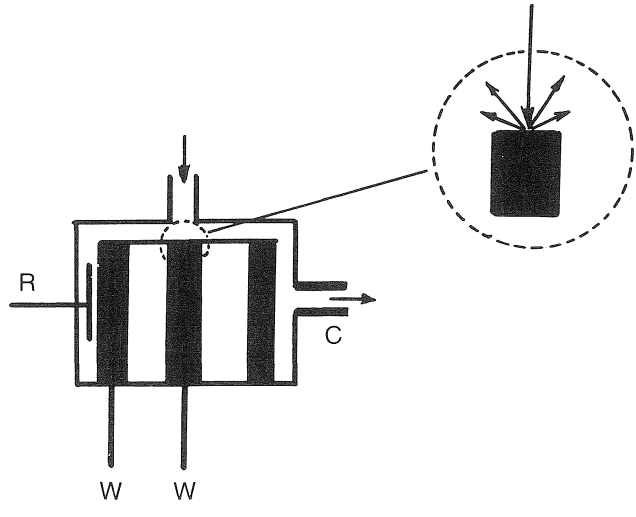

Figure 10.12 Principle of the wall-jet ring–disc electrode. W = working disc and ring electrodes. R = reference electrode. C = auxiliary or counter electrode incorporated into the outlet.

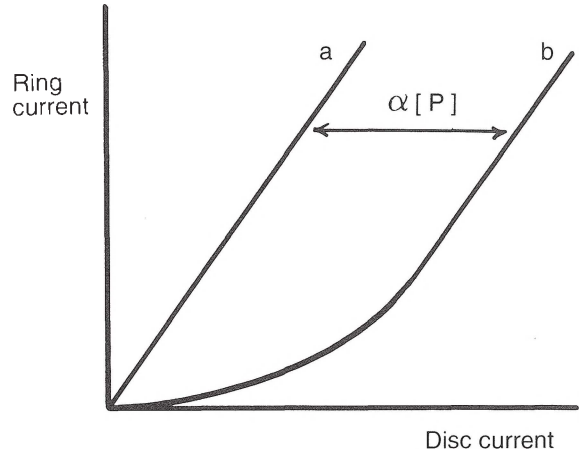

Figure 10.13 Titration of protein with electrolytically-generated bromine:

$$\textit{At the disc}: \ 2Br^- - 2e \longrightarrow Br_2$$
$$\textit{At the ring}: \ Br_2 + 2e \longrightarrow 2Br^-$$

The reaction $P + nBr_2 \longrightarrow PBr_{2n}$ reduces the ring current.
For explanation of curves (a) and (b) see text.

In the presence of protein, however, which will typically react rapidly with bromine in a molecular ratio of one to several hundreds, the amount of unreacted bromine available to react at the ring electrode is greatly reduced. The graph of ring current to disc current is now shifted, relative to its position in the absence of protein, by an amount proportional to the concentration of protein (Figure 10.13, curve (b)).

11 The exploitation of electrode processes

11.1 Mixed potentials and double electrodes

The potential adopted by a metal in aqueous solution is not always governed by the M^{n+}/M equilibrium which might be expected for simple cases. Other reactions may occur when the metal is thermodynamically unstable in aqueous solution. In particular, the reduction of hydrogen ions may interfere with the electrode equilibrium. Consider a metal such as zinc, with a fairly negative electrode potential, in an acidic solution containing its cations. If more positive potentials were to be imposed upon the zinc electrode the current density would vary according to the Tafel line as the metal ionized (assuming only activation polarization) a situation shown in Figure 11.1.

The standard potential of hydrogen is considerably more positive than that of zinc, but at potentials more negative than $E_H^{\ominus}$, the rate of hydrogen discharge increases according to its characteristic Tafel line. At the point where the two Tafel lines meet, both reactions must occur at the same current density, so that the potential corresponding to this intersection point is a steady one which is known as a mixed or corrosion potential. The situation may alternatively be represent by the current–potential relationships for the two reactions (Figure 11.2).

The actual potential adopted by the system for different currents will follow the resultant line AB which at $E = E_{corr.}$ gives equal currents flowing in opposite directions. The species co-reducing need not be hydrogen but may be any species reducing at a more positive than M^{n+}.

11.1.1 Pourbaix diagrams

Graphs of reversible metal electrode potentials versus pH of solutions into which they dip at fixed temperature and pressure, provide important information regarding the thermodynamic stability of various phases. Such Pourbaix diagrams provide a thermodynamic basis for the explanation of corrosion reactions. It must, however, be emphasized that the construction of such diagrams takes no account of the kinetics of reactions which occur under the conditions represented by various areas appearing on them. This means that they should be used with some caution when attempting to predict corrosion behaviour. A much simplified Pourbaix diagram for iron in aqueous solution is shown in Figure 11.3. Here the dashed lines labelled (a)

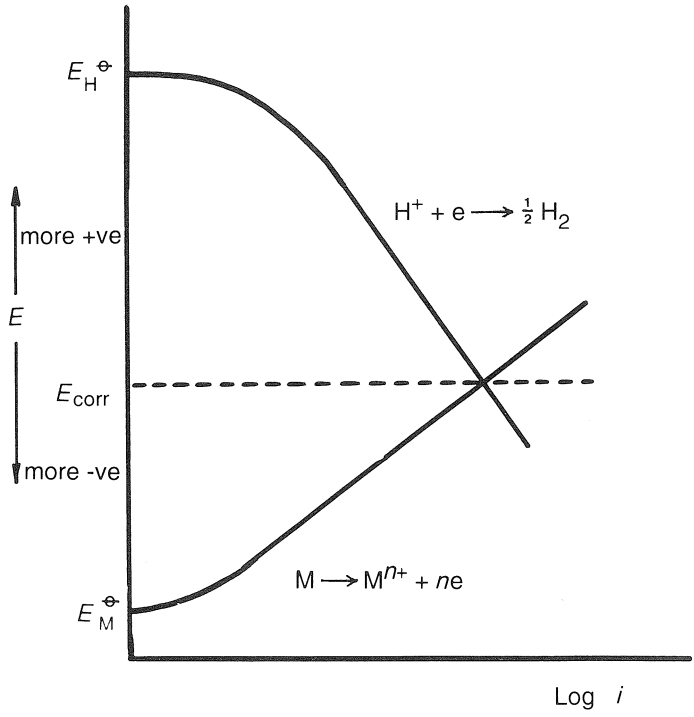

Figure 11.1 Mixed or corrosion potential in acid solution for a metal (e.g. zinc) with an electrode potential which is negative relative to hydrogen. Graphs showing such intersecting Tafel lines are often known as Evans diagrams.

and (b) give the pH dependence of the equilibrium potentials of hydrogen and oxygen electrodes. The area labelled 'passivation' corresponds to the formation of solid compound on the metal surface which protects the metal from attack.

High hydrogen overvoltages prevent high-purity metals from corroding at anything but very slow rates. In the presence of more noble metal impurities, however, corrosion rates may become greatly accelerated, the more noble metal regions acting as 'local cathodes' at which hydrogen evolution may take place.

In neutral and alkaline solutions, the mixed potential attained is usually insufficient to cause hydrogen evolution, at least at atmosphere pressure. In such cases oxygen, either adsorbed at the surface or in solution, may itself become a depolarizer undergoing reduction by the following cathodic processes.

$$O_2 + 2H_2O + 4e \longrightarrow 4OH^-$$

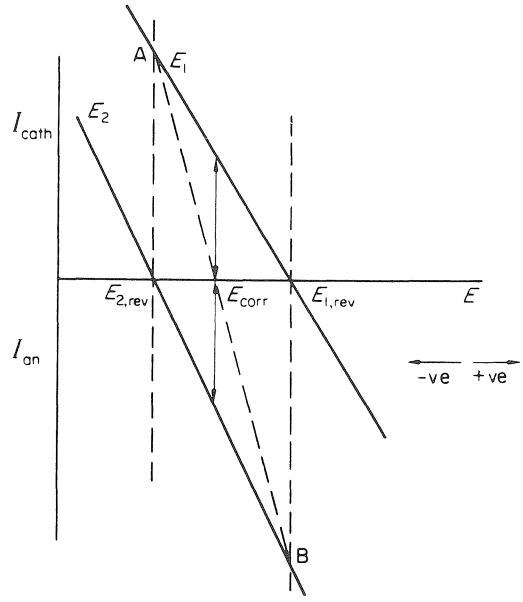

Figure 11.2 Resultant current–potential plot A–B for a mixed electrode: at the corrosion potential equal currents flow in opposite directions.

and

$$O_2 + 4H_3O^+ + 4e \longrightarrow 6H_2O$$

Such partial cathodic processes may well occur via adsorbed oxygen or oxides. Areas where oxide or oxygen are not adsorbed then correspond to anodes, and in this way local cells may be set up over the whole of the metal surface.

Corrosion rates involving oxygen consumption vary in a quite different manner to those involving hydrogen evolution. While the latter type starts very slowly, even in the presence of noble metal impurities, increasing dissolution exposes increasing areas of noble metal, to form an increasing number of local cathodes. The rate then accelerates rapidly. In corrosion involving oxygen, initial rates are high and drop to low steady values very rapidly, the rapid decline corresponding to the removal of adsorbed oxygen, after which the corrosion rate becomes largely dependent on the rate of diffusion of oxygen to the metal surface. In the rusting of iron, for instance, the initial reactions appear to be dissolution of iron to give Fe^{2+} ions at local anodes.

These Fe^{2+} ions then combine with hydroxyl ions, formed at local cathodes, to produce Fe(II) hydroxide. If sufficient oxygen is available, the

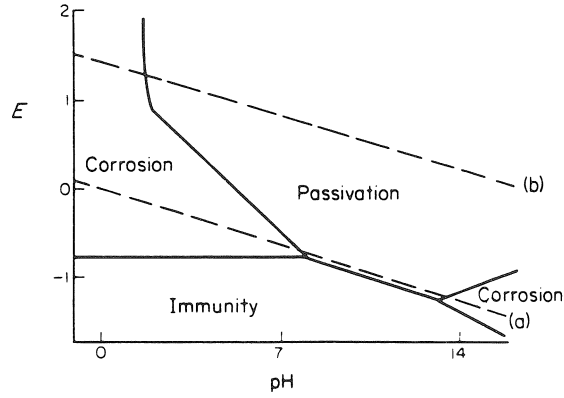

Figure 11.3 Simplified Pourbaix diagram for the iron–water system: the dashed lines (a) and (b) are the pH dependencies of E for hydrogen and oxygen electrodes, respectively, i.e.

$$\text{(a)}\quad 2H + 2e \rightleftharpoons H_2 \quad (pH < 7)$$

$$2H_2O + 2e \rightleftharpoons H_2 + 2OH^- \quad (pH > 7)$$

$$\text{(b)}\quad \tfrac{1}{2}O_2 + 2H^+ + 2e \rightleftharpoons H_2O \quad (pH < 7)$$

$$\tfrac{1}{2}O_2 + H_2O + 2e \rightleftharpoons 2OH^- \quad (pH > 7)$$

latter may be oxidized to rust, $Fe_2O_3 \cdot H_2O$. In practice the products of intermediate oxidation stages (Fe_3O_4 and hydrates) also occur due to lack of oxygen. Corroded surfaces show formation of these products in preferential layers, the true rust deposit being outermost.

The above reactions are not observed with metals which form an oxide surface layer in air, except in the neighbourhood of cracks or large pores in the layer. At such points anodic dissolution may occur. In cases where the anodically formed ions produce oxide after reacting with hydroxyl ions formed at a local cathode, the fault in the protective film becomes sealed against further corrosion. Should different products be formed, the development of further local cells is encouraged and severe local corrosion may result. These effects are summarized in Figure 11.4.

11.1.2 Corrosion prevention

Corrosion reactions may be minimized by two means—by covering surfaces with protective films or by using inhibition processes. Steel, for example may be protected to various degrees by surface layers of chromium, nickel, zinc or tin.

Cracks in a surface film of plated metal with a more positive electrode

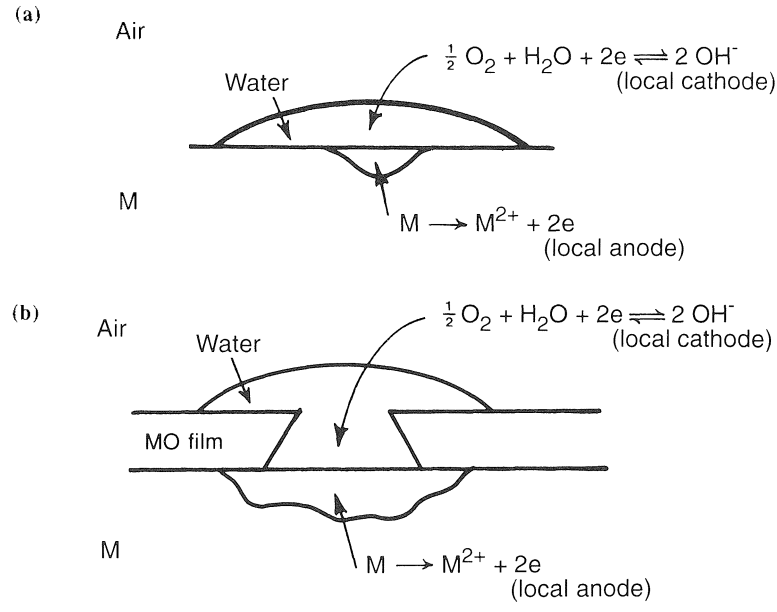

Figure 11.4 Corrosion of metal M in vicinity of oxygen-containing water droplets. (a) Dissolution of M occurs at local anode. (b) Dissolution of M occurs at local anode formed at site of a pore in protective oxide layer. Reaction with cathodically generated OH ions re-seals the oxide layer by: $M^{2+} + 2OH^- \rightarrow MO + H_2O$.

potential than ion, give rise to local cells in which the exposed, more base, metal becomes the anode and the erstwhile protective layer the cathode. This is a problem which can develop with tin plate as used in the canning industry; development of holes in the tin layer leads to the formation of a corrosion cell *between* the tin layer and the exposed iron at the bottom of the hole, a situation shown in Figure 11.5.

If the protective layer is of a less noble metal, such as is the arrangement in galvanized objects and other situations where zinc prevents ion from corroding, zinc becomes the anode and iron the cathode so that the status of the iron is preserved (Figure 11.6). This encouragement of an alternative corrosion process to the one causing harm is known as 'cathodic protection' and is employed extensively in the protection of metals in marine use and in pipelines.

Oxide layers formed by some metals in the atmosphere are most useful if they are physically tough and damage resistant. In any case, if damage should occur, the protective layer rapidly reforms. Thicker coatings may be obtained by anodizing, i.e. by anodically polarizing the material by electrolysis with some cathode in a suitable electrolyte.

Inhibiting reactions form an important part of corrosion prevention.

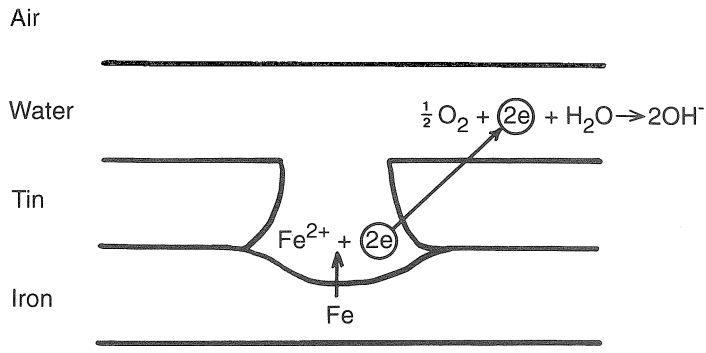

Figure 11.5 Corrosion of iron through hole in tinplate: a corrosion cell forms between the tin layer and the iron exposed at the bottom of the hole.

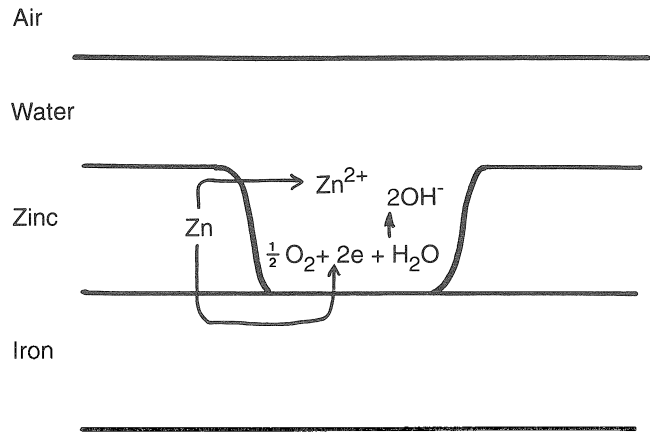

Figure 11.6 Corrosion of iron prevented by coating with a layer of less noble metal such as zinc.

Any material which inhibits, either partially or completely, the initial reaction at local anodes and cathodes comes within this category. Anodic inhibitors are species which can complex with anodically formed metal ions to produce protective layers. It is, however, vital that such species should be present in sufficient concentration to give protection at all local anodes, otherwise corrosion at a relatively few unprotected sites will cause extreme damage. Cathodic inhibitors increase the discharge overvoltage of hydrogen ions or prevent the formation of molecular hydrogen from atoms.

11.2 Electrochemical processes as sources of energy

Electrical energy may be produced through the operation of a chemical reaction taking place in a galvanic cell. The earliest, most rudimentary form of galvanic cell consisted of alternate sheets of copper and zinc separated by wet cloth. This arrangement subsequently gave rise, in a rather different form, to the Daniell cell.

Since we cannot normally expect to obtain reactions giving a free energy change of more than about 200 kJ per Faraday, application of $\Delta G = -nEF$ leads to the conclusion that about 2 V is the maximum emf obtainable from a simple cell. Higher voltages may, of course, be produced through appropriate banking of large numbers of cells.

There are three types of cell

1. *Primary cells*
   These are based upon reactions which are not reversible so that recharging is out of the question and once the cell reaction has proceeded to completion, the cell is discarded.
2. *Secondary cells*
   Such cells are based upon almost reversible electrode processes. All processes occurring during their discharge while used as a source of emf may to a large extent be reversed in the recharging process. The overall efficiency of the recharging reaction may be significantly reduced by side reactions.
3. *Fuel cells*
   In fuel cells an attempt is made to exploit to the fullest extent the *free energy* change of selected reactions to produce electrical energy. The functioning of fuel cells is fundamentally different to that of batteries: while the latter *store* electrical energy, fuel cells convert the energy of chemical processes *directly* into electricity.

11.2.1 Primary cells

As an example the Leclanché cell may be considered which may be represented as follows

$$\mathrm{Zn}|\mathrm{NH_4Cl},\underset{\uparrow}{\mathrm{ZnCl_2}}|\mathrm{MnO_2},\mathrm{C}$$

(forming a gel with starch)

Its construction is shown in Figure 11.7.

Such 'dry cells', with the electrolyte medium thickened by the use of suitable additives, may be used in any position without spillage. The reactions occurring in the cell are complex but the behaviour of the system may be largely explained in terms of the following:

At the anode

$$Zn \longrightarrow Zn^{2+} + 2e \ (E^{\ominus} = -0.76\,V)$$

At the cathode

$$MnO_2 + H_3O^+ + e \longrightarrow MnOOH + H_2O$$

followed by

$$2MnOOH \longrightarrow Mn_2O_3 + H_2O$$

Evolution of hydrogen gas at the cathode would be most undesirable and, in any case, would cause serious losses of energy. It is to prevent such an occurrence that the cathode is surrounded by manganese dioxide (the depolarizer), which discourages hydrogen formation by undergoing other reactions preferentially. The manganese dioxide proves to be more efficient in this respect when it contains lattice defects which may be artifically induced.

The Leclanché cell is irreversible, and therefore incapable of recharging, because of the occurrence of side reactions such as

$$OH^- + NH_4^+ \longrightarrow H_2O + NH_3$$

$$2NH_3 + Zn^{2+} + 2Cl^- \longrightarrow Zn(NH_3)_2Cl_2$$

(a sparingly soluble complex which forms a crystalline deposit)

$$Zn^{2+} + 2OH^- \longrightarrow ZnO + H_2O$$

The cell provides a cheap source of electrical energy with an emf of about 1.6 V, but since the cathode potential is a function of pH, this value falls rapidly on continuous discharge.

A more constant voltage is produced by the Ruben–Mallory cell in which a large excess of hydroxyl ions renders its operation less sensitive to pH change. This cell usually takes the form

$$Hg|HgO, KOH, Zn(OH)_2|Zn$$

Air or oxygen cells are modifications of the Leclanché cell in that the cathode is activated carbon in contact with atmospheric oxygen. Two forms are

$$Zn|NH_4Cl|C(O_2)$$

or

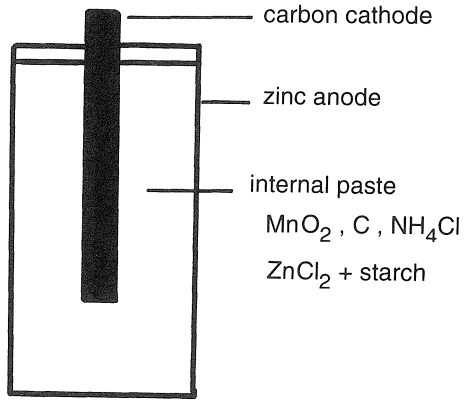

Figure 11.7 Components and their orientation within a Leclanché cell.

$$Zn|NaOH|C(O_2)$$

Such cells give maximum emf of about 1.5 V and have satisfactory voltage–time characteristics. Their major disadvantage is that they cannot be highly loaded due to the slow rate of oxygen polarization so that they operate most satisfactorily for very low currents or in intermittent use.

11.2.2 Secondary cells

The lead–acid battery is an example of a galvanic cell in which electrode processes are almost reversible. The action is based upon the pre-electrolysis of a solution of sulphuric acid saturated with lead sulphate between lead electrodes. Lead is deposited at the cathode, while Pb^{2+} ions are oxidized to the Pb^{4+} state at the anode. The Pb^{4+} ions are subsequently hydrolysed and deposited as PbO_2. In practice the electrodes are usually in the form of grids of a lead/antimony alloy (for mechanical strength) filled with a paste of red lead and litharge in sulphuric acid. As initially constructed, therefore, the system corresponds to the situation existing in the fully discharged cell.

During preliminary charging the electrode used as anode forms porous PbO_2; that used as the cathode forms spongy lead. During the subsequent discharge process, where the polarity is reversed and in which the cell acts spontaneously, the following reactions occur:

At the Pb anode

$$Pb + SO_4^{2-} \longrightarrow PbSO_4 + 2e$$

At the PbO_2 *cathode*

$$\text{(i)}\ PbO_2 + 4H^+ \longrightarrow Pb^{4+} + 2H_2O$$
$$\text{(ii)}\ Pb^{4+} + 2e \longrightarrow Pb^{2+}$$
$$\text{(iii)}\ Pb^{2+} + SO_4^{2-} \longrightarrow PbSO_4$$

Overall

$$Pb + PbO_2 + 2SO_4^{2-} + 4H^+ \underset{\text{charge}}{\overset{\text{discharge}}{\rightleftharpoons}} 2PbSO_4 + 2H_2O$$

The potential of the PbO_2 electrode, from a consideration of the electrochemical step (ii), is given by

$$E_{PbO_2} = E^{\ominus}_{Pb^{4+}/Pb^{2+}} + \frac{RT}{2F} \ln \frac{a_{Pb^{4+}}}{a_{Pb^{2+}}} \tag{11.1}$$

but, since $a_{Pb^{4+}} \sim a_{Pb^{2+}}$, and both are very small since the solution is saturated with PbO_2 and $PbSO_4$,

$$E \sim E^{\ominus}_{Pb^{4+}/Pb^{2+}} \sim +1.70\,V$$

The potential of the lead electrode is given by

$$E_{Pb} = E^{\ominus}_{Pb^{2+}/Pb} + \frac{RT}{2F} \ln a_{Pb^{2+}} \sim -0.28\,V \tag{11.2}$$

Therefore, the cell emf $\sim 1.70 - (-0.28) = +1.98$ V.

Charging and discharging curves for a lead accumulator are shown in Figure 11.8 from which it is evident that the processes are not completely reversible. Mixed potentials occurring at the electrodes cause them to corrode and give rise to 'spontaneous discharge', so that, even when no current is being drawn from the cell, the following (irreversible) reactions occur.

At the Pb electrode

$$Pb + 2H^+ \longrightarrow Pb^{2+} + H_2$$

Consideration of this reaction stresses the importance of eliminating any metal which has a lower hydrogen overvoltage than lead. Even traces of such metals will 'poison' the battery beyond repair.

At the PbO_2 *electrode*

$$PbO_2 + Pb + 2H_2SO_4 \longrightarrow 2PbSO_4 + 2H_2O$$

This constitutes attack of the lead supporting the effective electrode material. The sulphate deposit from both this spontaneous discharge and from the normal discharge, coagulates with time and retards further electrode

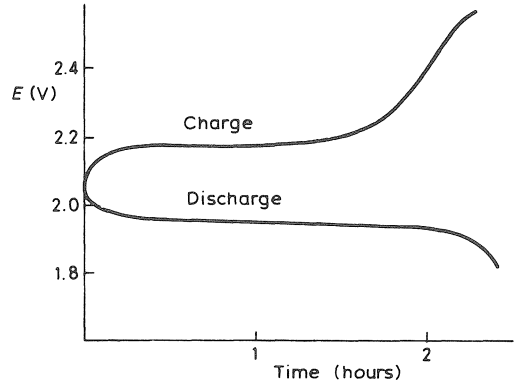

Figure 11.8 Constant current charging/discharging curves for the lead–acid battery.

processes—an effect known as 'sulphation'. Regular charging can reduce such effects to a minimum.

The efficiency of such cells may be expressed in two ways, current efficiency and energy efficiency.

Current efficiency (ε_I). This may be defined by

$$\varepsilon_I = \frac{\text{charge produced while discharging}}{\text{charge taken up during charging}}$$

The product of I (amps) and time (hours) at any point on the charging or discharging curve of Figure 11.8 gives the charge taken up or given out respectively in ampere hours. Thus,

$$\text{Current efficiency } \varepsilon_I = \frac{(It)_{\text{discharge}}}{(It)_{\text{charge}}} \tag{11.3}$$

which is about 95% for the lead acid cell.

Energy efficiency ε_U. This may be defined by

$$\varepsilon_U = \frac{\text{energy given out during discharge}}{\text{energy taken up while charging}}$$

$$= \frac{E_{\text{discharge}} \times (It)_{\text{discharge}}}{E_{\text{charge}} \times (It)_{\text{charge}}} \tag{11.4}$$

For the lead–acid battery this ratio is about 0.8. The voltage obtainable during discharge will be less than the reversible value, E_{rev}, by overvoltage and IR corrections, thus

$$E_{\text{discharge}} = E_{\text{rev}} - \eta - IR \tag{11.5}$$

η collecting both activation and concentration overvoltage effects. Conversely the voltage required for charging is in excess of E_{rev} according to

$$E_{charge} = E_{rev} - \eta' - IR \tag{11.6}$$

η' again collecting overvoltages.

It is seen therefore that the current and energy efficiencies are related through the expression

$$\varepsilon_U = \left(\frac{E_{dis} - \eta - IR}{E_{ch} - \eta' - IR}\right)\varepsilon_I \tag{11.7}$$

Activation contributions to the overvoltage terms are small for this system, by far the larger part of both η and η' arising from concentration polarization effects. The two energies may be obtained from the areas under the respective curves, the difference between them being the energy loss.

Although the lead–acid cell has high current and energy efficiencies, it leaves much to be desired when considered in the more important practical terms of its energy output to weight ratio. While improved output-to-weight ratios may be obtained by using larger surface area grid plates, these are less strong mechanically and current surges are liable to break up the delicate PbO_2 and $PbSO_4$ deposits to cause sludging. It is often more economical to use more durable electrode components at the expense of some efficiency.

In the Edison alkaline battery, a 20% solution of potassium hydroxide is electrolysed between a cathode of iron/iron(II) hydroxide and an anode of nickel hydroxide. These electrode materials are pressed into perforated steel containers along with mercury and finely divided nickel at cathode and anode respectively to raise the conductivity (which is low for hydroxides). During the charging process the following reactions occur.

At the $Fe(OH)_2$ *electrode* (*cathode*)

$$Fe(OH)_2 + 2e \longrightarrow Fe + 2OH^-$$

At the $Ni(OH)_2$ *electrode* (*anode*)

$$Ni(OH)_2 + OH^- \longrightarrow NiOOH + H_2O + e$$

The overall charging/discharging reaction may therefore be written

$$2NiOOH + Fe + 2H_2O \underset{\text{charge}}{\overset{\text{discharge}}{\rightleftharpoons}} 2Ni(OH)_2 + Fe(OH)_2$$

Side reactions such as

$$2NiOOH + Ni(OH)_2 \longrightarrow Ni_3O_2(OH)_4$$

cause the process to be less reversible than those in the lead–acid cell, the current efficiency being about 80% and the energy efficiency about 60%. The emf produced initially is close to the reversible value of 1.4 V, but drops rapidly to a fairly steady 1.3 V.

The lead–acid cell has proved to have the best characteristics for the regular and routine use required in motor cars. With modern sealed units the hazards associated with the domestic handling of such cells have been largely eliminated. This was not always so and people of a certain age with a rural upbringing will remember the weekly recharge of the 'accumulator' for powering the 'wireless' in homes without an electricity supply! The more easily handled Leclanché cell is unfortunately not rechargeable but the nickel–cadmium battery offers both advantages and operates on the following processes:

At the anode

$$Cd + 2H_2O \longrightarrow Cd(OH)_2 + 2H^+ + 2e$$

At the cathode

$$2NiOOH + 2H^+ + 2e \longrightarrow 2Ni(OH)_2$$

The overall process therefore is

$$Cd + 2NiOOH + 2H_2O \underset{\text{charge}}{\overset{\text{discharge}}{\rightleftharpoons}} Cd(OH)_2 + 2Ni(OH)_2$$

The apparent attractiveness of systems based upon more electropositive metals, such as those of the alkali group, coupled with the more electronegative non-metallic elements is rarely a straightforward matter to exploit. Quite apart from the reactivity of many of the materials, the complications of some systems are almost overwhelming; even so, some remarkably difficult ones have been made workable. The sodium–sulphur cell, although electrochemically simple and rechargeable works on the electrode reactions

$$2Na \longrightarrow 2Na^+ + 2e$$
$$S + 2e \longrightarrow S^{2-}$$

Overall

$$2Na + S \rightleftharpoons Na_2S$$

The electrolyte medium is solid alumina, and since an inert atmosphere of argon has to be used the cell requires careful sealing. Added to these factors the cell will only operate effectively at temperatures of the order of 300–400°C and the highly corrosive environment requires a mild steel container lined with chromium. It is hardly a suitable system for domestic purposes but has seen some pilot application for commercial traction purposes.

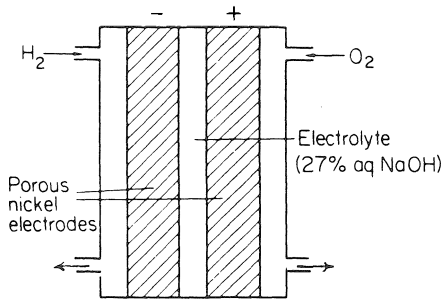

Figure 11.9 The Bacon hydrogen/oxygen fuel cell.

There is considerable current interest in aluminium as an electrode material and a rather unique combination of aluminium anode with air cathode has resulted in a cell which is rechargeable by mechanical rather than by electrochemical means. Electrode and overall reactions are

$$Al \longrightarrow Al^{3+} + 3e$$

$$\tfrac{3}{4}O_2 + \tfrac{3}{2}H_2O + 3e \longrightarrow 3OH^-$$

Overall

$$Al + \tfrac{3}{4}O_2 + \tfrac{3}{2}H_2O \rightleftharpoons Al(OH)_3$$

The electrolyte medium may be either sodium chloride ('saline') or sodium hydroxide ('alkaline').

Since the gelatinous aluminium hydroxide tends to adhere to the electrodes and cell walls and inhibit the reactions, it is necessary to agitate the solution to encourage precipitation. Removal of water from the electrolyte implied from the cell reaction means that this requires replenishing periodically along with the aluminium anode which dissolves. The recharging is thus effectively replacement of both the anode material and water; the aluminium lost in the discharge process may, however, be regenerated from the precipitated hydroxide.

11.2.3 Fuel cells

A fuel cell is based on the reversal of cause and effect of an electrolytic process and *generates a voltage* by supplying the products to appropriately constructed electrodes. The arrangement of components in the Bacon hydrogen/oxygen fuel cell is shown in Figure 11.9. Operation of the cell depends upon the following processes

$$2H_2 \longrightarrow 4H^+ + 4e;\ O_2 + 4H^+ + 4e \longrightarrow 2H_2O \text{ (in acid)}$$

or

$$2H_2 + 4OH^- \longrightarrow 4H_2O + 4e;\ O_2 + H_2O + 4e \longrightarrow 4OH^- \text{ (in alkali)}$$

The overall reaction is the production of water for both cases

$$2H_2 + O_2 \longrightarrow 2H_2O$$

For this reaction as written, tabulated thermodynamic data suggest the following values for free energy and enthalpy functions

$$\Delta G^{\ominus} \sim 476\,\text{kJ}$$

and

$$\Delta H^{\ominus} \sim 484\,\text{kJ}$$

From the first value it is clear that the theoretical voltage which could be developed follows from $\Delta G^{\ominus} = -nE_{eq}F$ as

$$E_{eq} = \frac{-476\,000}{-4 \times 96\,500} = 1.23\,\text{V}$$

In practice, voltages of the order of 1.0 to 1.1 V are obtained, which implies an efficiency of about 80%.

Another, more fundamental way of viewing the efficiency (ε) is in terms of the thermodynamics of the process as

$$\varepsilon = \frac{\Delta G}{\Delta H} = \frac{476}{484} \times 100 \sim 98\%$$

which is impressively high.

Indeed, when written in terms of the temperature coefficient of the cell voltage (see equation (8.17))

$$\varepsilon = \frac{E}{E - T\left(\dfrac{\partial E}{\partial T}\right)_P}$$

which implies that for a cell with a *positive* temperature coefficient, $\varepsilon >$ 100%!

Such a state of affairs cannot be realized because of the unavoidable overvoltage effects. Even so at a maximum these are likely to reduce the efficiencies by no more than 30%. Thus, for the case concerned, at least 68% efficiency should be realizable.

Combustion processes, and therefore all mechanical devices dependent for their operation upon them, are *intrinsically* of much lower efficiency. This is because the two types of process are *fundamentally* different: while the voltage of a fuel cell is directly dependent on ΔG of the reaction upon which it functions, the output of a heat engine depends on the *heat evolved* when the chosen fuel is *burnt*, i.e. $-\Delta H$, the enthalpy change for the combustion process. Now the efficiency of even an ideal heat engine is given in terms of the heat (Q_2) taken in at a higher temperature (T_2) and that given out (Q_1) at a lower temperature (T_1) as

$$\frac{Q_2 - Q_1}{Q_2} \tag{11.8}$$

and, since

$$\frac{Q_2}{T_2} = \frac{Q_1}{T_1} \qquad \text{(from the definition of entropy)}$$

it follows that

$$\varepsilon = \frac{T_2 - T_1}{T_2} \tag{11.9}$$

The value of this quantity might typically be 30%, which implies that 70% is lost through the thermodynamic nature of the proces—the so-called Carnot losses. Add to this the additional likely 15% loss due to the frictional effects of the engine and the final resultant efficiency could well be as low as 15%. This simple balance sheet approach brings home the likely advantages to be gained by developing fuel cell systems.

For an efficient cell, all processes must occur rapidly. Reactants must be able to reach the electrodes easily so that porous electrodes with large internal surface areas, saturated with electrolyte, are used. The pore sizes are often graded from large on the gas side of an electrode to small on the electrolyte side. Good catalyst materials ensure rapid electrochemical reactions and, in combination with a higher temperature, help to suppress the cathodic formation of perhydroxyl ions by the reaction.

$$O_2 + 4H_2O + 6e \longrightarrow 4OH^- + 2OH_2^-$$

With such precautions the hydrogen/oxygen cell can be made to show efficiencies of up to 75%. A Bacon-type cell has been successfully employed in space projects where the water produced (at the rate of about a pint per kilowatt-hour) is used to supplement the water supply.

Many other fuel cell systems have been devised with varying degrees of success. Provided that certain inherent difficulties can be overcome, a wide variety of designs and modes of operation could become available for specific purposes. Their use for traction purposes to replace engines with high

pollution risk is a major attraction. At the other extreme artificial hearts, powered by fuel cells consuming food fuels, have been suggested as a further possibility.

At present, a great drawback is that while the attractive prospect of the use of cheap fuels such as hydrocarbons presents itself, difficulties are encountered in practice by the poisoning of catalytic surfaces by intermediates.

11.3 Electrocatalysis and electrosynthesis

Inert electrodes which enable electron transfer between them and species in solution to take place at rates which are dependent upon the magnitudes of imposed electric fields, come within the classical definition of a catalyst. Rates of electron-transfer reactions are a function of both the electrode material and the applied potential but the electrode remains unchanged—a phenomenon known as *electrocatalysis*.

While in a broad sense, all such processes may be classed as heterogeneous, the term in this context is generally reserved for the more overtly heterogeneous character of reactions undergone by species during their adsorption on an electrode surface. This is a particularly common effect with organic compounds. The interplay of the adsorption and electron-transfer processes is a subtle one, the former being largely a function of the nature of the electrode surface, the latter of the potential that it has imposed upon it. Voltammetric/polarographic curves allow the study, albeit on a very small scale, of adsorption effects and indicate the properties and conditions required for scale-up synthetic applications.

The Arrhenius equation for the rate (current) of a heterogeneous electrochemical reaction whose overall activation energy comprises contributions of a chemical ($\Delta G^{\ddagger}_{\text{chem}}$), an adsorption ($\Delta G^{\ddagger}_{\text{ads}}$) and an overpotential ($\alpha\eta F$) kind may be written as

$$I = (\text{constant}) \left[-\frac{\Delta G^{\ddagger}_{\text{chem}} + \Delta G^{\ddagger}_{\text{ads}} - \alpha\eta F}{RT} \right] \tag{11.10}$$

Equation (11.10) emphasizes the significance of the magnitude of the $\Delta G^{\ddagger}_{\text{ads}}$ term on the rate; even more significant is the powerful control that η exerts on the reaction for it if becomes of such a magnitude that

$$\eta = \left[\frac{\Delta G^{\ddagger}_{\text{chem}} + \Delta G^{\ddagger}_{\text{ads}}}{\alpha F} \right] \tag{11.11}$$

the reaction takes place with effectively zero activation energy.

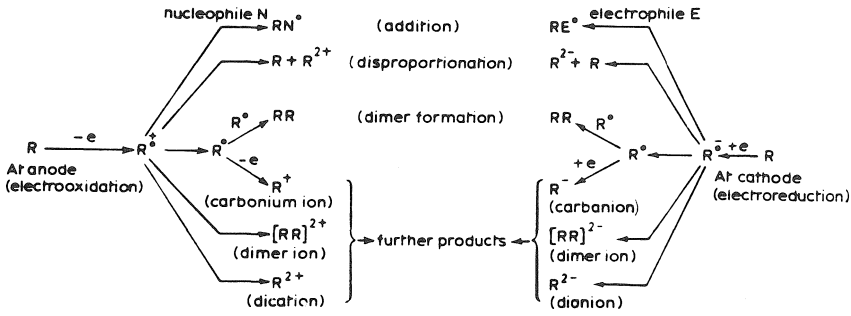

Figure 11.10 The main electro-organic reaction routes.

Electrochemical properties of different surface structures, even of the same material, can be quite distinct; indeed the nature of electrode surfaces may change during the course of electrolysis even to the extent of losing their effectiveness and showing passivity. Insulating oxide layers are not an uncommon feature at anodes and such (usually undesirable) effects may be reversed by a variety of mechanical and chemical methods.

Platinum has proved to be a versatile electrocatalyst; this versatility owes as much to its chemical and electrochemical stability as to its catalytic properties. It is possible, for instance, to oxidize ethene to carbon dioxide in a multistage process for which the rate-determining step is the reaction between adsorbed C_2H_4 and OH^-. The affinity of platinum for species of this sort is such that, while the bonding is of sufficient strength and duration to provide adequate opportunity for adsorbed species to react, it is not so overpowering as to prevent products removing themselves. Other noble metals such as osmium and iridium are often inferior to platinum for this reason.

Almost every kind of organic reaction may, in principle, be initiated electrochemically and, although this has been known for a very long while, it is only comparatively recently that electro-organic synthesis has emerged as a more general discipline from a somewhat empirical background. A major problem is that there are so many variables which, without fine tuning, give rise to alternative products. Variations of the electrode materials, solvent, electrolyte, pH and applied voltage can significantly alter the nature and/or proportions of products. While voltammetric methods may be used on a small scale to identify appropriate conditions, a major problem is to scale up laboratory experiments to arrangements of pilot and industrial size. Solvents themselves can cause something of a problem since those which offer ready solubility to species which must be used are often of low conductivity and mixed aqueous/non-aqueous media and the addition of supporting electrolytes may sometimes be necessary. Some idea of the

range of electrochemically promoted organic reactions, when R is an appropriate starting material, may be gained by scrutiny of Figure 11.10.

One example each of anodically and cathodically initiated processes will be considered briefly.

11.3.1 Anodically initiated process

The Kolbe reaction, based upon carboxylic acids, may be used to prepare a variety of products via both radical and carbonium ion mechanisms. Both the mechanism which operates and the products which result are dependent on the electrode material, the concentration of acid and the pH of the dispersive medium. A platinum anode favours a two-electron formation of radicals followed by dimerization—the classical Kolbe hydrocarbon chain extension, i.e.

$$2RCOO^- \xrightarrow{-2e} 2CO_2 + 2R^\bullet$$
$$2R^\bullet \longrightarrow RR$$

With carbon anodes, carbonium ions are formed which can, in the presence of other species, lead to a wide variety of products including alcohols, alkenes, esters, ethers and ketones.

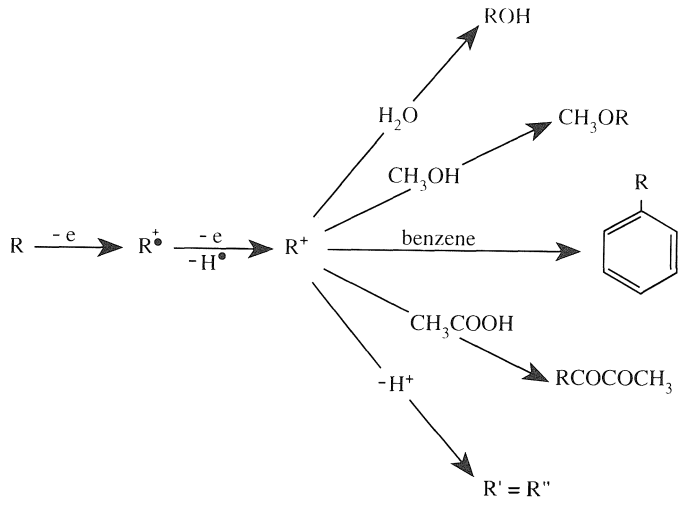

11.3.2 Cathodically initiated process

At present the largest electro-organic synthesis in the world is that of adiponitrile by the hydrodimerization of acrylonitrile which overall may be expressed by

$$2CH_2{=}CHCN + 2e + 2H^+ \longrightarrow NCCH_2CH_2CH_2CH_2CN$$

The low solubility of acrylonitrile in water alone necessitates the use of 30% tetraethylammonium *p*-toluene sulphonate in water; this not only improves the solubility of the reactant but provides the all-important high conductivity. If the pH is not strictly controlled to the range 7.5 to 9.5, side reactions become significant. In any case, the best yield of adiponitrile is some 90% the remainder being propionitrile. The balance of products may be completely altered if the quaternary ammonium salt is replaced by an alkali metal salt, the major product then being propionitrile.

11.4 Electrochemistry on an industrial scale

Electrochemical principles are used so widely on an industrial scale that for the present purposes it is necessary to be very selective in deciding on representative examples.

Where industry has a choice between electrochemical or other means to a commercial end, cheapness of the electricity supply will do much to influence the decision made. This is seen particularly in the range of methods used for the extraction of metals from their ores, although there are a number of instances such as those of aluminium and magnesium where there is little choice but to use electrochemistry.

A long-established application of the processes of electrodeposition is to be found in the electroplating industry. The nature and quality of an electrodeposit is strongly dependent upon the choice of conditions and the addition of certain materials (often strongly surface active organic species) known as 'brighteners'. Even nowadays the production of high-quality plated finishes is something of an art rather than the application of an understood science, the choice of many working conditions and materials being largely empirical. With the development of conducting paints which can key satisfactorily to plastic surfaces, it is now possible to electroplate metal finishes on to these materials.

The deposition process may be logically extended to the application of electroforming in which often intricate metal components may be made via deposition upon a cathode of appropriate shape and material. It is even possible to co-deposit more than one metal at a time to produce electrochemically formed alloys. In another context, careful control of the potentials of electrodes in large scale electrolyses forms the basis of electrorefining and separation processes.

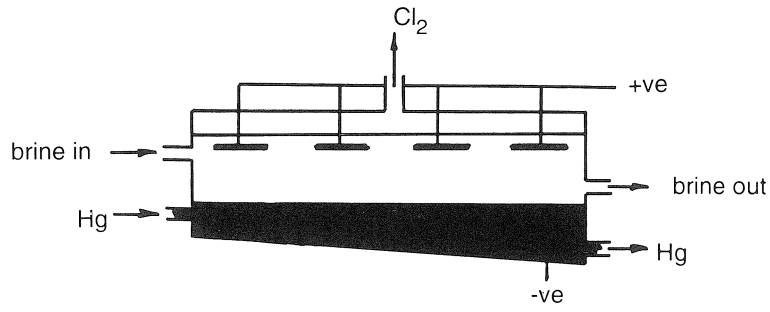

Figure 11.11 Flow system for electrolysis of brine between carbon anodes and mercury cathode. The foundation of the 'chlor-alkali' industry.

The reverse dissolution reactions at anodically polarized electrodes have been developed into the technologies of electropolishing and electromachining. Anodic dissolution of a thin layer of metal from the bulk often leaves a finish comparable in appearance to one which has been mechanically polished—but considerably more easily and cheaply and often of longer durability. Electrochemical 'drilling' of holes in metal components by such means, using a precision-operated controllable cathode, can be as rapid as any conventional power tool and may be performed with considerable accuracy.

To complement the earlier consideration of the world's largest electroorganic synthesis, it seems appropriate to briefly review the development of the world's largest scale electrolytic process. This is the electrolysis of brine to give chlorine and caustic soda and constitutes the 'chlor-alkali' industry.

Traditionally mercury was used as the cathode, making use of the high hydrogen overvoltage so that sodium was discharged in preference to hydrogen. With a carbon or graphite anode the two electrode reactions were

At the anode

$$2Cl^- \longrightarrow Cl_2 + 2e$$

At the cathode

$$2Na^+ + 2e + 2Hg \longrightarrow 2NaHg\,(\text{as amalgam})$$

Based on a flow system (Figure 11.11), the amalgamated mercury on treatment with water produced caustic soda after which the regenerated mercury was recycled. This system raised considerable technical and environmental problems. On the one hand, the continuous destruction of the anodes required continuous adjustment to retain their position relative to the liquid

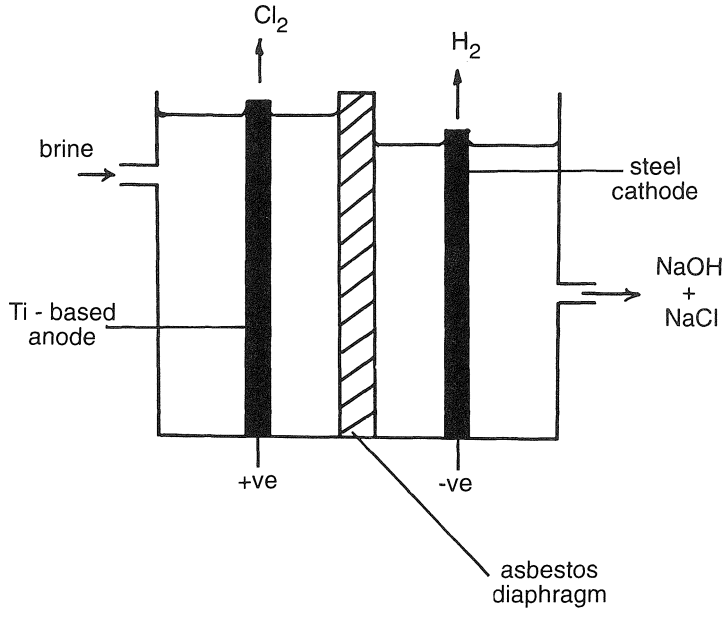

Figure 11.12 Principle of the diaphragm cell: generation of hydrogen at the cathode by $2H_2O + 2e \rightleftharpoons H_2 + 2OH^-$ produces dilute NaOH directly.

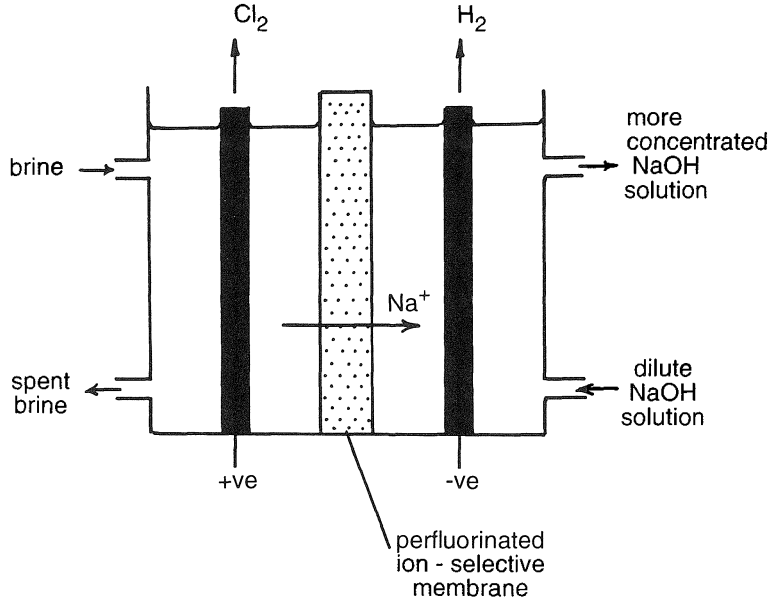

Figure 11.13 Principle of modern membrane cell for the electrolysis of brine.

cathode; on the other hand, the toxicity of mercury led to the development of arrangements involving alternative cathode materials.

Electrolysis between a steel cathode and a titanium-based anode generates chlorine and hydrogen. Caustic soda is effectively produced directly in the cathode region: this caustic solution must be prevented from mixing with that from the anode region where interaction of NaOH and Cl_2 would produce hypocholorite and chlorate. This may be achieved by separating the two regions by an asbestos diaphragm. The schematic arrangement of the *diaphragm cell* is shown in Figure 11.12.

There are a number of advantages offered by the diaphragm cell: the use of mercury is avoided, the applied voltage required is about 3.5 V (about 1V less than that needed for the mercury cell) and the anodes are 'dimensionally stable'. These are offset by the fact that the solution of sodium hydroxide produced is rather dilute (10–12%) and requires concentration. The additional cost of the associated evaporation process makes the two methods economically comparable.

The more modern *membrane cell* has the purely physical barrier between anode and cathode compartments replaced by an ion-selective membrane. Na^+ ions may cross the perfluorinated membrane but there is no flow of solution *between* the compartments (Figure 11.13). A significantly stronger solution of caustic soda is produced—of the order of 40%.

Problems

11.1 The zinc chloride battery, operating on the reaction $Zn + Cl_2 \rightarrow ZnCl_2$, has possibilities for exploitation as a source of power for driving vehicles in that a bank of 118 such cells, connected in series, has a capacity of approximately 90 kWh. Calculate (i) the standard emf of the cell, (ii) the mass of solid chlorine hydrate ($Cl_{12}.8 \quad H_2O$) which must be stored in the bank in order to sustain power capacity.

11.2 The following reactions may be made to operate in fuel cells at 298 K

$$CH_4(g) + 2O_2(g) = CO_2(g) + 2 \quad H_2O(l)$$
$$\Delta H^{\ominus}_{298} = -890.4\ \text{kJ mol}^{-1}; \qquad \Delta G^{\ominus}_{298} = -818.0\ \text{kJ mol}^{-1}$$
$$C_2H_6(g) + \tfrac{7}{2}O_2(g) = 2CO_2(g) + 3 \quad H_2O(l)$$
$$\Delta H^{\ominus}_{298} = -1560\ \text{kJ mol}^{-1}; \qquad \Delta G^{\ominus}_{298} = -1467.5\ \text{kJ mol}^{-1}$$
$$C_3H_8(g) + 5O_2(g) = 3CO_2(g) + 5 \quad H_2O(l)$$
$$\Delta H^{\ominus}_{298} = -2220\ \text{kJ mol}^{-1}; \qquad \Delta G^{\ominus}_{298} = -2108.0\ \text{kJ mol}^{-1}$$
$$CH_3OH(l) + \tfrac{3}{2}O_2(g) = CO_2(g) + 2 \quad H_2O(l)$$
$$\Delta H^{\ominus}_{298} = -764.0\ \text{kJ mol}^{-1}; \qquad \Delta G^{\ominus}_{298} = -706.9\ \text{kJ mol}^{-1}$$

For each case calculate (i) the number of electrons transferred overall in the cell reaction, (ii) the reversible emf of the cell at 298 K, (iii) the maximum efficiency of the cell.

Further reading

Chapter 1 (and general coverage)

Bockris, J.O'M. and Drazic, D.M. (1972) *Electrochemical Science*, Taylor and Francis, London.
Bockris, J.O'M. and Khan, S.U.M. (1979) *Quantum Electrochemistry*, Plenum Press, New York and London.
Bockris, J.O'M. and Reddy, A.K.N. (1973) *Modern Electrochemistry*, Plenum Press, New York.
Brett, C.M.A. and Brett, A.M.O.B. (1993) *Electrochemistry: Principles, Methods and Applications*, Oxford University Press, Oxford.
Goodisman, J. (1987) *Electrochemistry: Theoretical Foundations*, Wiley-Interscience, New York.
Hibbert, D.B. (1993) *Introduction to Electrochemistry*, Macmillan, Basingstoke and London.
Koryta, J. (1987) *Principles of Electrochemistry*, Wiley, Chichester.
Koryta, J., Dvorak, J. and Kavan, L. (1993) *Principles of Electrochemistry*, 2nd edn., Wiley, New York.

Chapter 2

Davies, C.W. (1962) *Ion Association*, Butterworths, London.
Robinson, R.A. and Stokes, R.H. (1959) *Electrolyte Solutions*, 2nd edn., Butterworths, London.

Chapter 3

Gurney, R.W. (1967) *Ionic Processes in Solution*, McGraw-Hill, London.
Prue, J.E. (1966) *Ionic Equilibria*, Pergamon Press, Oxford.
Rossotti, H. (1978) *The Study of Ionic Equilibria*, Longmans, London.

Chapter 4

Robbins, J. (1972) *Ions in Solution 2*. Clarendon Press, Oxford.
Selley, N.J. (1977) *Experimental Approach to Electrochemistry*, Edward Arnold, London.

Chapter 5

Delahay, P. (1965) *Double Layer and Electrode Kinetics*, Wiley-Interscience, New York.
Parsons, R. (1961) Structure of the electrical double layer and its influence on the rates of electrode reactions. In *Advances in Electrochemistry and Electrochemical Engineering*, Vol. 1 (Eds H. Gerischer and C.W. Tobias), Interscience, New York.
Sparnay, M.J. (1972) *The Electrical Double Layer*, Pergamon Press, Oxford.

Chapter 6

Ives, D.J.G. and Janz, G.I. (1961) *Reference Electrodes*, Academic Press, New York.
Koryta, J. (1991) *Ions, Electrodes and Membranes*, Wiley, Chichester.
Newman, J. (1973) *Electrochemical Systems*, Prentice-Hall, Englewood Cliffs, New Jersey.

Chapter 7

Albery, W.J. (1975) *Electrode Kinetics*, Clarendon Press, Oxford.
Bauer, H.H. (1972) *Electrodics*, Thieme, Stuttgart.
Brenet, J.P. and Traone, K. (1971) *Transfer Coefficients in Electrochemical Kinetics*, Academic Press, London.
Erdey-Gruz, T. (1972) *Kinetics of Electrode Processes*, Adam Hilger, London.
Fried, I. (1973) *The Chemistry of Electrode Processes*, Academic Press, London.
Hush, N.S. (1971) *Reactions of Molecules at Electrodes*, Wiley-Interscience, New York.
Pletcher, D. (1991) *A First Course in Electrode Processes*, The Electrochemical Consultancy, Romsey.
Thirsk, H.R. and Harrison, J.A. (1972) *A Guide to the Study of Electrode Kinetics*, Academic Press, London.

Chapter 8

Sawyer, D.T. and Roberts, J.L. (1974) *Experimental Electrochemistry for Chemists*, Wiley, New York.
Yaeger, E. and Salkind, A.J. (Eds) *Techniques of Electrochemistry*, Vol. I (1972), Vol. II (1973), Wiley-Interscience, New York.

Chapter 9

Adams, R.N. (1969) *Electrochemistry at Solid Electrodes*, Dekker, New York.
Albery, W.J. and Hitchman, M.L. (1971) *Ring–Disc Electrodes*, Oxford University Press, Oxford.
Bard, A.J. and Faulkner, L.R. (1980) *Electrochemical Methods, Fundamentals and Applications*, Wiley, New York.
Crow, D.R. (1969) *Polarography of Metal Complexes*, Academic Press, London.
Crow, D.R. (1986) Voltammetry. In *Metals Handbook, Materials Characterization*, Vol. 10, 9th edn. ASM International, Materials Park, Ohio.
Franklin Smyth, W. (1992) *Voltammetric Determination of Molecules of Biological Significance*, Wiley, Chichester.
Galus, Z. (1976) *Fundamentals of Electrochemical Analysis*, Ellis Horwood, Chichester.
Riley, T. and Tomlinson, C. (1987) *Principles of Electroanalytical Methods*, ACOL/Wiley, Chichester.
Southampton Electrochemistry Group (1985) *New Instrumental Methods in Electrochemistry*, Ellis Horwood, Chichester.

Chapter 10

Ammann, D. (1986) *Ion-Selective Microelectrodes*, Springer-Verlag, Berlin.
Covington, A.K. (1979) *Ion-Selective Electrode Methodology*, Vols I and II, CRC Press, Boca Raton, Florida.
Edmonds, T.E. (1988) *Chemical Sensors*, Blackie, London.
Evans, A. (1987) *Potentiometry and Ion-Selective Electrodes*, Wiley, New York.

Chapter 11

Baizer, M.M. and Lund, H. (1991) *Organic Electrochemistry*, Dekker, New York.
Fry, A.J. (1989) *Synthetic Organic Electrochemistry*, Wiley, New York.
Hine, F. (1985) *Electrode Processes and Electrochemical Engineering*, Plenum Press, New York.
Kyriacou, D.K. (1981) *Basics of Electroorganic Synthesis*, Wiley, New York.
McDougall, A. (1976) *Fuel Cells*, Macmillan, London.

Pletcher, D. and Walker, F.C. (1990) *Industrial Electrochemistry*, Chapman and Hall, London.
Shono, T. (1990) *Electroorganic Synthesis*, Academic Press, New York.
Wrangler, G. (1985) *Introduction to Corrosion and Protection of Metals*, Chapman and Hall, London.

Solutions to problems

Chapter 2

2.1 According to equation (2.13)

$$\kappa = \left(\frac{2 \times 10^3 \epsilon^2 N}{\varepsilon_0 \varepsilon k T}\right)^{1/2} \sqrt{I} = 0.503 \times 10^{12} \sqrt{\frac{I}{\varepsilon T}}$$

therefore radius $= 1/\kappa = (1.988 \times 10^{-12})\sqrt{\varepsilon T/I}$ for $1/\kappa$ in m.
(i) for 1:1 electrolyte in water at 298 K the following values are obtained:

I (mol kg^{-1})	0.1	0.01	0.001	0.0001
$1/\kappa$ (nm)	0.96	3.04	9.62	30.41

(ii) for 1:2 electrolyte in water at 298 K the following values arise:

I (mol kg^{-1})	0.3	0.03	0.003	0.0003
$1/\kappa$ (nm)	0.55	1.76	5.55	17.58

Corresponding values in DMF are:

(i)	0.66	2.08	6.57	20.79
(ii)	0.38	1.20	3.80	12.00

2.2 By equation (2.14)

$$I = \tfrac{1}{2}\sum m_i z_i^2 = \tfrac{1}{2}[(1 \times 0.0015 \times 2^2) + (2 \times 0.0015 \times 1^2)]$$

$$= 0.0045 \text{ mol kg}^{-1}.$$

(i) $\gamma_{Mg^{2+}} = 0.730$; $\gamma_{Cl^-} = 0.924$;
(ii) $\gamma_\pm = 0.854$. This may be obtained either from the individual activity coefficients using equation (2.7) or by the limiting law expression for $\log \gamma_\pm$ given in equation (2.17).

2.3 (i) $I = \tfrac{1}{2}[(1 \times 0.001 \times 3^2) + (3 \times 0.001 \times 1^2)] = 0.006 \text{ mol kg}^{-1}$
(ii) $I = \tfrac{1}{2}[(1 \times 0.001 \times 3^2) + (3 \times 0.001 \times 1^2)$
$+(1 \times 0.002 \times 1^2) + (1 \times 0.002 \times 1^2)] = 0.008 \text{ mol kg}^{-1}$

2.4 (i) $\gamma_\pm = 0.761$ for $I = 0.006$ mol kg^{-1}
$\gamma_\pm = 0.730$ for $I = 0.008$ mol kg^{-1}
(ii) $\gamma_\pm = 0.776$ for $I = 0.006$ mol kg^{-1}
$\gamma_\pm = 0.749$ for $I = 0.008$ mol kg^{-1}

$$2.5\ B = \left(\frac{2 \times 10^3 N^2 \epsilon^2}{\varepsilon_0 \varepsilon RT}\right)^{1/2}$$

$$= \left[\frac{2 \times 10^3 \times (6.023 \times 10^{23})^2 \times (1.6021 \times 10^{-19})^2}{8.8542 \times 10^{-12} \times 78.54 \times 8.314 \times 298}\right]^{1/2}$$

$$= 3.288 \times 10^9 \text{m}^{-1}\text{mol}^{-1/2}\,\text{kg}^{1/2}$$

$$A = \left[\frac{\epsilon^2 N}{2.303RT \times 8\pi\varepsilon_0\varepsilon}\right] B$$

$$= \left[\frac{(1.6021 \times 10^{-19})^2 \times 6.023 \times 10^{23}}{2.303 \times 8.314 \times 298 \times 8 \times 3.142 \times 8.8542 \times 10^{-12} \times 78.54}\right] \times 3.288 \times 10^9$$

$$= 0.509\ \text{mol}^{-1/2}\,\text{kg}^{1/2}$$

2.6 Use the Debye-Hückel equation in the form of equation (2.18), viz.

$$-\frac{A\,|z_+ + z_-|\,\sqrt{I}}{\log \gamma_\pm} = 1 + Ba\sqrt{I}$$

and plot values of LHS versus $\sqrt{I}$ to give slope = Ba and intercept = 1. Slope = 1.40 mol kg^{-1} which, with $B = 3.29 \times 10^9$ m^{-1}mol$^{-1/2}$ kg$^{1/2}$, gives $a = 0.43$nm.

2.7 Application of equation (2.20), $q = z_i z_j \epsilon^2 / 8\pi\varepsilon_0\varepsilon kT$ yields $q = 0.357$nm, 1.428 nm and 3.213 nm for the respective electrolyte types.

Chapter 3

3.1 (i) 3.00, (ii) 2.70, (iii) 11.30, (iv) 11.48, (v) 3.38, (vi) 10.78. Cases (i)–(iv) are strong acids or bases and allow direct assessment of $[H_3O^+]$ or $[OH^-]$. For case (v) consideration of weak acid dissociation equilibrium yields pH = $\frac{1}{2}(pK_a - \log C)$, while for case (vi) consideration of weak base dissociation equilibrium yields pOH = $\frac{1}{2}(pK_b - \log C)$.

3.2 From pH = $\frac{1}{2}(pK_a - \log C)$, $pK_a = 4.44$, whence pH of 0.15 mol dm^{-3} solution = 2.63.

3.3 From the Henderson–Hasselbalch equation (equation (3.50)) the required [salt] to [acid] ratio is 5.534. Therefore, since original number of moles of acid = 0.04.

$$\frac{\text{salt}}{\text{acid}} = 5.534 = \frac{\text{vol. of NaOH}}{\text{vol. of acid} - \text{vol. of NaOH}}$$

if vol. of NaOH = x, then $x/200 - x = 5.534$ giving $x = 169.4$ cm^3.

3.4 (i) pH = $\frac{1}{2}[pK_w - pK_b - \log C]$ (equation (3.43)) yields pH = 4.97;
(ii) pH = $\frac{1}{2}[pK_w + pK_a + \log C]$ (equation (3.41)) yields pH = 8.88;
(iii) pH = $\frac{1}{2}[pK_w + pK_a - pK_b]$ (equation (3.48)) yields pH = 7.01.

3.5 (i) pH = 4.94 (via equation (3.50)); (ii) pH = 9.55 (via equation (3.52)).

3.6 25 cm^3 of 0.15 mol dm^{-3} isopropylamine contain 0.00375 mol. 10 cm^3 of 0.12 mol dm^{-3} HCl contain 0.00120 mol, therefore amount of salt = 0.00120 mol and amount of base remaining = 0.00255 mol. Application of equation (3.52) gives pH = 10.30.

3.7 (i) 9.60, (ii) 10.19, (iii) 2.67, (iv) 2.09. pH values for (i) and (ii) are situated on either side of pK_{a2} and are given by equation (3.54) viz.

$$pH \sim pK_{a2} + \log \frac{[G^-]}{[G^\pm]}$$

pH values for (iii) and (iv) are situated on either side of pK_{a1} and are given by

$$pH \sim pK_{a1} + \log \frac{[G^\pm]}{[G^+]} \qquad \text{(see equation (3.53))}$$

3.8 Solution is 0.05 mol dm^{-3} in each component, with ionic strength given by

$$\begin{aligned} I &= \tfrac{1}{2}\{(C_{Na^+} \times 1^2) + (C_{H_2PO_4^-} \times 1^2) + (C_{HPO_4^{2-}} \times 2^2)\} \\ &= \tfrac{1}{2}\{(0.15 \times 1^2) + (0.05 \times 1^2) + (0.05 \times 2^2)\} \\ &= 0.2 \text{ mol dm}^{-3}. \end{aligned}$$

Second dissociation refers to $H_2PO_4^- \rightleftharpoons H^+ + HPO_4^{2-}$ therefore,

$$K_{a2} = \frac{a_{H^+} a_{HPO_4^{2-}}}{a_{H_2PO_4^-}} = \frac{a_{H^+} C_{HPO_4^{2-}} \gamma_{HPO_4^{2-}}}{C_{H_2PO_4^-} \gamma_{H_2PO_4^-}}$$

For equal concentrations of the two forms

$$K_{a2} = a_{H^+} \frac{\gamma_{HPO_4^{2-}}}{\gamma_{H_2PO_4^-}}$$

γ values may be calculated from the extended Debye–Hückel expression to be $\gamma_{HPO_4^{2-}} = 0.2349$ and $\gamma_{HPO_4^-} = 0.6968$ giving $a_{H^+} = 1.881 \times 10^{-7}$ and pH = 6.73.

3.9 (i) $pH \cong \frac{1}{2}(pK_a + 1) = 2.43$; (ii) $pH \cong 3.86 + \log(2.5)/(7.5) = 3.38$ (see equation (3.50)); (iii) $pH \approx pK_a = 3.86$; (iv) $pH \cong 3.86 + \log(7.5)/(2.5) = 4.16$ (see equation (3.50)); (v) $pH \cong \frac{1}{2}(14.00 + 3.86 - 1.301) = 8.28$ (see equation (3.41)); (vi) $[OH^-] = 0.001$ mol 30 cm^{-3}. i.e. 0.0033 mol dm^{-3}; pH = 12.52.

3.10 From $pH \cong \frac{1}{2}[(pK_w)_C + pK_a + \log C]$ (see equation (3.41))

$$(K_w)_C = 1.452 \times 10^{-14} = [H_3O^+][OH^-]$$

$$(K_w)_T = [H_3O^+][OH^-]\gamma_\pm^2; \gamma_\pm = 0.822$$

$$(K_w)_T = 1.452 \times 10^{-14}(0.676) = 0.982 \times 10^{-14}.$$

3.11 $pK_b = 3.911$; $\gamma_\pm = 0.813$. From equation (3.43)

$$pH \cong \tfrac{1}{2}[(pK_w)_C - pK_b - \log C]$$

$$(K_w)_C = 1.698 \times 10^{-15}; \; (K_w)_T = 1.122 \times 10^{-15}$$

The values stress the fairly strong temperature dependence of K_w.

Chapter 4

4.1 From data for KCl, cell constant $s = \kappa/G = 1.58\,\text{cm}^{-1}$.
From data for NaCl, $\kappa = 6.032 \times 10^{-4}\,\Omega^{-1}\,\text{cm}^{-1}$.
Therefore by equation (4.4c)

$$\Lambda = \frac{1000\kappa}{C} = \frac{0.6032}{0.005} = 120.6\,\Omega^{-1}\,\text{cm}^2\,\text{mol}^{-1}$$
$$= 1.206 \times 10^{-2}\,\Omega^{-1}\,\text{m}^2\,\text{mol}^{-1}.$$

4.2 From the Kohlrausch Law expressed by equation (4.9),

$$\Lambda_0 \text{ for propionic acid} = (0.8590 + 4.2126 - 1.2156) \times 10^{-2}\,\Omega^{-1}\,\text{m}^2\,\text{mol}^{-1}$$
$$= 3.856 \times 10^{-2}\,\Omega^{-1}\,\text{m}^2\,\text{mol}^{-1}.$$

4.3 (i) Use the Einstein equation, $D = \dfrac{uRT}{zF}$ (see equation (4.36))

thus $$D = \frac{6.4 \times 10^{-8}}{38.95} = 1.64 \times 10^{-9}\,\text{m}^2\,\text{s}^{-1}$$

(ii) Use the Nernst–Einstein equation, $\lambda = \dfrac{z^2F^2D}{RT}$ (see equation (4.24))

thus, $= 38.95 \times 96500 \times 1.64 \times 10^{-9} = 0.616 \times 10^{-2}\,\Omega^{-1}\,\text{m}^2\,\text{mol}^{-1}$

(iii) Use the Stokes–Einstein equation, $D = \dfrac{RT}{6\pi r\eta N}$ (see equation (4.38))

whence $r = 0.149\,\text{nm}$.

This is larger than the crystallographic value and is a partial reflection of the effects of solvation.

Chapter 5

5.1 $I = 0.003\,\text{mol dm}^{-3}$; $1/\kappa = (1.988 \times 10^{-12})\sqrt{\varepsilon T/I}$ (see question 2.1).
Therefore here $1/\kappa = \delta = 5.55\text{nm}$.

5.2 Use the Smoluchowski equation in the form

$$\zeta = \frac{\eta v}{\varepsilon_0 \varepsilon V} = \frac{\eta u_0}{\varepsilon_0 \varepsilon} \text{ (see equation (5.14))}$$
$$= \frac{8.94 \times 10^{-4} \times 3.5 \times 10^{-8}}{78.5 \times 8.8542 \times 10^{-12}}$$

Therefore

$$\zeta = 44.8\,\text{mV}$$

Since $I = 0.04\,\text{mol dm}^{-3}$;

$$\frac{1}{\kappa} = 1.988 \times 10^{-12}\sqrt{\frac{78.5 \times 298}{0.04}}$$
$$= 1.520 \times 10^{-9}\,\text{m}$$
$$\therefore \kappa a = 0.658 \times 10^{9} \times 2.5 \times 10^{-7} = 165$$

When such values of $\kappa a \gg 1$ operate, the Smoluchowski equation is applicable; it does not apply, however, to small particles such as were encountered in Chapter 2 with a characteristically of the order of 0.4 nm (and $\kappa a \sim 0.26$ for $I = 0.04\,\text{mol dm}^{-3}$).

5.3 Use equation (5.18) directly to yield a value for Φ of $5.89 \times 10^{-5}\,\text{cm}^3\,\text{s}^{-1}$.

Chapter 6

6.1 (i) Left hand
$Zn \longrightarrow Zn^{2+} + 2e$
Right hand
$Cu^{2+} + 2e \longrightarrow Cu$
Overall, $Zn + Cu^{2+} \longrightarrow Zn^{2+} + Cu$

(ii) Left hand
$Pb \longrightarrow Pb^{2+} + 2e$
Right hand
$Hg_2Cl_2 + 2e \longrightarrow 2Hg + 2Cl^-$
Overall, $Pb + Hg_2Cl_2 \longrightarrow 2Hg + Pb^{2+} + 2Cl^-$

(iii) Left hand
$Zn \longrightarrow Zn^{2+} + 2e$
Right hand
$2Fe^{3+} + 2e \longrightarrow 2Fe^{2+}$
Overall, $Zn + 2Fe^{3+} \longrightarrow Zn^{2+} + 2Fe^{3+}$

$\gamma_{\pm(ZnSO_4)} = 0.458$ (ionic strength $= 0.04\,\text{mol kg}^{-1}$),

$\gamma_{\pm(CuSO_4)} = 0.757$ (ionic strength $= 0.004\,\text{mol kg}^{-1}$),

$\gamma_{\pm(Pb(NO_3)_2)} = 0.708$ (ionic strength $= 0.03\,\text{mol kg}^{-1}$).

(i) Applying the Nernst equation (equation (6.23)) for both half-cells,

$$E_{Zn^{2+}/Zn} = -0.760 + \frac{0.0257}{2} \ln (0.01 \times 0.458) = -0.829\,\text{V}$$

$$E_{Cu^{2+}/Cu} = +0.340 + \frac{0.0257}{2} \ln (0.001 \times 0.757) = +0.248\,\text{V}$$

whence $E_{cell} = +0.248 - (-0.829) = 1.077\,\text{V}$.

(ii) $E_{cell} = +0.242 - (-0.194) = 0.436\text{V}$

(iii) For the redox half-cell

$$E_{Fe^{3+}/Fe^{2+}} = E^{\ominus} + \frac{RT}{F} \ln \frac{a_{Fe^{3+}}}{a_{Fe^{2+}}}$$

$$= +0.760 + 0.0257 \ln \frac{[Fe^{3+}]\,\gamma_{Fe^{3+}}}{[Fe^{2+}]\,\gamma_{Fe^{2+}}}$$

Since $-\log \gamma_{M^{z+}} = z^2 A\sqrt{I}/(1 + \sqrt{I})$ and here the ionic strength is $0.022\,\text{mol kg}^{-1}$, it may be shown that $\gamma_{Fe^{3+}} = 0.256$ and $\gamma_{Fe^{2+}} = 0.546$. Therefore, $E_{Fe^{3+}/Fe^{2+}} = +0.760 + 0.0257 \ln (0.256/0.546) = +0.741\text{V}$.
Thus $E_{cell} = +0.741 - (-0.829) = 1.570\text{V}$.

6.2 (i) $Pt|FeSO_4(aq.), Fe_2(SO_4)_3(aq.), H^+||Ce_2(SO_4)_3(aq.), Ce(SO_4)_2(aq.), H^+|Pt$

$$E^{\ominus} = 0.850\,\text{V}$$

(ii) $Zn|ZnSO_4(aq.)||Cl^-(aq.), AgCl, Ag$
$E^{\ominus} = 0.982\,\text{V}$.

6.3 $E^{\ominus}_{AgCl} = E^{\ominus}_{cell} = 0.222\,\text{V}$ (since $E^{\ominus}_{H_2} = 0.00\,\text{V}$)

6.4 $E_{right} - E_{left} = \left[0.222 - \frac{RT}{F} \ln m\gamma_{Cl^-}\right] - 0.242 = 0.051\,\text{V}$, giving $\gamma_{Cl^-} = 0.792$.
This compares with the values of 0.718 obtained from the limiting law and 0.772 obtained from the extended law.

6.5 $E^{\ominus}_{cell} = 0.014\,V; \Delta G^{\ominus} = -nE^{\ominus}F = -2.7 kJ\ mol^{-1}$

6.6 Liquid junction potential = $0.004\,V = (2t_- - 1)RT/F \ln(0.0735/0.00898)$, yields $t_- = 0.537$ and $t_+ = 0.463$.

6.7 The situation, both initially and after equilibrium is reached, may be summarized, for the general case involving protein Na_yR, as

NaCl, initial concn. = C_1	Na_yCl, initial concn. = C_2
At equilibrium have:	At equilibrium have:
Na^+ Cl^-	yNa^+ R^{y-} Cl^-
$(C_1 - x)$ $(C_1 - x)$	$(yC_2 + x)$ C_2 x

Therefore, $(C_1 - x)(C_1 - x) = C_2x$ (for $y = 1$) and $C_2x + 2C_1x - C_1^2 = 0$ from which the required relationship follows.

6.8 (i) $C_1 = 0.1\,mol\,dm^{-3}$: $yC_2 = 10 \times 0.01 = 0.1 mol\,dm^{-3}$
$x/C_1 = 0.1/0.1 + 0.2 = 0.333$ (using expression derived in question 6.7)
(ii) 0.286
(iii) 0.250

6.9 (i) Using equation (6.70) and the scheme from which it derives,

$$x = (K_w C)^{1/3} = [H^+]_{inside} = [OH^-]_{outside}$$

$$\therefore pH_{inside} = -\log[H^+] = -1/3[\log K_w + \log C] = -1/3[-14 - 1] = 5$$

$pOH_{outside} = 5$, therefore $pH_{outside} = 9$.

(ii)
$$\Delta\phi = \frac{RT}{F} \ln \frac{[H^+]_{inside}}{[H^+]_{outside}} = \frac{2.3RT}{F}[pH_{outside} - pH_{inside}]$$
$$= 0.236\,V$$

6.10 Schematically, the situation at equilibrium is:

R^- H^+ Cl^-	H^+ Cl^-
(x) $(x + y - z)$ $(y - z)$	z z

where x, y are the initial concentrations of RH and HCl, z is the equilibrium concentration of HCl in the right hand compartment. At equilibrium $[H^+]_L[Cl^-]_L = [H^+]_R[Cl^-]_R$

$$(x + y - z)(y - z) = z^2$$

$pH_L = 2.72 = -\log(x + y - z)$; $pH_R = 3.37 = -\log z$,
and since $\log(x + y - z) + \log(y - z) = 2\log z$.
$\log(y - z) = 2.72 - 6.74 = -4.02$. Therefore $(y - z) = 9.55 \times 10^{-5}\,mol\,dm^{-3}$
but since $\log(x + y - z) = -2.72$, $(x + y - z) = 1.905 \times 10^{-3}\,mol\,dm^{-3}$.
Thus $x = 1.810 \times 10^{-3}\,mol\,dm^{-3}$, and relative molecular mass of the acid
$= (15 \times 10^3)/(1.81) = 8290$.

6.11 ${}^{I}m_+{}^{I}m_- = {}^{II}m_+{}^{II}m_- = {}^{II}m^2 : {}^{I}m_+ = z{}^{I}m_{Rz-} + {}^{I}m_-$

Therefore ${}^{II}m^2 = (z{}^{I}m_{Rz-} + {}^{I}m_-){}^{I}m_-$

$$\approx \left({}^{I}m_- + \frac{z{}^{I}m_{Rz-}}{2}\right)^2 \text{ if square terms in } {}^{I}m_{Rz-} \text{ are neglected.}$$

Therefore ${}^{I}m_- \cong {}^{II}m - \dfrac{z{}^{I}m_{Rz-}}{2}$

Therefore $\Delta\phi \cong \dfrac{RT}{F} \ln \dfrac{{}^{I}m_-}{{}^{II}m_-} = \dfrac{RT}{F} \ln \left(\dfrac{{}^{II}m_- - \frac{z{}^{I}m_{Rz-}}{2}}{{}^{II}m} \right) \approx \dfrac{RT}{2F} \dfrac{z{}^{I}m_{Rz-}}{{}^{II}m}$

6.12 Graph of $\Delta\phi$ versus $m_{Hb^{z-}}$ has slope equal to $(RT/2F)(z/{}^{II}m)$ and has the value -0.240 V kg mol^{-1} so that $z = -8.5$.

Chapter 7

7.1 $\eta = a + b \log i$

$$a = -\frac{0.0591}{\alpha} \log i_0; \quad b = \frac{0.0591}{\alpha}, \text{ therefore } \alpha = \frac{0.0591}{0.119} = 0.497$$

$$1.54 = -\frac{0.0591}{0.497} \log i_0, \text{ therefore } \log i_0 = -12.951 \text{ and } i_0 = 1.12 \times 10^{-13} \text{A cm}^{-2}$$

7.2 For current densities i_1, i_2, overvoltages η_1, η_2 may be expressed as

$$\eta_1 = a + b \log i_1 \text{ and } \eta_2 = a + b \log i_2$$

Therefore

$$(\eta_2 - \eta_1) = b(\log i_2 - \log i_1)$$

$$0.394 - 0.148 = b(-2.000 - (-4.000)), \text{ therefore } b = 0.123$$

$$0.394 = a + (0.123 \times -2.00), \; a = 0.640 \text{ V}.$$

$$b = 0.123 = \frac{0.0591}{\alpha}, \text{ therefore } \alpha = 0.480$$

$$a = -\frac{0.0591}{0.48} \log i_0, \text{ therefore } \log i_0 = -5.198;$$

$$i_0 = 6.34 \times 10^{-6} \text{A cm}^{-2}$$

7.3 Draw up a table of η and $\ln i$ as follows

η (V)	0.02	0.05	0.07	0.10	0.12	0.15	0.20
i (mA cm^{-2})	2.13	6.63	11.35	23.45	37.26	73.85	229.08
$\ln i$ (mA cm^{-2})	0.756	1.892	2.429	3.155	3.618	4.302	5.434

Plot η versus $\ln i$. Slope $= -22.78 = -\alpha F/RT$, therefore $\alpha = 0.58$.
Intercept for linear portion $= 0.90 = \ln i_0$, therefore $i_0 = 2.45$ mA cm^{-2}

7.4 $E = E^{\ominus} = -0.760$ V, for i = 1 mA cm^{-2}
$\eta = 0.280 + 0.0591 \log (0.001) = 0.280 - 0.177 = 0.101$ V
Therefore plating occurs at $-0.760 - 0.101 = -0.861$ V
In neutral solution pH = 7, therefore $[H^+] \sim 10^{-7}$ mol dm^{-3}

$$E = E^{\ominus} = \frac{RT}{F} \ln a_{H^+} \sim 0.0591 \log (10^{-7}) = -0.414 \text{ V}$$

Thus zinc cannot be plated at −0.861 V because hydrogen is liberated at voltages 0.45 V more positive than this.

7.5
$$\frac{i}{i_0} = \exp\left[\frac{-\alpha F\eta}{RT}\right] - \exp\left[\frac{(1-\alpha)F\eta}{RT}\right] \text{ (see equation (7.18))}$$

$$\text{for } \eta = 0.07;\ i/i_0 = 0.206 - 3.143 = -2.937$$

$$i = 2.937 \times 2.5 = 7.34\,\text{mA cm}^{-2}$$

7.6 Draw up the following table

η (m V)	20	50	70	100	120	150	200	250
$\ln i$ (mA cm^{-2})	−0.562	0.336	0.718	1.212	1.517	1.969	2.711	3.452

Intercept of linear portion $= -0.25 = \ln i_0$

$$i_0 = 0.779\,\text{mA cm}^{-2}$$

$$\frac{\ln i}{\eta} = \frac{\alpha F}{RT} = 38.95\alpha = 14.808\,\text{V}^{-1} \text{ (from graph)}$$

Therefore
$$\alpha = \frac{14.808}{38.95} = 0.38$$

7.7 Using equation (7.18) the following table may be drawn up for the anodic and cathodic overvoltages corresponding to the values of applied potential to be considered.

E (V)	1.30	1.40	1.50	1.61	1.70	1.80	1.90
η (V)	0.31	0.21	0.11	0.00	−0.09	−0.19	−0.29
i/i_0	−20.46	−7.73	−2.88	0.00	13.45	257.18	4777.21
I (mA)	−0.82	−0.30	−0.12	0.00	0.54	10.29	191.1

(Taking anodic currents as negative)

7.8
$$\eta = \frac{-2.303RT}{\alpha nF}\ln i_0 + \frac{2.303RT}{\alpha nF}\ln i$$

Therefore
$$\eta = 0.278 + 0.059\log i, \quad a = 0.278, \quad b = 0.059$$

$$\eta = 0.278 + 0.059\log(5 \times 10^{-3}) = 0.142\,\text{V}.$$

Chapter 8

8.1 Plot $\log K$ versus $\sqrt{I}$ according to equation (8.2).
Intercept $= -4.0912 = \log K_T$; $K_T = 8.11 \times 10^{-5}$

8.2 Graphs of $\log k$ versus $\sqrt{I}$ are linear and lie on the same line for data obtained with both electrolytes. Effect is therefore confirmed as due to the ionic medium. Slope ~ 1.83, i.e. $z_A z_B \sim 2$, according to equation (8.10), consistent with the rate-determining step being reaction between $S_2O_8^{2-}$ and I^-.

8.3 $\kappa_{AgCl} = 1.853 \times 10^{-6}\,\Omega^{-1}\,\text{cm}^{-1}$; $\Lambda^{\infty}_{AgCl} = 138.25\,\Omega^{-1}\,\text{cm}^2\,\text{mol}^{-1}$

$$\text{Solubility} = \frac{1.853 \times 10^{-3}}{138.25} = 1.340 \times 10^{-5}\,\text{mol dm}^{-3}$$

Thus concentration solubility product $= 1.796 \times 10^{-10}\,\text{mol}^2\text{dm}^{-6}$

$$I = 1.34 \times 10^{-5}\,\text{mol dm}^{-3} \text{ and therefore } \gamma_{\pm} = 0.996$$

Thermodynamic $K_s = (1.796 \times 10^{-10})(0.996)^2 = 1.78 \times 10^{-10}$.

8.4 $C = \dfrac{\kappa}{\Lambda} = 1.003 \times 10^{-4}\,\text{mol m}^{-3} = 1.003 \times 10^{-7}\,\text{mol dm}^{-3}$, $K_w = 1.006 \times 10^{-14}$.

8.5 $\alpha \cong \dfrac{\Lambda}{\Lambda_0}$; plot of $\left(\dfrac{\alpha^2}{1-\alpha}\right)$ versus $1/C$ (equations (4.6), (4.8))
yields $K_a = 1.74 \times 10^{-5}\,\text{mol dm}^{-3}$ as slope.
The expression for α is approximate and the value of K_a is a concentration constant

8.6 Plot of E versus T (graph shows clear curvature) gives

$$\left(\frac{\partial E}{\partial T}\right)_P = -0.00148\,\text{V K}^{-1} \text{ at } 308\,\text{K}.$$

$$\Delta G_{308\,\text{K}} = -nEF = -271.4\,\text{k J mol}^{-1}$$

$$\Delta H_{308\,\text{K}} = -nEF + TnF\left(\frac{\partial E}{\partial T}\right)_P = -359.4\,\text{kJ mol}^{-1}$$

$$\Delta S_{308\,\text{K}} = nF\left(\frac{\partial E}{\partial T}\right)_P = -285.6\,\text{J K}^{-1}\,\text{mol}^{-1}$$

8.7
$$E_{\text{AgBr}} = E^{\ominus}_{Ag} + \frac{RT}{F}\ln a_{\text{Ag}^+} \quad \text{(see equation (8.61))}$$

$$= E^{\ominus}_{\text{Ag}} + \frac{RT}{F}\ln K_{\text{AgBr}} - \frac{RT}{F}\ln a_{\text{Br}^-} \quad \text{(see equation (8.62))}$$

$$= E^{\ominus}_{\text{AgBr}} - \frac{RT}{F}\ln a_{\text{Br}^-}$$

Or, $E^{\ominus}_{\text{AgBr}} - E^{\ominus}_{\text{Ag}} = \dfrac{RT}{F}\ln K_{\text{AgBr}} = -0.726\,\text{V}$

Therefore

$$\ln K_{\text{AgBr}} = -\frac{0.726}{0.0257} = -28.249$$

$$K_{\text{AgBr}} = 5.390 \times 10^{-13} \sim [\text{Ag}^+][\text{Br}^-]$$

$$\text{Solubility} = 7.34 \times 10^{-7}\,\text{mol kg}^{-1}$$

8.8 A plot of $[E_{\text{cell}} + (2RT/F)\ln m]$ versus $m^{1/2}$ gives an intercept of $E^{\ominus}$. At $m^{1/2} = 0$ (equation (8.24)) $E^{\ominus} = 0.2225\,\text{V}$. Substitution into equation (8.24) gives $\gamma_{\pm} = 0.798$.

8.9 At the start for every 10 g water there is $0.0758/170 = 0.0004459$ mole of silver; at end for every 28.755 g water there is $0.2701/170 = 0.0015888$ mole of silver (n). If the solution had remained unchanged in composition, 28.755 g of water would have been associated with $(0.0004459) \times (28.755)/10 = 0.0012822$ mole of silver (n_0). Copper deposited in coulometer $= 0.01857/31.75 = 0.0005849$ mole (n_e).
By equation (8.34),

$$t_+ = \frac{n_e + n_0 - n}{n_e}$$

whence

$$t_{Ag^+} = 0.476; t_{NO_3^-} = 0.524$$

8.10 $C = 10\text{mol m}^{-3}$; $V = 1.4139 \times 10^{-7}\,\text{m}^3$; $It = 1.65$ coulombs. By equation (8.35) $t_{H^+} = 0.827$.

8.11
$$\begin{aligned} E_{cell} &= E_{AgCl} - EH_2 \\ &= E^{\ominus}_{AgCl} - \frac{RT}{F}\ln a_{Cl^-} - \frac{RT}{F}\ln a_{H^+} \quad \text{(see equation (8.22))} \\ &\cong E^{\ominus}_{AgCl} - \frac{2RT}{F}\ln a_{H^+} \text{(assuming } \gamma_{H^+} \approx \gamma_{Cl^-}) \end{aligned}$$

Therefore
$0.4196 - 0.2225 = -0.1182 \log a_{H^+}$, giving pH = 1.668.
By the Debye–Hückel limiting law

$$\log \gamma_{H^+} \approx -0.509 \times 1^2 \times \sqrt{0.025} = -0.0805; \gamma_{H^+} \approx 0.8308$$

Therefore

$$a_{H^+} \approx 0.02077, \text{ giving pH} \approx 1.683$$

8.12 Data may be substituted into equation (8.49) assuming that the value of the activity quotient is approximately unity. Thus

$$\frac{0.6253 - 0.2225}{2.303RT/F} + \log\left[\frac{0.0079 \times 0.0082}{0.0075}\right] \approx -\log K_a$$

whence $K_a = 1.77 \times 10^{-5}$.

8.13 Isochore equation $\text{d}\ln K_w/\text{d}T = \Delta H_i/RT^2$ or $\ln K_w = -\Delta H_i/RT + \text{const}$. A graph of K_w versus $1/T$ yields a slight curve of negative slope from which ΔH_i may be estimated at the three temperatures as:
$58.1\,\text{kJ mol}^{-1}$(288 K), $56.4\,\text{kJ mol}^{-1}$(298 K), and $54.6\,\text{kJ mol}^{-1}$(308 K)
Heat of neutralization at 298 K = $-56.4\,\text{kJ mol}^{-1}$.

Chapter 9

9.1
$$\begin{aligned} i_{lim} &= \frac{DnF[Ag^+]}{\delta} \quad \text{(see equation (9.1))} \\ &= \frac{1.64 \times 10^{-5} \times 96500 \times 10^{-4}}{0.05} = 3.17\,\text{mA cm}^{-2} \end{aligned}$$

For rapid stirring, $\delta \sim 0.001$ cm, so i_{lim} is increased 50-fold to about $158.5\,\text{mA cm}^{-2}$.

9.2 A plot of $\log\{(\bar{I}_d - \bar{I})/\bar{I}\}$ versus E according to the Heyrovsky–Ilkovic equation (see equation (9.3)) gives $E_{1/2} = -1.00$ V vs. SCE. Slope = $0.0293 = 0.0591/n$, therefore $n = 2$.

$$\begin{aligned} D &= \left[\frac{\bar{I}_d}{607nm^{2/3}t^{1/6}C}\right]^2 \quad \text{from equation (9.2)} \\ &= 7.19 \times 10^{-6}\,\text{cm}^2\,\text{s}^{-1} \end{aligned}$$

9.3 The data are characteristic of an irreversible reduction. The same plot as for the previous question yields a value for the slope of $0.056 = 0.0591/\alpha n$. Since the limiting current is clearly diffusion controlled, its magnitude indicates that $n = 2$, so that $\alpha n = 1.06$.

9.4 Let the unknown concentration be C_1 and that of the standard solution be C_s: then by the Ilkovic equation

$$C_1 = \frac{I_1}{k}; \quad \Delta C = \frac{\Delta I}{k}$$

After addition of volume v of standard solution of concentration C_s to a volume V of the working solution of concentration C_1, the new concentration is

$$\left[C_s\left(\frac{v}{V+v}\right) + C_1\left(\frac{V}{V+v}\right)\right]$$

$$\therefore \Delta C = \left[C_s\left(\frac{v}{V+v}\right) + C_1\left(\frac{V}{V+v}\right)\right] - C_1$$

$$= (C_s - C_1)\left(\frac{v}{V+v}\right)$$

$$\therefore k = \frac{\Delta I}{\Delta C} = \frac{\Delta I(V+v)}{v(C_s - C_1)}$$

$$\therefore C_1 = \frac{I_1}{k} = \frac{I_1 v(C_s - C_1)}{\Delta I(V+v)}$$

which leads to

$$C_1 = \frac{I_1 v C_s}{\Delta I(V+v) + I_1 v}$$

Substitution of the experimental data into this last equation gives

$$C_{Ni^{2+}} = \frac{1.97 \times 4 \times 9.24 \times 10^{-3}}{(1.98 \times 79) + (1.97 \times 4)}$$

$$= 4.43 \times 10^{-4}\ \text{mol dm}^{-3}$$

$$= 0.026\ \text{g dm}^{-3}\ Ni^{2+}$$

$$= 0.0026\ \text{g}\ Ni^{2+}\ \text{per}\ 100\ \text{cm}^3$$

$$\therefore \%Ni^{2+} = \frac{0.0026 \times 100}{3} = 0.087\%$$

9.5 From equation (9.4) the shift of half-wave potential $\Delta E_{1/2}$ induced by ligand concentration [X] to form a complex MX_N is given by:

$$\frac{0.4343nF}{RT} \cdot \Delta E_{1/2} \sim \log \beta_N + N \log [X]$$

To apply the equation it must be assumed that both aqua and complexed ion are reduced reversibly. Then if complexation extends to formation of MX, substitution of data yields $\beta_1 = 2.9 \times 10^7$: if MX_2 is formed, it is found that $\beta_2 = 1.5 \times 10^8$.

Chapter 11

11.1 (i) $E^{\ominus}_{Zn^{2+}/Zn} = -0.76\ \text{V}$; $E^{\ominus}_{Cl_2/Cl^-} = +1.36\ \text{V}$ (see Table 6.1)

$E^{\ominus}_{cell} = 2.12\ \text{V}$.

(ii) Energy stored = 90 kWh. = $90 \times 1000 \times 60 \times 60$ J
Voltage of 118 cells = 250 V.

$$\text{Quantity of electricity stored} = \frac{90 \times 1000 \times 60 \times 60}{250}$$
$$= 1.296 \times 10^6 \text{C}$$

$$\text{Amount of } Cl_2 \text{ required} = \frac{1.296 \times 10^6}{2 \times 96500} = 6.72 \text{ mol } Cl_2 = 477.12 \text{ g } Cl_2$$

Corresponding amount of hydrate required = 638.4g.

11.2 (i) The overall reaction involving methane derives from the two half-cell reactions

$$CH_4 + 2H_2O = CO_2 + 8H^+ + 8e$$
$$2O_2 + 8H^+ + 8e = 4H_2O$$
$$\overline{CH_4 + 2O_2 = CO_2 + 2H_2O}$$

Similar treatment of all the cases cited yields the values 8, 14, 20 and 6 for the number of electrons transferred in each cell reaction.

(ii) Using $\Delta G^{\ominus} = -nE^{\ominus}F$ (see equation (6.19)), the respective $E^{\ominus}$ values are: 1.060 V, 1.086 V, 1.092 V, 1.221 V.

(iii) Since efficiency = $\Delta G/\Delta H$, the respective maximum efficiencies are: 91.9%, 94.0%, 95.0%, 92.5%.

Appendix I The electrical potential in the vicinity of an ion

By definition, the electrical potential, ϕ, at some point is the work done in bringing a unit positive charge from infinity (where $\phi = 0$) to that point (Figure I.i).

The concentration of positive and negative ions (N_+, N_-) at the point where the potential is ϕ may be found from the Boltzmann distribution law, thus

$$N_+ = N_+^0 \, e^{-(z_+ \epsilon \phi / kT)}$$

and

$$N_- = N_-^0 \, e^{+(z_- \epsilon \phi / kT)} \tag{I.i}$$

where ϵ is the unit electronic charge, k the Boltzmann constant, z_+, z_- the number of charges carried by positive and negative ions respectively, and N_+^0, N_-^0 the number of ions of each type per unit volume in the bulk.

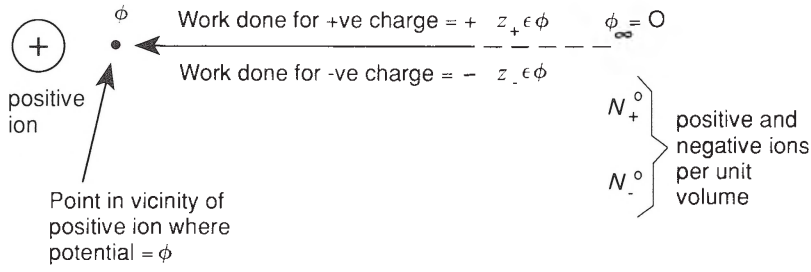

Figure I.i The work of bringing charges from infinity ($\phi_\infty = 0$) to a point near a selected ion where the potential = ϕ.

It is seen that these equations are consistent with the expected fact that there are, on average, more negative ions than positive ions in the vicinity of a given positive ion and vice versa.

The electrical density (ρ) at the point where the potential is ϕ is the excess positive or negative electricity per unit volume at that point. It is easily seen that for the present case this must be

$$\rho = N_+ z_+ \epsilon - N_- z_- \epsilon - N_+^0 z_+ \epsilon \, e^{-(z_+ \epsilon \phi / kT)} - N_-^0 z_- \epsilon \, e^{+(z_- \epsilon \phi / kT)} \tag{I.ii}$$

For the simplest case of a 1:1 electrolyte

$$z_+ = z_- = 1$$

and

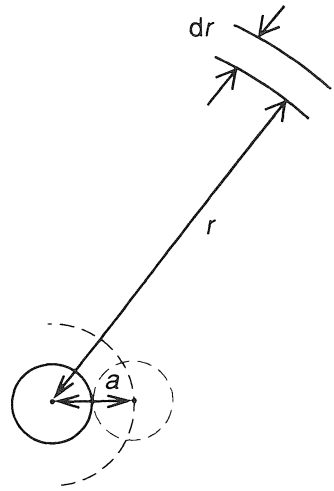

Figure I.ii Model for calculation of charge of an ion atmosphere about a central ion.

$$N_+^0 = N_-^0 = N_i$$

i.e.

$$\rho = N_i \epsilon \left[e^{-\epsilon\phi/kT} - e^{\epsilon\phi/kT} \right] \tag{I.iii}$$

If it is assumed that $\epsilon\phi/kT \ll 1$, the two exponential terms may be expanded and all but the first terms in the expansions neglected so that equation (I.iii) becomes

$$\rho \sim -2N_i \left[\frac{\epsilon^2\phi}{kT} \right] \tag{I.iv}$$

For the more general case where $z_+, z_- \neq 1$, equation (I.iv) becomes modified to

$$\rho \sim -\Sigma N_i z_i^2 \left[\frac{\epsilon^2\phi}{kT} \right] \tag{I.v}$$

The electrostatic potential and charge density are also related in the Poisson equation, viz.

$$\frac{\partial^2\phi}{\partial x^2} + \frac{\partial^2\phi}{\partial y^2} + \frac{\partial^2\phi}{\partial z^2} = -\frac{\rho}{\varepsilon_0\varepsilon} \tag{I.vi}$$

where ε_0 is the permittivity of a vacuum ($8.854 \times 10^{-12}\ C^2\ N^{-1}\ m^{-2}$) and ε is the relative permittivity, or dielectric constant, of the solvent. x, y, z are the rectangular coordinates of the point at which the potential is ϕ. In terms of polar coordinates equation (I.vi) becomes

$$\frac{1}{r^2}\frac{\partial}{\partial r}\left(r^2 \frac{\partial\phi}{\partial r} \right) = -\frac{\rho}{\varepsilon_0\varepsilon} \tag{I.vii}$$

Substituting for ρ from equation (I.v) we have that

$$\frac{1}{r^2}\frac{\partial}{\partial r}\left(r^2 \frac{\partial\phi}{\partial r} \right) = \frac{\epsilon^2}{\varepsilon_0\varepsilon kT}\Sigma N_i z_i^2 \tag{I.viii}$$

which we will express as $\kappa^2\phi$, where

$$\kappa = \left[\frac{\epsilon^2 \Sigma N_i z_i^2}{\varepsilon_0 \varepsilon k T}\right]^{1/2} \tag{I.ix}$$

A general solution of equation (I.viii) takes the form

$$\phi = \frac{A\,e^{-\kappa r}}{r} + \frac{A' e^{\kappa r}}{r} \tag{I.x}$$

in which A, A' are integration constants. The second term may, in fact, be ignored, since as $r \to \infty, \phi \to 0$, thus A' must be zero, i.e. ϕ must be finite even for very large values of r. Thus,

$$\phi = \frac{A\,e^{-\kappa r}}{r} \tag{I.xi}$$

and since

$$\kappa^2 \phi = -\frac{\rho}{\varepsilon_0 \varepsilon}$$

substitution of ϕ from equation (I.xi) into the expression

$$\rho = -\kappa^2 \phi \varepsilon_0 \varepsilon$$

yields

$$\rho = -A\left(\frac{\kappa^2 \varepsilon_0 \varepsilon}{r}\right) e^{-\kappa r} \tag{I.xii}$$

For electroneutrality, the total negative charge of the atmosphere about a given positively charged central ion is $-z_i\epsilon$. The total charge of the atmosphere is determined by considering the charge carried by a spherical shell of thickness dr and distance r from the central ion and integrating from the closest distance that atmosphere and central ions may approach out to infinity (Figure I.ii). Thus

$$\int_a^\infty 4\pi r^2 \rho\, dr = -z_i\epsilon \tag{I.xiii}$$

Therefore,

$$A\kappa^2 \varepsilon_0 \varepsilon \int_a^\infty 4\pi r\, e^{-\kappa r}\, dr = z_i\epsilon \tag{I.xiv}$$

Integration by parts gives A as

$$A = \left(\frac{z_i\epsilon}{4\pi\varepsilon_0\varepsilon}\right)\left(\frac{e^{\kappa a}}{1+\kappa a}\right) \tag{I.xv}$$

So that the potential ϕ may now be expressed by

$$\phi = \left(\frac{z_i\epsilon}{4\pi\varepsilon_0\varepsilon}\right)\left(\frac{e^{\kappa a}}{1+\kappa a}\right)\left(\frac{e^{-\kappa r}}{r}\right) \tag{I.xvi}$$

When r approaches a, the distance of closest approach, equation (I.xvi) becomes

$$\phi = \left(\frac{z_i\epsilon}{4\pi\varepsilon_0\varepsilon a}\right)\left(\frac{1}{1+\kappa a}\right) = \left(\frac{z_i\epsilon}{4\pi\varepsilon_0\varepsilon a}\right) - \left(\frac{z_i\epsilon}{4\pi\varepsilon_0\varepsilon}\right)\left(\frac{\kappa}{1+\kappa a}\right) \tag{I.xvii}$$

or, in the most general terms

$$\phi = \pm\left(\frac{z_i\epsilon}{4\pi\varepsilon_0\varepsilon a}\right) \mp \left(\frac{z_i\epsilon}{4\pi\varepsilon_0\varepsilon}\right)\left(\frac{\kappa}{1+\kappa a}\right) \tag{I.xviii}$$

or,

$$\phi = \phi_0 + \phi_i \tag{I.xvix}$$

where ϕ_0 is the contribution of the ion itself to ϕ while ϕ_i is the contribution of its atmosphere.

Appendix II Significance of the constant κ in the Debye–Hückel equation

In Appendix I, κ was expressed as

$$\kappa = \left[\frac{\epsilon^2}{\varepsilon_0 \varepsilon kT} \Sigma N_i z_i^2\right]^{1/2} \qquad \text{(see I.ix)}$$

in which $N_i = NC_i$, where N is the Avogadro constant and C_i is the ion concentration in mol m^{-3}. Thus,

$$\kappa = \left(\frac{\epsilon^2 N}{\varepsilon_0 \varepsilon kT} \Sigma C_i z_i^2\right)^{1/2}$$

or

$$\kappa = \left(\left(\frac{2\epsilon^2 N}{\varepsilon_0 \varepsilon kT}\right) \tfrac{1}{2} \Sigma C_i z_i^2\right)^{1/2} \qquad \text{(II.i)}$$

It is seen that equation (II.i) contains the expression $\frac{1}{2}\Sigma C_i z_i^2$. This is very similar in form to the expression defining the ionic strength, I, of the solution, viz.

$$I = \tfrac{1}{2} \Sigma m_i z_i^2 \qquad \text{(II.ii)}$$

where m_i represents the concentration of each ion of the electrolyte in the units mol kg^{-1}.

Now if C_i in mol m^{-3}, as used above, is replaced by c_i in mol dm^{-3}, then $N_i = 10^3 Nc_i$, and if the solution is of such dilution that 1dm^3 corresponds closely to 1dm^3 of pure solvent, i.e. 1 kg for the case of water, we may write

$$N_i = 10^3 Nm_i$$

Thus equation (II.i) becomes

$$\kappa = \left(\left(\frac{2 \times 10^3 \epsilon^2 N}{\varepsilon_0 \varepsilon kT}\right) \tfrac{1}{2} \Sigma m_i z_i^2\right)^{1/2}$$

or

$$\kappa = \left(\frac{2 \times 10^3 \epsilon^2 N}{\varepsilon_0 \varepsilon kT}\right)^{1/2} \sqrt{I} \qquad \text{(II.iii)}$$

Appendix III Derivation of the Lippmann equation

The expression $d\gamma = \Sigma\Gamma_i d\tilde{\mu}_i = 0$ (see equation (5.3)) may be applied to the four distinct phases of the following cell

$$\underset{1}{Pt(H_2)} \mid \underset{2}{HCl} \mid \underset{3}{Hg} \mid \underset{4}{Pt}$$

in which the hydrogen electrode may be regarded as non-polarizable and the mercury electrode as ideally polarizable.

Application of equation (5.3) to the interface between phase 2 and phase 3, gives

$$-d\gamma = [\Gamma_{Hg^+} d\tilde{\mu}_{Hg^+} + \Gamma_{e^-} d\tilde{\mu}_{e^-}] + [\Gamma_{H_3O^+} d\tilde{\mu}_{H_3O^+} \Gamma_{Cl^-} d\tilde{\mu}_{Cl^-} + \Gamma_{H_2O} d\mu_{H_2O}] \qquad \text{(III.i)}$$

Now, for an electrolyte, the chemical potential is the sum of the potentials of its component ions, e.g.

$$\mu = \nu_+ \mu_+ + \nu_- \mu_- \qquad \text{(III.ii)}$$

therefore,

and

$$\left.\begin{aligned} \mu_{Hg} &= \tilde{\mu}_{Hg^+} + \tilde{\mu}_{e^-} \quad \text{in phase 3} \\ \mu_{HCl} &= \tilde{\mu}_{H_3O^+} + \tilde{\mu}_{Cl^-} \quad \text{in phase 2} \end{aligned}\right\} \qquad \text{(III.iii)}$$

therefore,

$$\begin{aligned} -d\gamma = {} & [\Gamma_{Hg^+} d\mu_{Hg} - (\Gamma_{Hg^+} - \Gamma_{e^-}) d\tilde{\mu}_{e^-}] \\ & + [\Gamma_{Cl^-} d\mu_{HCl} + (\Gamma_{H_3O^+} - \Gamma_{Cl^-}) d\tilde{\mu}_{H_3O^+} + \Gamma_{H_2O} d\mu_{H_2O}] \end{aligned} \qquad \text{(III.iv)}$$

Now

$$\Gamma_i = \frac{n_i}{A} \qquad \text{(III.v)}$$

i.e. the number of particles of species i per unit area. It is possible to express the total number of charges per unit area, adsorbed by the interface from phase 2 and phase 3 as

and

$$\left.\begin{aligned} (\Gamma_{Hg^+} - \Gamma_{e^-})F &= \sigma_3 \\ (\Gamma_{H_3O^+} - \Gamma_{Cl^-})F &= \sigma_2 \end{aligned}\right\} \qquad \text{(III.vi)}$$

For electroneutrality at the interface

$$\sigma_2 + \sigma_3 = 0 \qquad \text{(III.vii)}$$

Also, for equilibrium to be maintained across the interface between mercury and platinum (phase 3 and phase 4)

$$(d\tilde{\mu}_{e^-})_3 = (d\tilde{\mu}_{e^-})_4 \qquad \text{(III.viii)}$$

Similarly, for equilibrium across the interface between phases 1 and 2,

$$(d\tilde{\mu}_{H_3O^+})_2 = -(d\tilde{\mu}_{e^-})_1 \qquad \text{(III.ix)}$$

Substituting equation (III.vi)–(III.ix) into equation (III.iv) yields

$$-d\gamma = \Gamma_{Hg^+}\, d\mu_{Hg} - \frac{\sigma_3}{F}(d\tilde{\mu}_{e^-})_4 + \Gamma_{Cl^-}\, d\mu_{HCl} + \frac{\sigma_2}{F}(d\tilde{\mu}_{e^-})_1 + \Gamma_{H_2O} d\mu_{H_2O} \qquad \text{(III.x)}$$

therefore

$$-d\gamma = \Gamma_{Hg^+}\, d\mu_{Hg} - \frac{\sigma_3}{F}[(d\tilde{\mu}_{e^-})_4 - (d\tilde{\mu}_{e^-})_1] + \Gamma_{Cl^-}\, d\mu_{HCl} + \Gamma_{H_2O} d\mu_{H_2O} \qquad \text{(III.xi)}$$

We may assume the equality of σ_2 and σ_3 since, as the mercury electrode is completely polarizable, no charge may be transferred across the interface; for the same reason the compositions of the phases must remain constant so that $d\mu$ terms = 0.

Now, at a given temperature and pressure, the potential of the hydrogen electrode is affected only by the activity of HCl and is not affected by an applied external voltage, E. Any variations, dE in E, may therefore be regarded as changes $d(\Delta\phi)$ at the Hg/HCl interface. Therefore,

$$(d\tilde{\mu}_{e^-})_1 - (d\tilde{\mu}_{e^-})_4 = F(\phi_1 - \phi_4) = F\, dE \qquad \text{(III.xii)}$$

therfore, equation (III.xi) becomes

$$-d\gamma = \Gamma_{Hg^+}\, d\mu_{Hg} + \Gamma_{Cl^-}\, d\mu_{HCl} + \Gamma_{H_2O}\, d\mu_{H_2O} + \sigma_3\, dE \qquad \text{(III.xiii)}$$

or,

$$\left(\frac{\partial\gamma}{\partial E}\right)_{P,T,\mu} = -\sigma_3 \qquad \text{(III.xiv)}$$

Equation (III.xiv) is known as the Lippmann equation.

Appendix IV Potentials in the diffuse double layer

For a single (x) direction it is possible, by analogy with equation (I.vi) to write

$$\frac{\partial^2\phi}{\partial x^2} = \frac{\epsilon^2\phi}{\varepsilon_0\varepsilon kT}\Sigma N_i z_i^2 = \kappa^2\phi = \frac{-\rho}{\varepsilon_0\varepsilon} \tag{IV.i}$$

whereas $1/\kappa$ in the Debye–Hückel theory is regarded as the effective radius of the ion atmosphere about an ion, here it is to be identified with δ the thickness of the diffuse double layer. For equation (IV.i) the general solution follows by analogy with that for (I.vi), viz.

$$= A\,e^{-\kappa x} + B e^{\kappa x} \tag{IV.ii}$$

and since $\phi \to 0$ as $x \to \infty$, $B = 0$. Now,

$$\frac{-\rho}{\varepsilon_0\varepsilon} = \kappa^2\phi$$

where ρ = charge/unit volume of electrolyte solution. Therefore,

$$\rho = -\varepsilon_0\varepsilon\kappa^2\phi \tag{IV.iii}$$

$$= -A\varepsilon_0\varepsilon\kappa^2\,e^{-\kappa x} \tag{IV.iv}$$

(by combining equations (IV.ii) and (IV.iii)).

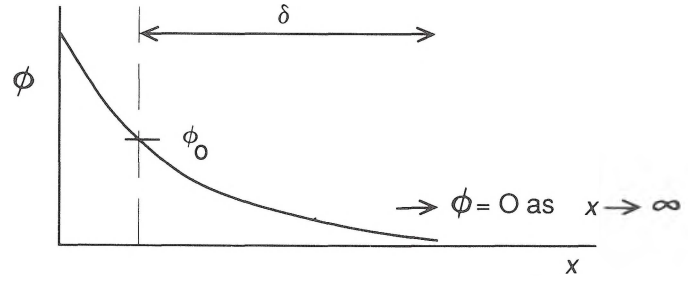

Figure IV.i The diffuse double layer in the region bounded by the conditions $\phi = \phi_0$ and $\phi = 0$.

Let the charge density at the electrode surface (i.e. at $x = 0$) be σ/unit area. This then is equal in magnitude, but of opposite sign, to the total volume charge in solution, i.e.

$$\sigma = -\int_a^\infty \rho\,dx \tag{IV.v}$$

a being the distance of closest approach of ions to the surface. Therefore,

$$\sigma = -A\varepsilon_0\varepsilon\kappa^2 \int_a^{\infty} e^{-\kappa x}\, dx \tag{IV.vi}$$

$$= A\varepsilon_0\varepsilon\kappa e^{-\kappa a} \tag{IV.vii}$$

therefore

$$A = \frac{\sigma}{\varepsilon_0\varepsilon\kappa} e^{\kappa a} \tag{IV.viii}$$

When the last expression for A is substituted into that for ϕ (equation (IV.ii)), we obtain

$$\phi = \frac{\sigma}{\varepsilon_0\varepsilon\kappa} e^{\kappa(a-x)} \tag{IV.ix}$$

Index